

THE UNIVERSITY OF TOKYO

DOCTORAL THESIS

**A Markovian route choice analysis
for trajectory-based urban planning**

Author:

Yuki OYAMA

*A thesis submitted in fulfillment of the requirements
for the degree of Doctor of Philosophy*

in the

**Behavior in Networks Studies Unit
Department of Urban Engineering**

March 31, 2017

"To be yourself in a world that is constantly trying to make you something else is the greatest accomplishment."

Ralph Waldo Emerson

The University of Tokyo

Abstract

School of Engineering
Department of Urban Engineering

Doctor of Philosophy

A Markovian route choice analysis for trajectory-based urban planning

by Yuki OYAMA

Route choice analysis predicts which route a given traveler takes to go from a location to another, and it evaluates the flow pattern on a transportation network. It is one of the most important issues of urban and transport planning; however, the evaluation of path choice probabilities is not a trivial task due to the requirement of the path set generation.

Markovian route choice model is an approach of route choice analysis and avoids to enumerate the path set by evaluating path choice probabilities as the products of link transition probabilities. It has originally been proposed in the context of traffic assignment and recently is gathering much attention again because of its consistency with the logity-type route choice model without path enumeration. In addition to its high operability, this thesis focuses on that the Markovian route choice model describes the sequence of decision-making process. The description of the sequential decision-making process in route choice behavior can expand the possibility of route choice analysis and would become important in the future urban planning. For these reasons, we aim at developing a framework of Markovian route choice analysis.

The Markovian route choice model mainly has the following challenges: 1) it includes the biases in observing route choice behavior and in estimating parameters of route choice model, which are caused from the initial parameter settings, 2) it is based on the assumption of global optimal decision, that is, travelers are assumed to have knowledge of the entire network and evaluate utilities of all links with the equivalent weight, and 3) there is the computational instability of the expected maximum utilities, which are the core idea of the Markovian route choice model, dependently on the relationship between the network structure and the size of link utilities. Therefore, 4) the application of the model is restricted into the daily vehicle route choice behavior, which is easier to observe and can be assumed to follow the global optimal decision based on the simple aspects such as travel time or travel cost.

This thesis presents the following several new methods for solving the above challenges and develops an integrated framework of the Markovian route choice analysis.

1) For reducing the biases in estimating parameters caused from the initial parameter settings, we propose a novel route measurement model and an estimation method. The *sequential link measurement model* identifies link-specific variance of GPS measurement error, which has been assumed as the given and constant value over the network in the previous probabilistic route measurement models. The *structural estimation* method removes the bias that is included in the prior information, which is used for correcting the measurement probability in the case that the measurement error is large. We have some numerical experiments and validate the effectiveness of the proposed methods. We also apply them to a real pedestrian network of the city center of Matsuyama city, Japan. This study is addressed in Chapter 3.

2) We propose a dynamic sequential route choice model, which is referred to as the β -scaled recursive logit model, to describe sequential and somewhat forward-looking decisions of travelers. It generalizes driver's sequential decision using the parameter of the discount factor in the dynamic discrete choice model. The model is consistent to the previous Markovian route choice model referred to as the recursive logit model as a special case, and it also can model the myopic decision that is dependent on only link utility that is directly connected with the current state link of a traveler. We show the model properties through illustrative examples. We also apply it to the taxi probe data collected in the Tokyo network on the day of the Great East Japan Earthquake and find out drivers' myopic decisions in the gridlock network. This study is shown in Chapter 4.

3) Focusing on that the computational problems of the Markovian route choice model are caused from the consideration of paths with infinite cycles, we propose several methods to solve the problems. The *time-structured network* is a state network that consists of decomposed networks by decision-making timing, and a route is described as a sequence of states in the time-structured network. Moreover, we propose a method of restricting path set based on the *time-space prism*, that is, only paths included in the time-space prism are considered in the route choice model. Thanks to these methods, infinite cyclic paths are removed, and it is possible to calculate the expected maximum utilities regardless of network structures, using the backward induction algorithm. The backward induction algorithm is a simple method for solving the Bellman equation and does not depend on whether the model is linear or non-linear. We present some illustrative examples to show that the computational challenges of the Markovian route choice model are solved. This study is shown in Chapter 5.

4) Using the proposed framework of a Markovian route choice analysis, we propose an activity path choice model, which describes a route choice behavior in time-space networks. By assuming that the time interval for state transitions is constant, it can describe the choices of routes, activity locations and durations simultaneously. We also propose an assignment model for activity-scheduling network using the activity path choice model, and it evaluates not only the spatial flow pattern but also the use of time at each node. We apply the activity assignment model to a pedestrian network design problem and investigate the Pareto front solutions of widening the sidewalk width, based on a framework of multi-level and multi-objective programming. This study is addressed in Chapter 6.

Acknowledgements

Many people have directly or indirectly helped me with the researches presented in this thesis. Although I cannot raise all names, I attempt to thank them here for their contributions.

First and foremost, I would like to thank my supervisor Eiji Hato for his relentless support, both academically and personally throughout these five years since my master's course. A lot of his strict but kind advices have brightened my future.

I would also like to thank my co-supervisor Aya kubota. She has been keeping an affectionate eye out for me since I started my study of urban planning and design about 6 years ago.

Michel Bierlaire has given me the opportunity to experience the stimulating environment in his lab at EPFL. He has also introduced me to Riccardo Scarinci and all members of Transport and Mobility Laboratory. I am very grateful them for their contribution to Chapter 6 of this thesis and the great time in Switzerland.

Kyosuke Chikamatsu and Yui Shoji, who are my colleagues at the University of Tokyo, have contributed a lot to Chapter 4 of this thesis. I really enjoyed the project with them and would like to thank them.

I am also grateful Moshe Ben-Akiva, Noboru Harata, Daisuke Fukuda, and Takuya Maruyama, the jury members of this thesis, for their critical and variable inputs towards improving this thesis. Also, Takashi Akamatsu gave me a lot of incisive comments.

My Ph.D. study and life have been supported by many senior researchers, Sachiyo Fukuyama, Hideki Yaginuma, Yusuke Hara, Junji Urata, Giancarlos Troncoso Parady, and all the current and previous members of Behavior in Networks studies unit.

Three years of my research and Ph.D life have been financed by Japan Society for the Promotion of Science, grant 14J10824 (April 2014 to March 2017).

Finally, I could not have finished this thesis without the continuous support of my parents and grandparents, sister and brother. I cannot enough express my gratitude to them.

Contents

Abstract	iii
Acknowledgements	v
1 Introduction	1
1.1 Trajectory-based urban planning	1
1.1.1 Background	1
1.1.2 Designing trajectories	3
1.2 Focus of the study	3
1.2.1 Route choice analysis	3
1.2.2 Markovian route choice analysis	5
1.2.3 Scopes of the thesis	5
1.3 Contributions	7
1.4 Outline of the thesis	8
2 Literature review	11
2.1 Route choice analysis	11
2.1.1 Shortest path problem	11
2.1.2 Multinomial logit model	12
2.1.3 Description of correlation structures	13
2.1.4 Path set generation algorithms	13
2.1.5 Route choice observation	14
2.1.6 Maximum likelihood estimation	15
2.1.7 Joint estimation of route choice models	16
2.2 Markovian route choice analysis	16
2.2.1 Dial's algorithm	18
2.2.2 Markov chain assignment	19
2.2.3 Proof of equivalence to the logit model	20
2.2.4 Stochastic user equilibrium based on Markovian model	22
2.2.5 Sequential link choice model	24
2.2.6 Description of correlation structures	25
2.2.7 Recursive logit model	27
2.3 Discussion	30
2.3.1 Biases in estimating route choice models	30
2.3.2 Computational property of Markovian route choice models	31
3 Structural estimation for route choice models under measurement uncertainties	35
3.1 Introduction	36
3.2 Literature review	37
3.2.1 Route measurement models	37
Map matching algorithms	37
Probabilistic route measurement models	38

3.2.2	Bayesian approaches	38
3.3	Biases in estimation process	39
	Framework and notations	40
3.3.1	Network	40
3.3.2	Route choice model	40
3.3.3	Route measurement model	41
3.4	Link-based route measurement model	42
3.4.1	Data decomposition	42
3.4.2	Sequential link measurement	42
3.4.3	Measurement probability	43
3.5	Structural estimation	45
3.5.1	Estimation of route choice models	45
3.5.2	Algorithm of structure estimation	45
3.6	Numerical examples	47
3.6.1	Simulation analysis	47
3.6.2	Real data analysis	51
3.7	Conclusion and discussion	53
3.7.1	Conclusion of the paper	53
3.7.2	Discussion for the future research	54
4	Dynamic sequential route choice model for dynamic network analysis	55
4.1	Introduction	56
4.2	Literature review	58
4.2.1	Route choice models in dynamic networks	58
4.2.2	Sequential route choice models	59
4.3	β -scaled recursive logit model	61
4.3.1	Sequential discount rate	61
4.3.2	Model formulation	62
4.3.3	Solving the Bellman equation	62
4.4	Illustrative examples	63
4.4.1	Path probabilities	63
4.4.2	Link flows	66
4.4.3	Cyclic paths	68
4.5	Parameter estimation	69
4.5.1	Maximum likelihood estimation	70
4.5.2	Simulation analysis	71
4.5.3	Case study	71
4.6	Conclusions and discussion	77
5	Path set restriction algorithm for Markovian traffic assignment	79
5.1	Introduction	80
5.2	Path set restriction based on prism constraints	81
5.2.1	Choice-stage-structured network	81
5.2.2	Choice-based prism constraints	81
5.2.3	Illustrative examples	83
5.3	Route choice model	84
5.3.1	Formulation	85
5.3.2	Solving Bellman equation	86
5.4	Stochastic traffic assignment	87
5.4.1	Preliminary	87
5.4.2	Assignment algorithm	87

5.4.3	Properties of the assignment model	89
5.5	Numerical examples	92
5.5.1	Computational examination	92
	Computational stability	92
	Computational efficiency	93
5.5.2	Cyclic flows	94
5.5.3	Overlapping paths in cyclic networks	95
	Formulation of a network-GEV model in CSN	95
	Path probability	97
	Assignment results	98
5.6	Conclusions and Discussion	98
6	Application to pedestrian activity-scheduling network	101
6.1	Introduction	102
6.2	Time-space constraints	103
6.2.1	Network description	103
6.2.2	Network restriction	104
6.2.3	Time-space prism	105
6.3	Activity assignment model	106
6.3.1	Activity path choice model	106
6.3.2	Path correlation	107
6.3.3	Solving the Bellman equation	108
6.3.4	Assignment algorithm	109
6.4	Illustrative example	109
6.4.1	Activity assignment	110
6.4.2	Time-space discount rate	110
6.4.3	Activity path correlation	111
6.5	Case study	112
6.5.1	Network standardization	113
6.5.2	Modeling utility	114
6.5.3	Assignment result in Matsuyama network	114
6.5.4	Application to network design	115
6.6	Conclusions and discussion	120
7	Conclusions and future works	121
7.1	Conclusion of the thesis	121
7.2	Future research	123
A	Appendix to Chapter 3	127
A.1	Link switching	127
A.2	Fluctuation of estimated values of parameters	129
B	Appendix to Chapter 5	131
B.1	Condition to solve Bellman equation	131
C	Appendix to Chapter 6	133
C.1	Equivalent optimization model	133
C.2	Activity patterns with different β s	134
C.3	Flow of the solution algorithm	135
D	Related publications	137

List of Figures

1.1 Data shift. (a) Trip data from conventional questionnaire survey. (b) Trajectory data from passive monitoring equipped with GPS sensors.	2
1.2 Framework of route choice analysis	4
1.3 Framework of Markovian route choice analysis	6
1.4 Contributions	7
2.1 An example network defining transition probabilities	17
2.2 Overview of Markovian models in the route choice context	18
2.3 Difference of measurement probability by the variance of GPS errors	31
2.4 Biases in estimation process of route choice models	31
2.5 Example networks	33
3.1 Biases in parameter estimation process of route choice model.	40
3.2 Image of the link-based route measurement model	43
3.3 Flow of structural estimation method	46
3.4 Simulation network	48
3.5 Examples of plots and the effect of σ_a	48
3.6 Convergence processes	51
3.7 Plot of estimated σ of each link	53
4.1 Framework of trajectory-oriented gridlock network management	56
4.2 Decision making dynamics with different sequential discount rates	61
4.3 (a) Example network and (b) path alternatives	64
4.4 Path probabilities of the three path alternatives of Figure 4.3	65
4.5 Value functions of links	66
4.6 Assignment results given by the β -SRL model with different β	67
4.7 Simulation network with cycles	69
4.8 Ratio of cyclic paths in 1000 observations	69
4.9 Link speed distribution at each time on the day of the Great East Japan Earthquake in the Tokyo metropolitan area network	73
4.10 The number of direction changes	74
4.11 Plots of estimated parameters. (a) The ratio of the parameter of travel time, (b) the ratio of the parameter of right turn dummy and (c) the estimated value of the discount factor.	76
5.1 Illustration of a constrained network by the prism	83
5.2 Constraint of transition by the prism	85
5.3 Illustration of a network assignment	88
5.4 A simple cyclic network	93
5.5 Grid network	94
5.6 Stochastic user equilibrium results	95
5.7 Network and alternatives	96
5.8 Logit-based and network-GEV-based assignment results with CSN	98

6.1	An activity path $\psi_{0:5} = [(8, 9), (9, 14), (14, 14), (14, 13), (13, 8)]$ in time-structured network and its projections. (a) Spatial network graph, (b) time-structured network with time constraint $T = 5$ and (c) time use pattern	104
6.2	Time-space constraints and path restriction. (a) <i>Prism</i> constraint when the constraints are $s_0 = 13$ and $s_T = 13$ ($T = 5$), (b) <i>Bundle</i> constraint when the constraints are $s_0 = s_2 = s_3 = s_5 = 13$ and (c) <i>Domain</i> constraint.	105
6.3	Example of activity paths which have similarity with each other	107
6.4	A simple network with three nodes for staying. (a) Network and parameter setting and (b) Time-structured network and prism constraint.	110
6.5	Evaluation of activity path and its change with various β	111
6.6	Scale parameter and path probabilities	113
6.7	Network standardization	113
6.8	Network of the city center in Matsuyama-city, Japan	115
6.9	Time constraint and pedestrian activity assignment results	117
6.10	Acceptance criterion of new solutions	118
6.11	Network design results. (a) Trade-off curve between total sojourn time and total area of widened sidewalk, the variation of (b) Total sojourn time and (c) Total area of widened sidewalk in iteration process.	119
6.12	Network design results. (a) Example of pedestrian network corresponding to <i>example solution A</i> in Figure 6.11(a) and (b) The activity assignment result in case of the network.	120
A.1	Example of errors in path estimation	127
A.2	Flow of link switching algorithm	128
A.3	Fluctuation of estimated values of parameters	129
B.1	A simple cyclic network	131
C.1	The most frequent activity patterns with different β s	135
C.2	Flow of Network Update algorithm	136

List of Tables

1.1	The number of simple paths in n-grid networks	5
2.1	Path probabilities in network (a)	34
2.2	Path probabilities in network (b)	34
2.3	Path probabilities in network (c)	34
2.4	Spectral radius of the incident matrix \mathbf{W} in network (c)	34
3.1	Accuracy and the difference of σ in each model	48
3.2	Structural estimation results	50
3.3	Average and standard deviation of estimated parameters, the number of iterations and computational time for 100 structural estimations	51
3.4	Structural estimation result using Probe Person data	52
4.1	Dynamic route choice models	58
4.2	Comparison of path choice probabilities given by several route choice models applied to the example in Figure 4.3	65
4.3	The maximum number of cyclic structures in a path of 10000 observations	70
4.4	Dataset used in simulation analysis	72
4.5	Estimation results of the β -SRL model using simulation data	72
4.6	Characteristics of observations used for estimation at each time period	74
4.7	Estimation result of the β -SRL model using the data on March 4, 2011	75
4.8	Estimation result of the β -SRL model using the data on March 11, 2011	75
4.9	Average of test error values over 40 holdout samples	77
5.1	Network definition and choice-stage constraint variables	83
5.2	Restricted path set $\mathcal{P}_{(0,7)}^{(5,14)}$	84
5.3	Assignment results in a cyclic network with $\theta = 1$	93
5.4	Assignment results in a cyclic network with $\theta = 0.2$	93
5.5	Loading time in seconds in grid networks	94
5.6	Path probabilities	97
6.1	Eight dominant activity paths and their utilities	112
6.2	Time-space discount rate and path probabilities	112
6.3	Addition of state constraint and path probabilities	114
6.4	Attributes of links	116
6.5	OD patterns	116
B.1	Spectral radius of the matrix \mathbf{W}	131

List of Abbreviations

AA	Activity Assignment
CNL	Cross Nested Logit
DCM	Discrete Choice Model
DDCM	Dynamic Discrete Choice Model
DDR	Domain of Data Relevance
DP	Dynamic Programming
GEJE	Great East Japan Earthquake
GEV	Generalized Extreme Value
GNL	Generalized Nested Logit
GPS	Global Positioning System
GRL	Generalized Recursive Logit
IIA	Independence from Irrelevant Alternatives
MCA	Markov Chain Assignment
MLE	Maximum Likelihood Estimation
MNL	MultiNomial Logit
MM	Map Matching
MPEC	Mathematical Programming with Equilibrium Constraints
MXL	MiXed Logit
NFXP	Nested FiXed Point algorithm
NL	Nested Logit
NPL	Nested Pseudo Likelihood algorithm
NRL	Nested Recursive Logit
PCL	Paired Combinatorial Logit
PL	Partial Linearization
PSL	Path Size Logit
PP	Probe Person
RCM	Route Choice Model
RL	Recursive Logit
RUM	Random Utility Maximization
SA	Stochastic Assignment
SE	Structural Estimation
SDR	Sequential Discount Rate
β-SRL	β -Scaled Recursive Logit
SUE	Stochastic User Equilibrium
TSA	Time-Structured Assignment
TSN	Time-Structured Network
TUP	Trajectory-based Urban Planning
UE	User Equilibrium

List of Symbols

a	link
c	travel cost
e	edge (Chapter 5, 6)
d	destination node (link)
f	edge flow (Chapter 5, 6)
g	state flow (Chapter 5, 6)
h	iteration number
i, j	node
l	link likelihood (Chapter 2), link length (Chapter 6)
\hat{m}	(GPS) measurement (Capter 3)
n	traveler
o	origin node (link)
$p(\cdot \cdot)$	conditional probability
q	generating flow
r	route
s	state (Chapter 5, 6)
t	discretized time
u	utility function
\tilde{u}	random utility function
v	exponential of expected maximum utility
w	link weight (Chapter 2)
x	pair of coordinates (Chapter 3), link attributes (Chapter 4, 6), link flow (Chapter 5)
y	link attributes (Chapter 3)
z	objective function (Chapter 6)
D	the minimum number of steps (Chapter 5, 6)
$\mathbb{E}[\cdot]$	expected value function
$G(\cdot)$	GEV-function
I	state existence indicator (Chapter 5, 6)
$LL(\cdot)$	log-likelihood function
N	total number
P_r	path choice probability
$\mathbb{P}(\cdot)$	probability function
T	time-constraint
$V(\cdot)$	value function
\mathcal{A}	set of links
\mathcal{C}_n	choice set of traveler n
\mathcal{D}	set of destination nodes
\mathcal{E}	set of edges
\mathcal{F}	set of Pareto front solutions
\mathcal{G}	network graph
\mathcal{L}	Lagrangian

\mathcal{M}	master choice set
\mathcal{N}	set of nodes
\mathcal{O}	set of origin nodes
\mathcal{R}	set of routes
\mathcal{S}	set of states
\mathcal{U}	universal set
\mathcal{Z}	domain
α	allocation parameter
β	discount factor
γ	Euler's constant
δ	indicator
Δ	state connection indicator
ϵ	index of error
ε	error term
η	white noise
θ	unknown parameter
κ	the maximum possible capacity
λ	eigenvalue
μ	scale parameter of i.i.d gumbel distribution
ξ	convergence tolerance
ρ	spectral radius
σ	variance
τ	timestamp
ψ	path
Ω	path set restricted by time-space prism
\hat{a}	measurement variable
\tilde{a}	estimated variable, random variable
\bar{a}	initial value, average value
\check{a}	convergence value
a^*	true value

To my dearest family ...

Chapter 1

Introduction

Transport planning has mainly dealt with the alleviation of traffic congestions as the primary problem, and a number of models for demand forecasting have been developed. Route choice analysis identifies which route a give traveler takes to go a place to another, and it has played a great role in transport planning. Recently, several paradigm shifts are appearing in the background of transport planning, and the relationship among transport planning, urban planning and information technologies is more and more closely connected. For this reason, a more flexible and more operable framework of route choice analysis is required.

In this thesis, we define the sequence of decision makings in the urban space as *trajectory* and aim at developing a method for urban planning based on modeling trajectories, which is referred to as *trajectory-based urban planning*. To do so, we focus on Markovian route choice models, which are powerful tools for describing trajectories in urban networks. The studies in this thesis present some extended methods for more flexible Markovian route choice analysis.

In this chapter, we first introduce the background of the thesis and also define the *trajectory-based urban planning* in Section 1.1. We then present an overview of route choice analysis and discuss its challenges in Section 1.2. In Section 1.3, we present our contributions, and finally, we show the outline of the thesis.

1.1 Trajectory-based urban planning

1.1.1 Background

Needless to say, the transformation of urban spaces are closely related to the development of transport technologies. The construction of *Via Appia* had developed cities along it, and the appearance of steamships and the sailing routes had simulated the development of port towns. The installation of railroads had changed the land-use in old towns, and automobiles had widely and continuously extended urban spaces. The progress of the motorization has affected not only the aspect of the macroscopic urban development but also microscopic structures of cities. The great part of the current urban spaces has already designed for cars, such as roads, parkings, roadside shops, and express ways, etc.

Transport studies have been developed for dealing with the increasing transport demand, and in the cradle, the transportation equilibrium theory was developed by Wardrop, 1952 and Beckmann, McGuire, and Winsten, 1956. In 1970s, the discrete choice model that is based on the random utility theory of McFadden, 1973 has been exploited, and the foundation of the transportation planning theory has been built. Thereafter, the theories have been applied to the four step model and the activity-based approach, which are the typical demand forecasting models in the transport planning context. In this way, transport planning studies have mainly dealt with

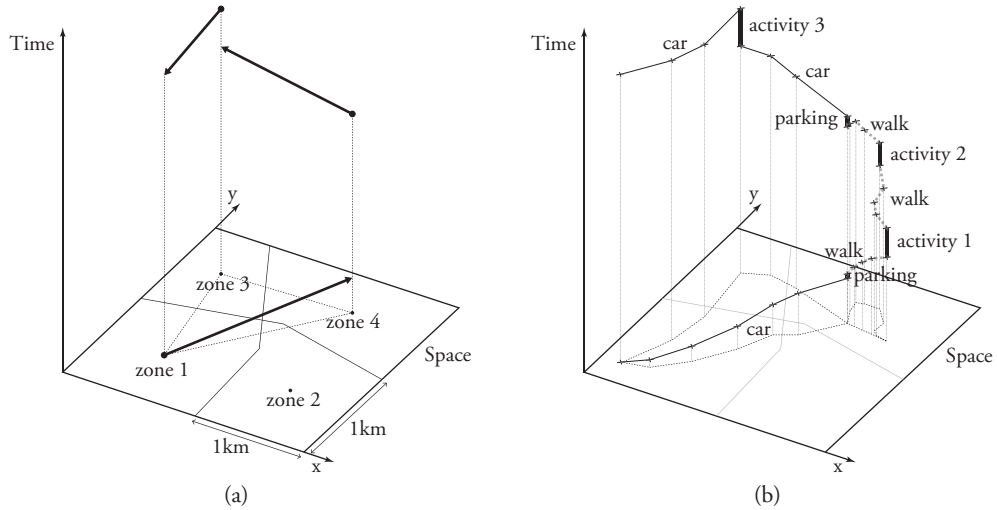


FIGURE 1.1: Data shift. (a) Trip data from conventional questionnaire survey. (b) Trajectory data from passive monitoring equipped with GPS sensors.

demand forecasting, and the alleviation of traffic congestions has been assumed to be the primary problem. For this reason, route choice analysis that is able to predict the traffic flow on each road is one of the most important topic in transport planning.

Recently, three big paradigm shifts in the background of transport studies are appearing. Firstly, social needs are changing. The negative effects of transportation on the environment have been mentioned so far, but recently, the global warming and the atmospheric pollution are making it gather much attention. In many areas over the world, the population is aging rapidly, and people are becoming more conscious of their health. For these reasons, the values of slow mobilities, such as walking and public transports, come to be reconsidered positively.

Secondly, new transportation systems are appearing. In cities, after the appearance of automobiles, any big shifts of the transportation mode have not been occurred. However, in recent years, the new technologies such as sharing mobilities and autonomous cars are appearing, and the concept of the ownership and urban space uses are changing.

Thirdly, the evolution of information technologies has been occurring. In this decades, mobile sensors that are equipped with Global Positioning System (GPS) or Wi-Fi, such as smartphones, are facilitating real-time observations of transport behavior. Using these technologies, we can observe e.g., pedestrian behavior inner city centers or buildings and the behavior at the time of emergency events or disasters, which have been difficult to observe with the conventional measurement tools. New transportation modes are also based on the development of these technologies.

These developments are transforming urban spaces again. In recent years, in real cases, the urban planning for making more human spaces have been developing, such as parking space re-locations for making pedestrian areas, which is referred to as *fringe parking* and seen in some European cities (e.g., Freiburg and Strasbourg, Germany), conversions of the parking space for other purposes (e.g., *Park(ing)* day in San Fransisco, the United States), and street space reallocations from for cars to for pedestrians (e.g., Matsuyama, Japan). In Japan, many cities focus on making better places for pedestrians, especially in city centers, in response to the aging society and the trend of urban residence. These trends are accelerated if shared autonomous

vehicles are installed and the traffic flows inner cities are decreased or controlled by the emerging systems. As the result, urban spaces that are designed for cars would be reallocated for other urban activities. Recently, some reports that illustrate the future urban spaces after the installation of autonomous cars are presented¹.

1.1.2 Designing trajectories

As discussed above, in the future urban planning, reallocation of urban spaces from cars to other transportation modes or human activities is becoming more and more important as a main issue. In previous transport planning, only the negative aspects of travels have been focused on, such as travel time and travel cost. Most of transport studies have assumed that travelers minimize their travel costs based on the global optimal decisions, in modeling travel behavior. However, since designs for making better places and changing the time use patterns in cities are gathering much attentions, it is getting more important to describe behavior different from previous assumptions, for instance, people react attractive spaces on the way of trips and change their scheduling.

Focusing on the requirement of modeling these continuous decision makings and availability of high-resolution behavioral data, we introduce the concept of *trajectory* as the planning unit into the urban planning field. We define a trajectory as the sequence of decision-making process and refer to the way of urban planning based on trajectories as *trajectory-based urban planning*. For this reason, in this thesis, we aim at developing a modeling framework for analyzing trajectories.

1.2 Focus of the study

For analyzing the sequence of decision-making process, we focus on the Markovian route choice model. Markovian models describe the sequential decision makings based on state transition probabilities, and the Markovian route choice model applies it to the context of the route choice model. The Markovian route choice model is important not only because it is suitable to describe sequential decisions but also because it can avoid the path set generation for the route choice analysis. In this section, we first present the framework of the general route choice analysis and afterward introduce the that of Markovian route choice analysis. In the end, we address the objectives of the thesis.

1.2.1 Route choice analysis

Consider a transport network with nodes and links. Generally, a node denotes an intersection, and a link denotes a road between two intersections. Route choice analysis deals with identifying route, which is a sequence of links (or nodes) and is taken by a given traveler who goes from a location to another. The most typical type of route choice model is the multinomial logit (MNL) model, which is based on the random utility maximization (RUM) theory (McFadden, 1973), and it is described as follows:

$$r = \arg \max_{r \in \mathcal{C}_n} \{\tilde{u}_{nr}\}, \quad (1.1)$$

¹"Making better places: Autonomous vehicles and future opportunities", 2016 by WSP | Parsons Brinckerhoff, Farrels.

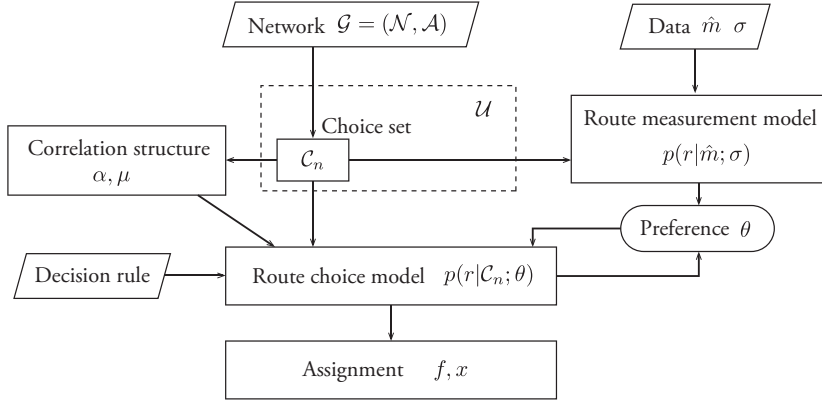


FIGURE 1.2: Framework of route choice analysis

where

$$\tilde{u}_{nr} = u_{nr} + \varepsilon_{nr} \quad (1.2)$$

is the random utility function when a traveler n chooses a route r from the choice set \mathcal{C}_n . u_{nr} is the deterministic component of the utility and ε_{nr} is the error term, which expresses model uncertainties, such as attributes that the modeler cannot observe and the heterogeneity of travelers, etc. In the MNL model, the error term is assumed as i.i.d extreme value type I, and the choice probability of r is formulated as follows:

$$P_{nr} = \frac{\exp(\mu u_{nr})}{\sum_{r' \in \mathcal{R}} \exp(\mu u_{nr}')}, \quad (1.3)$$

where μ is the scale parameter of the distribution and strictly positive. This is the fundamental model of route choice analysis. We show the framework of route choice analysis in Figure 1.2. For calculating route choice probabilities, rout choice models require the information of choice set, correlation structure, decision rule, and route choice preference. Using route choice probabilities, the network flow pattern is evaluated by assignment models. Route choice preferences are unknown, but they are estimated using route choice data. It is usually difficult to observe route choice behavior, and recently, passive monitoring with Global Positioning System (GPS) has been used in these decades. However, GPS data has measurement uncertainties, and probabilistic route measurement models have been developed. In this paper, we define the integrated framework of modeling route choices, evaluating network flow patterns, observing and estimating route choice models as the route choice analysis.

Route choice model is one of the most powerful framework of demand forecasting, because it can describe the sequence of choice behavior. It can identify not only a route between an origin-destination pair in a transportation network, but also multimodal routes including parking choice and activity paths in a time-space network, if we apply it to extended networks. However, since a route is a combination of links on a network, the number of alternative is often huge. For evaluating route choice probabilities based on route choice models, as is seen in Figure 1.2, the definition of the choice set \mathcal{C}_n is required, but it is a not trivial task. Consider simple grid networks with n links on each edge, the number of feasible paths of each network is shown in Table 1.1. Even in small networks, such as $n = 3$ or $n = 4$, the numbers of feasible paths are already 184 and 8,512. If n becomes larger, the number exponentially

TABLE 1.1: The number of simple paths in n-grid networks

n	simple paths
1	2
2	12
3	184
4	8,512
5	1,262,816
6	575,780,564
7	789,360,053,252
8	3,266,598,486,981,640
9	41,044,208,702,632,496,804
10	1,568,758,030,464,750,013,214,100
11	182,413,291,514,248,049,241,470,885,236
12	64,528,039,343,270,018,963,357,185,158,482,118
13	69,450,664,761,521,361,664,274,701,548,907,358,996,488
14	227,449,714,676,812,739,631,826,459,327,989,863,387,613,323,440
15	2,266,745,568,862,672,746,374,567,396,713,098,934,866,324,885,408,319,028

increases and becomes uncountable soon. A number of algorithms for generating the choice set have been proposed, and some method of sampling alternatives have been presented. However, they are not applicable to prediction yet, and moreover, the correct choice set is unknown especially in the case that cyclic paths or detour paths are considered, e.g., in pedestrian networks.

1.2.2 Markovian route choice analysis

For dealing with the problem that is discussed above, this thesis focuses on Markovian route choice analysis, which is based on Markovian route choice model. Markovian model is one of the most representative probability process models and has high operability. It was first applied to the traffic assignment model, and recently, it is linked to the framework of discrete choice model. The detailed review of Markovian route choice models is presented in Chapter 2. We show the framework of the current Markovian route choice analysis in Figure 1.3. The key point of the framework is that Markovian route choice models calculate node transition probabilities instead of route choice probabilities. Then, they do not require the choice set generation and can consider the set of all feasible paths, which is referred to as universal set \mathcal{U} , without path enumeration.

1.2.3 Scopes of the thesis

Markovian route choice analysis is high operable and gathers much attention recently; however, there are three main limitations that are addressed, which are shown as (a), (b) and (c) in Figure 1.3.

(a) Biases in estimating route choice model

First limitation is regarding data and estimation of route choice models. Despite the fact that Markovian route choice models do not require path enumeration for calculating route choice probabilities, most probabilistic route measurement models are still based on path-based and require the definition of the path set to evaluate the measurement probabilities of path candidates to observed data. For defining the path candidate set, the variance of GPS measurement error is often given as a constant value over network. However, in real cases, the value of the variance is

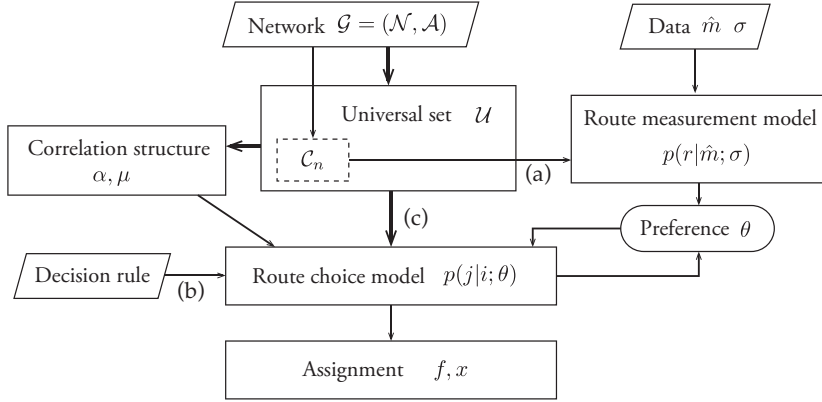


FIGURE 1.3: Framework of Markovian route choice analysis

unknown and heterogeneous over network. Since the measurement probabilities are dependent on the value of the variance, the variance that is given as arbitrary and constant over network can cause the biased measurement probabilities. As the result, the estimation of route choice model can be biased.

(b) Global optimal decision over network

Most of route choice models describe the global decision of a traveler, which means that he/she chooses the route between an origin-destination pair before departing from the origin (*pre-trip*). This is based on the assumption that travelers have information of the entire network and evaluate utilities of all links with the equivalent weight. Markovian route choice models that have been proposed so far are also based on this assumption, as the output of the models are proved to be equivalent to that of the *path-based* MNL model. However, this assumption may be strong in real cases, and it may be more realistic that travelers evaluate utilities of links close to them with larger weight than those of links distant from them. For instance, gridlock networks and pedestrian networks are typical cases. In high-congested networks, such as gridlock networks, travelers try to avoid congestions and make decisions at each intersection based on visible information. Pedestrians can also behave myopically, e.g., they react spacial attributes of walking space and unplanned activities are generated on the way of trips. For describing these behavior, existing models do not suit.

(c) Computational challenges regarding cyclic paths

Markovian route choice models use the expected maximum utility to the destination of each node to calculate transition probabilities that are equivalent to the MNL model with the universal set. However, in the case that networks have cyclic structures, the expected maximum utilities cannot always be solved. The condition of the solution is dependent on the balance between the network structure and the size of link utilities u_{ij} . More theoretically, the following equation has to be satisfied so that the Markovian route choice models has the solution:

$$\rho(\mathbf{W}) \equiv \max_h \{|\lambda_h|\} < 1, \quad (1.4)$$

where λ_h is the h -th eigenvalue of the incidence matrix \mathbf{W} defining link utilities, i.e., $w_{ij} = u_{ij}$, and $\rho(\mathbf{W})$ is known as the spectral radius. If the spectral radius is

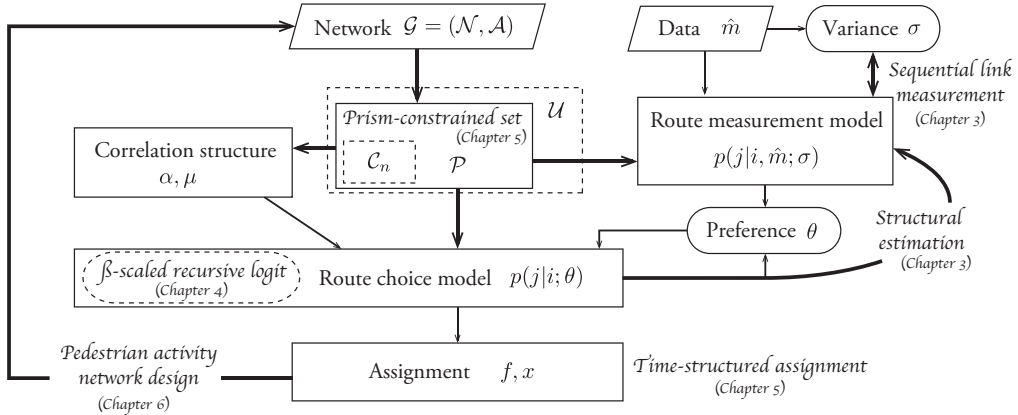


FIGURE 1.4: Contributions

larger or equal to one, the expected maximum utilities diverge and the transition probabilities of Markovian route choice models cannot be evaluated. As mentioned, this problem arises from the cyclic structures of the network. For example, if there is a cycle with positive utility, the expected utility of a route that passes the cycle again and again becomes large and finally diverges. Previous studies assume that the link utilities are always negative, $u_{ij} < 0, \forall(i, j)$; however, in the estimation process the computational instability remains, because parameters of route choice preferences vibrate and the link utilities can be larger or equal to zero. Moreover, $u_{ij} < 0$ means that we cannot consider link attributes that are possible to have positive effects to route choice behavior, such as the number of lanes, the attractiveness of shops along the street, the width of sidewalk, etc. In order to make Markovian route choice analysis more flexible and powerful tool, we have to deal with these computational challenges.

1.3 Contributions

We show the entire of contribution of the thesis in Figure 1.4. Our contributions can be divided into the main four topics: *Data and Estimation*, *Model formulation*, *Assignment algorithm*, and *Applications*, which are described as follows.

Data and Estimation

Our first contribution is regarding data and estimation of route choice models, which responds to problem (a) in the previous section. We propose an estimation framework for obtaining parameters of route choice models with less biases, using GPS data with measurement uncertainties. We focus on that the variance of GPS measurement errors is not uniform in high-resolution networks, and propose a *sequential link measurement model* based on the Bayesian approach. It enable us to estimate the variance as the specific value of each link, while the value is assumed as given and uniform over a network in previous works. Moreover, we introduce a *structural estimation method* in order to reduce the biases included in the uncertainty of prior information. We examine this approach through twins experiments, and apply to a real pedestrian network of Matsuyama-city, Japan.

Modeling

Secondly, we focus on that the sequential and somewhat forward-looking decisions in route choice behavior. This work is corresponding to the problem (b) in Section 1.2.3. We use the concept of time discount rate in the dynamic discrete choice models (e.g., Rust, 1987), and interpret it as a parameter describing a mechanism of route choice behavior. We propose a β -scaled recursive logit model as a generalized framework of the recursive logit (RL) model (Fosgerau, Frejinger, and Karlstrom, 2013) by incorporating the *sequential discount rate* into the RL model. We present illustrative examples which indicate the effect of the sequential discount rate on evaluating path probabilities, network patterns, and cyclic path selectivity. Moreover, we estimate the β -scaled RL model using taxi probe data in a disaster network of the Tokyo Metropolitan area.

Assignment algorithm

The third contribution is regarding the path set restriction. We focus on the fact that in real cases, it is very improbable that paths including infinite cycles are chosen by travelers. In order to describe this mechanism, we present a time-structured network, where travelers' states are decomposed by decision-making time period, and propose a method for restricting path sets based on the time-constraint. On this network, we model sequential link choice behavior of travelers based on Markovian route choice models. This idea is a solution of the three computational challenges of the assignment based on Markovian route choice model: unreasonable cyclic flows, computational instability (discussed in Section 1.2.3), and amplification of the IIA property, in reasonable time. We present several numerical examples to examine the model properties, and apply it to a stochastic user equilibrium (SUE) problem and a network-GEV based model.

Application

Finally, we apply the model and the algorithm to the description of pedestrian activity path choice behavior in city centers, for evaluating the continuity of moving and staying behavior of pedestrians in time-space networks. The activity assignment model can evaluate not only link flows but also duration time at each node integrally. The sequential discount rate and the time-constraint are important parameters for describing pedestrian activities. Moreover, we present a network design problem based on the activity assignment model. The problem is a multi-level and multi-objective programming, and the Pareto front solutions are investigated by a neighborhood search algorithm.

1.4 Outline of the thesis

This thesis consists of four main topics of which each topic has been presented in at least one international conference and is corresponding to one or two articles (see Appendix D). The outline is as follows.

- Chapter 2 reviews the literature. We present the state-of the-art of Markovian route choice analysis and discuss its challenges with some illustrative examples.
- Chapter 3 focuses on estimating route choice models using uncertain GPS data. We present a novel route measurement model and a estimation method to reduce biases in parameter estimation of route choice models. These methods are referred to as *sequential link measurement model* and *structural estimation method*.

- Chapter 4 focuses on modeling route choice behavior and deals with the problem regarding decision-making dynamics. We focus on that the utility evaluation is heterogeneous dependently on spatial relation, and propose a β -scaled recursive logit model.
- Chapter 5 focuses on the computational challenges of Markovian route choice models and the selectivity of cyclic paths. We introduce a novel network description referred to as *time-structured network*, and based on the network, we propose a method of the path set restriction.
- Chapter 6 applies the methods proposed in previous sections to pedestrian activities in time-space networks and extends it to the network design problem.
- Chapter 7 presents conclusions and future works.

Chapter 2

Literature review

In this chapter, we introduce the state-of-the-art studies of the route choice analysis. We focus on the route choice analysis in static and deterministic networks, not in dynamic and stochastic networks, where the link attributes are time-dependent and follow probability distributions (see Chapter 4 for this discussion). We first mention that Ben-Akiva and Lerman, 1985 introduced a comprehensive methodology of discrete choice analysis, and Bovy and Stern, 1990 presented an overview of route choice modeling through entire book. Ramming, 2001 and Frejinger, 2008 also presented comprehensive reviews of the route choice analysis. Regarding Markovian route choice models, which are discussed in Section 2.2, Mai, 2015 is also a helpful reference.

2.1 Route choice analysis

Consider a directed connected graph $\mathcal{G} = (\mathcal{N}, \mathcal{A})$ as a transportation network, where N is the set of nodes and A is the set of links. The route choice analysis deals with identifying which route a traveler takes to go from a node to another in the transportation network, and predicts the flows on the network. The route choice preferences are investigated using observed route choice data in real networks. In route choice analysis, a route is a combination of links; therefore, the route choice problem is often characterized by a large number of candidates in real road networks, and routes are spatially correlated with each other. These are the reason why the problem is complicated and is generally difficult to solve, and a number of studies have been presented in the transportation field.

2.1.1 Shortest path problem

The simplest description of a route choice model is the *shortest path problem* which assumes that a given traveler take a route with the minimum variable such as travel time or travel cost in a transport network. The problem is formulated as follows:

$$r = \arg \min_r \{c_r\}, \quad (2.1)$$

where r is a route in the network, which is described as a sequence of links

$$r = (a_1, \dots, a_j, \dots, a_J), \quad (2.2)$$

and c_r is the cost of route r . Naively, the number of paths is $|\mathcal{A}| \times |\mathcal{A}| \times \dots \times |\mathcal{A}| = |\mathcal{A}|^J$, which is often uncountable. Dijkstra's algorithm (Dijkstra, 1959) is a representative algorithm for solving shortest path problems in the case of single-source

problems with positive link costs. A shortest path problem is a simple and reasonable description; however, it is difficult to assume that the problem reflects the decisions of travelers, because travelers cannot necessarily get perfect information of a network and are heterogeneous with each other. Actually, shortest path problems are used in the process of evaluating network flows as *all-or-nothing* loading procedure, which is one of steps of the user equilibrium (UE) model. Therefore, in order to reflect individual decision making, the route choice problem is often described as a stochastic one based on the framework of the discrete choice analysis. In the following sections, we focus on the probabilistic route choice models and present their review.

2.1.2 Multinomial logit model

The (probabilistic) route choice model uses the framework of the discrete choice analysis, which is based on the random utility maximization (RUM) framework (McFadden, 1978; Ben-Akiva and Lerman, 1985), and it can be described as follows:

$$r = \arg \max_{r \in \mathcal{C}_n} \{\tilde{u}_{nr}\}, \quad (2.3)$$

where \tilde{u}_{nr} is the utility when individual n chooses route r , which is a stochastic variable, and it includes the unobserved attributes from the researchers. \mathcal{C}_n is the choice set of routes that individual n considers, and it is defined by the modeler. It is assumed that the utility of route r can be divided into the deterministic term u_{nr} and the error term ε_{nr} as

$$\tilde{u}_{nr} = u_{nr} + \varepsilon_{nr}. \quad (2.4)$$

The error term ε_{nr} captures the uncertainty of the model. The deterministic term includes attributes of the route such as the travel time, the distance and the number of crossings, as well as the socio-economic characteristics of the traveler. It is often described as a linear formulation $u_{nr} = u_{nr}(x_{nr}; \theta) = \sum_k \theta_k x_{nr,k}$, where x_{nr} is a vector of the attributes and θ is a vector of unknown coefficients to be estimated.

Route choice models evaluate the probability of paths that is included in the choice set. Equation 2.3 indicates that travelers are assumed to maximize their random utilities by choosing routes. That is, the probability that a traveler n chooses route r is formulated as follows:

$$P(r|\mathcal{C}_n) = \mathbb{P}[u_{nr} > u_{ns}; r \neq s, \forall s \in \mathcal{C}_n] = \mathbb{P}[u_{nr} + \varepsilon_{nr} > v_{ns} + \varepsilon_{ns}; r \neq s, \forall s \in \mathcal{C}_n], \quad (2.5)$$

then,

$$P(r|\mathcal{C}_n) = \mathbb{P}[\varepsilon_{nr} > u_{ns} - u_{nr} + \varepsilon_{ns}; r \neq s, \forall s \in \mathcal{C}_n]. \quad (2.6)$$

Defining the joint probability distribution function of the all error terms, $f(\varepsilon_{nr}; r \in \mathcal{C}_n)$, Equation (2.6) can be re-formulated as:

$$P(r|\mathcal{C}_n) = \int_{\varepsilon_{n1}=-\infty}^{+\infty} \int_{\varepsilon_{n2}=-\infty}^{u_{n1}-u_{n2}+\varepsilon_{n1}} \cdots \int_{\varepsilon_{n1}=-\infty}^{u_{n1}-u_{n|\mathcal{C}_n|}+\varepsilon_{n1}} f(\varepsilon_{nr}; r \in \mathcal{C}_n) d\varepsilon_{n|\mathcal{C}_n|} \cdots d\varepsilon_{n2} d\varepsilon_{n1}. \quad (2.7)$$

The joint distribution function $F(\varepsilon_{nr}; r \in \mathcal{C}_n)$ is given by the partial differential of Equation (2.7) by ε_{nr} :

$$F_r(\varepsilon_{nr}; r \in \mathcal{C}_n) = \frac{\partial F(\varepsilon_{nr}; r \in \mathcal{C}_n)}{\partial \varepsilon_{nr}} \quad (2.8)$$

The most representative model for describing the route choice probabilities is the multinomial logit (MNL) model. The MNL model assumes that the error term of the utility is independent and identically distributed (i.i.d) extreme value type I, and then the CDF and PDF are formulated as follows:

$$F(\varepsilon_{nr}) = \exp[-\exp(-\mu\varepsilon_{nr} - \eta)] \quad (2.9)$$

$$f(\varepsilon_{nr}) = \mu \exp[-\exp(-\mu\varepsilon_{nr} - \eta)] \cdot \exp(-\mu\varepsilon_{nr} - \eta) \quad (2.10)$$

where, μ is the positive scale parameter that means the degree of variation of ε_{nr} . η is the location parameter which means the mode of the distribution. In this case, the mean is $\eta + \gamma/\mu$, where γ is the Euler's constant, and the variance is $\pi^2/6\mu^2$. The MNL model is obtained by substituting Equation (2.9)(2.10) for Equation (2.7),

$$P(r|\mathcal{C}_n) = \frac{\exp(\mu u_{nr})}{\sum_{s \in \mathcal{C}_n} \exp(\mu u_{ns})}. \quad (2.11)$$

The MNL model introduce a fundamental framework for modeling route choice behavior; however, the MNL model cannot describe correlation structure among path alternatives due to its independence of irrelevant alternatives (IIA) property.

2.1.3 Description of correlation structures

Since routes in transportation networks are spatially correlated with each other, a number of route choice models for describing the correlation structures have been proposed.

The C-logit model (Cascetta et al., 1996) and the Path-Size logit (PSL) model (Ben-Akiva and Bierlaire, 1999) are the extended MNL models, which incorporate the commonality factors into the utility function of paths and describe the overlapping effect as the additional dis-utilities. Ramming, 2001 and Frejinger and Bierlaire, 2007 presented the alternatives of the Path Size correlation factors.

Another approach is developing the generalized extreme value (GEV) model, which is proposed by McFadden, 1978 and can describe the correlation structures among alternatives in the framework of the closed form expression. The cross nested logit (CNL) model (Vovsha and Bekhor, 1998), which is referred to as the link-nested logit (LNL) model, the paired combinatorial logit (PCL) model, and the generalized nested logit (GNL) model Bekhor and Prashker, 2001 have been proposed.

The multinomial probit (MNP) model, and the mixed logit (MXL) model, which is also referred to as the error component (EC) model, are also used for directly capturing the structure of variance-covariance among path alternatives by e.g., Bolduc and Ben-Akiva, 1991, Yai, Iwakura, and Morichi, 1997, Bekhor, Ben-Akiva, and Scott Ramming, 2002, and Frejinger and Bierlaire, 2007.

2.1.4 Path set generation algorithms

For the evaluation of the route choice probabilities using the route choice model, the choice set that traveler n considers, \mathcal{C}_n should be defined. However, as mentioned

in Chapter 1, the choice set of paths by traveler is unknown to the analyst. Also, the set of all possible paths, which is referred to as the universal choice set \mathcal{U} , cannot be enumerated, because paths are the combinations of links in transportation networks. For this reason, a number of algorithms for generating path set have been proposed so far. Regarding the comprehensive discussion of this topic, Bekhor, Ben-Akiva, and Ramming, 2006 reviews the path set generation algorithms and compares the estimation results of route choice models in large-scale urban networks from the view points of the selectivity of routes and computational times. Bovy, 2009 points out the difference of the choice set generation of route choice models from that of other discrete choice models and summarizes its characteristics.

In the context of route choice models, the master choice set by origin-destination pair $\mathcal{M} \subseteq \mathcal{U}$ is often first generated. Moreover, since the choice set is assumed to be individual-specific, the choice set defined by traveler $\mathcal{C}_n \subseteq \mathcal{M}$ should be generated. For the generation of \mathcal{M} and \mathcal{C}_n , the path generation algorithms are used. The *k-shortest path* algorithm (Eppstein, 1998), which enumerates the first k shortest paths from the origin to the destination, is one of the most well-known methods for generating the master choice set \mathcal{M} . The *link penalty* method (Barra, Perez, and Anez, 1993) and the *link elimination* method (Azevedo et al., 1993) are popular heuristics approaches, and they update the path set following their rules after identifying the shortest path. The *labeling* method (Ben-Akiva, Cyna, and Palma, 1984) extracts the optimal path for each link attribute, such as travel time, distance and generalized cost, and constructs the set of the optimal paths, which are labeled as "minimize time", "minimize distance", and so on. The *branch-and-bound* method (Friedrich, Hof-säß, and Wekeck, 2001; Prato and Bekhor, 2006) enumerates a tree, which consists of links, and restricts it by several constraints in terms of direction, travel time, detour, similarity, and turns. The *elimination by aspect* method (Tversky, 1972) restricts the master set \mathcal{M} into the choice set by traveler \mathcal{C}_n using several aspects of the alternatives. Frejinger, Bierlaire, and Ben-Akiva, 2009 propose a method for sampling alternatives, where the choice set by traveler \mathcal{C}_n is generated without the definition of the master set \mathcal{M} . Using the sampling probabilities of the alternatives, which are calculated based on a weighted random walk algorithm, the path probabilities are corrected.

2.1.5 Route choice observation

The more precious prediction of the route choice behavior requires its observation in real networks for investigating the route choice preferences of travelers. However, it is usually difficult to observe the route choice behavior by both conventional questionnaire surveys using mail or telephone and passive data collection from travelers who are equipped with the sensors with Global Positioning System (GPS). Since a route is a sequence of links in transportation networks, travelers often cannot answer the correct route that they take. Passive data based on GPS technology has several advantages over conventional surveys, because trip data is collected automatically. Moreover, in recent years, emerging technologies, such as probe vehicles and connected vehicles, contribute to facilitating a number of and real-time data collection. They are expected to develop extremely transportation studies. However, collected GPS data is usually characterized by coordinates in the two-dimensional surface; therefore, it is not corresponding in format to a network that the modeler uses for the route choice analysis. Moreover, GPS data often has localization error.

To deal with these problem, a number of methods for matching GPS dat to transportation networks, which are often referred to as *map matching* (MM) algorithms, have been proposed in these last few decades.

MM algorithms can be categorized into three groups: geometric (e.g., White, Bernstein, and Kornhauser, 2000), topological (e.g., Greenfeld, 2002; Quddus et al., 2003; Velaga, Quddus, and Bristow, 2009), and probabilistic (e.g., Ochieng, Quddus, and Noland, 2003; Quddus, Ochieng, and Noland, 2006; Hunter, Abbeel, and Bayen, 2014). Quddus, Ochieng, and Noland, 2007 comprehensively reviewed MM methods presented before early 2000s. Most of the algorithms are based on sequential link inferences, where the true location is inferred for each location data in chronological order, because they are aimed at applying on-line navigation systems. On the other hand, in transportation studies, researchers require the actual path as a sequence of links rather than on-line identification of the traveler locations (Bierlaire, Chen, and Newman, 2013).

Pyo, Shin, and Sung, 2001 and Bierlaire, Chen, and Newman, 2013 propose path-based and probabilistic MM algorithms, which evaluate the likelihoods of path candidates regarding all GPS data in a trip and do not identify to a specific path. Chen and Bierlaire, 2015 presents a MM algorithm that includes the transportation mode detection, for applying in multi-modal networks.

Recently, some studies proposed advanced methods based on bayesian approaches (Fuse and Nakanishi, 2012; Danalet, Farooq, and Bierlaire, 2014; Chen and Bierlaire, 2015). In bayesian approaches, the path likelihoods are evaluated by both measurement probabilities calculated by probabilistic MM algorithms and the path choice probabilities as the prior given by route choice models. Based on the path likelihoods, the paths are identified. The correction of the path likelihood using the path choice probabilities of route choice model is helpful of inferring paths in the case that the measurements have large uncertainties, e.g., when the localization is weak and the network is dense (Danalet, Farooq, and Bierlaire, 2014).

2.1.6 Maximum likelihood estimation

The parameter estimation of route choice models is generally implemented by the maximum likelihood estimation (MLE). The problem of estimating parameters is defined to maximize the following log-likelihood function:

$$\begin{aligned} \max_{\theta} LL(\theta) &= \log \left(\prod_{n=1}^N \prod_{r \in \mathcal{C}_n} P_n(r|\mathcal{C}_n; \theta)^{\delta_r^n} \right) \\ &= \sum_{n=1}^N \sum_{r \in \mathcal{C}_n} \delta_r^n \log P_n(r|\mathcal{C}_n; \theta) \end{aligned} \quad (2.12)$$

where δ_r^n equals one if an individual n chooses route r , which is defined from the route choice observation discussed in Section 2.1.5, and equals zero, otherwise. By solving this problem defined by Equation (2.12), we can investigate the route choice preferences of travelers.

2.1.7 Joint estimation of route choice models

Bierlaire and Freijinger, 2008 proposed a framework to estimate route choice models as the ambiguity of observations remains. In the framework, the following probability of reproducing the vector of observations \hat{m} is maximized to estimate parameters:

$$p(\hat{m}) = \sum_{r \in \mathcal{R}} p(\hat{m}|r; \sigma) p(r|\mathcal{R}; \theta), \quad (2.13)$$

where r is a route in choice set \mathcal{R} . $p(\hat{m}|r; \sigma)$ is the measurement equation, which gives the probability that \hat{m} is observed if r is the actual path, where σ is the parameter and often assumed as the variance of GPS measurement error. $p(r|\mathcal{R}; \theta)$ is the route choice model, which gives the probability that path r is selected within the choice set \mathcal{R} , where θ is the unknown parameters to be estimated. As is seen in Equation (2.13), the paths are regarded as latent variables, and a specific path is not identified. The measurement probabilities are calculated by e.g., path-based probabilistic MM algorithms. In evaluating the probabilities in Equation (2.13), similarly to route choice models, probabilistic models for route choice observations also suffer from the problem of the path set generation. Bierlaire and Freijinger, 2008 propose the concept of *domain of data relevance* (DDR) for restricting the set of observed path based on GPS localization errors. A path is included in the set of path candidates only if it is associated with the area of the sequence of data.

2.2 Markovian route choice analysis

Markovian model is one of the most fundamental and the most important stochastic processes, which has the Markov property. Consider a stochastic process $\{X_n; n = 0, 1, 2, \dots\}$ on a discrete state space \mathcal{S} , the Markov property can be expressed as follows:

$$\mathbb{P}(X_{n+1} = j | X_n = i, X_{n-1} = i_{n-1}, \dots, X_0 = i_0) = \mathbb{P}(X_{n+1} = j | X_n = i) \quad (2.14)$$

where $j, i, i_{n-1}, \dots, i_0 \in \mathcal{S}$ are the state variables. This means that the distribution of the future state is dependent on only the current state. If the stochastic process is time homogeneous, it is described using the transition probability matrix \mathbf{P} ($|\mathcal{S}| \times |\mathcal{S}|$), and Equation (2.14) is equal to an entry

$$\mathbb{P}(X_{n+1} = j | X_n = i) = p(j|i) \quad \forall n. \quad (2.15)$$

The transition probability satisfy

$$p(j|i) \geq 0, \quad \sum_{j \in \mathcal{S}} p(j|i) = 1. \quad (2.16)$$

Also, by the Chapman-Kolmogorov equation

$$p^{m+n}(j|i) = \sum_{k \in \mathcal{S}} p^m(k|i) p^n(j|k), \quad (2.17)$$

where $p^m(j|i)$ is the m -step transition probability, the following equation is established:

$$\mathbf{P}^n = \{p^n(j|i) | \forall i, j \in \mathcal{S}\}. \quad (2.18)$$

Therefore, if the transition probability matrix \mathbf{P} is obtained, the transition probabilities of any step can be calculated.

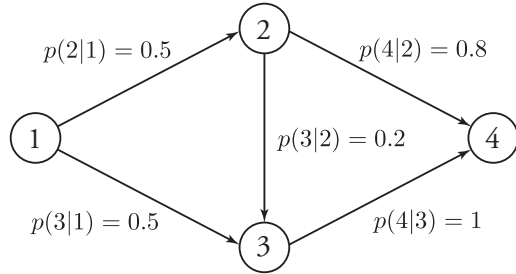


FIGURE 2.1: An example network defining transition probabilities

Markovian route choice models focus on that a path, which is a route in transportation network graphs, can be decomposed into the sequence of nodes (links), and they describe the flows or path choice probability using the state transition probabilities, where states correspond to nodes (links). For example, in the network with transition probabilities of Figure 2.1, the traffic flow departing from node 1, Q is assigned to the connecting links following the transition probabilities: $Q/2$ to link 12, and $Q/2$ to link 13. In the same way, the link flows x_{ij} are calculated as $x_{12} = Q/2$, $x_{13} = Q/2$, $x_{23} = Q/10$, $x_{24} = 2Q/5$, and $x_{34} = 3Q/5$. When we assume that the flow pattern has the Markov property, the flow conservation principle is hold at every node:

$$\sum_h x_{hi} - \sum_j x_{ij} = 0 \quad \forall i \in \mathcal{N}, \quad (2.19)$$

where we use Q instead of $\sum_h x_{hi}$ at the origin and instead of $\sum_j x_{ij}$ at the destination. As the result, the relationship between the transition probabilities and the link flows can be expressed as follows,

$$p(j|i) = \frac{x_{ij}}{\sum_{j'} x_{ij'}} \quad \forall (i, j) \in \mathcal{A}, \quad (2.20)$$

and using Equation (2.18), the path probability is given as the product of the transition probabilities:

$$\mathbb{P}(r = [i_0, \dots, i_J]) = \prod_{j=0}^{J-1} p(i_{j+1}|i_j). \quad (2.21)$$

With the advantage of this property, Markovian approaches have been developed as a alternative of Dial's algorithm for the logit-type network assignment, which can consider all possible paths including cyclic ones. It also has a high operability, because it is based on matrix representations, and recently, many models have been presented in the context of route choice analysis. We present an overview of the Markovian models in the route choice problem, which is summarized in Figure 2.2. In this section, we review the Markovian models for route choice analysis.

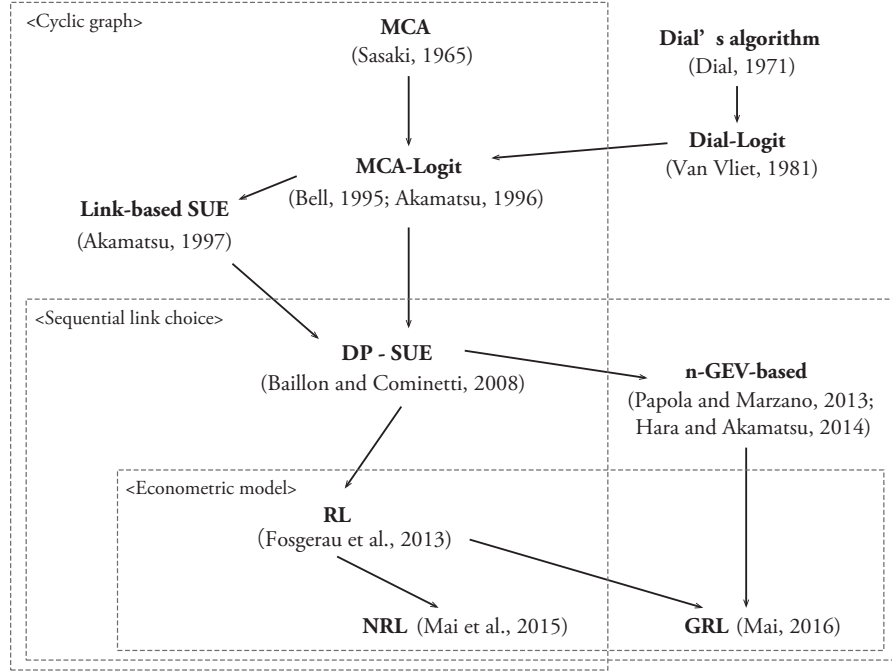


FIGURE 2.2: Overview of Markovian models in the route choice context

2.2.1 Dial's algorithm

We start to review the Dial's algorithm (Dial, 1971), which is one of the most popular procedures for the calculation of a logit-type route choice model in the traffic assignment context. Dial's algorithm is described as follows:

Step 1: Preliminaries. Calculating the shortest path cost from nodes o to i , $r(i)$, $\forall i \in \mathcal{N}$ and that from nodes i to d , $s(i)$, $\forall i \in \mathcal{N}$. Defining the *link likelihood* l_{ij} for each link as follows:

$$l_{ij} = \begin{cases} \exp[\mu\{r(j) - r(i) - c_{ij}\}], & \text{if } r(i) < r(j), s(i) > s(j) \\ 0, & \text{otherwise} \end{cases} \quad (2.22)$$

where c_{ij} is the cost of link (i, j) . The link likelihood always takes the value between zero and one.

Step 2: Forward pass. Calculating *link weight* w_{ij} for each link in ascending sequence with respect to $r(i)$,

$$w_{ij} = \begin{cases} l_{ij}, & \text{if } i = o \\ l_{ij} \sum_h w_{hi}, & \text{otherwise.} \end{cases} \quad (2.23)$$

When the destination node d is reached, go to Step 3.

Step 3: Backward pass. Assigning a flow x_{ij} in descending sequence with respect to $r(i)$, which is starting with the destination node d ,

$$x_{ij} = \begin{cases} q_{od} \frac{w_{ij}}{\sum_h w_{hj}}, & \text{if } j = d \\ (\sum_k x_{jk}) \frac{w_{ij}}{\sum_h w_{hj}}, & \text{otherwise.} \end{cases} \quad (2.24)$$

Equation (2.22) means that Dial's algorithm considers only paths that never include any move which goes away from the destination in terms of travel time, which are referred to *efficient paths*.

This algorithm is proven to be equivalent to the logit-type assignment model by Van Vliet, 1981.

Proof. In Dial's algorithm, based on the procedure of Equation (2.24), the choice probability of route $r = [o, i_1, i_2, \dots, i_J, d]$ can be given as

$$P_r = \frac{w_{i_J d}}{\sum_h w_{hd}} \frac{w_{i_{J-1} i_J}}{\sum_h w_{hi_J}} \dots \frac{w_{i_1 i_2}}{\sum_h w_{hi_2}} \frac{w_{o i_1}}{\sum_h w_{hi_1}}. \quad (2.25)$$

By the definition of the link weights, $w_{ij} = l_{ij} \sum_h w_{hi}$, Equation (2.25) is transformed as

$$P_r = l_{i_J d} l_{i_{J-1} i_J} \dots l_{i_1 i_2} l_{o i_1} \Big/ \sum_h w_{hd}, \quad (2.26)$$

and, moreover, by the definition of the link likelihood, the numerator of the right side of Equation (2.26) is

$$\begin{aligned} & l_{i_J d} l_{i_{J-1} i_J} \dots l_{i_1 i_2} l_{o i_1} \\ &= e^{\mu\{r(d)-r(i_J)-c_{i_J d}\}} e^{\mu\{r(i_J)-r(i_{J-1})-c_{i_{J-1} i_J}\}} \dots e^{\mu\{r(i_2)-r(i_1)-c_{i_1 i_2}\}} e^{\mu\{r(i_1)-r(o)-c_{o i_1}\}} \\ &= e^{\mu\{r(d)-\sum_{ij \in r} c_{ij}\}} \\ &= e^{\mu\{r(d)-c_r\}}, \end{aligned} \quad (2.27)$$

where c_r is the cost of path r . By the flow conservation principle,

$$\sum_r P_r = \sum_r \frac{e^{\mu\{r(d)-c_r\}}}{\sum_h w_{hd}} = \sum_r \frac{e^{\mu\{r(d)-c_r\}}}{\sum_h w_{hd}} = \frac{e^{\mu\{r(d)\}}}{\sum_h w_{hd}} \sum_r e^{-\mu c_r} = 1, \quad (2.28)$$

finally, we obtain the following expression by substituting Equation (2.27) and (2.28) for Equation (2.26),

$$P_r = \frac{e^{-\mu c_r}}{\sum_{r'} e^{-\mu c_{r'}}}. \quad (2.29)$$

This is the probability of the logit-type route choice model. ■

Dial's algorithm is equivalent to the Logit-type assignment model without requirement of the path enumeration, and it has an advantage in that it can be easily applied to a large scale network. However, the algorithm sometimes produces an unrealistic flow pattern due to restricting the path set to the set of *efficient paths*, e.g., no flow is loaded on paths that are often used by travelers in reality. Moreover, the stochastic user equilibrium using Dial's algorithm does not converge to the exact solution because the set of *efficient paths* can change dependently on link flows at each iteration. Leurent, 1997 proposed a solution of the latter problem; however, it also can generate unreasonable flow patterns and cannot consider cyclic paths.

2.2.2 Markov chain assignment

Sasaki, 1965 is the first to propose a method for traffic assignment based on a Markovian model, which is described as follows. Consider a directed connected graph

$\mathcal{G} = (\mathcal{N}, \mathcal{A})$, where \mathcal{N} is the set of nodes and \mathcal{A} is the set of links. \mathcal{N} contains the set of origins $\mathcal{O} \subseteq \mathcal{N}$ and the set of destinations $\mathcal{D} \subseteq \mathcal{N}$. The number of nodes included in each set is $|\mathcal{N}| = n$, $|\mathcal{O}| = n_o$ and $|\mathcal{D}| = n_d$. We assume that the nodes correspond to the states in Markovian model, and travelers repeat the transition from one node to another until they arrive at their destinations. The MCA uses the matrix of transition probabilities as follows:

$$\mathbf{P} = \begin{pmatrix} \mathbf{I} & \mathbf{0} & \mathbf{0} \\ \mathbf{0} & \mathbf{0} & \mathbf{Q}_1 \\ \mathbf{R} & \mathbf{0} & \mathbf{Q}_2 \end{pmatrix} \begin{matrix} n_d \\ n_o \\ n - n_o - n_d \end{matrix} \quad (2.30)$$

$$\begin{matrix} n_d & n_o & n - n_o - n_d \end{matrix}$$

where \mathbf{I} ($n_d \times n_d$) is the identity matrix, \mathbf{Q}_1 and \mathbf{Q}_2 are the matrices of transition probabilities to nodes that are not included in \mathcal{O} or \mathcal{D} (transient nodes), from origins and from transient nodes, respectively. \mathbf{R} is the matrix of transition probabilities from transient nodes to destinations. In Markovian model, the probability that a traveler at the initial state i takes the state j through k -step is given as the (i, j) element of the matrix \mathbf{Q}^n . Considering all number of steps, the total probability of the transition probabilities from i to j is given as follows (assuming both of two nodes are the transient nodes):

$$\mathbf{I} + \mathbf{Q}_2 + \mathbf{Q}_2^2 + \dots = (\mathbf{I} - \mathbf{Q}_2)^{-1}, \quad (2.31)$$

where $(\mathbf{I} - \mathbf{Q}_2)^{-1}$ is the inverse matrix of $(\mathbf{I} - \mathbf{Q}_2)$, and we can get this inverse matrix only if the matrix \mathbf{Q}_2 is a convergence matrix. Because the first step of transition is necessarily from origin, the matrix of node choice probabilities by origin is given as $\mathbf{Q}_1(\mathbf{I} - \mathbf{Q}_2)^{-1}$. Using this node choice probability $P(i)$ and the transition probability $p(j|i)$, which is the element of \mathbf{P} , the link choice probability by origin is given as,

$$p_{ij}^o = P^o(i) \cdot p(j|i) \quad \forall(i, j) \in \mathcal{A}, \forall o \in \mathcal{O}. \quad (2.32)$$

Therefore, the flow of link (i, j) x_{ij} is:

$$x_{ij} = \sum_{o \in \mathcal{O}} p_{ij}^o q_o = \sum_{o \in \mathcal{O}} (P^o(i) p(j|i) \sum_{d \in \mathcal{D}} q_{od}) \quad \forall(i, j) \in \mathcal{A}. \quad (2.33)$$

where q_{od} is the OD flow and q_o is the total flow that departs from the origin o .

2.2.3 Proof of equivalence to the logit model

In MCA of Sasaki, 1965, it is difficult to define the transition probabilities, and they have been assumed to be estimated based on observed link flows. In that case, MCA does not based on any behavioral mechanism. Akamatsu, 1996 is the first to give MCA the behavioral interpretation theoretically by proving that MCA is equivalent to the Logit-type assignment model.

Proof. Akamatsu, 1996 defines the transition probability from nodes i to j $p(j|i)$ as follows:

$$p^d(j|i) \equiv \exp[-\mu(c_{ij} + \varphi_{jd} - \varphi_{id})] = \exp(-\mu c_{ij}) \frac{v_{jd}}{v_{id}} \quad \forall(i, j) \in \mathcal{A}, \forall d \in \mathcal{D}. \quad (2.34)$$

where,

$$v_{id} \equiv \sum_{r \in \mathcal{R}^{id}} \exp(-\mu c_r^{id}) \quad \forall i \in \mathcal{N}, \forall d \in \mathcal{D}, \quad (2.35)$$

$$\varphi_{id} \equiv -\frac{1}{\mu} \log \sum_{r \in \mathcal{R}^{id}} \exp(-\mu c_r^{id}) = -\frac{1}{\mu} \log v_{id} \quad \forall i \in \mathcal{N}, \forall d \in \mathcal{D}, \quad (2.36)$$

μ is the scale parameter of i.i.d. extreme value type I, c_{ij} is the cost of link (i, j) , and c_r^{id} is the cost of route r from nodes i to d . In MCA, a path is a sequence of nodes; therefore, the path choice probability is formulated as the product of transition probabilities as follows:

$$P_r^{od} = \prod_{(i,j) \in r} p(j|i) \quad \forall r \in \mathcal{R}^{od}, \forall o \in \mathcal{O}, \forall d \in \mathcal{D}, \quad (2.37)$$

where P_r^{od} is the probability that one chooses the route r in order to travel from nodes o to d . By substituting Equation (2.34) and (2.35), Equation (2.50) can be re-expressed as follows:

$$\begin{aligned} P_r^{od} &= \prod_{ij \in r} \exp(-\mu c_{ij}) \frac{v_{jd}}{v_{id}} \\ &= \exp\left(\sum_{ij \in r} -\mu c_{ij}\right) \cdot \exp\left(\sum_{ij \in r} \log \frac{v_{jd}}{v_{id}}\right) \\ &= \exp(-\mu c_r^{od}) \cdot \exp(\log v_{dd} - \log v_{od}) \\ &= \frac{\exp(-\mu c_r^{od})}{\sum_{r \in \mathcal{R}^{od}} \exp(-\mu c_r^{od})} \end{aligned} \quad (2.38)$$

where c_r^{od} is the cost of route r that travels from nodes o to d . This is the formulation of multinomial logit model. ■

Note that we have to calculate v_{id} by solving Equation (2.35) in order to evaluate the transition probabilities; however, since the equation contains the sum of variables related to infinite paths, it is impossible to calculate it naively. Bell, 1995 and Akamatsu, 1996 proposed efficient methods for the evaluation, and Akamatsu, 1996's method is described here as follows. Consider a matrix \mathbf{W} ($n \times n$) with entries

$$w_{ij} = \begin{cases} \exp(-\mu c_{ij}), & (i, j) \in \mathcal{A}, \\ 1, & \text{otherwise.} \end{cases} \quad (2.39)$$

Based on this matrix, the element of the matrix \mathbf{W}^m ($n \times n$) is given as follows:

$$w_{ij}^{[m]} = \sum_{k \in \mathcal{K}_m^{ij}} \exp(-\mu c_{k,m}^{ij}) \quad (2.40)$$

where \mathcal{K}_m^{ij} is the set of paths that connect nodes i and j by passing through m links and $c_{k,m}^{ij}$ is the cost of the k -th path belonging to \mathcal{K}_m^{ij} . Therefore, the matrix \mathbf{V} ($n \times n$), which has entries $v_{ij} = \sum_{r \in \mathcal{R}^{ij}} \exp(-\mu c_r^{ij})$, is given as

$$\mathbf{V} = \mathbf{W} + \mathbf{W}^2 + \mathbf{W}^3 + \dots = (\mathbf{I} - \mathbf{W})^{-1} - \mathbf{I}. \quad (2.41)$$

If the matrix \mathbf{W} is a convergence matrix, Equation (2.41) has the solution and the transition probabilities in Equation (2.34) can be evaluated.

2.2.4 Stochastic user equilibrium based on Markovian model

The Markovian models are based on link choice probabilities $p(j|i)$, while the traditional traffic assignment models deal with path choice probabilities. One of the most popular frameworks for the stochastic traffic assignment is Fisk's formulation (Fisk, 1980), which is the optimization model equivalent to the Logit-type stochastic user equilibrium of Daganzo and Sheffi, 1977, and it is formulated as follows:

$$\min .Z(\mathbf{x}(\mathbf{f})) = \sum_{a \in \mathcal{A}} \int_0^{x_a} t_a(\omega) d\omega - \frac{1}{\mu} \sum_{o \in \mathcal{O}} \sum_{d \in \mathcal{D}} HP(\mathbf{f}^{od}), \quad (2.42)$$

where,

$$HP(\mathbf{f}^{od}) = - \sum_{r \in \mathcal{R}^{od}} f_r^{od} \log \frac{f_r^{od}}{q_{od}} \quad (2.43)$$

subject to,

$$x_a = \sum_{o \in \mathcal{O}} \sum_{d \in \mathcal{D}} \sum_{r \in \mathcal{R}^{od}} \delta_{a,r}^{od} f_r^{od}, \quad \forall a \in \mathcal{A}, \quad (2.44)$$

$$\sum_{r \in \mathcal{R}^{od}} f_r^{od} = q_{od}, \quad \forall o \in \mathcal{O}, \forall d \in \mathcal{D}, \quad (2.45)$$

$$f_r^{od} \geq 0 \quad \forall o \in \mathcal{O}, \forall d \in \mathcal{D}, \forall r \in \mathcal{R}^{od}, \quad (2.46)$$

$$x_a \geq 0, \quad \forall a \in \mathcal{A}. \quad (2.47)$$

This is a formulation that adds the entropy term to the Beckman's formulation Beckmann, McGuire, and Winsten, 1956. As seen in Equation (2.42), the entropy term is calculated based on the path flows. Akamatsu, 1997 proposed a method of decomposing the entropy term into the function defined by link flows, which is consistent with the Logit-type Markovian route choice models, such as Dial, 1971 and Akamatsu, 1996. The entropy function based on link flows is developed as follows. The relationship between path probabilities and path flows is

$$P_r^{od} = \frac{f_r^{od}}{q_{od}}, \quad \forall o \in \mathcal{O}, \forall d \in \mathcal{D}, \forall r \in \mathcal{R}^{od}, \quad (2.48)$$

and that between path flows and link flows is

$$x_{ij}^{od} = \sum_{r \in \mathcal{R}^{od}} f_r^{od}, \quad \forall o \in \mathcal{O}, \forall d \in \mathcal{D}, \forall (i,j) \in \mathcal{A}. \quad (2.49)$$

Moreover, the path choice probabilities that satisfy the Markov property can be decomposed into the link choice probabilities $p(j|i)$,

$$P_r^{od} = \prod_{ij \in \mathcal{A}} p^{od}(j|i)^{\delta_{ij,r}^{od}} \quad \forall o \in \mathcal{O}, \forall d \in \mathcal{D}, \forall r \in \mathcal{R}. \quad (2.50)$$

where,

$$p^{od}(j|i) = \frac{x_{ij}^{od}}{\sum_h x_{hj}^{od}} \quad \forall o \in \mathcal{O}, \forall d \in \mathcal{D}, \forall (i,j) \in \mathcal{A}. \quad (2.51)$$

Using these relationships, the entropy term $HP(\mathbf{f}^{od})$, which is defined by the path flow in Equation (2.42), can be decomposed into as follows:

$$\begin{aligned}
HP(\mathbf{f}^{od}) &= - \sum_{r \in \mathcal{R}^{od}} f_r^{od} \log \frac{f_r^{od}}{q_{od}} \\
&= - \sum_{r \in \mathcal{R}^{od}} f_r^{od} \log P_r^{od} \\
&= - \sum_{r \in \mathcal{R}^{od}} f_r^{od} \log \left[\prod_{ij \in \mathcal{A}} p(j|i)^{\delta_{ij,r}} \right] \\
&= - \sum_{r \in \mathcal{R}^{od}} f_r^{od} \sum_{ij \in \mathcal{A}} \delta_{ij,r} \log p(j|i) \\
&= - \sum_{ij \in \mathcal{A}} \left(\sum_{r \in \mathcal{R}^{od}} f_r^{od} \delta_{ij,r} \right) \log p(j|i) \\
&= - \sum_{ij \in \mathcal{A}} x_{ij}^{od} \log \frac{x_{ij}^{od}}{\sum_h x_{hj}^{od}} \\
&= - \sum_{ij \in \mathcal{A}} x_{ij}^{od} \log x_{ij}^{od} + \sum_j \left(\sum_i x_{ij}^{od} \right) \log \left(\sum_i x_{ij}^{od} \right)
\end{aligned} \tag{2.52}$$

Furthermore, Akamatsu, 1997 showed that it can be replaced to a more compact one, where the unknown variables are not the link flows by OD pair, \mathbf{x}^{od} , but the link flows by origin, \mathbf{x}^o . As shown in Dial, 1971, the proportion of flows at each is replaced as follows:

$$\frac{x_{ij}^{od}}{\sum_h x_{hj}^{od}} = \frac{x_{ij}^o}{\sum_h x_{hj}^o}, \quad \forall o \in \mathcal{O}, \forall d \in \mathcal{D}, i \neq d \tag{2.53}$$

where,

$$x_{ij}^o = \sum_{d \in \mathcal{D}} x_{ij}^{od}, \quad \forall o \in \mathcal{O}, \forall (i, j) \in \mathcal{A} \tag{2.54}$$

Using Equation (2.53) and (2.55), the entropy function can be replaced to one defined by the link flows by origin,

$$\begin{aligned}
\sum_{o \in \mathcal{O}} \sum_{d \in \mathcal{D}} HP(\mathbf{f}^{od}) &= - \sum_{o \in \mathcal{O}} \sum_{d \in \mathcal{D}} \sum_{ij \in \mathcal{A}} x_{ij}^{od} \log \frac{x_{ij}^{od}}{\sum_h x_{hj}^{od}} \\
&= - \sum_{o \in \mathcal{O}} \left\{ \sum_{ij \in \mathcal{A}} x_{ij}^o \log \frac{x_{ij}^o}{\sum_h x_{hj}^o} \right\} \\
&= - \sum_{o \in \mathcal{O}} \left\{ \sum_{ij \in \mathcal{A}} x_{ij}^o \log x_{ij}^o + \sum_j \left(\sum_i x_{ij}^{od} \right) \log \left(\sum_i x_{ij}^o \right) \right\}
\end{aligned} \tag{2.55}$$

Therefore, the SUE formulation (Equation 2.42) can be replaced into one defined by only the link flows as follows:

$$\min .Z(\mathbf{x}) = \sum_{a \in \mathcal{A}} \int_0^{x_{ij}} t_{ij}(\omega) d\omega - \frac{1}{\mu} \sum_{o \in \mathcal{O}} \{ HL(\mathbf{x}^o) - HN(\mathbf{x}^o) \}, \tag{2.56}$$

where,

$$HL(\mathbf{x}^o) \equiv - \sum_{ij \in \mathcal{A}} x_{ij}^o \log x_{ij}^o \quad (2.57)$$

$$HN(\mathbf{x}^o) \equiv - \sum_j \left(\sum_i x_{ij}^{od} \right) \log \left(\sum_i x_{ij}^o \right) \quad (2.58)$$

subject to,

$$\sum_h x_{hi}^o - \sum_j x_{ij} + \sum_d q_{od} \delta_{oi} - q_{od} \delta_{di} = 0 \quad \forall o \in \mathcal{O}, \forall i \in \mathcal{N}, \quad (2.59)$$

$$x_{ij} = \sum_{o \in \mathcal{O}} x_{ij}^o, \quad \forall (i, j) \in \mathcal{A}, \quad (2.60)$$

$$x_{ij}^o \geq 0, \quad \forall o \in \mathcal{O}, \forall (i, j) \in \mathcal{A}. \quad (2.61)$$

In the same way, the entropy function with only the link flows by destination, \mathbf{x}^d , can be defined. This work has been extended to the formulation with state specific scale parameters in Baillon and Cominetti, 2008.

2.2.5 Sequential link choice model

As seen in Equation (2.36), φ_{id} is the expected minimum cost from nodes i to d when the error term of link costs is i.i.d. extreme value type I with the scale parameter μ . Therefore, φ is formulated as the dynamic programming (Bellman, 1957):

$$\varphi_{id} = \mathbb{E} \left[\min_{j \in \mathcal{N}_i^+} (\tilde{c}_{ij} + \varphi_{jd}) \right] \quad \forall i \in \mathcal{N}, \forall d \in \mathcal{D}. \quad (2.62)$$

where,

$$\tilde{c}_{ij} \equiv c_{ij} + \varepsilon_{ij} \quad \forall (i, j) \in \mathcal{A}, \quad (2.63)$$

\mathcal{N}_i^+ is the set of nodes that is directly connected with node i by a link, and ε_{ij} is the error term of the link cost and i.i.d. extreme value type I. Gentile and Papola, 2006 and Baillon and Cominetti, 2008 clearly mentioned that route choice is not an issue to be solved once and for all at the origin of each trip, but instead it is considered as the outcome of sequential choices of links at every intermediate node. In the case of a logit Markovian model, the expected minimum cost in Equation (2.62) is formulated as a logsum:

$$\varphi_{id} = -\frac{1}{\mu_{id}} \log \sum_{j \in \mathcal{N}_i^+} \exp[-\mu_{id}(c_{ij} + \varphi_{jd})] \quad \forall i \in \mathcal{N}, \forall d \in \mathcal{D}, \quad (2.64)$$

where μ_{id} is the state-specific scale parameter in general discrete choice schemes (Gentile and Papola, 2006; Baillon and Cominetti, 2008). It is equivalent to Equation (2.36) when $\mu_{id} = \mu, \forall i \in \mathcal{N}$. In that case, the transition probability from nodes i to j is given as follows:

$$p^d(j|i) = \frac{\partial \varphi_{id}}{\partial c_{ij}}(\mathbf{c}) = \frac{\exp[-\mu_{id}(c_{ij} + \varphi_{jd})]}{\sum_{j' \in \mathcal{N}_i^+} \exp[-\mu_{id}(c_{ij'} + \varphi_{jd})]} \quad \forall (i, j) \in \mathcal{A}, \forall d \in \mathcal{D}, \quad (2.65)$$

where the fact that the change rate of the expected minimum cost to each cost corresponds to the choice probability is proved in e.g., Baillon and Cominetti, 2008.

Equation (2.65) is a well-known multinomial logit model; therefore, we can get the interpretation of the transition probability as the choice probability of a link at each node. It indicates that a traveler at node i chooses a link (i, j) that minimizes the sum of the link cost c_{ij} and the expected minimum cost from the sink node of the link j to the destination node d , φ_{jd} .

2.2.6 Description of correlation structures

The logit-type route choice models suffer from the IIA (*Independence from Irrelevant Alternatives*) property of the logit model and can assign excessive probabilities to paths that overlap each other. Daganzo and Sheffi, 1977 proposed a probit-based network loading algorithm without the path enumeration to solve the overlapping problem, but it requires heavy computational burden and the application to break networks is difficult. On the other hand, in recent, a route choice model that is based on the network-GEV model (Bierlaire, 2002; Daly and Bierlaire, 2006) have been proposed by Papola and Marzano, 2013, Hara and Akamatsu, 2014, and Mai, 2016. Ma and Fukuda, 2015 applied the model to a hyperpath-based model to analyze route choice behavior under uncertainties. The network-GEV based route choice model can consider the correlation structure among paths without enumerating paths, by assuming the structure of a road network as that of a GEV network, where an intersection corresponds to a state node.

The network-GEV based route choice model is developed as follows. Daly and Bierlaire, 2006 showed that the GEV network, which is proposed in the paper and represents the correlation structure among alternatives, can always generate RUM-based discrete choice models if the network satisfies that 1) it has a unique root and 2) has no cyclic structure in it. In the GEV network $(\mathcal{S}, \mathcal{E})$, where \mathcal{S} is the set of nodes and \mathcal{E} is the set of arcs, every node i has the specific GEV function G^i . The relationship between the GEV function of node i G^i and that of the successive node j G^j is described as follows:

$$G^i(y) = \sum_{j \in \mathcal{S}_i} \alpha_{ji} G^j(y)^{\mu_i / \mu_j}, \quad (2.66)$$

and the choice probability of node j conditional on node i is

$$p(j|i) = \frac{\alpha_{ji} G^j(y)^{\mu_i / \mu_j}}{\sum_{j' \in \mathcal{S}_i} \alpha_{j'i} G^{j'}(y)^{\mu_i / \mu_{j'}}}, \quad (2.67)$$

where \mathcal{S}_i is the set of the successive nodes of node i , the allocation parameter α_{ji} and the scale parameter μ_i are strictly positive. In the GEV network, the set of nodes with no successor represents the choice set \mathcal{C} and all other nodes represent nests. The expected maximum utility corresponding to each G^i is given as:

$$\begin{aligned} \bar{U}_i &= \mathbb{E} \left[\max_{r \in \mathcal{C}} (u_k + \varepsilon_r^i - \frac{\gamma}{\mu_i}) \right] \\ &= \int_{-\infty}^{\infty} \max_{r \in \mathcal{C}} (u_k + \varepsilon_r^i - \frac{\gamma}{\mu_i}) f(\varepsilon) d\varepsilon \\ &= \frac{\log G^i(y)}{\mu_i}, \end{aligned} \quad (2.68)$$

where γ is the Euler's constant and the error utility component ϵ_r^i follows the distribution $F(\epsilon_1^i, \dots, \epsilon_r^i) = \exp[-G^i(\exp(-\epsilon_1^i), \dots, \exp(\epsilon_r^i))]$. Using Equation (2.67), the relationship between the expected maximum utility of node i \bar{U}_i and that of its successive node j \bar{U}_j is expressed as a recursive form:

$$\bar{U}_i = \begin{cases} \frac{1}{\mu_i} \log \sum_{j \in \mathcal{S}_i} \alpha_{ji} e^{\mu_i \bar{U}_j} & \forall i \notin \mathcal{C} \\ 0 & \forall i \in \mathcal{C} \end{cases} \quad (2.69)$$

More detailed development of the formulas is seen in McFadden, 1978 and Daly and Bierlaire, 2006.

Hara and Akamatsu, 2014 uses the GEV network to describe the sequential link choice behavior in a road network. In the context of route choice model, each intermediate arc $(i, j) \in \mathcal{E}$ has the attribute corresponding to the link cost $-c_{ij}$; therefore, the expected maximum utility is defined as link specific value as follows:

$$\bar{U}_{ij} = -(c_{ij} + \varphi_j^d), \quad (2.70)$$

where φ_j^d is the expected minimum cost from node j to the destination. Also, the choice probability of node j conditional on node i is:

$$\begin{aligned} p(j|i) &= \frac{\alpha_{ji} G^{ij}(y)^{\mu_i/\mu_j}}{\sum_{j' \in \mathcal{S}_i} \alpha_{j'i} G^{ij}(y)^{\mu_i/\mu_{j'}}} \\ &= \frac{\alpha_{ji} \exp[-\mu_i(c_{ij} + \varphi_j^d)]}{\sum_{j' \in \mathcal{S}_i} \alpha_{j'i} \exp[-\mu_i(c_{ij'} + \varphi_{j'}^d)]}, \end{aligned} \quad (2.71)$$

where

$$G^{ij}(y) = \exp(\mu_j \bar{U}_{ij}) \quad (2.72)$$

The probability of path $r = [i_0, \dots, i_J]$ is given as the product of the link choice probabilities. The relationship between the expected minimum cost of node i φ_i^d and that of its successive node j φ_j^d is expressed using Equation (2.69),

$$\begin{aligned} \varphi_i^d &= \frac{1}{\mu_i} \log \sum_{j \in \mathcal{S}_i} \alpha_{ji} e^{\mu_i \bar{U}_{ij}} \\ &= \frac{1}{\mu_i} \log \sum_{j \in \mathcal{S}_i} \alpha_{ji} \exp[-\mu_i(c_{ij} + \varphi_j^d)]. \end{aligned} \quad (2.73)$$

In the case that $\mu_i = \mu, \forall i \in \mathcal{S}$ and $\alpha_{ji} = 1, \forall (i, j) \in \mathcal{E}$, the expected minimum utility from the origin o to the destination d is

$$\varphi_o^d = \frac{1}{\mu} \log \sum_{r \in \mathcal{R}^{od}} \exp \left(-\mu \sum_{ij \in r} c_{ij} \right) = \frac{1}{\mu} \log \sum_{r \in \mathcal{R}^{od}} \exp(-\mu c_r). \quad (2.74)$$

This corresponds to the well-known expected minimum cost of the logit-type Markovian route choice model. For this reason, the network-GEV based route choice model can be considered as a generalized form of the Markovian route choice model.

2.2.7 Recursive logit model

Fosgerau, Freijinger, and Karlstrom, 2013 is the first to deal with the sequential link choice model in the context of economic discrete choice models, based on a dynamic discrete choice model (Rust, 1987). We first review the dynamic discrete choice model (DDCM), and we then present the formulation of the recursive logit (RL) model proposed by Fosgerau, Freijinger, and Karlstrom, 2013.

Rust, 1987 proposed a DDCM, which is also referred to as dynamic programming conditional logit model. Aguirregabiria and Mira, 2010 presented a comprehensive review of DDCMs. In DDCMs, an individual at every time period t observes the vector of state variables s_t and chooses the alternative a_t that maximizes the *discounted* expected utility (Samuelson, 1937):

$$\mathbb{E} \left(\sum_{j=t}^T \beta^{j-t} \tilde{u}(a_j, s_j) | a_t, s_t \right), \quad (2.75)$$

where $\beta \in (0, 1)$ is the discount factor and $\tilde{u}(a_t, s_t)$ is the utility function at period t . T is the terminal period of the decisions. This is the dynamic programming (DP) problem of the individual. By the Bellman's principle of optimality (Bellman, 1957), the value function can be expressed as the recursive expression:

$$V(s_t) = \max_{a \in \mathcal{C}} \left\{ \tilde{u}(a, s_t) + \beta \int V(s_{t+1}) dF(s_{t+1} | a, s_t) \right\}, \quad (2.76)$$

where $F(s_{t+1} | a_t, s_t)$ is a Markov transition distribution function that represents the individual's beliefs about future states. The optimal decision rule $\alpha(s_t)$ is then:

$$\alpha(s_t) = \arg \max_{a \in \mathcal{C}} \{v(a, s_t)\}, \quad (2.77)$$

where

$$v(a, s_t) \equiv \tilde{u}(a, s_t) + \beta \int V(s_{t+1}) dF(s_{t+1} | a, s_t) \quad \forall a \in \mathcal{C} \quad (2.78)$$

is a choice-specific value functions. This DP problem can be solved by starting determining the value function at the terminal period T $V(s_T)$ and calculating Equation (2.76) in descending order. However, the procedure includes a number of maximization problems and it is computationally very expensive.

Rust, 1987 defined six assumptions to solve the problem more easily: AS (*Additive Separability*), IID (*iid Unobservables*), CI-X (*Conditional Independence of Future x*), CI-Y (*Conditional Independence of y*), CLOGIT, and DIS (*Discrete Support of x*) (see Rust, 1987; Aguirregabiria and Mira, 2010, for more detail). By these assumptions, the choice-specific value function is:

$$v(a, s_t) = u(a, x_t) + \varepsilon_t(a) + \beta \int \int V(x_{t+1}, \varepsilon_{t+1}) dG_\varepsilon(\varepsilon_{t+1}) dF_x(x_{t+1} | a_t, x_t), \quad (2.79)$$

where the state variables and the utility functions are distinguished into two subsets, $s_t = (x_t, \varepsilon_t)$ and, $\tilde{u}(a, x_t, \varepsilon_t) = u(a, x_t) + \varepsilon_t(a)$, respectively. By the assumption IID and CI-X, $F(s_{t+1} | a, s_t)$ can be decomposed as $F(x_{t+1}, \varepsilon_{t+1} | a, x_t, \varepsilon_t) = G_\varepsilon(\varepsilon_{t+1}) F_x(x_{t+1} | a_t, x_t)$, where $G_\varepsilon(\varepsilon_{t+1})$ is the CDF of the iid distributed unobserved value ε_{t+1} and $F_x(x_{t+1} | a_t, x_t)$ is the distribution function conditional on the current decision and observed state variables. By defining the integrated value function $\bar{V}(x_t) = \int V(x_t, \varepsilon_t) dG_\varepsilon(\varepsilon_t)$

and assuming that the state space X is discrete and finite, Equation (2.79) can be re-defined as:

$$v(a, s_t) = v(a, x_t) + \varepsilon_t(a) \quad (2.80)$$

where

$$v(a, x_t) = u(a, x_t) + \beta \sum_{x_{t+1}} \bar{V}(x_{t+1}) F_x(x_{t+1} | a_t, x_t). \quad (2.81)$$

Moreover, by the assumption CLOGIT, this can be expressed as DP conditional logit model with the Bellman equation

$$\bar{V}(x_t) = \log \left[\sum_{a \in \mathcal{C}} \exp \left\{ u(a, x_t) + \beta \sum_{x_{t+1}} \bar{V}(x_{t+1}) F_x(x_{t+1} | a_t, x_t) \right\} \right], \quad (2.82)$$

and choice probabilities:

$$P(a|x_t) = \frac{\exp\{v(a, x_t)\}}{\sum_{a' \in \mathcal{C}} \exp\{v(a', x_t)\}}. \quad (2.83)$$

This is similar to the static multinomial logit model, and it has contributed to the extensive development of DDCMs. A review of the applications of DDCMs in transportation studies are presented by Cirillo and Xu, 2011.

Fosgerau, Frejinger, and Karlstrom, 2013 proposed the recursive logit model as a network route choice model with unrestricted choice set, using the DDCM framework above. In the RL model, the route choice model is assumed as a utility-based and link-based one, while the above discussion is cost-based and node-based. At each current link k , a traveler chooses the next link a from the set of outgoing links $\mathcal{A}(k)$. An instantaneous utility $\tilde{u}(a|k) = u(a|k) + \varepsilon(a)$, where the random utility term $\varepsilon(a)$ is i.i.d. extreme value type I with the scale parameter μ , is associated with each link in the choice set $\mathcal{A}(k)$ conditional on current link k . In the context of sequential route choice models, the decision a corresponds to the state at the next period. Moreover, the state variables are link-specific and deterministic. Travelers are assumed to know the link utilities over the network deterministically; therefore, the discount factor β equals one and Equation (2.76) can be expressed as:

$$V^d(k) = \mathbb{E} \left[\max_{a \in \mathcal{A}(k)} (\tilde{u}(a|k) + V^d(a)) \right] \quad \forall k \in \mathcal{A}, \quad (2.84)$$

where d is a dummy link for a destination that has no successors, and $\tilde{\mathcal{A}} = \mathcal{A} \cup d$. This corresponds to the expected maximum utility from links k to d . Also, based on Equation (2.81)-(2.83), the link choice probability can be formulated as

$$p^d(a|k) = \frac{\exp[\mu\{u(a|k) + V^d(a)\}]}{\sum_{a' \in \mathcal{A}(k)} \exp[\mu\{u(a'|k) + V^d(a')\}]} \quad \forall k, a \in \mathcal{A}, \quad (2.85)$$

and the value function is formulated as a logsum:

$$V^d(k) = \begin{cases} \frac{1}{\mu} \log \sum_{a \in \mathcal{A}} \delta(a|k) \exp[\mu\{u(a|k) + V^d(a)\}], & \forall k \in \mathcal{A}, \\ 0, & k = d. \end{cases} \quad (2.86)$$

where an indicator $\delta(a|k)$ is equal to one if $a \in \mathcal{A}(k)$ and zero otherwise. Since d has no successive state, $V^d(d)$ equals to zero. This corresponds to Equation (2.64), which is the expected maximum utility in the DP framework. Equation (2.86) is transformed by multiplying μ and taking the exponential:

$$e^{\mu V^d(k)} = \begin{cases} \sum_{a \in \mathcal{A}} \delta(a|k) e^{\mu \{u(a|k) + V^d(a)\}}, & \forall k \in \mathcal{A}, \\ 1, & k = d. \end{cases} \quad (2.87)$$

which is corresponding to v in Equation (2.35) and (2.36) in Akamatsu, 1996. Using the matrix forms: \mathbf{M} ($|\tilde{\mathcal{A}}| \times |\tilde{\mathcal{A}}|$) with entries $\delta(a|k)e^{\mu u(a|k)}$, which is the incidence matrix defining instantaneous utilities, \mathbf{z}^d ($|\tilde{\mathcal{A}}| \times 1$) with entries $z_k^d = e^{\mu V^d(k)}$, and \mathbf{b}^d ($|\tilde{\mathcal{A}}| \times 1$) with entries $b_k = 0$ if $k \neq d$, and $b_d = 1$, Equation (2.87) can be written as a system of linear equations:

$$\mathbf{z}^d = \mathbf{M}\mathbf{z}^d + \mathbf{b}^d \Leftrightarrow (\mathbf{I} - \mathbf{M})\mathbf{z}^d = \mathbf{b}^d \quad (2.88)$$

which has the solution if the matrix \mathbf{M} is a convergence matrix. The main difference of Fosgerau, Freijinger, and Karlstrom, 2013 from previous route choice models based on Markovian model is that the deterministic component of instantaneous utility is expressed as $u_n(a|k) = u(x_{n,a|k}; \theta)$, where $x_{n,a|k}$ is a vector of observed characteristics of the link pair (k, a) that may include characteristics of traveler n and θ is an unknown parameter vector to be estimated by maximum likelihood. The log likelihood function defined for observations $n = 1, \dots, N$ is:

$$LL(\theta) = \log \prod_{n=1}^N P(r_n) = \mu \sum_{n=1}^N \sum_{i=0}^{I_n-1} u_n(k_{i+1}|k_i; \theta) - V(k_0) \quad (2.89)$$

where the choice probability of path $r_n = [k_0, \dots, k_{I_n}]$ is the product of link choice probabilities. The log likelihood function is maximized using structural estimation method, such as the nested fixed point (NFXP) algorithm (Rust, 1987) and the nested pseudo likelihood (NPL) algorithm (Aguirregabiria and Mira, 2002), which consist of two steps: the non-linear optimization to search over the parameter space and the evaluation of the system of linear Equation (2.88).

Mai, Fosgerau, and Freijinger, 2015 and Mai, 2016 has extended the RL model to the nested RL (NRL) model and the generalized RL (GRL) model, which are the framework for considering the correlation structure among paths based on the RL model, respectively. In Mai, Fosgerau, and Freijinger, 2015, the scale parameter of the error term distributions of the instantaneous utility is assumed to be link-specific μ_k , and Equation (2.87) is re-formulated as

$$e^{\mu_k V^d(k)} = \begin{cases} \sum_{a \in \mathcal{A}} \delta(a|k) e^{\mu_k \{u(a|k) + V^d(a)\}}, & \forall k \in \mathcal{A}, \\ 1, & k = d. \end{cases} \quad (2.90)$$

In the same way with Fosgerau, Freijinger, and Karlstrom, 2013, this is replaces by the matrix expression defining the matrix \mathbf{M} and \mathbf{z}^d :

$$z_k^d = \begin{cases} \sum_{a \in \mathcal{A}} M_{ka}^d (z_a^d)^{\mu_k / \mu_a}, & \forall k \in \mathcal{A}, \\ 1, & k = d, \end{cases} \quad (2.91)$$

then

$$\mathbf{z}^d = \mathbf{MX}(\mathbf{z}^d) + \mathbf{b}^d \quad (2.92)$$

where $\mathbf{X}(\mathbf{z}^d)$ is a matrix of size $|\tilde{\mathcal{A}}| \times |\tilde{\mathcal{A}}|$ with entries $X(z)_k a^d = (z_a^d)^{\mu_k / \mu_a}$. This is a system of non-linear equations, and it is solved by a value iteration approach. Mai, 2016 proposed a generalized recursive logit (GRL) model, which describes correlation structures among path alternatives integrally, based on the network-GEV model (Daly and Bierlaire, 2006) similarly to the method shown in Section 2.2.6. Moreover, Mai, Frejinger, and Bastin, 2015 proposed a dynamic programming approach to quickly solve the large scale network models with correlation structures.

2.3 Discussion

2.3.1 Biases in estimating route choice models

We discussed the estimation methods of route choice models using GPS data in Section 2.1.5 and 2.1.7. For observing route choices, passive monitoring with the GPS technology is used; however, it is required to match the data format to transportation networks and to deal with the measurement errors. As mentioned in Section 2.1.5, in the case that the measurement uncertainty is large, bayesian approaches are used, which incorporate route choice models as the prior to correct the measurement probabilities. In bayesian approaches, the parameters of the route choice model that is used as the prior are required to be given. These parameters that are given by the modeler are not consistent with those that are estimated in route choice models. As the results, the parameter estimation, which is the objective of discrete choice analysis, can be biased.

In the framework of the joint estimation of Bierlaire and Frejinger, 2008, the definition of the set of path candidates is required, and for this purpose, the concept of DDR is used. For defining the DDRs, the variance of GPS measurement error σ should be given and often regarded as the constant value over the network. However, it is assumed that the localization errors largely depends on spacial attributes on which travelers move, especially in pedestrian networks. The probability that is evaluated by the measurement equation with given σ can be biased. Figure 2.3 shows the measurement probabilities with different variances, which are often assumed to be a Rayleigh distribution here as:

$$p(\hat{x}|x; \sigma) = \frac{\|\hat{x} - x\|}{\sigma} \exp\left(-\frac{\|\hat{x} - x\|^2}{2\sigma^2}\right), \quad (2.93)$$

where measurement probability $p(\hat{x}|x; \sigma)$ is the probability that measurement \hat{x} is observed if x is the true location. The figure shows that the measurement probabilities are largely dependent on the value of the variance, that is, the error of the variance parameter can cause biases in evaluating the measurement probabilities. Also, as the result, the estimated parameters of the route choice model can also be biased.

The above discussion demonstrates that previous frameworks for estimating route choice models using uncertain measurements, such as GPS data, often result in biased parameters due to the initial parameter settings of both the measurement model and the prior information. We show the illustration of the process in Figure 2.4,

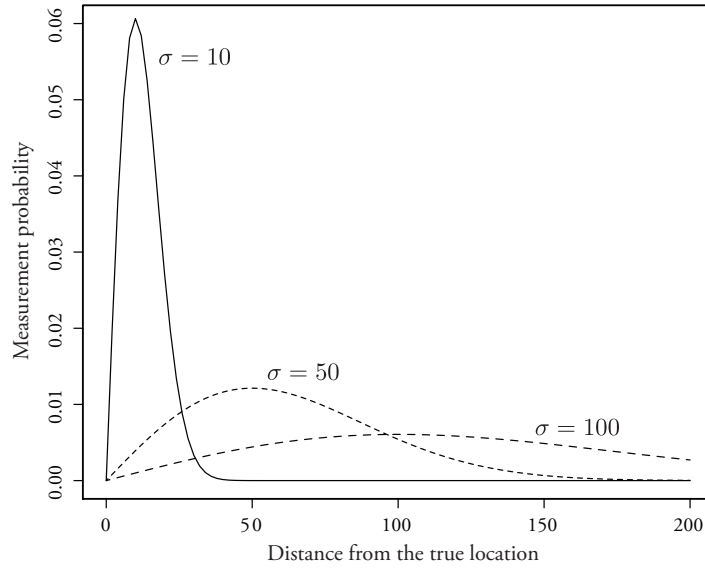


FIGURE 2.3: Difference of measurement probability by the variance of GPS errors

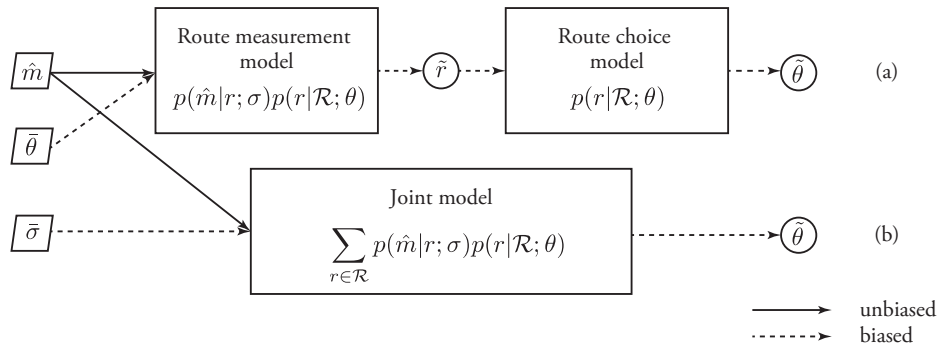


FIGURE 2.4: Biases in estimation process of route choice models

where solid lines indicate the unbiased inputs and dash lines denote the biased inputs or outputs. In bayesian approaches shown in Figure 2.4(a), the parameters $\bar{\theta}$ of route choice preferences have to be given to calculate the route choice probability $p(r|\mathcal{R}; \theta)$ of the prior, while the modeler cannot know the true preferences of route choices. Therefore, the biases included in the initial parameters are retained into the inferred routes \tilde{r} , and also into the estimated parameters $\tilde{\theta}$. In the joint estimation method of Bierlaire and Frejinger, 2008, which is shown in Figure 2.4(b), the assumption of the variance $\bar{\sigma}$ is required to define the set of path candidates. The value of the variance is assumed as the constant value over a network; however, in the case that the variances have spatial dependence, the measurement probabilities $p(\hat{m}|r; \sigma)$ can be biased, and as the result, the estimated parameters $\tilde{\theta}$ are biased. For this reason, a new method for reducing the biases is needed, especially in the case of high resolution networks, such as pedestrian networks.

2.3.2 Computational property of Markovian route choice models

In this section, we point out a challenge of Markovian route choice models using the example networks of Figure 2.5. The number associated with each link is link

cost c_{ij} , which is the only attribute of utilities, and the link utility is $u_{ij} = \theta c_{ij}$, where $\theta = -1.5$. For the path-based MNL model and the PSL model, the choice set includes 3 paths: [o1, 12, 23, 3d] (path 1), [o1, 12, 24, 43, 3d] (path 2), and [o1, 13, 3d] (path 3). In Markovian model, which is referred to as the RL model in this section, the universal set is considered. Table 2.1, 2.2 and 2.3 show the choice probabilities of the three paths given by the path-based MNL model, the PSL model with $\theta_{PS} = 2.5$, the RL model, and the RL model with the link size attributes and $\theta_{LS} = -0.75$ in network (a), (b), and (c) of Figure 2.5, respectively. We denote the three path probabilities as P_1 , P_2 , and P_3 , respectively. As is seen in Table 2.1, in network (a), which has no cyclic structure, the path probabilities given by the MNL model and the RL model are equivalent to each other: $P_1 = P_2 = P_3 = 0.333$, because the universal set is path 1, 2 and 3 in the case of network (a). As mentioned in Section 2.2.3, the path probabilities given by the logit-type Markovian route choice model is consistent with that of the path-based MNL model with the universal choice set. The RL model can also consider the overlapping effect of paths by incorporating the link size attributes into the model. The tables show that the RL model with link size attributes output the values of the path probabilities close to those given by the PSL model, which is one of the most popular models for considering the overlapping effects.

In network (a), the total value of the path probabilities given by every model is equivalent to one; however, in network (b) and (c), the total value is lower than one, because the probabilities are assigned to the cyclic paths. In the case of the RL model in network (b) and (c), probability 0.050 and 0.214 are assigned to the cyclic paths, respectively. This assignment of probabilities to cyclic paths causes a problem for solving the Bellman equation. Consider the incident matrix \mathbf{W} defining the link utilities, and the logit-type Markovian model has to satisfy the following inequality to solve the expected minimum cost:

$$\rho(\mathbf{W}) \equiv \max_h \{|\lambda_h|\} < 1, \quad (2.94)$$

where λ_h is the h -th eigenvalue of the matrix \mathbf{W} and $\rho(\mathbf{W})$ is the spectral radius, which is the maximum absolute value of the eigenvalues of \mathbf{W} . Equation (2.94) is then the necessary and sufficient condition for the matrix \mathbf{W}^m to converge as $m \rightarrow +\infty$. When the network has no cyclic structure as network (a), $\rho(\mathbf{W})$ is always zero and satisfies Equation (2.94), theoretically. However, when the network has cyclic structures, it depends on the balance between the number of paths that connect the nodes in the network and the size of the link utilities.

We investigate this conditions using network (c), which has two cyclic structures: [12, 24, 41] and [24, 42]. We change the coefficient of the link cost in the link utility function, θ , and report the change of the spectral radius, $\rho(\mathbf{W})$ in Table 2.4. The $\rho(\mathbf{W})$ values that are larger than one indicate that the matrix \mathbf{W} is not a convergence matrix and $(\mathbf{I} - \mathbf{W})$ is not invertible. Table 2.4 shows that in the case of network (c), the maximum expected utilities diverge and the Bellman equation cannot be solved when θ is larger and equal to -0.4 . That is, we cannot solve the path probabilities of the Markovian route choice models when the link utilities are large and the network has cyclic structures.

In Fosgerau, Freijinger, and Karlstrom, 2013, the link utilities are defined to be always lower than zero, and a fixed large penalty to each u-turn is introduced so that their probability is close to zero. However, the computational stability is retained in the parameter estimation process, because the values of coefficients fluctuate and the spectral radius can be larger or equal to one in the process. Moreover, the setting that the utilities are always negative do not allow one to introduce variables that can

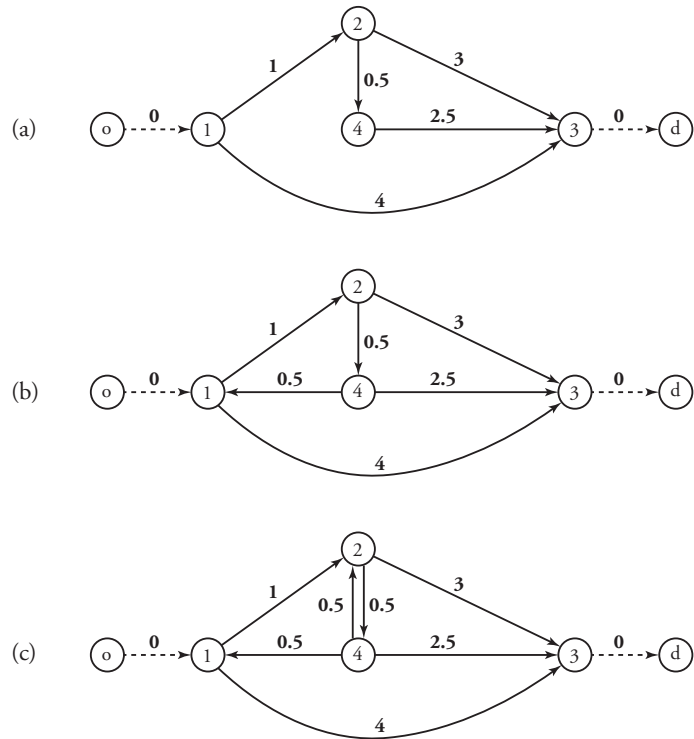


FIGURE 2.5: Example networks

have positive effects to the utilities, such as the number of lanes, the attractiveness of shops along the road, the width of sidewalk, and so on.

TABLE 2.1: Path probabilities in network (a)

Path	MNL	PSL	RL	RLwithLS
1:[o1,12,23,3d]	0.333	0.294	0.333	0.292
2:[o1,12,24,43,3d]	0.333	0.294	0.333	0.227
3:[o1,13,3d]	0.333	0.411	0.333	0.481
total	1	1	1	1

TABLE 2.2: Path probabilities in network (b)

Path	MNL	PSL	RL	RLwithLS
1:[o1,12,23,3d]	0.333	0.294	0.317	0.283
2:[o1,12,24,43,3d]	0.333	0.294	0.317	0.212
3:[o1,13,3d]	0.333	0.411	0.317	0.485
total	1	1	0.950	0.979

TABLE 2.3: Path probabilities in network (c)

Path	MNL	PSL	RL	RLwithLS
1:[o1,12,23,3d]	0.333	0.294	0.262	0.262
2:[o1,12,24,43,3d]	0.333	0.294	0.262	0.161
3:[o1,13,3d]	0.333	0.411	0.262	0.504
total	1	1	0.786	0.927

TABLE 2.4: Spectral radius of the incident matrix \mathbf{W} in network (c)

θ	-1.5	-1.4	-1.3	-1.2	-1.1	-1	-0.9	-0.8
$\rho(\mathbf{W})$	0.559	0.591	0.626	0.662	0.701	0.742	0.785	0.832
θ	-0.7	-0.6	-0.5	-0.4	-0.3	-0.2	-0.1	0
$\rho(\mathbf{W})$	0.881	0.934	0.989	1.048	1.111	1.178	1.249	1.325

Chapter 3

Structural estimation for route choice models under measurement uncertainties

In this chapter, we propose an estimation method for obtaining parameters of route choice models without biases dependent on parameter settings, using GPS data with measurement uncertainties.

Passive monitoring with the Global Positioning System (GPS) is increasingly used to observe trip data because it contributes to facilitating the automatic observation of trip data. However, data from monitoring with GPS includes measurement errors that are dependent on device, network description, and spatial attributes. The errors result in a biased observation of route choices, and therefore, the parameter estimation results of route choice models are biased. In this study, we propose a link-based route measurement model that is based on a Bayesian approach and incorporates a link-based route choice model as the prior. It allows the inference of links based on both measurements and behavioral mechanisms, and to simultaneously estimate the variance of GPS measurement error on each link. Additionally, we propose a structural estimation method for route choice models to remove biases with respect to the initial parameter settings. The performance of the framework is examined through a numerical example and a case study involving a real pedestrian network. As a result, the estimated preferences of route choices using the structural estimation method are less biased and show the different trend from those using the biased route choice observations. Also, the estimated variances of GPS measurement errors are realistic.

Keywords: Route choice model, Route choice observation, GPS data, Structural estimation, Sequential link measurement, map matching

3.1 Introduction

Observations corresponding to models are required to estimate the parameters of discrete choice models. In the context of route choice model, we need the information of paths that are sequences of links connecting between the origin-destination pairs. Conventionally, mail and telephone surveys were conducted to ask travelers as to which routes were taken. However, it is difficult to assume that many travelers correctly state their routes. Conversely, passive monitoring with the Global Positioning System (GPS) is currently used to automatically observe trip data. Probe cars and connected vehicles contribute to obtaining real-time trip data, and recently emerging monitoring technologies allow the observation of trajectories of vehicles as well as pedestrians in districts (Hato, 2010; Kasemsuppakorn and Karimi, 2013; Asakura, Hato, and Maruyama, 2014; Shafique, Hato, and Yaginuma, 2014).

It is increasingly important to understand pedestrian route choice behavior in districts as a solution for recent problems involving urban and transportation planning (Scarinci, Markov, and Bierlaire, 2017) and human health (Borst et al., 2008). Several studies report that pedestrian route choice behavior exhibits preferences different from other means of transport (Timmermans, Hagen, and Borgers, 1992; Kurose, Borgers, and Timmermans, 2001). Also, pedestrian behavior is described as a series of decisions and activities (Borgers and Timmermans, 1986a). While these characteristics of pedestrian behavior have been studied in microscopic scale, such as in transportation hubs (Hoogendoorn and Bovy, 2004), the behavior has not been sufficiently investigated at the urban network level such as in shopping streets and city center districts. This problem depends on data collection. At the microscopic scale, various sensors or video tracking are used to follow trajectories. On the other hand, in urban networks, this type of monitoring is typically not applicable, and it is difficult to observe the complicated series of behavior by questionnaire surveys. Although trajectory monitoring using mobile instruments is currently under development (Danalet, Farooq, and Bierlaire, 2014; Shafique, Hato, and Yaginuma, 2014; Danalet et al., 2016), there is a paucity of studies examining the method for detecting route choices in urban pedestrian networks.

Specifically, the observation accuracy of trajectory monitoring is continuously improved. Nevertheless, high measurement uncertainties persist especially in pedestrian networks. First, pedestrian networks are often dense, and thus the number of candidates of the true path corresponding a sequence of measurements increases. Therefore, it is more difficult to identify the true state as opposed to networks of the other transportation modes. Second, the spatial attributes of links are different from each other and affect on measurement errors. For example, we can accurately observe trajectories on wide streets or streets along open spaces, while the observation accuracy worsen on narrow streets or streets with arcades. That is, the variance of the measurement error is heterogeneous in pedestrian networks.

Probabilistic route measurement models that explicitly consider the measurement error and probabilistically identify routes are used to deal with the measurement uncertainties. However, in the previous models, the variance of the measurement error is assumed as a given and constant value over a network to define the route candidate set (Bierlaire and Frejinger, 2008; Bierlaire, Chen, and Newman, 2013). This causes a trade-off problem between measurement accuracy and computational efficiency and also has the risk of inaccurate evaluation of the measurement probabilities. If the route identification is uncertain, then the route choice model that is estimated with the uncertain route information is consequently biased. Also, Bayesian approaches that incorporate route choice models as the prior information

(e.g., Danalet, Farooq, and Bierlaire, 2014; Chen and Bierlaire, 2015) remain a problem to correct the route measurement in the wrong direction in the case when the incorporated model is not consistent with the finally estimated model.

Focusing on the mechanism of the increase in estimation biases that depends on the relationship between route measurement and route choice models, this paper proposes a novel framework for estimation with less biases. The study considers and estimates the *link-specific* variance of measurement error, and this has been ignored in extant studies as mentioned above. To do so, we introduce a link-based route measurement model that is based on the assumption of sequential link choice behavior. Furthermore, we propose an estimation method that ensures consistency of route choice model with the route measurement model to remove the biases included in the prior information of Bayesian approaches. The proposed framework is examined through numerical examples, and it is shown that it converges to a point close to the true value and is computationally efficient. We also apply the framework to the real trajectory data of pedestrians in a city center. The analysis not only shows realistic results in terms of estimation results of both the measurement error variance and route choice preference of pedestrians, but also reveals a hidden behavioral mechanism under the measurement uncertainties.

The structure of this paper is as follows. In Section 3.2, we present a literature review of estimation methods for route choice models with uncertain measurements. In Section 3.3, we present a framework of this study and notations. In Section 3.4, we introduce a link-based route measurement method and show how to estimate link-specific variances. In Section 3.5, we propose a structural estimation method and explain its algorithm. In Section 3.6, we examine the performance of our model in a simulation analysis and a case study of applying the framework to a real pedestrian network. Conclusions and discussion for future research directions are provided in the end.

3.2 Literature review

In this section, we present a literature review of frameworks to estimate the parameters of route choice models with uncertain measurement. We first introduce studies on route measurement models that observe route choices with GPS data for route choice models. We then review Bayesian approaches that incorporates behavioral route choice information into route measurement models.

3.2.1 Route measurement models

Raw data from sensors is typically not useful for behavior analyses without the pre-processing, because GPS location data is not consistent with network graphs in format and includes measurement errors that are dependent on the devices and spatial contexts. Given these reasons, several methods have been proposed within the last two decades to estimate behavioral states from the passive data.

Map matching algorithms

Map matching (MM) methods that involve the aim of matching GPS data to transportation networks are typical techniques. MM algorithms are categorized into the three following groups: geometric (e.g., White, Bernstein, and Kornhauser, 2000), topological (e.g., Greenfeld, 2002; Quddus et al., 2003; Velaga, Quddus, and Brishtow, 2009), and probabilistic (e.g., Ochieng, Quddus, and Noland, 2003; Quddus,

Ochieng, and Noland, 2006; Hunter, Abbeel, and Bayen, 2014). Quddus, Ochieng, and Noland, 2007 comprehensively reviewed map matching methods presented prior to the early 2000s. Most algorithms are based on sequential position inferences where the true location is inferred for each location data in chronological order, because the aim involves application to on-line navigation systems. However, in transportation studies, researchers require the actual path as a sequence of links rather than the on-line identification of the traveler locations (Bierlaire, Chen, and Newman, 2013).

Probabilistic route measurement models

Conversely, Pyo, Shin, and Sung, 2001 and Bierlaire, Chen, and Newman, 2013 proposed path-based and probabilistic route measurement models that evaluate the likelihoods of path candidates with respect to all GPS data in a trip. Chen and Bierlaire, 2015 presented a probabilistic route measurement model that includes the transportation mode detection for route choice analysis in multi-modal networks. However, in order to probabilistically evaluate path candidates, the set of paths to which the probabilities are assigned should be defined. It is widely known that the choice set definition of route choice models is challenging, and probabilistic route measurement models involve the same problem.

Bierlaire and Frejinger, 2008 proposed the concept of *domain of data relevance* (DDR) that indicates a region where each data is related, in order to generate the set of path candidates for route measurement models. Based on the DDR concept, Bierlaire and Frejinger, 2008 also proposed a framework to estimate route choice models as the ambiguity of observations remains (Figure 3.1 a). In the case of GPS data, links included in a DDR are assumed as candidates of the true state of each data, and paths that include those links are considered in the path candidate set. Based on the DDR concept, Bierlaire, Chen, and Newman, 2013 proposed a path generation algorithm. Danalet, Farooq, and Bierlaire, 2014 applied it to Wi-Fi data to generate candidate locations of activity episode for each measurement. The application of the DDR concept involves, however, a trade-off problem between measurement accuracy and computational efficiency because the number of path candidates depends on the size of DDRs. Furthermore, it is required to give the probability distribution of the measurement error in advance to define a DDR, and this can cause the bias on evaluation of the route measurement probabilities.

Bayesian approaches

Recently, a few studies proposed advanced methods based on Bayesian approaches (e.g., Danalet, Farooq, and Bierlaire, 2014; Chen and Bierlaire, 2015). Bayesian approaches in the context of route choice analysis correct the route measurement probabilities by incorporating the prior information of the route choice probabilities given by route choice models. When localization is weak and a network is dense, the difference among route measurement probabilities is not significantly high and it is typically not possible to obtain information enough to identify routes (Danalet, Farooq, and Bierlaire, 2014). Especially in such cases with large measurement uncertainties, Bayesian approaches that correct for the measurement probabilities based on behavioral information are helpful. However, when the prior (i.e., the parameters of route choice model) is uncertain, the results of route identification of a Bayesian approach can be worse than that without the prior. The estimated parameters of route choice

model are theoretically biased unless the route choice model of the prior is consistent with one that is finally estimated by using the identified route information.

3.2.2 Biases in estimation process

As mentioned above, probabilistic route measurement models are mainly used in recent years to estimate route choice models with uncertain measurement. This study focuses on the effect of initial parameter settings of these types of models on the estimation process of the route choice model. To discuss it, we let r denote a route and let \mathcal{R} denote the route set that travelers consider. $p(\hat{m}|r; \sigma)$ is the route measurement model that yields the probability that data \hat{m} is observed if r is the actual path, where σ is the measurement parameter. $p(r|\mathcal{R}; \theta)$ is the route choice model that gives the probability that path r is selected within the choice set \mathcal{R} , where θ is the unknown parameters to be estimated. Hats (^), bars (‐) and tildes (~) over symbols respectively indicate observed, given (initial) and estimated values.

First, a path-based probabilistic measurement model requires the definition of path candidate set. As discussed above, the DDR concept is used for this purpose (Bierlaire and Frejinger, 2008), and the variance of measurement error σ should be given in advance to define the DDR of each location data. In previous works, the variance is often considered as a constant value over the network (Bierlaire, Chen, and Newman, 2013; Danalet, Farooq, and Bierlaire, 2014; Chen and Bierlaire, 2015). Given that σ defines the probability distribution of the measurement error, the evaluation of the route measurement probabilities is biased when the given value of σ is significantly different from the true value. Also, the number of path candidates, i.e., the definition of \mathcal{R} depends on the size of DDR. This indicates the possibility that the true path is not included in the path candidate set. Thus, the arbitrary setting of the parameter of route measurement model causes the bias in the estimation result of route choice model (Figure 3.1 b). This is assumed as a critical issue in urban pedestrian networks. Such networks are often dense, and the number of path candidates to consider is large compared to road networks even if the size of measurement error is same. For the sake of computational efficiency, we need to define smaller DDRs, and this means the higher risk of ignoring the true path. Also in urban pedestrian networks, localization errors can largely depend on spatial attributes, such as width of a street and height of buildings along a street. A constant value of σ over a network thus causes the biases in the evaluation of measurement probabilities.

Second, the Bayesian approach corrects for the measurement probability by using prior information. In the context of route choice analysis, the prior is assumed as the parameter of route choice model θ that represents route choice preference of travelers Chen and Bierlaire, 2015. This parameter is supposed to be finally estimated by using route choice data observed through route measurement model, namely, it is not possible to obtain its true value in advance. In previous studies, θ is defined as, e.g., estimated parameters from historical or external data sources (Chen and Bierlaire, 2015), arbitrarily given (Danalet, Farooq, and Bierlaire, 2014), and assumed as uniformly distributed if no information is available (Chen and Bierlaire, 2015; Hunter, Abbeel, and Bayen, 2014). However, when the prior is uncertain, the results of route identification can be worse rather than the case without prior information, and subsequently the final parameter estimation result of route choice model is worse. This theoretically implies that the estimated parameters are biased unless the route choice model of the prior is consistent with one that is finally estimated by using the identified route information (Figure 3.1 a).

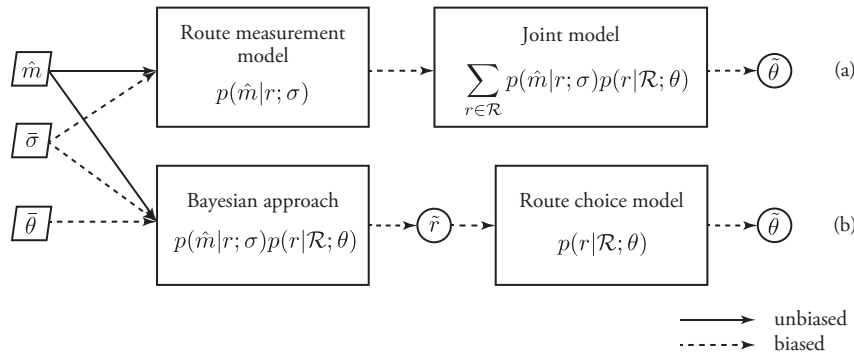


FIGURE 3.1: Biases in parameter estimation process of route choice model.

To summarize, the existing frameworks to estimate route choice models with measurement uncertainties involve possibilities of causing biased results dependently on the initial parameter settings that are required in route measurement models (Figure 3.1). In this study, we propose a novel framework to estimate route choice models with less biases, by estimating σ as a link-specific parameter and solving a fixed point problem of θ between the prior and the estimation result. Note that the framework of joint estimation of Bierlaire and Frejinger, 2008 is theoretically clear; however, it leads to expensive computation and/or biased estimation results (Figure 3.1 a). This study proposes another approach with the aims at making computation simple and reducing parameter biases.

3.3 Framework and notations

The main goal of this study involves estimating the parameters of route choice model with less biases based on a sequence of GPS location data with measurement error. In this section, we present the framework of the study by defining the route choice model and the route measurement model with the notations used in the models.

3.3.1 Network

We first define a transportation network $\mathcal{G} = (\mathcal{N}, \mathcal{A})$, where \mathcal{N} is the set of nodes and \mathcal{A} is the set of links. The horizontal position of each node $i \in \mathcal{N}$ is described by $x_i = \{x_{i1}, x_{i2}\}$, which is a pair of coordinates that typically consist of latitude and longitude. Link $a \in \mathcal{A}$ is a line and is characterized by the vector of spatial attributes y_a and the pair of its up-node and down-node (u_a, d_a) . We define $\mathcal{A}(a)$ as the set of possible next states of link a and $\delta(a'|a)$ as the indicator that equals one if the pair consisting of link a and link $a' \in \mathcal{A}(a)$ is directly connected, and zero otherwise, i.e., $\mathcal{A}(a) = \{a' \in \mathcal{A} | \delta(a'|a) = 1\}$.

3.3.2 Route choice model

We assume that travelers move continuously on the network $\mathcal{G} = (\mathcal{N}, \mathcal{A})$ to go from a place (an origin) to another (a destination). In this study, it is assumed that travelers do not determine their routes *pre-trip* but *sequentially* choose a link at every node. In the link-based route choice model, a route is not directly chosen but the output of

sequential link choices. At each period t , each traveler is associated with the current state $a_t \in \mathcal{A}$ and chooses the next state link a_{t+1} that maximizes the utility from the set $\mathcal{A}(a_t)$. The link choice probability is formulated as follows:

$$p(a_{t+1}|a_t) = \mathbb{P} \left(\tilde{u}(a_{t+1}|a_t) = \max_{a'_{t+1} \in \mathcal{A}(a_t)} \tilde{u}(a'_{t+1}|a_t) \right), \quad (3.1)$$

where

$$\tilde{u}(a_{t+1}|a_t) = u(a_{t+1}|a_t) + \varepsilon(a_{t+1}). \quad (3.2)$$

The deterministic utility component of the transition from link a_t to link a_{t+1} is the function of the vectors of spatial attributes y_{a_t}, y_{a+1} and the vector of unknown parameters θ , i.e., $u(a_{t+1}|a_t) = u(y_{a_t}, y_{a+1}, \theta)$. The error term of the utility $\varepsilon(a_{t+1})$ is i.i.d. extreme value type I. Based on Equation (3.1), the path choice probability is given as the product of the link choice probabilities:

$$\mathbb{P}(r = [a_0, \dots, a_T]) = \prod_{t=0}^{T-1} p(a_{t+1}|a_t; \theta) \quad (3.3)$$

where a_0 and a_T are defined as the origin link and the destination link, respectively. As a link-based route choice model in the context of discrete choice model, Fosgerau, Frejinger, and Karlstrom, 2013 proposed the recursive logit (RL) model that does not require path enumeration and is consistent with the conventional MNL route choice model with the universal set. Mai, Fosgerau, and Frejinger, 2015 proposed RL models that consider the correlation structures among paths, based on the GEV model (McFadden, 1978; Bierlaire, 2002; Daly and Bierlaire, 2006). Oyama and Hato, 2017 presented a framework of link-based route choice model with the discount factor for integrating the description of myopic and global decisions and mentioned that the model can be applied to pedestrian myopic route choice analysis.

3.3.3 Route measurement model

We observe routes and estimate a route choice model, based on the data as sequences of GPS measurements recorded by the built-in sensors in devices that are carried by travelers. We denote a measurement as $\hat{m} = (\hat{x}, \hat{\tau})$, where $\hat{x} = (\hat{x}_1, \hat{x}_2)$ is the pair of coordinates (usually latitude and longitude) and $\hat{\tau}$ is the measurement timestamp. For a given trip z , we obtain a chronologically ordered sequence of N_z measurements $\hat{\mathbf{m}} = (\hat{m}_1, \dots, \hat{m}_n, \dots, \hat{m}_{N_z})$, which are recorded by the same device. It is assumed that the recorded locations \hat{x} always include the measurement errors while the timestamps $\hat{\tau}$ have no measurement error. The true location of \hat{x}, x , is a point on a link, and the difference between \hat{x} and x follows a probability distribution $p(\hat{x}|x; \sigma)$, where σ is the variance of GPS measurement error. As discussed in Section 3.2, the variance has been assumed as a given and constant value over a network in previous works. The measurement error of GPS localization is a variable specific for each measurement, and the error arises from various factors such as atmosphere, noise of receiver, interception and multipath reflection. Also, the presences of buildings or structures have large effects. In this study, we focus on the fact that the spatial attributes do not significantly change in the same street between two intersections, and we assume that the variance of measurement error is a *link-specific* value, i.e., $\sigma = \sigma_a$. That is, we

estimate a route choice model under the assumptions of inter-link heteroscedasticity of measurement error, which has ignored in previous works but is important for urban pedestrian networks.

3.4 Link-based route measurement model

In this section, we propose a link-based route measurement model. Path-based probabilistic route measurement models evaluate the probability of each possible route based on all of measurements that are included in a trip. In this case, the link on which the true location of each measurement is located is unknown, and moreover, it is impossible to consider all links as the candidates from the computation viewpoint. Thus, the restriction of the set of possible routes is performed in advance by using links included in the domain relevant to each measurement that is defined by the variance of measurement error (Bierlaire and Frejinger, 2008).

In contrast, we focus on that the sequential link identification gives us the set of possible next links as the output of the model; namely, if link a is specified as the state link at a period, then we can assume that the next link is included in $\mathcal{A}(a)$. This explicitly specifies the spatial relationship between a measurement and the set of link candidates on which the true location is possible to be located, and thus it is possible to calculate the measurement equation of each possible link. Based on the measurement equation, we can estimate the link-specific variance of measurement error.

Furthermore, the link-based route measurement model is based on a Bayesian approach. The incorporation of a link-based route choice model as the prior corrects the observation by a behavioral route choice mechanism without requiring the path enumeration.

3.4.1 Data decomposition

In the link-based route measurement model, sequential link choice behavior is the shared framework for both measurement and behavioral models. In order to consider both route choice model and route measurement model in the same framework, we first process the unit of the route measurement.

We define the discretized time sequence $(1, \dots, t, \dots, T_z)$ where $t^- \leq t \leq t^+$ is a time period and the interval $\bar{t} = t^+ - t^-$ is consistent for all time periods. t^-, t^+ indicate elapsed times from the beginning of a trip, i.e., $\hat{\tau}_{N_z} - \hat{\tau}_1 = T_z^+$. Note that \bar{t} is defined by using the information of network structure to satisfy the link connection condition.

Let $\hat{\mathbf{m}}^t = (\hat{m}_1^t, \dots, \hat{m}_j^t, \dots, \hat{m}_{J_t}^t)$ denote a vector of measurements that are observed within a time period t and satisfy $t^- \leq \hat{\tau}_j^t \leq t^+$. J_t is the number of measurements included in $\hat{\mathbf{m}}^t$ and satisfies $\sum_t J_t = N_z$. Therefore, the sequence of measurements for a trip $\hat{\mathbf{m}}$ is decomposed as $(\hat{\mathbf{m}}^1, \dots, \hat{\mathbf{m}}^t, \dots, \hat{\mathbf{m}}^T)$. At each period, we use a vector $\hat{\mathbf{m}}^t$ and observe the state link a_t . We assume that the true states of all measurements observed within the same period are located in the same link and sequentially perform link measurement from $t = 1$ to $t = T$.

3.4.2 Sequential link measurement

At every time period t , we use a decomposed data $\hat{\mathbf{m}}^t$ and observe the link a_t based on link likelihood. The candidates of state link are defined as the links that are

connected to the previous state a_{t-1} , $\mathcal{A}(a_{t-1})$. Given a vector of measurements $\hat{\mathbf{m}}^t$ and the previous state a_{t-1} , the link likelihood $p(a_t | \hat{\mathbf{m}}^t, a_{t-1})$ is formulated from the Bayes' theorem:

$$p(a_t | \hat{\mathbf{m}}^t, a_{t-1}) \propto p(\hat{\mathbf{m}}^t | a_t; \sigma_{a_t}) p(a_t | a_{t-1}; \theta), \quad (3.4)$$

where $p(\hat{\mathbf{m}}^t | a_t; \sigma_{a_t})$ denotes a measurement equation, giving the probability that the measurement vector $\hat{\mathbf{m}}^t$ is observed if a_t is the actual link, and σ_{a_t} is the unknown link-specific variance of GPS measurement error. $p(a_t | a_{t-1}; \theta)$ denotes a route choice model, and we use a link-based route choice model as mentioned in Section 3.3.2. θ is a vector of unknown parameters to be finally estimated. In the route choice context, the state variable a_t can be discretized, and thus Equation (3.4) is replaced as the following standardization form:

$$p(a_t | \hat{\mathbf{m}}^t, a_{t-1}) = \frac{p(\hat{\mathbf{m}}^t | a_t; \sigma_{a_t}) p(a_t | a_{t-1}; \theta)}{\sum_{a_t \in \mathcal{A}(a_{t-1})} p(\hat{\mathbf{m}}^t | a_t; \sigma_{a_t}) p(a_t | a_{t-1}; \theta)}. \quad (3.5)$$

Based on the link likelihood, we sequentially identify the state link at each time:

$$a_t = \arg \max_{a_t \in \mathcal{A}(a_{t-1})} p(a_t | \hat{\mathbf{m}}^t, a_{t-1}). \quad (3.6)$$

The iteration of this process until $t = T$ obtains an inferred path $r = [a_1, \dots, a_t, \dots, a_T]$ as a sequence of identified links. The process of the link-based measurement model is summarized in Figure 3.2. It should be noted that we propose an algorithm to avoid a problem specific for the link-based route measurement model (see Appendix A.1).

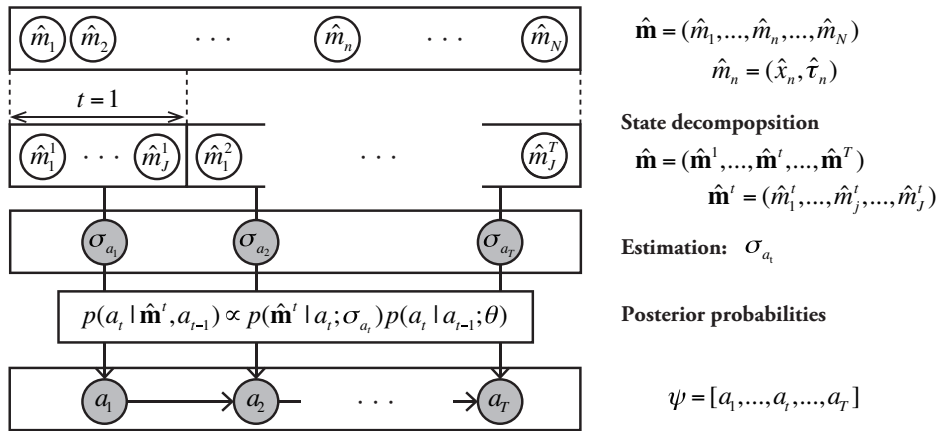


FIGURE 3.2: Image of the link-based route measurement model

3.4.3 Measurement probability

Given the assumption that timestamps $\hat{\tau}$ include no measurement error, the probability that the vector of measurements $\hat{\mathbf{m}}^t = (\hat{m}_1^t, \dots, \hat{m}_{J_t}^t)$ is observed if a_t is the actual state is given as

$$p(\hat{m}_1^t, \dots, \hat{m}_{J_t}^t | a_t; \sigma_{a_t}) = p(\hat{x}_1^t, \dots, \hat{x}_{J_t}^t | a_t; \sigma_{a_t}). \quad (3.7)$$

Also, we assume that traveler locations on a link depend on only elapsed time from the arrival at the link, and traveler moves at the constant speed with white noise on the link (Equation (3.9) - (3.11)). Hence, Equation (3.7) is decomposed as follows:

$$\begin{aligned} p(\hat{x}_1^t, \dots, \hat{x}_J^t | a_t; \sigma_{a_t}) &= \prod_{j=1}^J p(\hat{x}_j^t | a_t; \sigma_{a_t}), \\ &= \prod_{j=1}^J \int_{x_j \in a_t} p(\hat{x}_j^t | x_j, a_t; \sigma_{a_t}) p(x_j | a_t) dx_j \end{aligned} \quad (3.8)$$

where,

$$x_j = l x_{d_{a_t}} + (1-l) x_{u_{a_t}}, \quad (3.9)$$

$$l = \frac{\hat{\tau}_j^t - t^-}{t^+ - t^-} + \eta, \quad (3.10)$$

$$\eta \sim N(0, \sigma_\eta^2). \quad (3.11)$$

Equation (3.8) indicates that the true location x_j is probabilistically distributed on link a_t , and we calculate the line integral of the probability on the link. $p(\hat{x}_j^t | x_j, a_t; \sigma_{a_t})$ denotes the probability distribution that the measurement error of the GPS location follows. The errors in horizontal directions are generally assumed as independently normally distributed (Diggelen, 2007), and thus the distance between the measurement and the true location, d , follows a Rayleigh distribution. Therefore, the probability that a location x_j on link a_t generates the measurement \hat{x}_j^t is formulated as follows:

$$p(\hat{x}_j^t | x_j, a_t; \sigma_{a_t}) = \frac{\|\hat{x}_j^t - x_j\|}{\sigma_{a_t}^2} \exp\left(-\frac{\|\hat{x}_j^t - x_j\|^2}{2\sigma_{a_t}^2}\right), \quad (3.12)$$

where the variance σ_{a_t} relates to the localization error of GPS measurements. The variance is assumed to consist of the errors of network data and GPS devices (Qudus, Noland, and Ochieng, 2005; Bierlaire, Chen, and Newman, 2013). As mentioned above, the error in previous studies is assumed as given and constant over the network, and thus the measurement probabilities are biased. Conversely, our link-based measurement model allows the value to change independently on each link $a_t \in \mathcal{A}(a_{t-1})$. The parameter σ_{a_t} is estimated by the maximum likelihood estimation at each link:

$$\sigma_{a_t} = \arg \max_{\sigma} p(\hat{\mathbf{m}}^t | a_{t-1}; \sigma), \quad (3.13)$$

where

$$p(\hat{\mathbf{m}}^t | a_{t-1}; \sigma) = \sum_{a_t \in \mathcal{A}(a_{t-1})} p(\hat{\mathbf{m}}^t | a_t; \sigma_t) p(a_t | a_{t-1}; \theta). \quad (3.14)$$

The link likelihood $p(a_t | \hat{\mathbf{m}}^t, a_{t-1})$ in Equation (3.5) is also calculated using the estimated variance σ_{a_t} by Equation (3.13).

3.5 Structural estimation

In the context of route choice analysis, identified routes by route measurement model are used as the data set to estimate the behavioral parameters of route choice model. This section focuses on the relationship between the measurement model and the behavior model, and proposes a method of structural estimation as a framework to reduce biases in the process of route measurement and parameter estimation.

3.5.1 Estimation of route choice models

A route choice model is usually estimated by the maximum likelihood estimation. In this study, the log-likelihood function of the link-based route choice model is formulated as the function of a vector of parameters θ as follows:

$$\begin{aligned} LL(\theta) &= \ln \left(\prod_z \prod_{t=2}^{T_z} p(a_t | a_{t-1}; \theta)^{\delta_{a_t}^{z,t}} \right) \\ &= \sum_z \sum_{t=2}^{T_z} \delta_{a_t}^{z,t} \ln (p(a_t | a_{t-1}; \theta)), \end{aligned} \quad (3.15)$$

where z indicates the suffix of trip, and $\delta_{a_t}^{z,t}$ equals one if trip z uses link a_t at time t , and zero, otherwise. It is assumed that $p(a_t | a_{t-1}; \theta)$ is the link-based route choice model, and the same model is used as the prior in the link-based route measurement model. θ is estimated by maximizing the log-likelihood function $LL(\theta)$:

$$\tilde{\theta} = \arg \max_{\theta} LL(\theta). \quad (3.16)$$

Note that in the case of link-based route choice models based on the recursive formulation of the dynamic programming (Fosgerau, Freijinger, and Karlstrom, 2013; Mai, Fosgerau, and Freijinger, 2015; Oyama and Hato, 2017), the algorithms that include the process of solving the Bellman equation, such as the nested fixed point (NFXP) algorithm (Rust, 1987), the nested pseudo likelihood (NPL) algorithm (Aguirregabiria and Mira, 2002), are used for parameter estimation.

3.5.2 Algorithm of structure estimation

The route measurement model based on a Bayesian approach requires a route choice model as the prior behavioral information. The vector of parameters θ is initially required to evaluate the route choice model. It is not possible to know the true value of θ in advance, and thus θ in previous studies is defined as, e.g., estimated parameters from historical or external data sources (Chen and Bierlaire, 2015), arbitrarily given (Danalet, Farooq, and Bierlaire, 2014), and assumed as uniformly distributed if no information is available (Chen and Bierlaire, 2015; Hunter, Abbeel, and Bayen, 2014). However, in any cases, it is clear that the given parameters are not consistent with the finally estimated parameters. This results in biases in both the route measurement probabilities and the estimated parameters because θ is supposed to be consistent with the final estimation result. In this study, we focus on that θ is a shared vector of parameters in the measurement and behavior models and propose a method for estimating the models while retaining the consistency of the parameters. The structural estimation method is described in Figure 3.3 and given by the following steps:

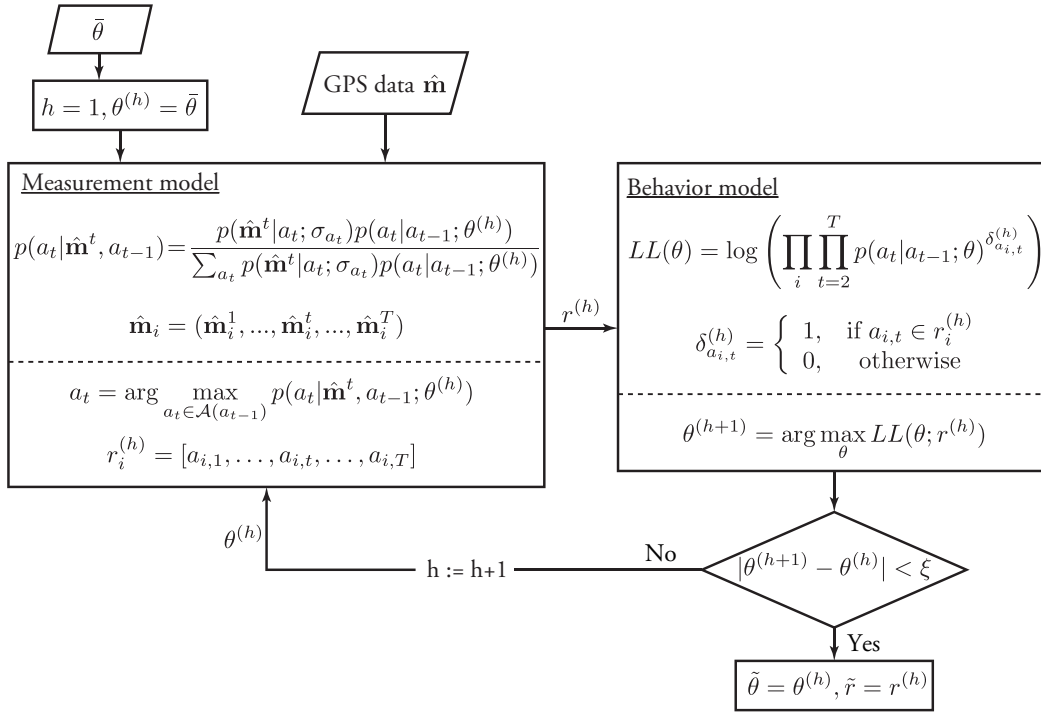


FIGURE 3.3: Flow of structural estimation method

Step 1: Initialization. Input data \hat{m} and initial parameters $\bar{\theta}$, and set $h = 1$.

Step 2: Estimation of the route measurement model. Estimate link variance σ_a and paths r by using the link-based measurement model, and set $\sigma^{(h)} = \sigma$ and $r^{(h)} = r$.

Step 3: Estimation of the route choice model. Estimate parameters θ of the link-based route choice model by the maximum likelihood estimation using estimated behavior data set $r^{(h)}$. Set $\theta^{(h+1)} = \theta$.

Step 4: Convergence Check. Finish the algorithm if the following inequality with convergence tolerance ξ is satisfied:

$$|\theta^{(h+1)} - \theta^{(h)}| < \xi, \quad (3.17)$$

then $\tilde{\theta} = \theta^{(h)}$, $\tilde{\sigma} = \sigma^{(h)}$ and $\tilde{r} = r^{(h)}$. Otherwise, set $h = h + 1$ and back to Step 2.

The algorithm iterates the process of measurement and estimation until the parameters of the route choice model arrive at a fixed point. Note that this study leads to an efficient computation and reduces the memory space by sequentially identifying links sequentially in the measurement model. For this reason, we optimize the likelihood for each model in two-stages. We consider the extension to the framework of joint estimation and the proofs of solution's existence and uniqueness as the future works, which are discussed in the end. In this paper, we use several numerical examples to examine the properties of our models.

3.6 Numerical examples

In this section, we show two numerical examples. In the simulation analysis based on a simple network, we examine the link measurement accuracy and the parameter estimation results, under the condition that we know the true values. Subsequently, we use real data of a pedestrian network in a city center and estimate a route choice model by using the proposed framework.

3.6.1 Simulation analysis

We first examine the proposed models using a simple network of Figure 3.4. The numbers in the parenthesis on each link indicates the continuous cost CC_a , the discrete cost DC_a (1 or 0) and the variance of the measurement error σ_a , respectively. In the network, we assume the inter-link heteroscedasticity of the measurement errors: links on the line $x_2 = 30$ and $x_2 = 60$ have large variances $\sigma = 10$ and $\sigma = 20$, respectively, and the other links have small variance $\sigma = 5$. Figure 3.5 shows examples of the plots of two sampled paths that pass links with different variances from each other. The locations generated from path (b) have larger errors (are observed as more distant from the true values) compared to path (a), because path (b) uses the links with large variances. Simulations assume pedestrian route choice behavior and are conducted with a first-order Markov model that corresponds to the myopic link choice (MyL) model (Oyama and Hato, 2017). The link utility function and the link choice probability are formulated as follows:

$$u(a_{t+1}|a_t) = \theta_1 LC_{a_{t+1}} + \theta_2 CC_{a_{t+1}} + \theta_3 DC_{a_{t+1}} + \theta_4 UT_{a_{t+1}|a_t}, \quad (3.18)$$

and

$$p(a_{t+1}|a_t) = \frac{\exp\{u(a_{t+1}|a_t)\}}{\sum_{a_{t+1} \in \mathcal{A}(a_t)} \exp\{u(a_{t+1}|a_t)\}}, \quad (3.19)$$

where LC_a is the length of link a and $UT_{a'|a}$ is a u-turn dummy variable that equals one, if the up node of link a corresponds to the down node of link a' , and zero otherwise. We set the interval of the time discretization as $\bar{t} = 30s$ and the interval of measurements as $\hat{\tau}_n - \hat{\tau}_{n-1} = 10s$. Given the parameter $\bar{\theta} = [-0.1, -2, -1.5, -4]$ (TRUE values), we generate 50 routes and the sequences of measurements corresponding to the routes.

Table 3.1 indicates the measurement accuracy and the difference of estimated $\tilde{\sigma}$ from the true value σ^* in each model. The measurement accuracy is calculated as the ratio of correspondence of the identified link \tilde{a}_t to the true (simulated) link a_t^* . The estimation error of σ is,

$$\frac{1}{|\mathcal{Z}||T|} |\tilde{\sigma}_a - \sigma_a^*|, \quad (3.20)$$

where $|\mathcal{Z}||T|$ is the sample size, i.e., the number of link observations.

In Table 3.1, $\theta = [0, 0, 0, 0]$ means that the measurement model does not use the prior (no information). Model 1 also assumes the constant variance of measurement error over the network, $\sigma_a = 20$ ($\forall a \in \mathcal{A}$), and the measurement accuracy is 54.57 %. Model 2 estimates the link-specific variances, and the measurement accuracy is 76.86 %, and this indicates that the estimation of σ refines the measurement accuracy. Also, in all cases, the switching algorithm (Appendix A.1) refines both the link measurement accuracy and the estimation result of σ .

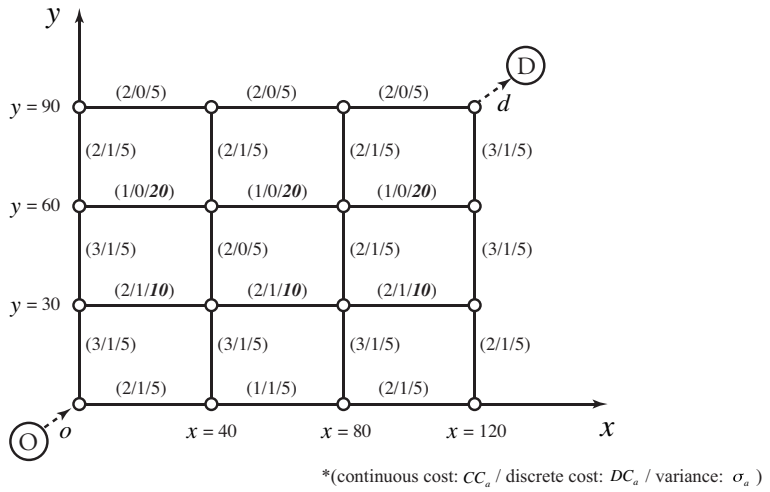
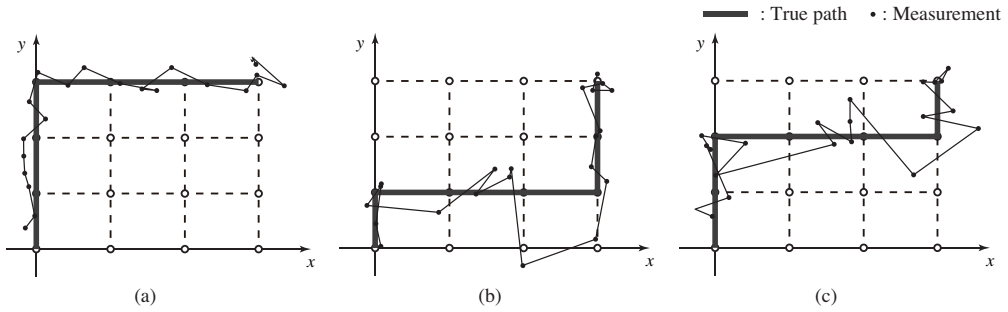


FIGURE 3.4: Simulation network


 FIGURE 3.5: Examples of plots and the effect of σ_a

Model 3 and 4 incorporate the prior probability into the measurement model. In the case that we use the true parameters as the prior and the switching algorithm (model 4), we achieve 91.71 % accuracy of link measurement. Conversely, in the case of model 3 that uses the parameters completely different from the true values, the results are less accurate compared to the case without the prior information (model 1, 2). This indicates that the inaccurate prior has a large effect on and corrects the measurement in the wrong direction, in the situation that the measurement uncertainty is large, e.g., when we have few measurements, when localization is weak, and when the network is dense.

 TABLE 3.1: Accuracy and the difference of σ in each model

Model	σ	$\bar{\theta}$	Link accuracy(%)		Ave. $ \tilde{\sigma}_a - \sigma_a^* $	
			-	Switching	-	Switching
1	Given	[0, 0, 0, 0]	54.57	68.86	-	-
2	Estimated	[0, 0, 0, 0]	76.86	82.86	5.848	4.40
3	Estimated	[-1.5, -0.1, -2, -10]	4.86	38.29	41.99	21.21
4	Estimated	[-0.1, -2, -1.5, -4]	76.86	91.71	7.58	4.06

Using model 2 and model 3 in Table 3.1, we identify the routes and estimate the route choice model of Equation (3.18) and (3.19). Table 3.2 reports the estimation results. "One-way" in the table denotes the estimation result obtained by using behavioral data reproduced from the measurement model with $\bar{\theta}$, which denotes the

initially given parameters. "Structural estimation" indicates the result from the iteration process of the structural estimation in Figure 3.3.

We set the convergence tolerance as $\xi = 1e - 10$. The sample is the number of observed link choices (in the 50 routes). Note that the initial log-likelihoods $LL(0)$ of "One-way" are different between model 2 and 3 because the identified route sets, which is the data sets for estimating route choice models, depend on the initial value of the prior $\bar{\theta}$.

In both cases of (a) $\bar{\theta} = [0, 0, 0, 0]$ (model 2) and (b) $\bar{\theta} = [-1.5, -0.1, -2, -10]$ (model 3), "One-way" estimation results are largely different from the true values: the total differences correspond to 3.643 and 6.058, respectively. As seen in Table 3.1, the link measurement accuracies of model 2 and 3 are not high, and the estimation results of route choice models are biased. In model 3, it is also seen that positive and negative signs are reversed, and the estimated values differ from the initial values as well as from the true values. It is assumed that the prior does not correct the measurement and instead functions as a noise.

In contrast, the results of the structural estimation are refined by the iteration process of measurement and estimation, and the estimated parameters exhibit values close to the true values. Moreover, both of two tested models converge to the same values, irrespective of $\bar{\theta}$. The t-values and $\bar{\rho}^2$ are also refined. These results indicate the effectiveness of our structural estimation method. It should be noted that we obtain the same converged values in the cases that we set initial value of the prior as $\bar{\theta} = [-10, -10, -10, -10], [-100, 0, 0, 0], [-100, -100, -100, -100], [10, 10, 10, 10]$.

We also test the convergence process for several cases with different initial parameters of the route choice model $\bar{\theta}$ in Figure 3.6. The horizontal axis and the vertical axis of the figure indicate the difference between the convergence value and the h -th estimated value of θ and σ , respectively. We use the two cases discussed above: (a) $\bar{\theta} = [0, 0, 0, 0]$ (no information) and (b) $\bar{\theta} = [-1.5, -0.1, -2, -10]$ (wrong parameter set), and additional two cases (c) $\bar{\theta} = [-0.1, -2, -1.5, -4]$ (the true values) and (d) $\bar{\theta} = [10, 10, 10, 10]$ (another wrong parameter set). In all cases, regardless of the largely different values from the true parameters, the models converge in a small number of iterations and with little vibration.

Additionally, in order to examine the dependence of estimation results on samples, we generate 100 datasets using model 2 ($\bar{\theta} = [0, 0, 0, 0]$) and implement the structural estimation for each dataset. Table 3.3 reports the averages and the standard deviations of estimated parameters of route choice model, the number of iterations, and computational time. While we obtain the estimate with respect to travel time (θ_1) close to the true value stably, the estimates of the other parameters are different from the true values. However, all parameters are closer to the true value than the initial parameters ($\bar{\theta} = [0, 0, 0, 0]$), and it is expected that enriching the measurement model improves the estimation results. With respect to the estimated parameter of the u-turn dummy variable, the standard deviation is large. It is assumed that the number of path observations including u-turns is small because we consider the large resistance for u-turns in the true model ($\theta_4^* = -4$). The averages of the number of iterations and the computational time correspond to 4.086 and 858.2 seconds, respectively. Note that in these experiments, there are seven cases in which the structural estimation does not converge out of 100 cases. We show the possibility that the structural estimation converges regardless of the initial parameter settings; however, the experiment indicates that the convergence depends on samples and the structural estimation remains a challenge for the convergence property. We consider an extension to the analytical framework as an important future study, which is addressed in further detail in Section 3.7.2.

TABLE 3.2: Structural estimation results

(a) Input: $\bar{\theta} = [0, 0, 0, 0]$ (model 2, no information)

	One-way			Structural Estimation			
	TRUE	Estimates	abs(diff.*)	t-value	Estimates	abs(diff.)	t-value
θ_1	-0.1	0.002	0.102	0.101	-0.064	0.036	-2.562
θ_2	-2	-0.755	1.245	-4.164	-1.727	0.273	-6.882
θ_3	-1.5	-1.312	0.188	-4.772	-1.046	0.454	-3.519
θ_4	-4	-1.892	2.108	-8.864	-3.519	0.481	-9.739
total error		3.643			1.244		
sample			350			350	
$LL(0)$				-373.221			-371.887
$LL(\tilde{\theta})$				-269.872			-211.308
$\bar{\rho}^2$			0.266				0.421
iteration							6

(b) Input: $\bar{\theta} = [-1.5, -0.1, -2, -10]$ (model 3, wrong values)

	One-way			Structural Estimation			
	TRUE	Estimates	abs(diff.)	t-value	Estimates	abs(diff.)	t-value
θ_1	-0.1	-0.097	0.003	-5.312	-0.064	0.036	-2.562
θ_2	-2	-0.419	1.581	-2.710	-1.727	0.273	-6.882
θ_3	-1.5	0.178	1.678	0.963	-1.046	0.454	-3.519
θ_4	-4	-1.204	2.796	-6.774	-3.519	0.481	-9.739
total error		6.058			1.244		
sample			350			350	
$LL(0)$				-373.560			-371.887
$LL(\tilde{\theta})$				-328.587			-211.308
$\bar{\rho}^2$			0.110				0.421
iteration							8

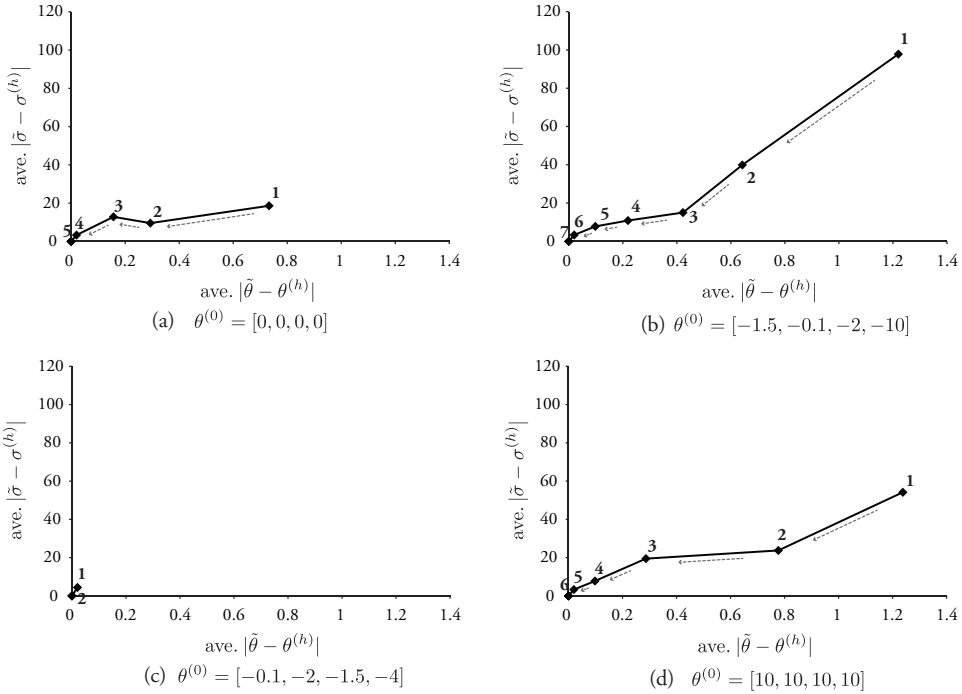


FIGURE 3.6: Convergence processes

TABLE 3.3: Average and standard deviation of estimated parameters, the number of iterations and computational time for 100 structural estimations

	$\bar{\theta}_1$	$\bar{\theta}_2$	$\bar{\theta}_3$	$\bar{\theta}_4$	Iteration	CPU time (s)
Ave.	-0.112	-1.140	-1.006	-2.916	4.086	858.2
Std. err.	0.023	0.663	0.413	4.006	1.007	229.7

3.6.2 Real data analysis

Finally, we test the proposed method based on real GPS data of pedestrians in a dense city center network. The data is obtained from Probe Person (PP) surveys in Matsuyama city, Japan. The PP surveys use an automatic recording system of position and time based on GPS and Internet communications by using cellular phones (Hato, 2006), where the accurate travel information such as trajectories and behavior contexts is observed throughout the survey (Hato, 2010). The data is used to observe routes and estimate parameters of the pedestrian route choice model by the structural estimation method.

We use a MyL model in a manner similar to the simulation analysis. The utility function when a pedestrian moves from link a_t to a_{t+1} are defined as follows:

$$u(a_{t+1}|a_t) = \theta_1 \text{LU}_{a_{t+1}} + \theta_2 \text{CU}_{a_{t+1}} + \theta_3 \text{DU}_{a_{t+1}} + \theta_4 \text{UT}_{a_{t+1}|a_t}, \quad (3.21)$$

where LU_a is the link length [m], CU_a is the width of sidewalk [m], DU_a is the arcade dummy variable, and $\text{UT}_{a'|a}$ is the u-turn dummy variable. The link choice probability is given by Equation (3.19). We set the initial values as $\bar{\theta} = [0, 0, 0, 0]$ and randomly select 30 trips that include a total of 792 locations and 270 link choices. The route choice model is estimated with the structural estimation method. The convergence tolerance is set as $\xi = 1e - 10$.

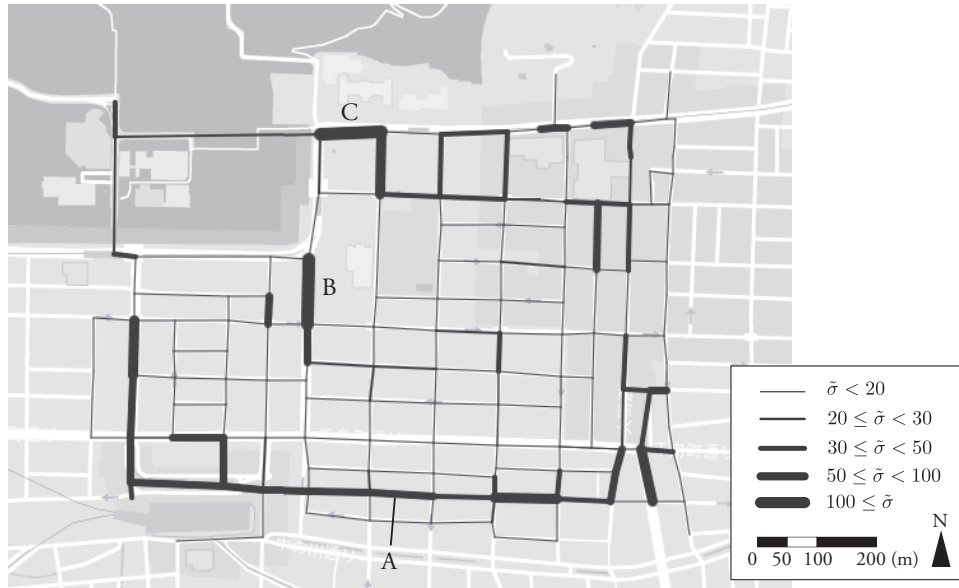
TABLE 3.4: Structural estimation result using Probe Person data

Input: $\bar{\theta} = [0, 0, 0, 0]$ (No information)		One-way		Structural Estimation	
	Estimates	t-value	Estimates	t-value	
$\tilde{\theta}_1$	-0.007	-2.473	-0.001	-0.428	
$\tilde{\theta}_2$	0.088	1.497	0.134	1.582	
$\tilde{\theta}_3$	-0.004	-0.011	2.760	4.288	
$\tilde{\theta}_4$	0.774	0.532	0.469	3.344	
sample		270		270	
$LL(0)$		-307.608		-309.066	
$LL(\tilde{\theta})$		-302.174		-225.162	
$\bar{\rho}^2$		0.005		0.259	
iteration					11

Table 3.4 reports the estimation result. "One-way" shows the result in which we estimate the route choice model based on the identified routes without prior information. Compared to the result, the structural estimation exhibits better values of final log-likelihood $LL(\tilde{\theta})$ and $\bar{\rho}^2$. With respect to the result of the one-way model, the parameter of link length (travel time) θ_1 shows the significant sign. In contrast, with respect to the result of the structural estimation, θ_1 is not significant; or rather, the parameters of arcade dummy variable (θ_3) and the u-turn dummy variable (θ_4) show the significant signs. These results indicate a possibility that without the prior behavioral information, it is not possible to observe the choice of links with arcade due to large measurement uncertainty, and thus the biased preference of route choice behavior is estimated, as the travel time is the sole significant parameter in the one-way model. In fact, several previous studies report that pedestrian route choices are affected by the presence of attractors rather than congestion level or travel time, differently from other transportation modes (Kurose, Borgers, and Timmermans, 2001; Borst et al., 2008).

Moreover, we plot the estimation results of link-specific variance of measurement error σ_a that are obtained in the link-based route measurement model, on the network (Figure 3.7). The line weights in Figure 3.7 show the size of variance. The result shows that the spatial distribution of the variance is not at all uniform over the network. This suggests that the assumption in previous studies of a given and constant value of variance over network can lead to biases in the route measurement process.

Also, we check the estimated variance on each link and obtain several meaningful results. Street A in Figure 3.7 that consists of linearly connected multiple links corresponds to the main shopping street that has an arcade with a low height. It is assumed that the existence of the arcade makes the variance larger than other streets. Specifically, B and C are the links in front of the city hall and the prefecture hall, respectively. These halls are often chosen as the destination of travelers in the data used for the case study. On the PP surveys, participants manually report the end of trips on their cellar phones. Therefore, it is assumed the information of locations after they enter the buildings of the destination is often included in trips, and the variances of links B and C increase due to the errors of the inside of buildings. In both cases, they are realistic results for the Matsuyama network.

FIGURE 3.7: Plot of estimated σ of each link

3.7 Conclusion and discussion

3.7.1 Conclusion of the paper

In extant studies, the estimation process of route choice model with measurement uncertainty includes biases caused from the initial parameter settings that are required in probabilistic route measurement models. This study focuses on the mechanism of the increase in estimation biases that depends on the relationship between route measurement and route choice models, and we propose a novel framework to estimate route choice parameters with less biases.

This study begins to introduce the link-based route measurement model, based on the assumption of sequential link choice behavior. The sequential link identification helps in clarifying the relationship between each measurement and the candidate set of true links, and thus the link-based route measurement model allows the estimation of the *link-specific* variance of GPS measurement error. In previous studies, this variance has been assumed to be a given and constant value over network, which leads to biases in the evaluation of route measurement probability. The biases can significantly increase in urban pedestrian networks because the network is often dense compared to the size of measurement error, and the variance depends on spatial attributes of each link. The link-based route measurement model is proposed to consider and solve this problem.

Also, we use a link-based route choice model as the prior information based on the Bayesian approach to correct the measurement probability by considering the route choice mechanism without the path enumeration. Furthermore, we focus on the possible bias due to the incorporation of the prior and propose a framework of structural estimation to reduce the biases. The parameter of route choice model that is used as the prior is supposed to be finally estimated based on route choice data identified by route measurement model. The structural estimation is the method for solving the fixed point problem between the prior and the estimation result of the route choice model.

The numerical results involve confirming the effectiveness of the estimation of

the link-specific variance and the switching algorithm to refine the route measurement. We also recognize that the measurement result is highly dependent on the behavioral parameters when we incorporate the prior into the measurement model and the measurement uncertainty is large. With respect to the structural estimation results, the parameters converge to the same values irrespective of initial parameter settings, and we obtain estimates closer to the true values compared to the case without the structural estimation. Ultimately, we use a real GPS data of pedestrians in a city center network, and the structural estimation reveals the choice mechanism of arcade link that is typically difficult to identify. Moreover, the distribution of the estimated variances of measurement error is realistic. The results verify the effectiveness of our framework.

3.7.2 Discussion for the future research

In the end, we would like to discuss prospects for the future research. In this paper, we propose a framework to sequentially determine links in a route measurement model. Through the numerical examples, we obtain the convergence and meaningful results. However, it is expected to clarify the theoretical properties of the framework, such as existence, uniqueness, and convergence of the solution, in future studies. The next work should focus on extending the framework to the joint estimation of route measurement and route choice models by maximizing the following likelihood function:

$$p(\hat{\mathbf{m}}_{1:T}; \sigma, \theta) = \sum_{a_{1:T} \in \mathcal{P}} p(\hat{\mathbf{m}}_{1:T}|a_{1:T}; \sigma)p(a_{1:T}; \theta), \quad (3.22)$$

where \mathcal{P} is the set of path candidates that is generated in the process of the link-based route measurement model, and $\hat{\mathbf{m}}_{1:T}$ and $a_{1:T}$ are the arrays of measurements and links from $t = 1$ to $t = T$, respectively. Equation (3.22) indicates the probability that the sequence of measurements $\hat{\mathbf{m}}_{1:T}$ is reproduced by the route measurement model and the route choice model. Both σ and θ are estimated at the same time as the solutions of the maximization problem of Equation (3.22). However with respect to the calculation of Equation (3.22), in the link-based route measurement model it is required to preserve the link measurement probabilities at each time period and then to calculate the path measurement probabilities as the products of link measurement probabilities. The calculation cost depends on the number of paths $|\mathcal{P}|$ and is expensive due to the combinatorial complexity. Bierlaire, Chen, and Newman, 2013 proposed a method for efficiently calculating measurement probabilities of paths; however, the path-based approach cannot identify the link-specific variances of measurement errors as we discussed in Section 3.2. Therefore, a future study should include the development of algorithms of preserving link measurement probabilities and maximizing the likelihood of the joint estimation. The examination of the above-mentioned theoretical properties of the framework is included. Additionally, the statistical test of the relationship between the spatial attributes of links and σ_a and the elaboration of the simulation analysis in various cases are interesting topics for future research.

Chapter 4

Dynamic sequential route choice model for dynamic network analysis

In this chapter, we propose a dynamic sequential route choice model, which is a generalized formulation of global and myopic decisions in route choice behavior.

Emerging sensing technologies such as probe vehicles equipped with Global Positioning System (GPS) devices on board provide us real-time vehicle trajectories that are helpful for the understanding of the cases, which are significant, but difficult to observe because of its infrequency, such as gridlock networks. On the premise of this type of emerging technology, this paper propose a novel route choice model that describes route choice behavior, both in ordinary networks, where drivers acquire spatial knowledge of networks through their experiences, and in extraordinary networks, which are situations that drivers rarely experience, and applicable to real-time traffic simulations. In extraordinary networks, drivers do not have any experience or appropriate information. In such a context, drivers have little spatial knowledge of networks and choose routes based on dynamic decision making, which is sequential and somewhat forward-looking. In order to model these decision-making dynamics, we propose a dynamic sequential route choice model using a sequential discount rate, which is a discount factor of expected future utility. Through illustrative examples, we show that the sequential discount rate reflects drivers' decision-making dynamics, and myopic decisions can confound the network congestion level. We also estimate the parameters of the proposed model using a probe taxis' trajectory data collected on March 4, 2011 and on March 11, 2011, when the Great East Japan Earthquake occurred in the Tokyo Metropolitan area. The results show that the sequential discount rate has a lower value in gridlock networks than in ordinary networks.

Keywords: Route choice model, Dynamic discrete choice model, Sequential discount rate, Urban gridlock, Trajectory data, Probe vehicles

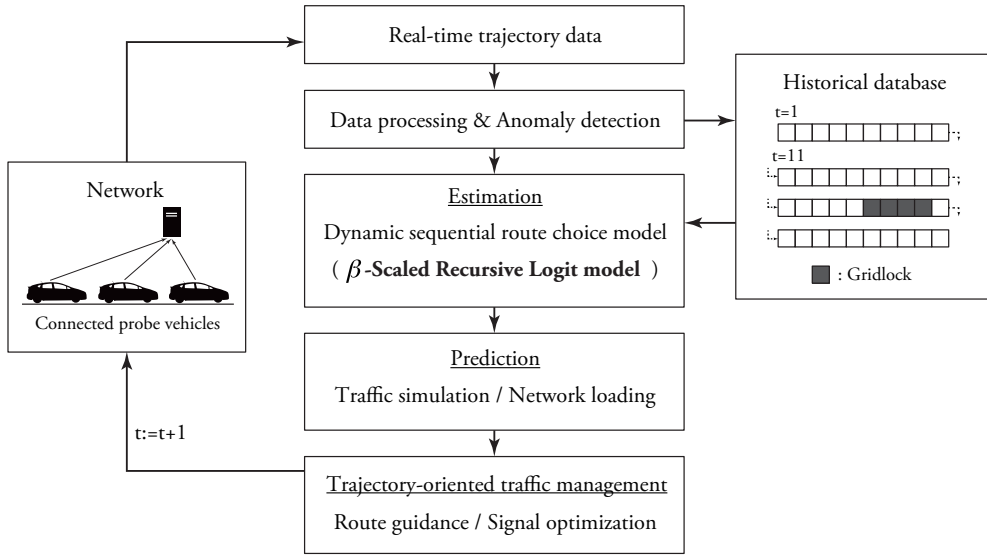


FIGURE 4.1: Framework of trajectory-oriented gridlock network management

4.1 Introduction

A gridlock network is an extraordinary situation that drivers do not usually experience, unlike congestion due to accidents, construction, rush hour, and special events. In gridlock networks, drivers cannot make global decisions for their route choice because of which they travel in confusion. These extraordinary route choice mechanisms may confound the network situation. Therefore, technologies to observe and analyze these behaviors are needed.

The mainstream method of traffic congestion control is the crossing or area control (Daganzo, 2007; Geroliminis and Daganzo, 2008) that is based on traditional vehicle detection sensors, but this method cannot deal with network-based congestion spread, which is critical in dealing with gridlock networks. On the other hand, emerging sensor technologies such as probe vehicles equipped with global positioning system (GPS) devices are helpful to understand the infrequent but significant behavior of each vehicle in gridlock networks. Using certain type of vehicles as probe vehicles, such as taxis or buses, has increased the monitoring capability (Dailey and Cathey, 2002). This emerging sensor technique is now ubiquitous and provides real-time information of vehicle trajectories, while traditional vehicle detection sensors provide only flow or density at fixed locations.

In this paper, on the premise of this type of emerging technology, we aim at developing a novel route choice model applicable to a trajectory-oriented framework for gridlock network analysis and management (Figure 4.1). The management method is based on traffic simulations using trajectories from real-time and ubiquitous technologies in contrast to the previous route choice models that require the choice set generation (e.g., Bekhor, Ben-Akiva, and Ramming, 2006) and the information regarding entire trips, including origin and destination for estimating parameters. Herein, we propose a dynamic sequential route choice model that does not require the information of entire trips to estimate parameters. Using the model, in the framework of Figure 4.1, the parameter estimation is implemented at each time period, because we assume that not only network situations but also behavioral preferences can change at different time periods.

Moreover, previous route choice models describe only the route choice behavior of habitual drivers in daily networks. In a route choice modeling context, it is assumed that drivers usually acquire spatial knowledge of networks through direct environmental experiences (Gale et al., 1990). That is, they postulate that drivers have global spatial cognition to evaluate the path utilities of all alternatives. Contrary to such a daily route choice model, in extraordinary situations such as natural hazards or urban gridlocks, drivers' route choice behavior has distinctive features. They are non-habitual situations where drivers' have no experience. Moreover, drivers cannot gain appropriate information because of network disarray, as a result, they have little spatial knowledge of networks. In such a situation, route choice decisions become sequential and somewhat forward-looking, that is, drivers choose routes based on dynamic decision making.

This study aims at developing a route choice model, which describes both route choice behavior in ordinary networks and gridlock networks, and focuses on the decision-making dynamics in sequential route choice models. Existing sequential route choice models (e.g., Baillon and Cominetti, 2008; Fosgerau, Freijinger, and Karlstrom, 2013) formulate route choice behavior based on sequential link choices conveniently; however, they do not discuss the serializability of decisions and result in the equivalent path probability to the path-based MNL model. To the contrary, we deal with the dynamic sequential decisions of drivers, which mean that the decisions at possible future states affect the decision at the current state. For this reason, we apply the concept of a discount factor in the dynamic discrete choice model (Rust, 1987) and formulate a dynamic sequential route choice model, where the dynamics is within a trip. Note that we model the dynamics of decisions as the mechanism of route choice behavior, as opposed to dealing with the route switching/adaptation behavior in time-dependent networks as previous dynamic route choice models do: therefore, the targets are different from each other. It is possible to combine both the dynamics of decisions and networks; however, in this study we concentrate on the former and assume a static and deterministic network to clarify the impact of decision-making dynamics in route choice models.

We also estimate parameters of the route choice model as a disaggregate discrete choice model, rather than macroscopic analyses of extraordinary networks (Daganzo, 2007; Mahmassani, Saberi, and Zockaei, 2013). Real-time parameter estimation and traffic simulations are significant for gridlock network management; however, path-based route choice models require the information on entire paths of trips and choice set generations. On the other hand, sequential route choice models require the information of only link transitions and the destination, for parameter estimation, and these are applicable to emerging real-time sensing technologies. Moreover, we focus on the change of route choice mechanisms in each network condition and compare the estimation results among multiple time periods over two very different days (ordinary/extraordinary) using probe-vehicle data. One of the days is that of the Great East Japan Earthquake.

The paper is organized as follows. In Section 4.2, we present a literature review of dynamic route choice models, which describe the route decision-making process en-route, as opposed to pre-trip route choice models and sequential link choice models. In Section 4.3, we formulate a route choice model as a simple extension of the recursive logit model (Fosgerau, Freijinger, and Karlstrom, 2013) using the concept of a sequential discount rate. In Section 4.4, we give illustrative examples to show the difference between route choice models based on global decision and those based on myopic decisions. In Section 4.5, we then discuss the comparison of estimation results using probe-vehicle data in the Tokyo Metropolitan area. Conclusions and

discussion of future research directions are provided in the end.

4.2 Literature review

Most existing route choice models describe the route choice behavior of habitual drivers in deterministic networks, e.g., C-logit (Cascetta et al., 1996), Link-Nested Logit (Vovsha and Bekhor, 1998) and Path Size Logit (Ben-Akiva and Bierlaire, 1999). In these studies, drivers choose routes *pre-trip* and do not change the routes *en-route*: that is, the dynamics of route choice behavior is ignored. We review here dynamic route choice models, which describe the route decision processes *en-route* rather than *pre-trip* route choices, and classify them into two kind of models: route choice models in dynamic networks and sequential link choice models. We summarize dynamic route choice models in Table 4.1.

TABLE 4.1: Dynamic route choice models

Model type	Authors	Network	Choice set	Routing	Decision making	Parameter estimation (Data requirement)
Static route choice model	Cascetta(1996), Ben-Akiva and Bierlaire (1999)	Static/Deterministic	Given	Pre-trip	Global	✓ (O, D, whole paths)
Route switching model	Ben-Akiva(1991), Mahmassani and Liu(1999)	Dynamic/Deterministic	Given	Pre-trip+En-route	Global	✓ (O, D, whole paths)
Routing policy model	Gao(2005), Gao et al.(2010)	Dynamic/Stochastic	Given	Pre-trip+En-route	Global	✓ (O, D, whole paths)
Markov chain model	Sasaki(1965)	Static/Deterministic	No enumeration	En-route	Myopic	
Sequential route choice model	Gentile and Papola(2006), Baillon and Cominetti (2008)	Static/Deterministic	No enumeration	En-route	Global	
Recursive logit model	Fosgerau et al.(2013), Mai et al.(2015), Mai (2016)	Static/Deterministic	No enumeration	En-route	Global	✓ (D, link transitions)
β -scaled recursive logit model	This study	Static/Deterministic	No enumeration	En-route	Global+ Myopic	✓ (D, link transitions)

4.2.1 Route choice models in dynamic networks

In the context of route choice model, "dynamics" usually indicates that network conditions are stochastic and dependent on real-time information (e.g., Ben-Akiva, De Palma, and Isam, 1991; Abdel-Aty, Kitamura, and Jovanis, 1997; Mahmassani and Liu, 1999; Dia, 2002; Abdel-Aty and FathyAbdalla, 2006) or uncertainty (e.g., Peeta and Yu, 2005; Palma and Picard, 2005; Gao, Freijinger, and Ben-Akiva, 2010). Dynamic route choice models describe the route switching behavior from a previous chosen or experienced route and have been applied in DYNASMART (Mahmassani, 2001), DynaMIT (Ben-Akiva et al., 1997; Ben-Akiva et al., 2002) and EVAQ (Pel, Bliemer, and Hoogendoorn, 2009). Route choice studies in networks with risks have incorporated the concept of decision rules, including elimination by aspects (Tversky, 1972), fuzzy logic (Zadeh, 1965) and cumulative prospect theory (Tversky and Kahneman, 1992). Morikawa and Miwa, 2006 and Li, Miwa, and Morikawa, 2014 have analyzed driver's decision process. We can see the review of travel behavior modeling from the viewpoint of evacuation behavior in Pel, Bliemer, and Hoogendoorn, 2012.

However, previous dynamic route choice models deal with the route choice behavior in habitual networks, where drivers have spatial knowledge based on environmental experiences, regardless of whether there are risks or not. In such a context, route choice behavior is based on global spatial cognition over networks and described as path-based choice, which is a joint choice of the links identifying a path. In this study, to describe route choice behavior not only in habitual but

also non-habitual networks, where drivers have little experiences or network knowledge, we model the dynamics of decision making within a trip rather than dynamics of network conditions.

4.2.2 Sequential route choice models

Decision making dynamics refers to the drivers' forward-looking decision mechanism. Sequential route choice models (e.g., Gentile and Papola, 2006; Baillon and Cominetti, 2008; Fosgerau, Frejinger, and Karlstrom, 2013) assume that drivers reach destinations through successive link choices rather than choosing jointly all the links identifying a path. In these studies, path choice probability is described as a product of link transition probabilities as follows:

$$\mathbb{P}(\sigma = [a_1, \dots, a_J]) = \prod_{j=1}^{J-1} p(a_{j+1}|a_j), \quad (4.1)$$

where a path σ is a sequence of links $a_1, \dots, a_J \in \mathcal{A}$ and \mathcal{A} is the set of all links of the network. This assumption that drivers choose the next link at each intersection is realistic, especially in non-habitual networks. Moreover, Baillon and Cominetti, 2008 and Fosgerau, Frejinger, and Karlstrom, 2013 can consider all possible paths including cyclic ones, which are also assumed to be important in gridlock networks. Note that the idea of using link transition probabilities was proposed in the context of traffic assignment (Sasaki, 1965; Bell, 1995; Akamatsu, 1996; Baillon and Cominetti, 2008) to avoid the path enumeration. Fosgerau, Frejinger, and Karlstrom, 2013 link the idea to the infinite multinomial logit model in the context of route choice analysis, using dynamic discrete choice models (Rust, 1987). We briefly introduce the recursive logit (RL) model proposed by Fosgerau, Frejinger, and Karlstrom, 2013 here, since our model is an extension of the RL model.

Consider a directed connected graph $\mathcal{G} = (\mathcal{A}, \mathcal{N})$, where \mathcal{A} is the set of links and \mathcal{N} is the set of nodes. It is assumed that a driver chooses a link a_{j+1} in the set of outgoing links $\mathcal{A}(a_j)$, which maximizes the sum of instantaneous utility $u(a_{j+1}|a_j)$ associated with each link pair and expected downstream utility to destination link d $V^d(a_{t+1})$ that is given as a value function and formulated via the Bellman equation (Bellman, 1957) as follows:

$$V^d(a_j) = \mathbb{E} \left[\max_{a_{j+1} \in \mathcal{A}(a_j)} \{v(a_{j+1}|a_j; \theta) + V^d(a_{j+1}) + \mu \varepsilon(a_{j+1})\} \right] \quad \forall a_j \in \mathcal{A}, \quad (4.2)$$

where $v(a_{j+1}|a_j; \theta) = v(x_{a_{t+1}|a_t}; \theta)$ is the deterministic utility component, $x_{a_{t+1}|a_t}$ is a vector of observed characteristics of the link pair (a_j, a_{j+1}) and θ is an unknown parameter vector to be estimated. It is the main difference of the RL model from previous sequential link choice models (e.g., Gentile and Papola, 2006; Baillon and Cominetti, 2008) that it allows to estimate its parameters by providing an interpretation of the model as a dynamic discrete choice model. The random term ε is assumed to be an i.i.d extreme value I with zero mean, the dummy link for the destination d has no successor, and the union of the link set and the dummy link is denoted as $\tilde{\mathcal{A}} = \mathcal{A} \cup d$. The probability of choosing a link a_{j+1} given state a_j is:

$$p(a_{j+1}|a_j) = \frac{e^{\frac{1}{\mu} \{v(a_{j+1}|a_j) + V(a_{j+1})\}}}{\sum_{a'_{j+1} \in \mathcal{A}(a_j)} e^{\frac{1}{\mu} \{v(a'_{j+1}|a_j) + V(a'_{j+1})\}}}, \quad (4.3)$$

which is the multinomial logit model. Path probability in the RL model is also given by Equation (4.1). By the assumption of the random term distribution, Equation (4.2) is re-formulated as a logsum:

$$V^d(a_j) = \begin{cases} \mu \log \sum_{a_{j+1} \in \mathcal{A}} \delta(a_{j+1}|a_j) e^{\frac{1}{\mu} \{v(a_{j+1}|a_j) + V^d(a_{j+1})\}}, & a_j \in \mathcal{A} \\ 0, & a_j = d, \end{cases} \quad (4.4)$$

where $\delta(a_{j+1}|a_j)$ is an indicator that equals one if $a_{j+1} \in \mathcal{A}(a_j)$ and zero otherwise. Since the destination link d has no outgoing link, $V^d(d)$ is set to zero.

In order to calculate the probability of link choices, the Bellman equation must be solved, and Equation (4.4) is transformed by taking the exponential,

$$e^{\frac{V^d(a_j)}{\mu}} = \begin{cases} \sum_{a_{j+1} \in \mathcal{A}} \delta(a_{j+1}|a_j) e^{\frac{1}{\mu} \{v(a_{j+1}|a_j) + V^d(a_{j+1})\}}, & a_j \in \mathcal{A} \\ 1, & a_j = d. \end{cases} \quad (4.5)$$

Moreover, the matrix $\mathbf{z}(|\tilde{\mathcal{A}}| \times 1)$ and $\mathbf{M}(|\tilde{\mathcal{A}}| \times |\tilde{\mathcal{A}}|)$ are defined with entries

$$z_{a_j} = e^{\frac{V^d(a_j)}{\mu}}, M_{a_j a_{j+1}} = \delta(a_{j+1}|a_j) e^{\frac{v(a_{j+1}|a_j)}{\mu}} \quad (4.6)$$

The value functions are the solutions to the following equation:

$$\mathbf{z} = \mathbf{Mz} + \mathbf{b} \quad (4.7)$$

where $\mathbf{b}(|\tilde{\mathcal{A}}| \times 1)$ is a vector with zero value for all states except for the destination, where it equals 1. The value functions are evaluated by solving the system of linear Equation (4.7), and in Fosgerau, Freijinger, and Karlstrom, 2013, it is solved using the inverse matrix of $\mathbf{I} - \mathbf{M}$.

The RL model describes the decision-making dynamics, which is a sequential and forward-looking decision, by incorporating the value function into the link utility function. However, it assumes global spatial cognition similar to previous *pre-trip* route choice models, because it is known that the path probabilities of the RL model correspond to those of the *pre-trip* MNL model. In other words, drivers choose routes with perfect information of all states over networks.

This study focuses on the parameter of the discount factor in dynamic discrete choice models (e.g., Rust, 1987). The review of studies of dynamic discrete choice models can be found in Cirillo and Xu, 2011, and the models describe the sequential decision in the time axis. In the context of dynamic discrete choice models, the expected future utility is described as a "discounted" utility, because decision makers regard the future states as uncertain and do not have perfect information. We assume the route choice behavior in non-habitual networks is similar to such a situation. In the context of route choices, the uncertainty of the future state means

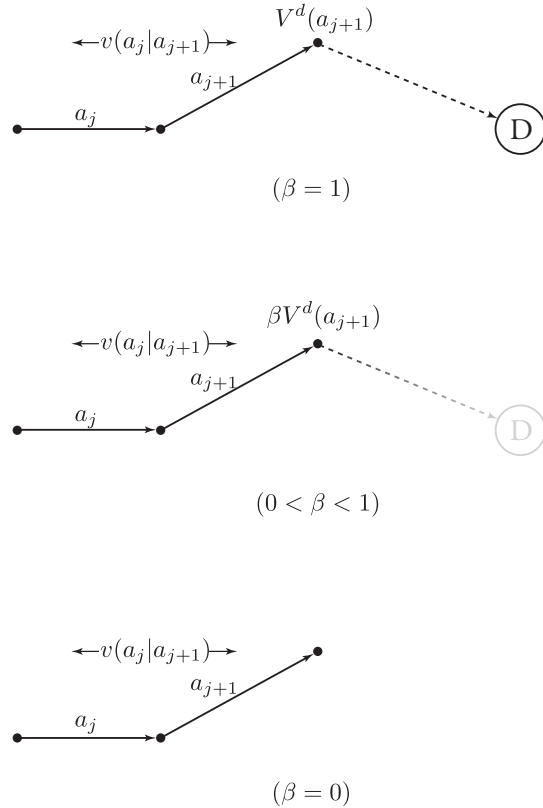


FIGURE 4.2: Decision making dynamics with different sequential discount rates

the ambiguity or lack of spatial knowledge, and a driver cannot evaluate utilities of distant space with the same weight with the utility of current links. It is natural that in extraordinary networks, such as urban gridlocks drivers find ways to get out of congestions anyway. In this study, we define the discount factor in the dynamic discrete choice model as a "sequential discount rate", which is the parameter that represents decision-making dynamics, and incorporate it into the sequential route choice models.

4.3 β -scaled recursive logit model

In this section, we present the concept of a sequential discount rate and the formulation of a route choice model referred to as the β -scaled recursive logit (β -SRL) model. Our model is an extension of the RL model that is based on sequential link choices. Note here that we model the route choice behavior in static and deterministic networks to clarify and emphasize the impact of the sequential discount rate.

4.3.1 Sequential discount rate

We first present the concept of sequential discount rate β . It is a generalization of drivers' decision-making dynamics and also a representation of the degree of spatial cognition of networks as a parameter. The sequential discount rate β is assumed to be between zero and one, and can be estimated together with other parameters θ . A large value of β means that drivers evaluate the future expected utility with great weight. Figure 4.2 shows the difference of drivers' decision making with different β .

in the context of a sequential route choice model. When β is one, drivers evaluate the expected utility of forward space V and the instantaneous utility of the next link v with equal weights, that is, route choice behavior depends on global decision over networks. On the other hand, when β is zero, drivers myopically choose the next link based only on its instantaneous utility v . In this case, the utility and probability of choosing link a_{j+1} , given a state link a_j are respectively:

$$u(a_{j+1}|a_j) = v(a_{j+1}|a_j) + \mu\varepsilon(a_{j+1}) \quad (4.8)$$

and

$$p(a_{j+1}|a_j) = \frac{e^{\frac{1}{\mu}v(a_{j+1}|a_j)}}{\sum_{a'_{j+1} \in \mathcal{A}(a_j)} e^{\frac{1}{\mu}v(a'_{j+1}|a_j)}}. \quad (4.9)$$

Equation (4.9) is the transition probability of first-order Markov chain models and indicates that drivers have only visible link conditions as the information for decision making. We define this model as a myopic link choice (MyL) model in this study.

4.3.2 Model formulation

Using the sequential discount rate, we re-formulate the value function of Equation (4.2) as follows:

$$\begin{aligned} V^d(a_j) &= \max_{a_{j+1} \in \mathcal{A}(a_j)} \mathbb{E} \left[\sum_{t=j}^{\infty} \beta^{t-j} u(a_{t+1}|a_t; \theta) \right] \\ &= \mathbb{E} \left[\max_{a_{j+1} \in \mathcal{A}(a_j)} \{v(a_{j+1}|a_j; \theta) + \beta V^d(a_{j+1}) + \mu\varepsilon(a_{j+1})\} \right], \end{aligned} \quad (4.10)$$

where $t \in \mathbb{N}_0$ is the number of decision-making from the origin link and β ($0 \leq \beta \leq 1$) is the sequential discount rate of the value function. The transition probability from link a_j to a_{j+1} is given by the multinomial logit model,

$$p(a_{j+1}|a_j) = \frac{e^{\frac{1}{\mu}\{v(a_{j+1}|a_j) + \beta V^d(a_{j+1})\}}}{\sum_{a'_{j+1} \in \mathcal{A}(a_j)} e^{\frac{1}{\mu}\{v(a'_{j+1}|a_j) + \beta V^d(a'_{j+1})\}}}. \quad (4.11)$$

The path probability of the β -SRL model is also given by Equation (4.1).

4.3.3 Solving the Bellman equation

The Bellman equation (4.10) is transformed by taking a logsum and exponential form in the same way with Equation (4.4) and (4.5),

$$e^{\frac{V^d(a_j)}{\mu}} = \begin{cases} \sum_{a_{j+1} \in \mathcal{A}} \delta(a_{j+1}|a_j) e^{\frac{1}{\mu}\{v(a_{j+1}|a_j) + \beta V^d(a_{j+1})\}}, & a_j \in \mathcal{A} \\ 1, & a_j = d. \end{cases} \quad (4.12)$$

Based on the recursive logit model, we define the matrix $\mathbf{z}(|\tilde{\mathcal{A}}| \times 1)$ and $\mathbf{M}(|\tilde{\mathcal{A}}| \times |\tilde{\mathcal{A}}|)$ with the entries of Equation (4.6). In our case, the value functions are the solutions to the following system of non-linear equations with the sequential discount rate,

$$z_{a_j} = \begin{cases} \sum_{a_{j+1} \in \mathcal{A}} M_{a_j a_{j+1}} (z_{a_{j+1}})^\beta, & a_j \in \mathcal{A} \\ 1, & a_j = d. \end{cases} \quad (4.13)$$

This equation is written in matrix notations as:

$$\mathbf{z} = \mathbf{MX(z)} + \mathbf{b}, \quad (4.14)$$

where $\mathbf{X}(\mathbf{z})(|\tilde{\mathcal{A}}| \times |\tilde{\mathcal{A}}|)$ is the matrix with entries $X(z)_{a_j} = (z_{a_j})^\beta$. We solve Equation (4.14) by iterative computations until the value function arrives a fixed point (the use of the same solution method is found in e.g., Mai, Fosgerau, and Freijinger, 2015). We first initialize the vector $\mathbf{z}^{(0)}$ and then update as $\mathbf{z}^{(1)} = \mathbf{MX(z}^{(0)}) + \mathbf{b}$. If \mathbf{z} converges, i.e., it satisfies $|\mathbf{z}^{(n+1)} - \mathbf{z}^{(n)}| < \gamma$ where γ is a convergence tolerance, we finish the iteration, and otherwise, we update \mathbf{z} using Equation (4.14). As mentioned in Fosgerau, Freijinger, and Karlstrom, 2013, it depends on the balance between the network structure and the size of the instantaneous utilities $v(a_{j+1}|a_j)$. Cyclic structures in networks may cause the divergence of the value functions. In this paper, this is discussed in more detail in Section 4.4.3.

Note here that this model corresponds, as special cases, to the recursive logit model when β equals one and to the myopic link choice model when β equals zero. Therefore, the proposed model can be assumed as a generalized version of these previous models. We also note that we do not consider the correlation structure among path alternatives, which is addressed in e.g., Mai, Fosgerau, and Freijinger, 2015 and Mai, 2016, though our model can be developed in the same way with the literatures. In this paper, we would like to focus on the effect of the sequential discount rate.

4.4 Illustrative examples

In this section, we present illustrative examples to show the difference between our model and previous route choice models. We use simple networks, where the only attribute in the instantaneous utility $v(a)$ is the link cost, and its parameter is set $\theta_{cost} = -1$ for simplicity.

4.4.1 Path probabilities

The first example uses the network of Figure 4.3(a), and we have three alternative paths in Figure 4.3(b): [1,2,4] (path 1), [1,3,4] (path 2), and [1,3,2,4] (path 3). The number on each link is the link cost. We denote the path probabilities as P_1 , P_2 and P_3 , respectively.

In order to compare the path probabilities, given by the model incorporating the sequential discount rate, to previous route choice models, we calculated the probability of the pre-trip MNL model, the recursive logit model (Fosgerau, Freijinger, and Karlstrom, 2013), the MyL model defined in the previous section, and the β -SRL model. Table 4.2 shows the results. The probabilities of MNL, RL and β -SRL with

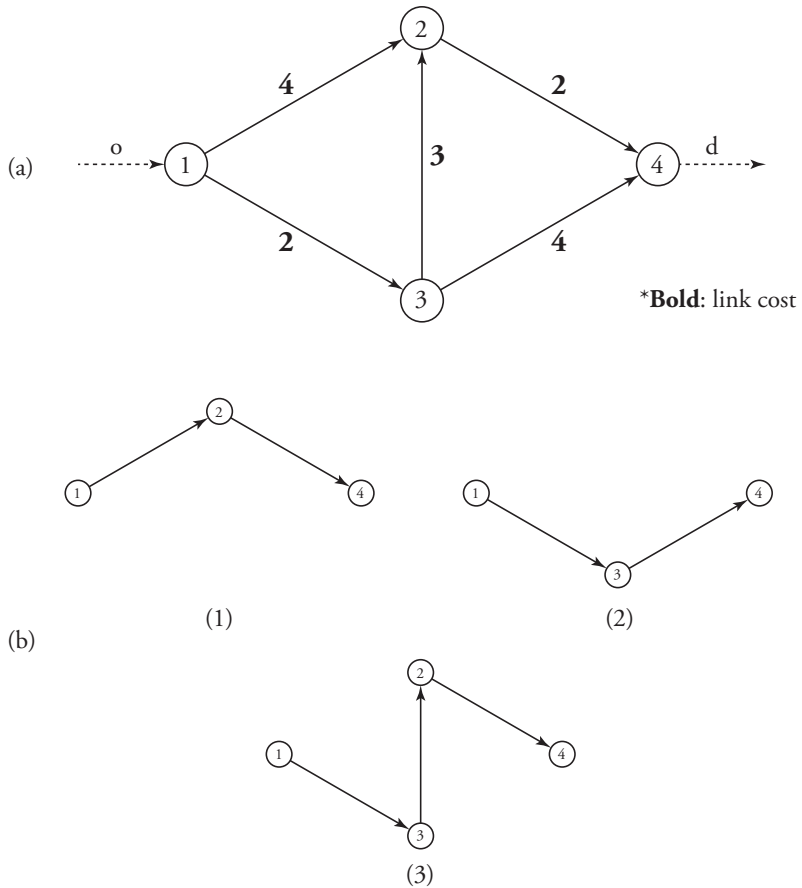


FIGURE 4.3: (a) Example network and (b) path alternatives

$\beta = 1$ give the same results; P_1 and P_2 are equivalent and higher than P_3 . Since path-based costs of route 1 and 2 are lower than that of route 3, these models reflect the global decision making of travelers. As proven in Akamatsu, 1996 and mentioned in Fosgerau, Freijinger, and Karlstrom, 2013, the path probabilities of the RL model correspond with those of the path-based MNL model if the universal choice set, which is the set of path 1, 2 and 3 in this case, can be defined. This result indicate that those of the β -SRL model with $\beta = 1$ are also equivalent. On the other hand, the result given by β -SRL with $\beta = 0.5$ shows the difference between P_1 (0.206) and P_2 (0.397), and in the case of MyL and β -SRL with $\beta = 0$, P_3 is the highest of all routes. The smaller β becomes, the more link 1-3 and 3-2 are likely to be chosen at node 1 and 3, respectively, and as a result of sequential decisions, the probability of route 3 becomes higher. While previous path-based route choice models could not describe such a myopic decision, the model proposed in this study generalizes the decision-making dynamics as the parameter of the sequential discount rate, and it includes the RL and the MyL models as special cases, as the results show.

To analyze the impact of β on travelers' route choice behavior in detail, we report the relationship between β and path probabilities in Figure 4.4. Despite that the path-based costs of route 1 and 2 are equivalent, P_2 is always equal to or higher than P_1 , because there is difference between the costs of links 1-2 and 1-3, which are connected with link o . It is realistic that the difference of the costs of the first links changes the selectivity of routes; therefore, the result represents a contribution of our model to previous route choice models, which evaluate the probabilities of route 1 and 2 equally. Moreover, in Figure 4.4, we show the fluctuations of the three

TABLE 4.2: Comparison of path choice probabilities given by several route choice models applied to the example in Figure 4.3

	β	P_1	P_2	P_3
MNL	-	0.422	0.422	0.155
RL	-	0.422	0.422	0.155
β -SRL	1	0.422	0.422	0.155
β -SRL	0.5	0.206	0.397	0.397
β -SRL	0	0.119	0.237	0.644
MyL	-	0.119	0.237	0.644

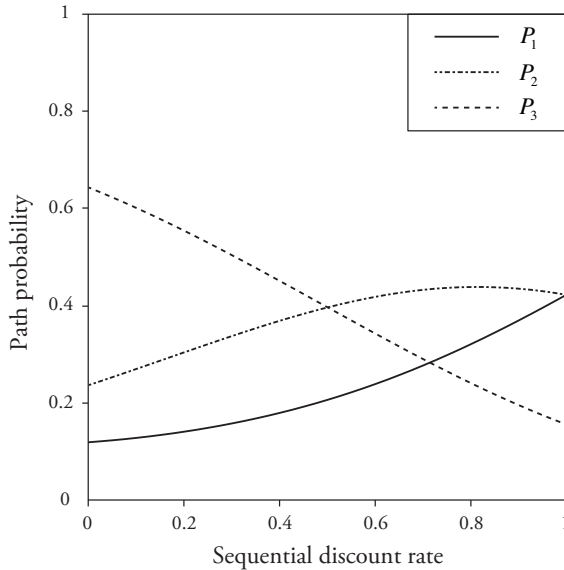


FIGURE 4.4: Path probabilities of the three path alternatives of Figure 4.3

path probabilities when β changes. With respect to β , P_2 monotonically increases and P_3 monotonically decreases. The figure indicates that β has a large impact on not only path probabilities but also their ranking: $P_3 > P_2 > P_1$ when $0 \leq \beta < 0.5$, $P_2 > P_3 > P_1$ when $0.5 \leq \beta < 0.75$ and $P_2 \geq P_1 > P_3$ when $0.75 \leq \beta \leq 1$. The fact that P_3 is the largest of the three suggests that most of travelers make decisions at each node and choose the links with smaller instantaneous costs; link 1-3 at node 1, link 3-2 at node 3, and link 2-4 at node 2. Assuming that link costs mean the level of congestion, it seems to be likely that travelers choose links myopically in order to avoid the congestion. This result indicates that β -SRL model can describe both a myopic decision and a global decision in route choice behavior.

In order to examine the mechanism of path probability change, we show the values of $V^d(a)$ (Figure 4.5a), $\beta V^d(a)$ (Figure 4.5b) and $v(a) + \beta V^d(a)$ (Figure 4.5c) of each link $a \in [o, 1-2, 1-3, 2-4, 3-2, 3-4]$. V and βV of link 2-4 and 3-4 are always $\log(\exp(0)) = 0$ because the unique outgoing link of these links is link d . In this case, the deterministic component of link transition utility v depends on only link cost; therefore, the value functions of links that share the sink node are equal to each other in the network of Figure 4.3, where $V(1-2) = V(3-2)$. The link choice probability of the β -SRL model is given by $\exp(v + \beta V) / \sum \exp(v + \beta V)$ and dependent on $(v + \beta V)$, which is the sum of instantaneous utility v and the product of the sequential discount rate and value function βV . Comparison between $(v + \beta V)$ of link 1-2 and

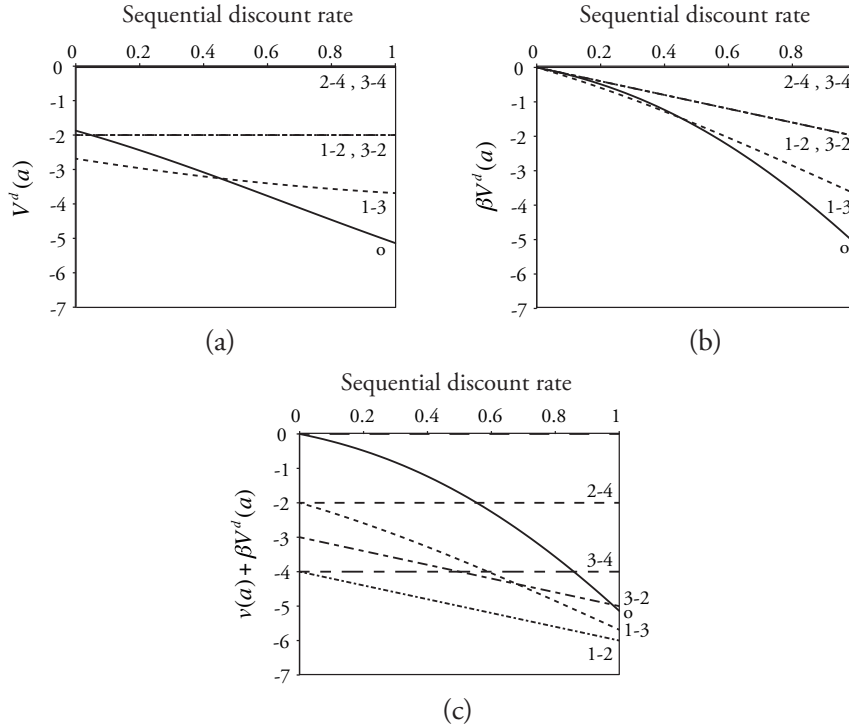


FIGURE 4.5: Value functions of links

1-3 indicates that the value of link 1-2 is always higher than that of link 1-3, but the difference becomes gradually smaller as β becomes large. On the other hand, the order of $(v + \beta V)$ of link 3-2 and 3-4 reverses at $\beta = 0.5$, and the reverse causes the inversion of the order of P_2 and P_3 .

The results of path probabilities demonstrates that the sequential discount rate in the β -SRL model reflects the decision-making dynamics. The smaller β is, the more important myopic decision (instantaneous utility) is regarded. In contrast, the larger β is, the more significant expected downstream utility is. It also can be assumed that the sequential discount rate indicates the spatial heterogeneity of link cost cognition, because drivers consider future expected utility with small weight when the sequential discount rate is small. Moreover, the β -SRL model can describe the global decision as well as previous models, since the β -SRL model includes the RL model as a special case.

4.4.2 Link flows

In order to analyze the effect of the sequential discount rate on prediction of traffic flow, we report on the results of traffic assignment, using a simple grid network in Figure 4.6. We calculated link flows using the assignment method based on link transition probabilities, which are detailed in Sasaki, 1965 and Akamatsu, 1996. Panels in the top row indicate the three network settings used for assignments, where the number on each link is the link cost. Network 2 and 3 are the networks with some high cost links and low cost links compared to network 1, respectively. The lower part in Figure 4.6 shows the assignment results that are based on link transition probabilities given by the β -SRL model with different sequential discount rates ($\beta = 0, 0.5, 1$), where the line weight indicates the link flow. In this example, we set the OD flow to 1000. In the case of $\beta = 1$, the assignment results reflect the effect

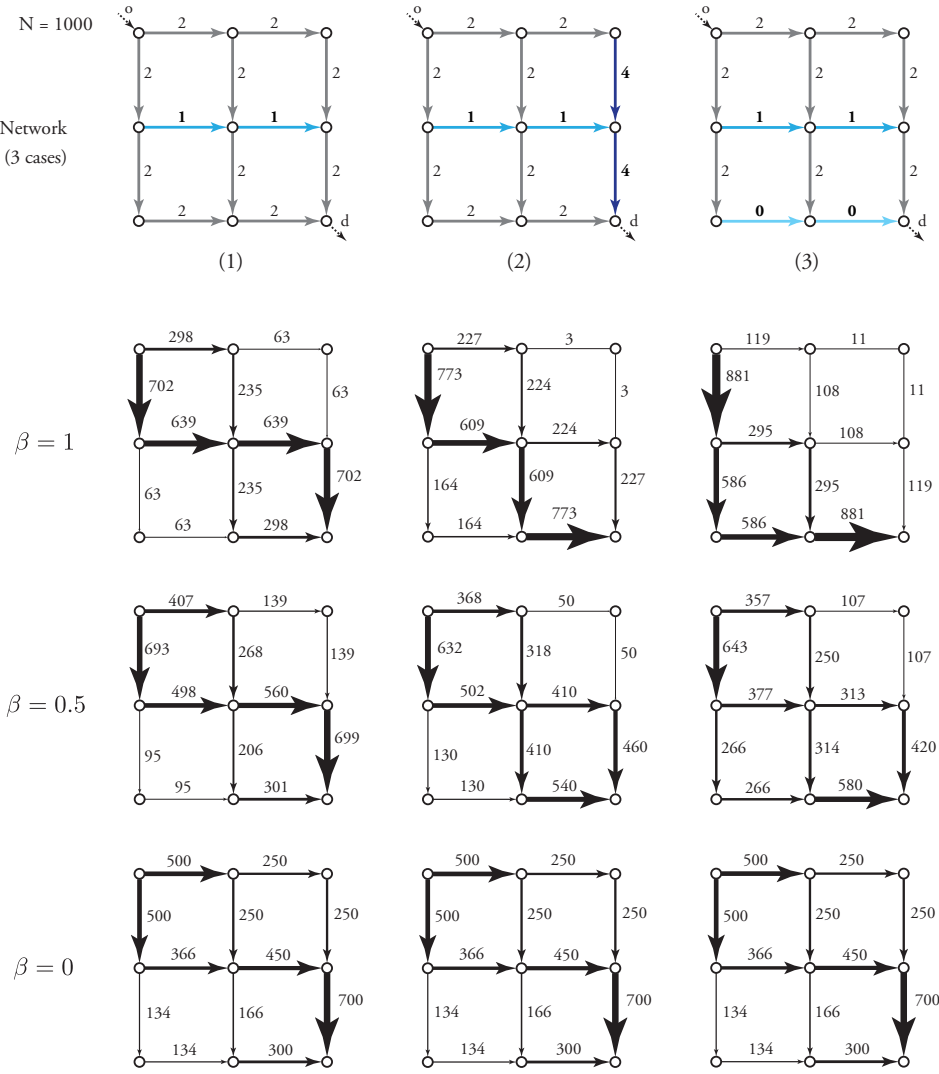


FIGURE 4.6: Assignment results given by the β -SRL model with different β

of the link cost changes, where the links with cost 4 have little flow in network 2. The links with zero cost have large flow in network 3, because when $\beta = 1$, travelers consider path-based cost from origin to destination, rather than separated link costs. The smaller β becomes, the more flow we can see on links with cost 4 in network 2. Moreover, when $\beta = 0$, the assignment results are the same regardless of network settings in these examples. When $\beta = 0$, travelers myopically choose links. Therefore, larger flows are assigned to high cost links, which drivers should ordinarily avoid to travel in network 2, and smaller flows are assigned to zero cost links in network 3. The fact that larger flows are assigned to high cost links shows that myopic route choice decisions can worsen the congestion of networks, and it may suggest the mechanism of gridlock occurrence.

We conclude that the sequential discount rate has a large impact on predicted link flows, and existing route choice models with global decision may cause erroneous predictions in terms of network flow, and, therefore, the estimation of β using real data is useful for real-time traffic management.

4.4.3 Cyclic paths

The advantage of sequential route choice models compared to general route choice models is that we do not need path enumeration and can consider all possible paths including cyclic paths. In the case of gridlock networks, where route choice behavior is confusing, the generation of cyclic paths, which pass the same node more than once, is an important issue. Cyclic paths are generally assumed to be chosen, not under global decisions, but myopic decisions in route choice behavior. In order to analyze the impact of the sequential discount rate on the selectivity of cyclic paths, we simulated the network of Figure 4.7(1). Instantaneous utility associated with the link pair (a_j, a_{j+1}) is given by $v(a_{j+1}|a_j) = \theta_{cost}x_{a_j} - 10x_{a_{j+1}|a_j}$, where x_{a_j} is the link cost, and $x_{a_{j+1}|a_j}$ is the u-turn dummy variable that equals one, if the source node of link a_j corresponds to the sink node of link a_{j+1} , and zero otherwise.

We first the coefficient of link costs θ_{cost} to -2 . With respect to every β , we have 100 sets of 1000 path observations, and we present the maxima, the minima and the means of the ratio of cyclic paths, in Figure 4.8. When β is large (close to one), there are few cyclic paths because travelers choose routes with global decision making. Maxima, minima and means are zero when $\beta = 1$ and 0.9 . This result indicates that no cyclic path is generated by the RL model, which is the special case of β -SRL when $\beta = 1$, in this network. As we decrease β , we first observe cyclic paths when $\beta = 0.8$: the maximum equals 0.001 . Further, there are sets that contain no cyclic path (the minima are equal to zero), when β is equal to or greater than 0.6 . The smaller β becomes, the more cyclic paths are observed, and when $\beta = 0$ the maximum is 0.253 , the minimum is 0.200 and the mean of ratio of cyclic paths is 0.225 .

In order to examine the relationship between the values of parameters and the generation of cyclic paths, we observe 10000 paths for each parameter set of θ_{cost} and β and report the maximum number of cyclic structures in a path among the observations in Table 4.3. When the absolute values of both θ_{cost} and β are large, no cyclic path is contained in the 10000 observations, where the results are shown as 0 in Table 4.3. On the other hand, when the absolute value of θ_{cost} or that of β is small, a path that includes two figures of cyclic structures is observed. Paths with a number of cyclic structures are observed, especially when β is close to one and θ_{cost} is close to zero. In the case of $\beta = 1$ and $\theta_{cost} = -0.1$, an observed path includes 6398 cyclic structure, and in the case of $\beta = 1$ and $\theta_{cost} = 0$, Equation (4.14) has no solution and we cannot observe paths.

When $\beta = 1$, the β -SRL model corresponds to the RL model. The condition of solution existence of the RL model is that the incidence matrix \mathbf{M} is a convergence matrix, i.e., the following equation is satisfied:

$$\rho(\mathbf{M}) = \max_h \{|\lambda_h|\} < 1, \quad (4.15)$$

where λ_h is the eigenvalue and $\rho(\mathbf{M})$ is the spectral radius of matrix \mathbf{M} . The matrices \mathbf{M} with θ_{cost} equal to or smaller than -0.1 satisfy Equation (4.15); however, when $\beta = 0$, the spectral radius of \mathbf{M} is 1.189 , which is larger than one. In this case, the value functions diverge due to the cyclic structures with large utilities. When β is smaller than one, Equation (4.14) has the solution even though Equation (4.15) is not satisfied, in the network of Figure 4.8(1). This is because the value functions are discounted by the sequential discount rate β and do not diverge.

These results demonstrate that the sequential discount rate, which describes decision making dynamic in route choices, has a large impact on the selectivity of cyclic

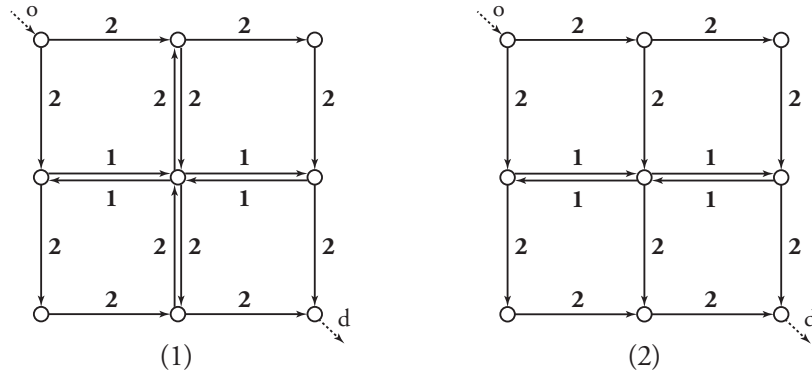


FIGURE 4.7: Simulation network with cycles

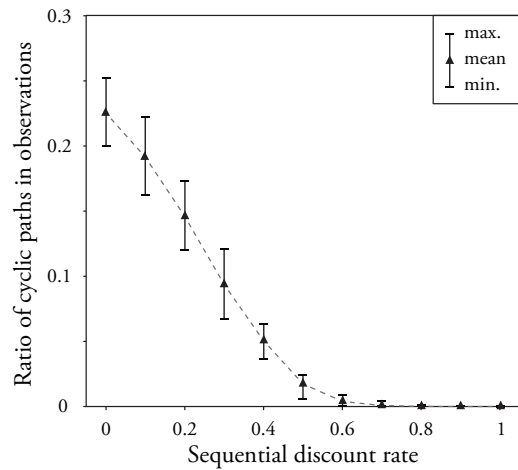


FIGURE 4.8: Ratio of cyclic paths in 1000 observations

paths. Especially in non-habitual networks, such as gridlock networks, it is thus important that the proposed model can simulate the generation of cyclic paths.

4.5 Parameter estimation

In this section we present parameter estimations given by the β -SRL model. First, we discuss the estimation methods for the β -SRL model, and then we present validation results using simulated route choice data. Finally, we present the estimation results using real observations.

TABLE 4.3: The maximum number of cyclic structures in a path of 10000 observations

θ_{cost}	sequential discount rate β										
	1	0.9	0.8	0.7	0.6	0.5	0.4	0.3	0.2	0.1	0
-2	0	0	0	3	4	6	10	22	22	28	30
-1.9	0	0	3	4	5	8	12	20	22	30	32
-1.8	0	0	1	4	7	12	20	26	30	29	30
-1.7	0	2	1	8	4	12	16	22	28	34	30
-1.6	0	0	3	4	7	12	14	20	28	28	34
-1.5	0	1	1	4	7	11	16	22	28	28	28
-1.4	0	3	4	5	8	16	20	22	32	30	34
-1.3	1	3	4	4	16	14	22	30	24	30	44
-1.2	0	3	4	8	10	12	16	20	26	24	34
-1.1	1	4	7	6	8	16	22	24	26	28	34
-1	3	4	6	8	12	18	26	24	28	28	32
-0.9	3	4	7	8	11	20	36	26	24	32	32
-0.8	4	10	8	11	12	18	24	22	38	30	32
-0.7	4	8	8	14	20	26	30	28	38	42	30
-0.6	5	10	12	18	16	24	20	26	24	30	32
-0.5	7	10	16	16	22	26	32	32	34	36	40
-0.4	16	20	18	20	28	30	32	40	32	30	32
-0.3	23	24	32	32	40	44	30	32	38	28	34
-0.2	44	50	42	36	40	36	32	26	28	30	32
-0.1	6398	80	56	54	38	38	46	30	28	28	28
0	-	216	80	46	42	32	44	48	30	34	24

*: The Bellman equation has no solution.

4.5.1 Maximum likelihood estimation

Parameters of the β -SRL model are estimated by the method of maximum likelihood estimation. The log-likelihood function LL is defined as follows:

$$\begin{aligned}
 LL(\theta, \beta) &= \ln \prod_{n=1}^N \mathbb{P}_n(\sigma_n = [a_1, \dots, a_{J_n}]) \\
 &= \sum_{n=1}^N \sum_{j=1}^{J_n-1} \ln p_n(a_{j+1}|a_j) \\
 &= \sum_{n=1}^N \sum_{j=1}^{J_n-1} \frac{1}{\mu} (v_n(a_{j+1}|a_j) + \beta V_n^d(a_{j+1}) - V_n^d(a_j)),
 \end{aligned} \tag{4.16}$$

where N is the number of paths, and J_n is the number of links included in path n . As Equation (4.16) shows, the link choice probability p depends on the value function V , which has a recursive structure as shown in Equation (4.2). That is, p includes an endogenous variable, and we have to solve the fixed point problem of the parameters. In the field of economics, several estimators for dynamic discrete choice models have been proposed. One can see the reviews in Aguirregabiria and Mira, 2010. Most methods are two-step iterative solutions, e.g., the nested fixed point (NFXP) algorithm (Rust, 1987), and the nested pseudo likelihood (NPL) algorithm (Aguirregabiria and Mira, 2002). Recently, Su and Judd, 2012 proposed a constrained optimization method for structural estimation, which is referred to as the mathematical programming with equilibrium constraints (MPEC) approach.

In order to estimate β , we adopt a two-step iterative method, which includes the first step for maximization of the log-likelihood function and the second step is for

calculating the value functions, because the estimation of β includes a problem regarding parameter identification in the case of simultaneous estimation, such as the MPEC approach. NPL does not solve the fixed point problem of the value functions in the second step. Therefore, it is useful when the value functions are costly to evaluate. However, in the case of dynamic sequential link route choice models, the first step takes much more time because the number of links is usually huge. In this study, we use another approach, which is also based on two-step procedures: 1) set $m = 0$ and initialize the value functions $V^{(0)}$ and the parameters $\theta^{(0)}, \beta^{(0)}$, 2) maximize the log-likelihood function and solve the parameters $\theta^{(m+1)}, \beta^{(m+1)}$, 3) solve the Bellman equation and update the value functions $V^{(m+1)}$, and 4) finish the algorithm if the parameters and the value functions satisfy $|\theta^{(m+1)} - \theta^{(m)}| < \xi$, $|\beta^{(m+1)} - \beta^{(m)}| < \xi'$, and $|V^{(m+1)} - V^{(m)}| < \xi''$, where ξ, ξ' and ξ'' are the convergence tolerances, return step 2 otherwise.

4.5.2 Simulation analysis

In order to confirm the estimability of parameters in the β -SRL model, we present a simulation analysis using the cyclic network of Figure 4.7(2) and simulation data is generated on the five conditions in Table 4.4. The instantaneous utility associated with the link pair (a_j, a_{j+1}) is given by $v(a_{j+1}|a_j) = \theta_{cost}x_{a_j} - 10x_{a_{j+1}|a_j}$, where x_{a_j} is the link cost and $x_{a_{j+1}|a_j}$ is a u-turn dummy variable that equals one, if the source node of link a_j corresponds to the sink node of link a_{j+1} , and zero otherwise. In this case, θ and β are estimated.

Table 4.5 shows the estimation results of the β -SRL model using simulation data. Note that we do not estimate β directly, but γ , where the relationship between them is $\beta = \exp(\gamma)/(1 + \exp(\gamma))$, and evaluate β using γ . For this reason, the table have no information of the standard errors of β .

Regarding the estimated θ , the difference from the true value is the maximum in dataset 5 (0.060), and in all datasets, we get the estimates close to this true value. We also can estimate γ and evaluate β , and the results show close values to each true value. In the case of dataset 1, the difference between estimated β and true β is 0.070 and larger than the other datasets. All estimates of θ and γ are not significantly different from their true values at the 5% significance level.

4.5.3 Case study

We used data of vehicle trajectories in the network of the Tokyo Metropolitan area, collected by the *Vehicle Information and Communication Systems Center*, which is a typical corporation collecting and providing driver's road traffic information. The data includes vehicle trajectories of taxis, as sequences of consecutive geo-referenced coordinates and the corresponding timestamps, which are typically recorded every few seconds. It is important to note that this emerging sensor technology, using taxis, enabled us to observe trajectories anytime, therefore the data includes the traces on March 11, 2011, which is the day of the Great East Japan Earthquake. We use the data on that day, and the day a week before (March 4, 2011) for comparison. They include 33,858,752 locations and 872,070 trips. We here briefly introduce a summary of the Great East Japan Earthquake.

At 14:46 on March 11, 2011, a magnitude-9 earthquake shook eastern Japan. The Tokyo Metropolitan area also experienced the large earthquake, the throughput of the entire transportation network declined. The Metropolitan Expressway

TABLE 4.4: Dataset used in simulation analysis

Set	utility function	parameters		Travelers
	$v(a_{j+1} a_j)$	θ	β	N
1	$\theta_{cost}x_{a_j} - 10x_{a_{j+1} a_j}$	-2	0.9	2000
2	$\theta_{cost}x_{a_j} - 10x_{a_{j+1} a_j}$	-2	0.7	2000
3	$\theta_{cost}x_{a_j} - 10x_{a_{j+1} a_j}$	-2	0.5	2000
4	$\theta_{cost}x_{a_j} - 10x_{a_{j+1} a_j}$	-2	0.3	2000
5	$\theta_{cost}x_{a_j} - 10x_{a_{j+1} a_j}$	-2	0.1	2000

* x_{a_j} : Link cost, $x_{a_{j+1}|a_j}$: U-turn dummy

TABLE 4.5: Estimation results of the β -SRL model using simulation data

Set	θ			$\beta = \exp(\gamma)/(1 + \exp(\gamma))$			
	Estimate (θ)	Std. err.	t-value* ¹	Estimate (γ)* ²	Std. err.	t-value* ¹	β
1	-2.012	0.067	-0.178	3.477	1.046	1.223	0.970
2	-2.031	0.065	-0.473	0.890	0.109	0.394	0.709
3	-2.005	0.060	-0.086	0.026	0.067	0.381	0.506
4	-1.969	0.056	0.547	-0.827	0.083	0.248	0.304
5	-2.060	0.058	-1.050	-2.250	0.198	-0.267	0.095

*1: t-value is reported with respect to the true value.

*2: In order to satisfy $0 < \beta < 1$, γ in $\beta = \exp(\gamma)/(1 + \exp(\gamma))$ is estimated instead of β .

was closed and all railways stopped. As a consequence of the concentration of all demand on road traffic, the network was heavily congested. It is the first time that a Japanese city experienced the gridlock phenomenon.

We report the mapping of the average link speeds at each time period (14:00-15:00, 15:00-16:00, 16:00-17:00, 17:00-18:00) on March 11, 2011 in Figure 4.9. At 14-15, most links were ordinary and link speeds were equal to and faster than 30km/h, over the network, and we can see a little congestion on narrow streets in the city center. However, after the earthquake occurred, congestion started to spread from the right side of the figure, where the density of the network was high, at 15-16. In the left side area with low network density, we can observe many green links with 20-30 km/h, but arterial roads were already congested, because a number of people started to go home from the city center to the suburbs. At 16-17, the link speeds declined over the network and most links were under 20km/h. Then at 17-18, especially surrounding the Imperial Palace (the empty spot at the center of the figure), the links under 10km/h connected with each other, and the congestion spread widely. As a result of the congestion propagating from one link to the next, the system achieved minimal throughput. This state can be referred to as a gridlock.

Figure 4.10 shows the variation of the average number of right or left turns per vehicle per five kilometers in time series: the broken line is for March 4 and the solid line is for March 11. Before 14:46, which is the time when the earthquake occurred on March 11, 2011, the two lines are consistent; however, after the time, the number of direction changes on March 11 rapidly increases, while that on March 4 gradually does not significantly change during 14-17 and decreases afterward. This result suggests that in the disaster network, the mechanisms of route choice behavior can dynamically fluctuate as the network situation changes. We guess that the myopic decision causes the increase of direction changes after the earthquake, and examine the route choice mechanisms through estimating parameters of the β -SRL model.

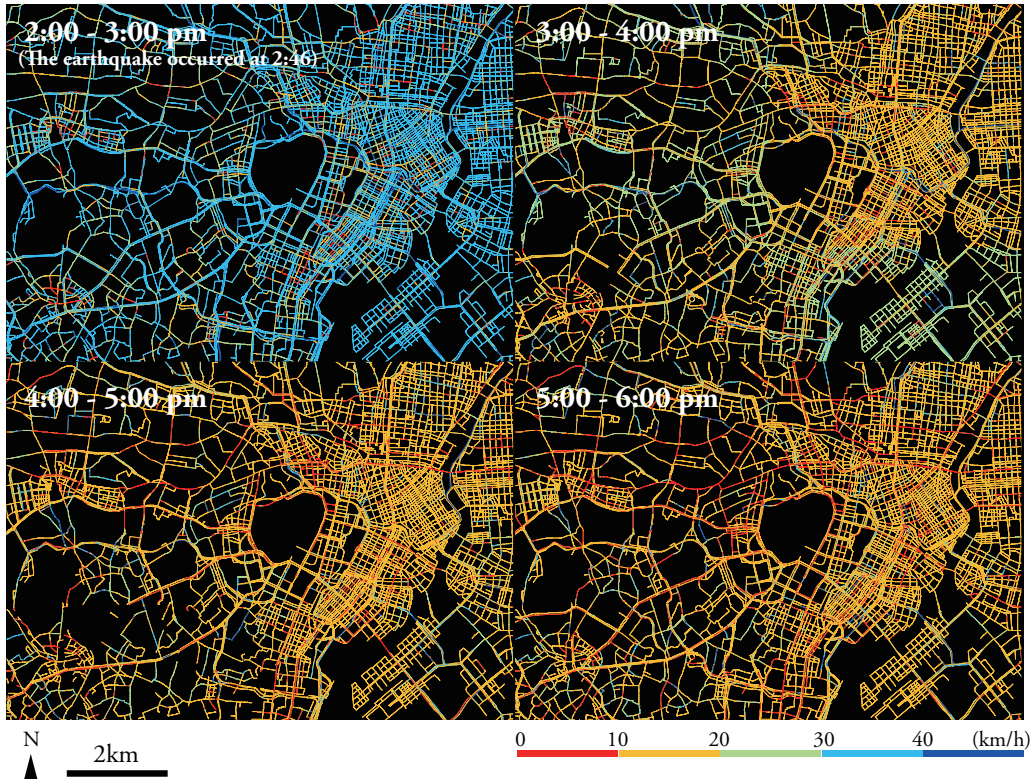


FIGURE 4.9: Link speed distribution at each time on the day of the Great East Japan Earthquake in the Tokyo metropolitan area network

Note that a multifaceted analysis of route choice behavior in the gridlock network using the same data is shown in Oyama et al., 2016.

In order to examine the route choice mechanism in such a situation, we estimated the β -SRL model for each time period on each day. For estimating parameters, we extracted a smaller one of the network in Figure 4.9, which includes 2724 links, and we used all of samples, which are the number of observations of link choices, at every period. The average number of destinations for periods is 110.5. More detailed characteristics of observations used for estimating parameters are reported on Table 4.6. In this case study, we define the deterministic component of instantaneous utility function as follows:

$$v(a_{j+1}|a_j) = \theta_{TT} TT_{a_{j+1}} + \theta_{RT} RT_{a_{j+1}|a_j}. \quad (4.17)$$

where TT_{a_j} is the travel time, in minutes, of link a_j , which is calculated by the length divided by the average link speed. The average link speed is calculated at each time using processing data with a map-matching algorithm, or it is set via the average over the network in the corresponding zone (as the second-order grid square), if the link has no observation. $RT_{a_{j+1}|a_j}$ is a right turn dummy variable that equals one, if the turn from link a_j to a_{j+1} is a right turn with an angle between 40° and 177° compared to the direction of the link a_j , and zero otherwise. We focused on right turns because in Japan people drive their cars in the left lane and are reluctant to turn right. Note that this study does not include the link size (LS) attribute, which is proposed by Fosgerau, Freijinger, and Karlstrom, 2013 to consider the overlapping effect

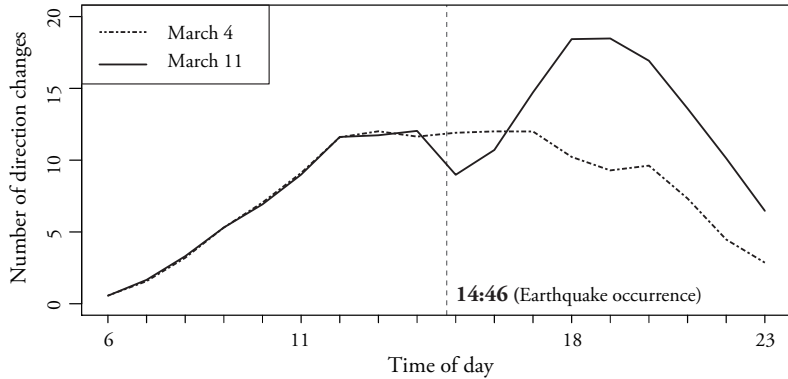


FIGURE 4.10: The number of direction changes

TABLE 4.6: Characteristics of observations used for estimation at each time period

Date	Time of day	No. of paths	No. of samples*	No. of destinations	CPU-time [s]
March 4	14-15	309	5043	132	393.1
	15-16	337	5469	133	380.2
	16-17	287	4634	114	340.9
	17-18	312	4353	121	326.4
March 11	14-15	256	4493	99	306.2
	15-16	307	4864	126	294.5
	16-17	184	2728	82	172.8
	17-18	138	2108	77	161.0
Total		2130	33692	884	2375.1
Average		266.25	4211.5	110.5	296.9

* It is the number of observed link choices, and all observations are used as samples for estimation.

among path alternatives. The LS attribute is based on the given parameters, but we do not have the prior information of the parameters in extraordinary networks. Since we aim at comparing the estimation results assuming that the parameters can change in different time periods, we do not include the LS attribute that is based on the given parameters. In this study, we focus on examining the effect and the difference of the discount factor rather than pursuing goodness-of-fit of the model.

We report the parameter estimation results in Table 4.7 and Table 4.8. We can estimate the parameters of the β -SRL model at all time periods, and the average estimation time for a period was 296.9 seconds. The computational time of each estimation is reported on Table 4.6, and it depends on the number of samples. Every computational time is sufficiently short for estimating at every one hour, which indicates the applicability of the model to frameworks of traffic management, as we will discuss in the last section.

The reported t-value is with respect to zero for θ_{TT} and θ_{RT} and with respect to one for β . All estimates are highly significant, and all estimated β s are significantly different from one. Signs and magnitudes are also reasonable, and there are differences among estimated values: θ_{TT} is estimated between -2.976 and -1.069, and θ_{RT} is between -1.162 and -0.991. The result that β is estimated between 0.176 and 0.463 suggests the possibility for both ordinary and extraordinary situations that route choice behavior is not necessarily based on global decisions.

In order to examine the temporal change of each parameter, we present the plots

TABLE 4.7: Estimation result of the β -SRL model using the data on March 4, 2011

Date	March 4, 2011					
Time of day	14:00-15:00			15:00-16:00		
	Estimates	Std. err.	t-value*	Estimates	Std. err.	t-value
θ_{TT}	-2.488	0.115	-21.69	-2.498	0.228	-10.97
θ_{RT}	-0.991	0.065	-15.13	-1.052	0.071	-14.75
β	0.455	0.037	-14.63	0.439	0.031	-18.12
LL			-2884.8			-3141.1

Time of day	16:00-17:00			17:00-18:00		
	Estimates	Std. err.	t-value	Estimates	Std. err.	t-value
θ_{TT}	-2.976	0.152	-19.57	-2.347	0.138	-17.05
θ_{RT}	-1.100	0.075	-14.68	-1.089	0.074	-14.64
β	0.463	0.036	-15.11	0.424	0.043	-13.34
LL			-2530.5			-2438.7

* We report t-value for θ_{TT} and θ_{RT} with respect to zero and that for β with respect to one.

TABLE 4.8: Estimation result of the β -SRL model using the data on March 11, 2011

Date	March 11, 2011					
Time of day	14:00-15:00			15:00-16:00		
	Estimates	Std. err.	t-value*	Estimates	Std. err.	t-value
θ_{TT}	-2.698	0.125	-21.65	-1.646	0.108	-15.28
θ_{RT}	-1.088	0.080	-13.62	-1.121	0.072	-15.54
β	0.408	0.042	-13.97	0.265	0.044	-16.54
LL			-2554.9			-2807.1

Time of day	16:00-17:00			17:00-18:00		
	Estimates	Std. err.	t-value	Estimates	Std. err.	t-value
θ_{TT}	-1.524	0.134	-11.36	-1.069	0.120	-8.89
θ_{RT}	-1.162	0.097	-11.97	-1.073	0.107	-9.99
β	0.176	0.066	-12.41	0.249	0.082	-9.16
LL			-1558.6			-1213.5

* We report t-value for θ_{TT} and θ_{RT} with respect to zero and that for β with respect to one.

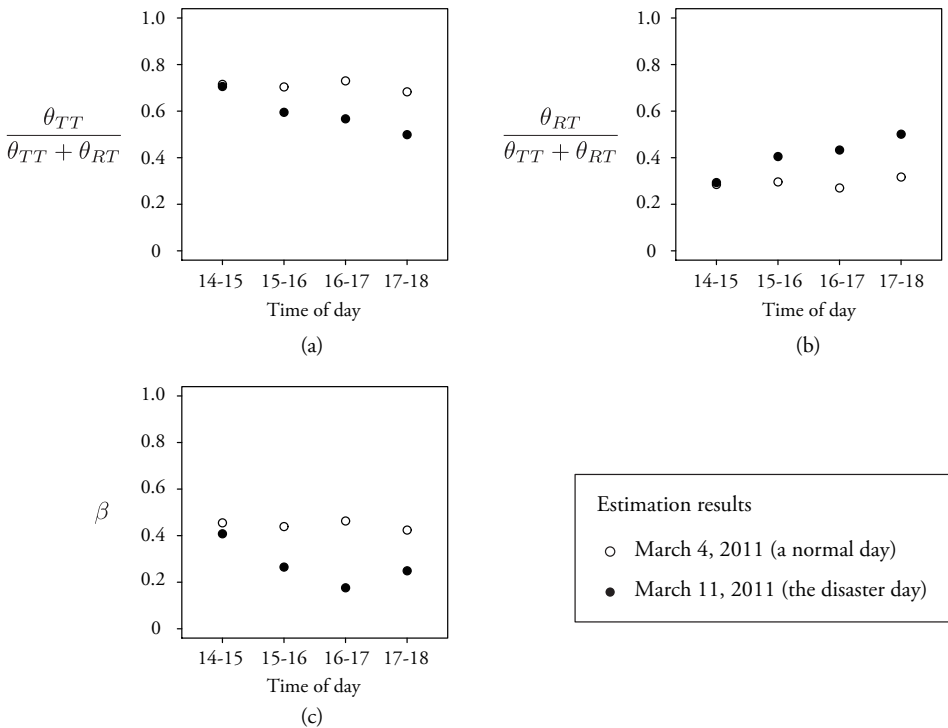


FIGURE 4.11: Plots of estimated parameters. (a) The ratio of the parameter of travel time, (b) the ratio of the parameter of right turn dummy and (c) the estimated value of the discount factor.

of estimated parameters in Figure 4.11. For the sake of comparison, we show the ratios of parameters, $\theta_{TT}/(\theta_{TT} + \theta_{RT})$ and $\theta_{RT}/(\theta_{TT} + \theta_{RT})$, in Figure 4.11(a) and (b), respectively. Figure 4.11(c) shows the change of β . The white and black plots are the estimation results on March 4 (normal day) and March 11 (disaster day), respectively.

$\theta_{TT}/(\theta_{TT} + \theta_{RT})$ on the normal day is the largest at 16-17, when people start returning home; however, the difference of the value among time periods is small. It suggests that the ratio of the parameters is stable on the normal day. On the other hand, $\theta_{TT}/(\theta_{TT} + \theta_{RT})$ on the disaster day shows a different trend from the normal day. At 14-15 on the disaster day, the value is almost same with that on the normal day (0.715 vs 0.713), and it decreases systematically as time goes by. The change indicates that after the earthquake occurrence at 14:46, as the congestion becomes worse, they cannot evaluate the travel time appropriately.

We can see the opposite dynamics between estimated $\theta_{RT}/(\theta_{TT} + \theta_{RT})$ on the normal and the disaster day. On the disaster day, the value increases as time goes by, while it barely changes on the normal day. At 17-18 on the disaster day, $\theta_{RT}/(\theta_{TT} + \theta_{RT})$ is the largest on the day and larger than $\theta_{TT}/(\theta_{TT} + \theta_{RT})$. That is, the cost of right turns becomes very high because of urban gridlock.

Regarding β , the estimated values on the disaster day are smaller than those on the normal day at all time periods. This result suggests that the earthquake occurrence makes drivers' decision myopic. At 14-15 on the disaster day, β shows the value close to β at 14-15 on the normal day. After the occurrence of the earthquake, β decreases as time goes by, and drivers have to choose routes myopically because the congestion has reached levels never experienced before. Afterwards β becomes the smallest at 16-17, just before the urban gridlock incidence. The result suggests

that the myopic decisions of drivers may worsen the network situation and cause gridlock networks.

Finally, we examined the prediction performance of the estimated β -SRL model at every period, comparing to the RL model, using a cross validation approach (Mai, Fosgerau, and Frejinger, 2015). We divide the sample of observations at each time period t \mathcal{I}^t into two sets by drawing observations at random, and the set that has 80 % of observations \mathcal{I}_e^t is used for estimating the models and the set that has 20 % of observations \mathcal{I}_p^t is used for evaluation of the following likelihood loss:

$$\overline{err}_t = \frac{1}{K - K_f^t} \sum_{k=1}^{K - K_f^t} \left[-\frac{1}{|\mathcal{I}_{k,p}^t|} \sum_{n \in \mathcal{I}_{k,p}^t} \sum_{j=1}^{J_n-1} \ln p_n(a_{j+1}|a_j; \hat{\theta}_k^t, \hat{\beta}_k^t) \right], \quad (4.18)$$

where K is the number of trials, and K_f^t is the number of failure of estimation among K trials. $\hat{\theta}_k^t$ and $\hat{\beta}_k^t$ are the estimated parameters of the models using the sample of $\mathcal{I}_{k,e}^t$. We set $K = 40$ and generate holdout samples of the same size by reshuffling the original sample for all time periods. Table 4.9 reports the results. The β -SRL model can be estimated at all time periods, i.e., $K_f^t = 0, \forall t$, while in the case of the RL model estimation results cannot always be obtained, as we discussed in Section 4.4.3. Moreover, the β -SRL model perform better than the RL model at all time periods. The loss of the β -SRL model is the largest at 17-18 on March 11 and the smallest at 16-17 on March 4, but there is not large difference among the averages of test error value of the eight β -SRL models. The result indicates that the change of the discount factor does not have a large effect on the out-of-sample fits of the model.

TABLE 4.9: Average of test error values over 40 holdout samples

		$\overline{err}_t (K - K_f^t)^*$			
		14-15	15-16	16-17	17-18
March 4	β -SRL	0.576 (40)	0.573 (40)	0.543 (40)	0.557 (40)
	RL	0.873 (10)	0.640 (5)	0.689 (2)	0.586 (22)
March 11	β -SRL	0.572 (40)	0.581 (40)	0.567 (40)	0.587 (40)
	RL	- (0)	0.832 (12)	0.760 (1)	- (0)

* $K - K_f^t$ is the number of completion of estimation.

4.6 Conclusions and discussion

This paper proposed the discounted recursive logit (β -SRL) model, which incorporates the discount factor for capturing the diversity of decisions under congestions.

Through some illustrative examples using simple networks, we presented the properties of the β -SRL model in terms of path probability and link flow prediction, and showed the differences from several existing route choice models. The discount factor reflected the effect of links that travelers pass early and had a large impact on the order of path probabilities of routes. It also affected network assignment results, and we concluded that the evaluation of appropriate discount factors was important for precise demand forecasting. Moreover, we mentioned the selectivity of cyclic paths, which have not been discussed in detail in previous works and may cause the divergence of expected utilities, and showed the effect of the balance between the parameter of link cost and the discount factor.

We then presented estimation results using both simulation data and real data, including GPS traces in the time of the Great East Japan Earthquake. The estimated parameters using real data showed that the difference of route choice mechanisms between the normal day and disaster day, and among the time periods. On the disaster day, all parameters systematically changed as time went by after the earthquake occurrence, and the estimation results of the discount factor indicated myopic route choice behavior in gridlock networks. We conclude that the β -SRL model enable us to examine the decision-making dynamics in route choices by estimating appropriate discount factors.

Regarding the limitations in this paper, we mention the characteristics of probe vehicle data of taxis. In the first place, it is difficult to detect trips from the sequence of continuous GPS data because the stop time of taxis is often very short. We defined the end of a trip, if the interval between successive two data is larger than 120 seconds; however, some sorts of methods for more accurate inference of origins and destinations may be possible. Regarding the estimation of the discount factor, we assumed the unique value at each time period. It means that all travelers have a common value of the discount factor; however, more realistically, its value is assumed to depend on the characteristics of each traveler. The variation, e.g., among travelers or networks at the same time period, should be discussed in the future work. A mixed logit model or a latent class model can be applied for this purpose. Moreover, the extension of the model to a dynamic model that considers a time-dependent network is also a future work.

As an application of the β -SRL model, we refer to the framework of trajectory-oriented gridlock network management in Figure 4.1, again. The β -SRL model is applicable for both trajectory data in ordinary and extraordinary situations, thanks to its generalized description of myopic decisions and global decisions in route choices. Regarding the parameter estimation, the calculation of log-likelihood function in Equation (4.16) does not require the information of whole paths in trips, because the link choice probability is based on only the information of link transition and the destination. Therefore, the β -SRL model goes well with the traffic simulations using emerging sensing technologies, such as full-time connected vehicles. As seen in the case study, our management method is based on the parameter estimation at each time period. We are based on the assumption that travelers' route choice preferences and the discount factor can change at different time periods, and estimate the β -SRL model at each period. We set the unit as one hour, because we assume that the changes depend on the macroscopic situation of the network. For the parameter estimation, the network is assumed to be static and deterministic during each time period. We do not use a dynamic model but a static one to detect anomaly of route choice mechanism. The case study actually showed that the estimated parameters dynamically changed after the earthquake occurrence on the disaster day, while the difference among time periods is small on the normal day. These results indicate the importance of real-time traffic management for the control of the extraordinary networks, and the β -SRL model that can capture the diversity of drivers' decision-making mechanism is applicable to the framework. Moreover, the implementation of the estimation of the β -SRL model is sufficiently fast for estimating at every one hour, and even in the case that larger size of data is available and the time unit is shorter, the framework is expected to work well. Of course, faster and efficient estimation algorithms help for making the framework more feasible. Based on a traffic simulation using the β -SRL model, information provision, route guidance and signal control can be implemented for real-time traffic management. This trajectory-oriented traffic management will be helpful for gridlock network control.

Chapter 5

Path set restriction algorithm for Markovian traffic assignment

In this chapter, we propose a method of path set restriction for the Markovian route choice model to solve its computational challenges dependent on cyclic structures in networks.

It is known that Markovian traffic assignment models remain main three computational challenges caused from cyclic structures included in networks: unreasonable cyclic flows, computational instability of the expected utilities, and amplification of the IIA property. To solve these challenges, this study proposes a method of restricting path set based on the concept of time-space prism. We assume the sequential link choice behavior of travelers and introduce a network description where traveler's states are decomposed by choice-stage. Based on the network, we introduce several variables to define a prism. Traveler's route choice considering all feasible paths within the prism is modeled. This framework is quite flexible and shown to be a solution of the challenges of Markovian traffic assignment models through several numerical examples, which include the validation of computational time, applications to a stochastic user equilibrium problem and a network-GEV based model.

Keywords: Route choice model; Markovian traffic assignment; Path generation algorithm; Time-space prism; Cyclic paths; Choice-stage-structured network

5.1 Introduction

Stochastic traffic assignment (STA) is a technique of loading the origin-destination (OD) entries to a network based on travelers' perceived travel times (Sheffi, 1985). Though the simplest definition of the path set for STA is the set of *simple paths* that do not pass the same node more than once, the path enumeration of all simple paths is impossible due to the combinatorial explosion. Indeed, approaches based on implicit path enumeration have provided significant contributions to STA. This paper proposes a new implicit approach of STA that is referred to as a choice-stage-structured assignment (CSA).

The most popular algorithm of the implicit approach is the algorithm proposed by Dial, 1971. It restricts the path set to the set of so-called *efficient paths* that never include any move that goes away from the destination in terms of travel time. Dial's algorithm is popular in STA because of its computational efficiency and the equivalence to the logit-based assignment model (Van Vliet, 1981); however, two large problems remain in the algorithm. First, it often generates unreasonable flow patterns as a result of restriction of the path set to efficient paths. Secondly, the stochastic user equilibrium that is solved with Dial's algorithm does not converge to an exact solution because the set of efficient paths can change at each iteration independently on the link flows. Though Leurent, 1997 proposed a solution to the second problem, it can also generate unreasonable flow patterns and is not able to consider cyclic paths.

Another representative approach without explicitly enumerating paths is the Markovian traffic assignment (MTA) algorithm that is able to consider the universal set, i.e., the set of infinite paths including cyclic paths. MTA was first proposed by Sasaki, 1965 and then was linked to the logit-based assignment by Bell, 1995 and Akamatsu, 1996. Akamatsu, 1997 showed the link-based equivalent optimization problem for implicit STA models, and thus the stochastic user equilibrium problem based on MTA was formulated. Recently, it gathers much attention once again because of its high operability. Baillon and Cominetti, 2008 mentioned the interpretation of decision-making dynamics of the MTA model, and Fosgerau, Frejinger, and Karlstrom, 2013 linked it to disaggregate discrete choice analysis based on a dynamic discrete choice framework (Rust, 1987). However, the MTA model still has computational challenges to be solved: it can output excessive cyclic flows, and the existence of solutions depends on network structure and network condition (see the discussion of Oyama and Hato, 2017).

The logit-based assignment models including Dial's algorithm and the MTA also suffer from the Independence from Irrelevant Alternatives (IIA) property of the logit model and can load excessive flows to paths that overlap each other. Although Daganzo and Sheffi, 1977 proposed a probit-based assignment algorithm to solve the overlapping problem, it requires heavy computational burden, and thus the application to stochastic user equilibrium in real networks is difficult. Route choice models that are based on the GEV model (McFadden, 1978) such as the CNL model (Vovsha and Bekhor, 1998; Prashker and Bekhor, 1998; Prashker and Bekhor, 2004) and the GNL-based STA model (Bekhor and Prashker, 2001) are able to consider the underlying correlation structure among path alternatives. Since the GEV-based models require the path enumeration, network-GEV (Bierlaire, 2002; Daly and Bierlaire, 2006) based route choice models that are able to capture the correlation structure without explicitly enumerating paths were proposed (Papola and Marzano, 2013; Hara and Akamatsu, 2014; Ma and Fukuda, 2015; Mai, 2016). However, the application of the

network-GEV model requires editing of the network to remove cyclic structures, and thus these models are not able to consider original networks that include cycles.

The CSA algorithm proposed in this paper is based on the MTA and describes the sequential link choice behavior at each choice-stage. We incorporate the choice-stage-constraint into the route choice model and decompose the state of the network at each choice-stage. Given the novel network description, we propose a path set restriction method based on the concept of time-space prism. Thanks to this idea, we can solve the challenges of the MTA: excessive cyclic flows, computational instability dependent on network structure and conditions, and the amplification of the IIA property. Note that our method is a static model and does not consider any dynamics of link flows or network.

The structure of the paper is as follows. In Section 2, we first introduce the description of the choice-stage-structured network (CSN). Given the network description, we propose a novel method of restricting path set based on the concept of time-space prism. In Section 3, we formulate a route choice model in the CSN and explain how to calculate the state transition probabilities. In Section 4, we propose the choice-stage-structured assignment (CSA) algorithm. In Section 5, we give some numerical examples to examine computational characteristics of the CSA algorithm, from the viewpoints of computational instability and efficiency, cyclic flows and overlapping of routes. Conclusions and discussion of future research are provided in the end.

5.2 Path set restriction based on prism constraints

5.2.1 Choice-stage-structured network

Consider a directed connected graph $\hat{\mathcal{G}} = (\mathcal{N}, \mathcal{A})$, where \mathcal{N} is the set of nodes and \mathcal{A} is the set of links. The spatial connection indicator $\delta(n'|n)$ equals one if a link connecting the node pair $(n \rightarrow n')$ exists, and it equals zero otherwise. This is a general spatial network. We aim at modeling which route a traveler takes from origin node o to destination node d in the network and calculating the aggregate flow on each link.

To do so, this paper introduces a choice-stage-structured network (CSN). We first define choice-stage $\mathcal{T} = \{0, 1, \dots, T\}$ and let $\mathcal{G} = (\mathcal{S}, \mathcal{E})$ denote a CSN, where $\mathcal{S} = [\mathcal{S}_0, \dots, \mathcal{S}_t, \dots, \mathcal{S}_T]$ is the array of state sets with entries of state $s = (t_s, n_s)$, $t_s \in \mathcal{T}$, $n_s \in \mathcal{N}$, and $\mathcal{E} = [\mathcal{E}_0, \dots, \mathcal{E}_t, \dots, \mathcal{E}_{T-1}]$ is the array of edge sets with entries of edge $e = (s, s')$, $s, s' \in \mathcal{S}$, $(n_s, n_{s'}) \in \mathcal{A}$, respectively. Especially, \mathcal{S}_t contains only the states s at $t_s = t$, and the edges that are included in \mathcal{E}_t always connect a state s at $t_s = t$ with a state s' at $t_{s'} = t + 1$. Given the notation, a path on a CSN is described as a sequence of T states $[s_0, \dots, s_T] = [(0, n_{s_0}), \dots, (T, n_{s_T})]$. In a CSN, it is important that s and s' ($t_s \neq t_{s'}$) are strictly different from each other even if both of them are at the same spatial node n , i.e., $n_s = n_{s'} = n$. Thanks to this property, we can avoid the cyclic structures from the network, while we are able to retain and consider spatial cycles.

5.2.2 Choice-based prism constraints

The key parameter of the CSN is T , which is called choice-stage constraint (CC) and indicates the maximum number of choice-stages that a traveler experiences in a trip. The state and edge sets at a certain choice-stage \mathcal{S}_t , \mathcal{E}_t are restricted based on the constraint as follows.

Given the origin and destination node pair $o, d \in \mathcal{N}$, we consider the initial and final states: $s_o = (t_{s_o}, o)$ and $s_d = (t_{s_d}, d)$, where $t_{s_o} = 0$ and $t_{s_d} = T$. We first introduce variables $D^o(n)$ and $D^d(n)$ that are defined as the minimum number of steps (choice-stages) from node o to n and from node n to d in the spatial network, respectively. With respect to $D^o(n)$ and $D^d(n)$, the relations between connected two nodes are given by dynamic programming as follows:

$$D^o(n) = \min_{i \in \mathcal{N}_n^-} [D^o(i) + 1], \quad (5.1)$$

$$D^d(n) = \min_{j \in \mathcal{N}_n^+} [D^d(j) + 1], \quad (5.2)$$

where \mathcal{N}_n^- and \mathcal{N}_n^+ are the set of upstream and downstream nodes directly connected to node n , respectively. Given these variables, the set of states at t , \mathcal{S}_t is described as follows:

$$\mathcal{S}_t = \{(t, n) | I_t(n) = 1\}, \quad (5.3)$$

where

$$I_t(n) = \begin{cases} 1, & \text{if } D^o(n) \leq t, D^d(n) \leq T - t \\ 0, & \text{otherwise.} \end{cases} \quad (5.4)$$

$I(s) = I_t(n)$ is the state existence condition. Then, we define the state connection indicator Δ , and the constrained set of edges \mathcal{E}_t is described as follows:

$$\mathcal{E}_t = \{((t, n), (t + 1, n')) | \Delta_t(n'|n) = 1\}, \quad (5.5)$$

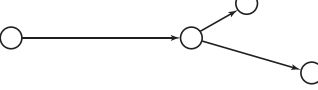
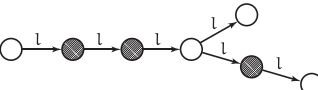
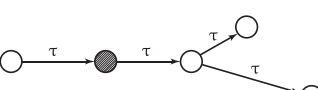
where

$$\Delta_t(n'|n) = I_t(n)\delta(n'|n)I_{t+1}(n'), \quad (5.6)$$

and $\delta(n'|n)$ is the spatial connection indicator as already defined. These constraints indicate that the link choice set that a traveler faces is constrained and changes at each choice-stage, even if at the same spatial node. That is, above-mentioned procedure not only reduces the number of states considered in the model by removing unused states but also expresses the limitations on the travel of individuals. Paths on a CSN use only states and edges that satisfy the constraints, and the set of the paths that travelers are able to take forms a prism that shows individuals' possible behavior in time-space (Hägerstrand, 1970).

Note that what the constraints mean with respect to path depends on the definition of spatial network and choice-stage. It is typically assumed that a traveler chooses link at each intersection as shown in Table 5.1 (a). In this case, the number of links that are included in a path r is constrained by T . The following sections and numerical examples in the paper are based on this assumption. On the other hand, if we modify the network by adding pseudo nodes, T is able to express other path constraints. If we edit the network so that all links have the same length l (Table 5.1 b), only paths whose trip length is shorter than $T \cdot l$ are considered by travelers. Also, in the case that all links are associated with the same travel time τ (Table 5.1 c), the path is constrained with respect to travel time.

TABLE 5.1: Network definition and choice-stage constraint variables

	Choice-stage	Spatial network	Constraint of path r
(a)	Intersection		$(\#links)_r \leq T$
(b)	Unit distance l		$(triplength)_r \leq T \cdot l$
(c)	Unit time τ		$(traveltime)_r \leq T \cdot \tau$

5.2.3 Illustrative examples

Figure 5.1 shows an example of the set of the restricted paths by the prism. Consider the directed and connected spatial graph in the left panel of Figure 5.1, where the origin and destination are node 7 and 14, i.e., $s_o = (0, 7)$ and $s_d = (T, 14)$. When we set $T = 5$, the set of possible paths is restricted within the prism as shown in the right panel in Figure 5.1. We focus on node 18 as an example. Given that $D^7(18) = 3$ and $D^{14}(18) = 2$, the vector of state existence indicators with respect to node 18 is

$$\mathbf{I}(18) = \begin{pmatrix} 0 & 1 & 2 & 3 & 4 & 5 \\ 0 & 0 & 0 & 1 & 0 & 0 \end{pmatrix}. \quad (5.7)$$

Regarding the state connection condition, $\Delta_2(18|17) = \Delta_2(18|13) = \Delta_3(19|18) = \Delta_3(13|18) = 1$ and otherwise $\Delta_t(18|n)$ and $\Delta_t(n|18)$ equal to zero. In this way, we have \mathcal{S}_t s in layers and obtain the prism as shown on the right panel of Figure 5.1. The prism also indicates the set of feasible paths $\mathcal{P}_s^{s'}$ that is based on the fundamental states s and s' . In the case of Figure 5.1, the prism-based path set $\mathcal{P}_{(0,7)}^{(5,14)}$ includes forty one paths that are exhibited in Table 5.2. While the number of feasible paths is restricted into an enumerable number by the prism, reasonable cyclic paths may exist within the prism. Note that we use an example of $T = 5$ but are able to control the path set by adjusting the value of T .

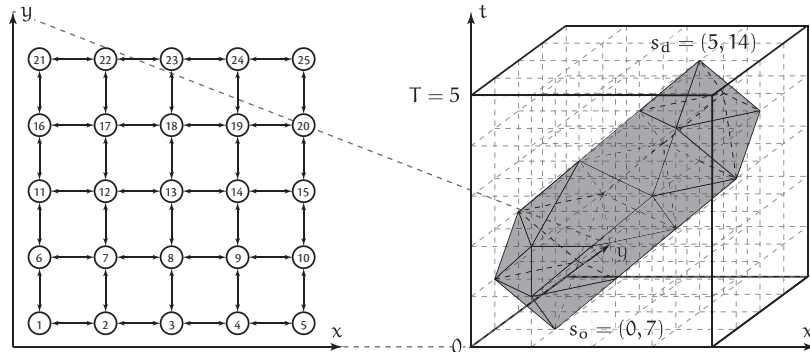


FIGURE 5.1: Illustration of a constrained network by the prism

TABLE 5.2: Restricted path set $\mathcal{P}_{(0,7)}^{(5,14)}$

path	node number at each time					path	node number at each time				
	$t = 0$	1	2	3	4		$t = 0$	1	2	3	4
1	7	2	3	4	9	14	22	7	8	9	14
2	7	2	3	8	9	14	23	7	8	13	8
3	7	2	3	8	13	14	24	7	8	13	8
4	7	2	7	8	9	14	25	7	8	13	12
5	7	2	7	8	13	14	26	7	8	13	14
6	7	2	7	12	13	14	27	7	8	13	18
7	7	6	7	8	9	14	28	7	8	13	18
8	7	6	7	8	13	14	29	7	12	7	8
9	7	6	7	12	13	14	30	7	12	7	8
10	7	6	11	12	13	14	31	7	12	7	12
11	7	8	3	4	9	14	32	7	12	11	12
12	7	8	3	8	9	14	33	7	12	13	8
13	7	8	3	8	13	14	34	7	12	13	8
14	7	8	7	8	9	14	35	7	12	13	12
15	7	8	7	8	13	14	36	7	12	13	14
16	7	8	7	12	13	14	37	7	12	13	18
17	7	8	9	4	9	14	38	7	12	13	18
18	7	8	9	8	9	14	39	7	12	17	12
19	7	8	9	8	13	14	40	7	12	17	18
20	7	8	9	10	9	14	41	7	12	17	18
21	7	8	9	10	15	14				19	14

As discussed in the beginning, MTA overpredicts the flows of cyclic paths by considering the universal set that includes infinite cyclic paths, especially in the case that the costs of cyclic structures are small. In contrast, this paper focuses on that infinite cyclic paths are unrealistic from the viewpoint of decision making of travelers and proposes a method of systematically restricting path set by introducing the parameter of the CC. Even though it is an exogenous parameter, the CC can be interpreted as a behavioral parameter that defines the prism such as constraints of the number of links, trip length or travel time. Indeed, these aspects are used by previous methods of defining path sets, such as the k-shortest path algorithm (Eppstein, 1998), the link elimination method (Azevedo et al., 1993), the labeling method (Ben-Akiva, Cyna, and Palma, 1984) and the branch-and-bound method (Prato and Bekhor, 2006). Compared to these literatures, our method contribute to consider all feasible paths within the prism without explicitly enumerating paths. It is reasonable enough to apply to traffic assignment problems. Moreover, since $I(s) = 0$ for states exterior to the prism, the matrix Δ_t has a sparser structure than the original incidence matrix δ . Focusing on this structure and using the description of sparse matrix that memorizes only non-zero elements, we can significantly reduce the volume of computation and the memory capacity.

5.3 Route choice model

In this section, we formulate a route choice model in choice-stage-structured networks.

5.3.1 Formulation

We assume that a traveler in state $s_t = (t, n)$ chooses the state $s_{t+1} = (t + 1, m)$ that minimizes the sum of the cost of link (n, m) , c_{nm} , and the expected minimum cost from state s_{t+1} to the final state s_d , $\mu_{t+1}^{s_d}(m)$. The transition probability from state s_t to state s_{t+1} is given by the multinomial logit model as follows (for the sake of simplicity, we omit the index of the absorbing state s_d):

$$p_t(m|n) = \frac{\Delta_t(m|n)e^{-\theta\{c_{nm} + \mu_{t+1}(m)\}}}{\sum_{m' \in \mathcal{N}} \Delta_t(m'|n)e^{-\theta\{c_{nm} + \mu_{t+1}(m')\}}}, \quad (5.8)$$

where θ is the perception parameter of the travel cost that is strictly positive. The expected minimum cost $\mu_t(n)$ is recursively formulated by the Bellman equation (Bellman, 1957):

$$\mu_t(n) = \mathbb{E} \left[\min_{(t+1,m) \in \mathcal{S}_{(t,n)}^+} \{\tilde{c}_{nm} + \mu_{t+1}(m)\} \right], \quad (5.9)$$

where

$$\mathcal{S}_{(t,n)}^+ = \{(t+1, m) \in \mathcal{S}_{t+1} | \Delta_t(m|n) = 1\}, \quad (5.10)$$

$$\tilde{c}_{nm} = c_{nm} + \varepsilon_{nm}. \quad (5.11)$$

$\mathcal{S}_{(t,n)}^+$ is the following set of successive states of $s = (t, n)$. ε is the i.i.d. extreme value type I. By this assumption of the random term distribution, Equation (5.9) is re-formulated as the logsum

$$\mu_t(n) = \begin{cases} -\frac{1}{\theta} \log \sum_{m \in \mathcal{N}} \Delta_t(m|n) e^{-\theta\{c_{nm} + \mu_{t+1}(m)\}}, & t \neq T \wedge n \neq d, \\ 0, & t = T \vee n = d. \end{cases} \quad (5.12)$$

The above formulations of dynamic programming are shown in Markov chain assignment models, such as Akamatsu, 1996, Baillon and Cominetti, 2008 and Fosgerau, Frejinger, and Karlstrom, 2013; however, our model is the first to incorporate the concept of choice-stage t and prism constraints $\Delta_t(m|n)$ into route choice modeling. This means that any state transition going outside of the prism is not permitted even if the two states are spatially connected (Figure 5.2), thus the probability of unrealistic cyclic paths become zero.

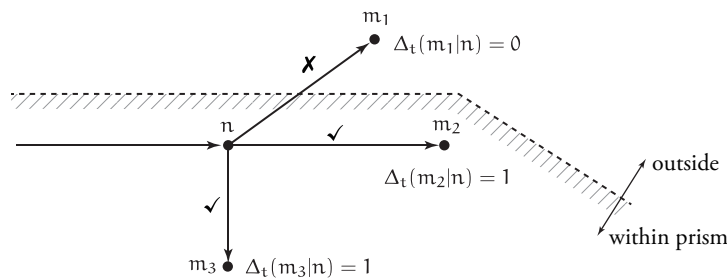


FIGURE 5.2: Constraint of transition by the prism

5.3.2 Solving Bellman equation

The incorporation of the prism constraints also enables one to solve the Bellman equation easily. We transform Equation (5.12) by taking the exponential.

$$e^{-\theta\mu_t(n)} = \begin{cases} \sum_{m \in \mathcal{N}} \Delta_t(m|n) e^{-\theta\{c_{nm} + \mu_{t+1}(m)\}}, & t \neq T \wedge n \neq d, \\ 1, & t = T \vee n = d. \end{cases} \quad (5.13)$$

We then define an array of vectors $\mathbf{v} = [\mathbf{v}_0, \dots, \mathbf{v}_t, \dots, \mathbf{v}_T]$, where the size of vector \mathbf{v}_t is $|\mathcal{N}| \times 1$, and an array of matrices $\mathbf{W} = [\mathbf{W}_0, \dots, \mathbf{W}_t, \dots, \mathbf{W}_{T-1}]$, where the size of matrix \mathbf{W}_t is $|\mathcal{N}| \times |\mathcal{N}|$, with entries

$$v_{tn} = e^{-\theta\mu_t(n)}, W_{tnm} = \Delta_t(m|n) e^{-\theta c_{nm}}. \quad (5.14)$$

The expected minimum costs μ are the solutions of the following equations:

$$v_{tn} = \begin{cases} \sum_{m \in \mathcal{N}} W_{tnm} v_{t+1,m}, & t \neq T, \\ 1, & t = T. \end{cases} \quad (5.15)$$

Finally, the Bellman equation Equation (5.15) can be written as:

$$\mathbf{v}_t = \mathbf{W}_t \mathbf{v}_{t+1} + \mathbf{b}, \quad (5.16)$$

where $\mathbf{b}(|\mathcal{N}| \times 1)$ is a vector with zero values for all states except for the destination that equals 1.

For previous Markovian traffic assignment models (e.g., Bell, 1995; Akamatsu, 1996; Baillon and Cominetti, 2008; Fosgerau, Frejinger, and Karlstrom, 2013), the Bellman equation is similar to Equation (5.16) but does not have the index of t , i.e., $\bar{\mathbf{v}} = \bar{\mathbf{W}}\bar{\mathbf{v}} + \mathbf{b}$, and thus they somehow need to solve the system of linear equations. In the case of the system of linear equations, the following inequality regarding the spectral radius $\rho(\bar{\mathbf{W}})$ of the incidence matrix $\bar{\mathbf{W}}$ (not including the concept of time) should be satisfied:

$$\rho(\bar{\mathbf{W}}) = \max_h \{|\lambda_h|\} < 1, \quad (5.17)$$

where λ_h is the h -th eigenvalue, and the inequality (5.17) is the necessary and sufficient condition for the matrix $\bar{\mathbf{W}}^k$ to converge as $k \rightarrow \infty$. That is, the computational stability of the MTA depends on the structure and condition of network; especially, the convergence becomes unstable when the network includes cyclic structures, and the perception parameter of the travel cost is small (see a numerical example in Appendix B.1 for the further discussion).

In contrast, in this paper, the expected minimum cost is defined for each state that is decomposed by choice-stage t , and thus the Bellman equation can be solved with the following backward induction:

Step 1: Set $s_o = (0, o)$, $s_d = (T, d)$ and $\mu_t^{s_d}(d) = 0, \forall t$. Calculate Δ , then \mathbf{W} .

Step 2: Initialize $t = T$, and $\mu_t^{s_d}(n) = 0, \forall n \in \mathcal{N}$.

Step 3: Set $t = t - 1$, and calculate $\mu_t^{s_d}(n)$ with Equation (5.16).

Step 4: Finish the algorithm if $t = 0$, otherwise back to STEP 3.

It is very simple and does not require convergence, and the computational burden is always same order ($T \times |\mathcal{N}|$), as long as the time constraint T is finite. Also, since unrealistic states are removed beforehand thanks to the prism constraint Δ , we are stably able to solve the Bellman equation. Moreover, the backward induction can be applied to the GEV-based Markovian models (Mai, Fosgerau, and Freijinger, 2015; Mai, 2016; Oyama and Hato, 2017), because the algorithm does not depend on whether the equation is linear or non-linear.

5.4 Stochastic traffic assignment

In this section, we present a STA algorithm on the choice-stage-structured network. As well as previous STA algorithms (Dial, 1971; Bell, 1995; Akamatsu, 1996), it aims to calculate the spatial link flow x_{nm} , $(n, m) \in \mathcal{A}$ in flow-independent networks without path enumeration.

5.4.1 Preliminary

We introduced an indicator $I_t(n)$, based on only one pair of origin and destination (OD), i.e., $I_t(n) = I_t^{od}(n)$, for the sake of making it clear to understand the formation process of the prism in Figure 5.1. However, in the context of traffic assignment, it is usual to deal with multiple OD pairs. The previous STA algorithms (Dial, 1971; Akamatsu, 1996) use variables specific for not each pair of origin and destination but each origin (or each destination), in order to implement the assignment for an origin and multiple destinations (or multiple origins and a destination) simultaneously. For this reason, we herein re-define $I_t(n)$ as a destination-specific variable, i.e., $I_t(n) = I_t^d(n)$ as follows:

$$I_t^d(n) = \begin{cases} 1, & \text{if } \min_{o \in \mathcal{O}} \{D^o(n)\} \leq t, D^d(n) \leq T - t \\ 0, & \text{otherwise.} \end{cases} \quad (5.18)$$

where $\mathcal{O} \subseteq \mathcal{N}$ is the set of origin nodes. The state connection indicator Δ and the transition probability p can be calculated using Equation (5.6) and (5.8) with $I_t^d(n)$ as the destination-specific variables. In the followings, we use the destination-specific variables, namely, the assignment is based on a many-to-one procedure.

5.4.2 Assignment algorithm

We define $y_n^{d,t}$ and $x_{nm}^{d,t}$ as the state flow at $s = (t, n)$ and edge flow from $s = (t, n)$ to $s' = (t + 1, m)$, respectively. The relationship between state and edge flows is formulated as follows:

$$y_n^{d,t} = \begin{cases} \sum_{i \in \mathcal{N}} x_{in}^{d,t-1}, & t \neq 0 \\ q_{nd}, & t = 0 \wedge n \in \mathcal{O} \\ 0, & t = 0 \wedge n \notin \mathcal{O} \end{cases} \quad (5.19)$$

and

$$x_{nm}^{d,t} = y_n^{d,t} p_t^d(m|n), \quad \forall t \in \mathcal{T} \setminus T \quad (5.20)$$

where q_{od} is a given generating flow between each OD pair. For each state $s = (t, n)$, the following condition of flow conservation is satisfied:

$$\sum_{i \in \mathcal{N}} x_{in}^{d,t-1} - \sum_{m \in \mathcal{N}} x_{nm}^{d,t} + \sum_{o \in \mathcal{O}} \eta_{(t,n)}^{s_o} q_{od} - \eta_{(t,n)}^{s_d} \sum_{o \in \mathcal{O}} q_{od} = 0, \quad \forall t \in \mathcal{T}, \forall n \in \mathcal{N}, \quad (5.21)$$

where $\eta_s^{s_o}$ and $\eta_s^{s_d}$ are indicators that equal to one when $s = s_o = (0, o)$ and $s = s_d = (T, d)$, and are zero when $s \neq s_o$ and $s \neq s_d$, respectively.

Lemma 5.4.1. *In a CSN, all flows with the same destination d are absorbed into the unique final state $s_d = (T, d)$.*

Proof. The condition of flow conservation for $s = s_d$ is formulated by Equation (5.21) as

$$\sum_{i \in \mathcal{N}} x_{id}^{d,T-1} - \sum_{o \in \mathcal{O}} q_{od} = 0, \quad (5.22)$$

and namely by Equation (5.19),

$$y_d^{d,T} = \sum_{o \in \mathcal{O}} q_{od}. \quad (5.23)$$

This indicates that the state flow at $s = (T, d)$ is equivalent to the sum of generating flows. \blacksquare

Note that Lemma 5.4.1 is provided by the prism constraint. Since $p_t^d(m|n)$ includes the state connection indicator $\Delta_t^d(m|n)$, no transition from states within the prism to states external to the prism is considered, and thus the traffic volume always flows within the prism.

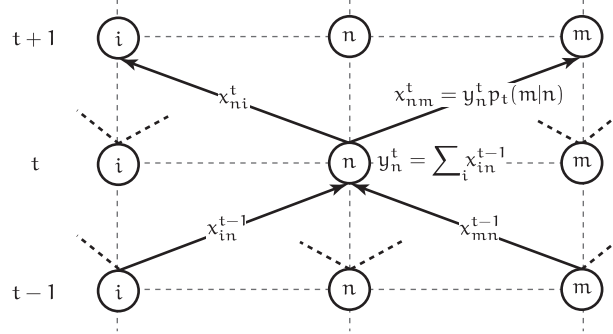


FIGURE 5.3: Illustration of a network assignment

Figure 5.3 shows the assignment algorithm on a CSN: we first set $t = 0$ and $y_0^{d,0} = q_{od}, \forall o \in \mathcal{O}$ and then alternately calculate state and edge flows using Equation (5.20) and (5.19) until the choice-stage arrives at T . After calculating flows for all destinations, we finally obtain spatial link flow of $(n, m) \in \mathcal{A}$, x_{nm} by the summation of $x_{nm}^{d,t}$ as follows:

$$x_{nm} = \sum_{d \in \mathcal{D}} x_{nm}^d = \sum_{d \in \mathcal{D}} \sum_{t=0}^{T-1} x_{nm}^{d,t}. \quad (5.24)$$

where $\mathcal{D} \subseteq \mathcal{N}$ is the set of destination nodes.

The procedures of the assignment algorithm are summarized below.

Algorithm 1 Choice-stage-structured assignment**Input:**Spatial network graph $\mathcal{G} = (\mathcal{N}, \mathcal{A})$ OD flow entries $\{(o, d, q_{od})\}$ Choice-stage constraint T **Output:**Link flow $\{x_{nm}\}$

```

1: Calculate the matrix  $\mathbf{D}^n(m)$  ( $|\mathcal{N}| \times |\mathcal{N}|$ ).
2: for  $d = 1$  to  $|\mathcal{D}|$  do
3:   #Step1: Choice-stage-structured network
4:   Set  $t = 0$ . For  $n \in \mathcal{O}$ ,  $I_t^d(n) = 1$ , and otherwise  $I_t^d(n) = 0$ .
5:   for  $t = 1$  to  $T$  do
6:     Calculate the vector  $\mathbf{I}_t^d$  ( $|\mathcal{N}| \times 1$ ).
7:     Calculate the matrices  $\Delta_{t-1}^d$  ( $|\mathcal{N}| \times |\mathcal{N}|$ ) and  $\mathbf{W}_{t-1}^d$  ( $|\mathcal{N}| \times |\mathcal{N}|$ ).
8:   end for
9:   #Step2: Transition probabilities
10:  Set  $t = T$ . For  $n = d$ ,  $v_{tn}^d = 1$ , and otherwise  $v_{tn}^d = 0$ .
11:  for  $t = T - 1$  to  $0$  do
12:    Calculate the vector  $\mathbf{v}_t^d$  ( $|\mathcal{N}| \times 1$ ).
13:  end for
14:  #Step3: Assignment
15:  Set  $t = 0$ . For  $n \in \mathcal{O}$ ,  $y_n^{d,t} = q_{od}$ , and otherwise  $y_n^{d,t} = 0$ .
16:  for  $t = 1$  to  $T$  do
17:    Calculate the matrices  $\mathbf{p}_{t-1}^d$  ( $|\mathcal{N}| \times |\mathcal{N}|$ ) and  $\mathbf{x}^{d,t-1}$  ( $|\mathcal{N}| \times |\mathcal{N}|$ ).
18:    Calculate the vector  $\mathbf{y}^{d,t}$  ( $|\mathcal{N}| \times 1$ ).
19:  end for
20:  Calculate the matrix  $\mathbf{x}^d$  ( $|\mathcal{N}| \times |\mathcal{N}|$ ).
21: end for
22: Calculate the matrix  $\mathbf{x}$  ( $|\mathcal{N}| \times |\mathcal{N}|$ ).
23: return Spatial aggregate link flow  $\{x_{nm}, \forall (n, m) \in \mathcal{A}\}$ .
```

5.4.3 Properties of the assignment model

Proposition 5.4.1. *The set of flow calculated by the CSA algorithm is equivalent to the solution of the following optimization problem (CSA-STA):*

[CSA-STA]

$$\min Z(\mathbf{f}) = \sum_{nm} c_{nm} x_{nm} + \frac{1}{\theta} \sum_d \sum_t \sum_{nm} x_{nm}^{d,t} \ln x_{nm}^{d,t} - \frac{1}{\theta} \sum_d \sum_t \sum_n (\sum_m x_{nm}^{d,t}) \ln (\sum_m x_{nm}^{d,t}) \quad (5.25)$$

s.t., Equation (5.21) and

$$x_{nm} = \sum_d \sum_t x_{nm}^{d,t}, \quad \forall (n, m) \in \mathcal{A}, \quad (5.26)$$

$$x_{nm}^{d,t} \geq 0, \quad \forall d \in \mathcal{D}, \forall t \in \mathcal{T}, \forall (n, m) \in \mathcal{A}. \quad (5.27)$$

Proof. We define the Lagrange \mathcal{L} as

$$\begin{aligned}\mathcal{L}(\mathbf{f}, \boldsymbol{\gamma}, \boldsymbol{\lambda}) &= Z(\mathbf{f}) \\ &+ \sum_d \sum_t \sum_n \gamma_n^{d,t} \left(\sum_h x_{hn}^{d,t-1} - \sum_m x_{nm}^{d,t} + \sum_o \eta_{(t,n)}^{s_o} q_{od} - \eta_{(t,n)}^{s_d} \sum_o q_{od} \right) \\ &+ \sum_{nm} \lambda_{nm} \left(x_{nm} - \sum_d \sum_t x_{nm}^{d,t} \right).\end{aligned}\quad (5.28)$$

The Karush-Kuhn-Tucker (KKT) condition of the CSA-STA is

$$\frac{\partial \mathcal{L}}{\partial x_{nm}^{d,t}} \cdot x_{nm}^{d,t} = 0, \quad (5.29)$$

$$\frac{\partial \mathcal{L}}{\partial x_{nm}^{d,t}} \geq 0, \quad (5.30)$$

and Equations (5.21), (5.26) and (5.27). Therefore, we obtain the following equation when $x_{nm}^{d,t} \geq 0$:

$$c_{nm} + \log \frac{x_{nm}^{d,t}}{\sum_j x_{nm}^{d,t}} + \gamma_j^{d,t+1} - \gamma_i^{d,t} = 0. \quad (5.31)$$

By transforming Equation (5.31), we obtain

$$p_t^d(m|n) = \frac{x_{nm}^{d,t}}{\sum_j x_{nm}^{d,t}} = e^{-\theta(c_{nm} + \gamma_m^{d,t+1} - \gamma_n^{d,t})}. \quad (5.32)$$

Since the summation of transition probabilities $p_t(m|n)$ is conserved as one for any state $s = (t, n)$,

$$e^{-\theta \gamma_n^{d,t}} = \sum_m e^{-\theta c_{nm}} e^{-\theta \gamma_m^{d,t+1}} \quad (5.33)$$

is satisfied. Assuming $\gamma_n^{d,t}$ as the expected maximum utility $\mu_t^{s_d}(n)$ at state $s = (t, n)$, Equation (5.33) is equivalent to the Bellman equation of Equation (5.16), that is, Equation (5.32) is the route choice model in the CSN. ■

Proposition 5.4.2. *The CSA-STA is equivalent to the logit-based assignment with the prism-based path set.*

Proof. The expansion of Equation (5.33) to time T with the notations $v_{t,n} = e^{-\theta \gamma_n^{d,t}}$ and $\bar{w}_{nm} = e^{-\theta c_{nm}}$ is

$$v_{t,n_t} = \sum_{n_{t+1}} \bar{w}_{n_t n_{t+1}} \sum_{n_{t+2}} \bar{w}_{n_{t+1} n_{t+2}} \cdots \sum_{n_{T-1}} \bar{w}_{n_{T-2} n_{T-1}} \cdot \bar{w}_{n_{T-1} d} v_{T,d}. \quad (5.34)$$

At any time $t+l$ ($0 < l < T-t$), only the state $s_{t+l} = (t+1, n_{t+l})$ that satisfies $D^{n_t}(n_{t+l}) \leq l$ and $D^d(n_{t+l}) \leq T - (t+l)$ is considered; therefore Equation 5.34 is

transformed as:

$$\begin{aligned} v_{t,n_t} &= v_{T,d} \sum_{r \in \mathcal{P}_{(t,n_t)}^{(T,d)}} \prod_{nm \in r} \bar{w}_{nm} \\ &= v_{T,d} \sum_{r \in \mathcal{P}_{(t,n_t)}^{(T,d)}} e^{-\theta c_r}, \end{aligned} \quad (5.35)$$

where $\mathcal{P}_{(t,n_t)}^{(T,d)}$ is the set of all feasible paths that arrives at d from n_t within $(T-t)$ steps, which is the time-space prism defined by the states (t, n_t) and (T, d) , and c_r is the cost of path r . By assuming $v_{T,d} = 1$, we obtain

$$v_{t,n_t} = \sum_{r \in \mathcal{P}_{(t,n_t)}^{(T,d)}} e^{-\theta c_r}, \quad (5.36)$$

which is also satisfied at (T, d) (the right side equals to one). Given Equations (5.32) and (5.36), the probability of path $r = [n_0, n_1, \dots, n_{T-1}, n_T]$ ($n_0 = o$, $n_T = d$) is formulated as

$$\begin{aligned} P(r) &= \prod_{t=0}^{T-1} p_t(n_{t+1}|n_t) \\ &= e^{-\theta \sum_{t=0}^{T-1} c_{n_t n_{t+1}}} \frac{v_{T,d}}{v_{0,o}} \\ &= \frac{e^{-\theta c_r}}{\sum_{r \in \mathcal{P}_{(0,o)}^{(T,d)}} e^{-\theta c_r}}. \end{aligned} \quad (5.37)$$

This is equivalent to the logit-based assignment with the prism-based path set $\mathcal{P}_{(0,o)}^{(T,d)}$ that is defined in Section 5.2.

From the above, it is proved that the CSA-STA is equivalent to the logit-type assignment with the path set defined by the prism. ■

Proposition 5.4.3. *The CSA-STA has the unique solution.*

Proof. The first term of the objective function (5.25) is a strictly convex function of x . The second and third terms are entropy terms and can be decomposed into the entropy function for each state $s = (t, n)$, as follows:

$$-H(\mathbf{f}) = \sum_d \sum_t \sum_n -H_{tn}^d(\mathbf{f}), \quad (5.38)$$

where,

$$H_{tn}^d(\mathbf{f}) = -\sum_m x_{nm}^{d,t} \ln x_{nm}^{d,t} + (\sum_m x_{nm}^{d,t}) \ln (\sum_m x_{nm}^{d,t}). \quad (5.39)$$

$-H_{tn}^d$ is a strictly convex function for the edge flows $\{x_{nm}^{d,t}, \forall m \in \mathcal{N}_n^+\}$ at state $s = (t, n)$ (Akamatsu, 1997). Also, since Equations (5.21), (5.26) and (5.27) are the constraints of only linear equations and the non-negative condition, the solution space is a closed convex set. Therefore, the CSA-STA is a convex programming problem with a strictly convex objective function, and the solution is always unique if it has the solution. ■

Given the discussion above, we also obtain the equivalent optimization problem to the stochastic user equilibrium (SUE) problem that is based on the proposed route choice model with the prism-based path set. The SUE problem is formulated as follows:

[CSA-SUE]

$$\begin{aligned} \min Z(\mathbf{f}) = & \sum_{nm} \int_0^{x_{nm}} t_{nm}(\omega) d\omega + \frac{1}{\theta} \sum_d \sum_t \sum_{nm} x_{nm}^{d,t} \ln x_{nm}^{d,t} \\ & - \frac{1}{\theta} \sum_d \sum_t \sum_n (\sum_m x_{nm}^{d,t}) \ln (\sum_m x_{nm}^{d,t}), \end{aligned} \quad (5.40)$$

s.t., Equation (5.21), (5.26) and (5.27).

In the same way with the CSA-STA, by considering the Lagrangian, we obtain the same KKT conditions and prove that the CSA-SUE is the equivalent optimization problem of the stochastic user equilibrium in a CSN. Furthermore, if the link performance function $t_a(x_a)$ is monotonically increasing for the link flow x_a , the first term of the objective function (5.40) is a strictly convex function of x . Since the entropy terms are the same with CSA-STA, the CSA-SUE is a convex programming problem with a strictly convex objective function, and the solution is always unique if it has the solution.

5.5 Numerical examples

In this section, we present several numerical examples to validate the proposed model compared to existing approaches.

5.5.1 Computational examination

We first have the STA examples using simple networks to show the computational stability and the efficiency of the model. Examinations of cyclic flows and path correlation structures are shown, too.

Computational stability

To confirm the consistency with previous STA models and the computational stability, we implement the assignment using the simple cyclic network of Figure 5.4. The number associated with each link is the link cost c_{nm} . We set generating flow to $q_{od} = 1000$ for one OD pair and compare the assignment results given by Dial's algorithm, MTA and CSA. Table 5.3 shows the assignment results when the perception parameter $\theta = 1$. The results show that the CSA with $T = 20$ outputs the same flow with the MTA (the difference from the Dial's assignment result comes from its restriction to efficient paths). That is, CSA is a generalized formulation of MTA, since it theoretically corresponds to MTA as a special case, if T is large enough. We also calculate link flow when $\theta = 0.2$ to check the computational stability of the models, and the results are shown in Table 5.4. Thanks to the restriction of efficient paths, Dial's algorithm is able to calculate the link flow, though cyclic flow cannot be considered. CSA is able to output results including cyclic flows regardless of the value of θ , while MTA fails to do so because of a large spectral radius (in this example, $\rho(\mathbf{W}) = 1.058$). These results demonstrate that the proposed method is consistent with the MTA approach as a special case, and moreover, it enables solving network flow even if the link cost and/or the perception parameter are small.

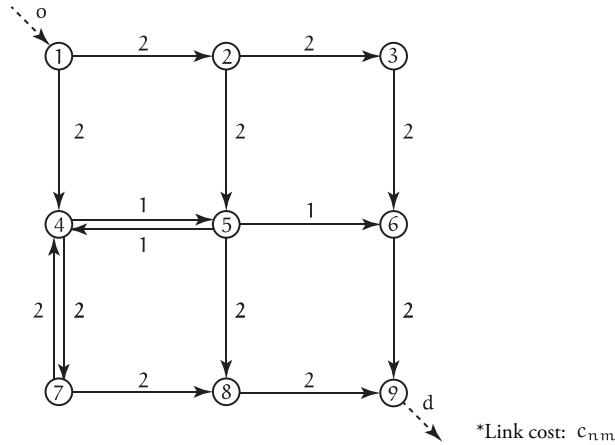


FIGURE 5.4: A simple cyclic network

TABLE 5.3: Assignment results in a cyclic network with $\theta = 1$

	1-2	2-3	1-4	2-5	3-6	4-5	5-6	4-7	5-8	6-9	7-8	8-9	5-4	7-4
Dial	269	0	731	269	0	731	731	0	269	731	0	269	0	0
MTA	290	54	710	236	54	797	643	83	236	697	67	303	154	16
CSA (T=5)	298	63	702	235	63	639	639	63	235	702	63	298	0	0
CSA (T=10)	290	54	710	236	54	795	642	83	236	697	67	303	153	16
CSA (T=20)	290	54	710	236	54	797	643	83	236	697	67	303	154	16

TABLE 5.4: Assignment results in a cyclic network with $\theta = 0.2$

	1-2	2-3	1-4	2-5	3-6	4-5	5-6	4-7	5-8	6-9	7-8	8-9	5-4	7-4
Dial	269	0	731	269	0	731	731	0	269	731	0	269	0	0
MTA	-	-	-	-	-	-	-	-	-	-	-	-	-	-
CSA (T=5)	465	144	535	320	144	391	391	144	320	535	144	465	0	0
CSA (T=10)	363	36	637	327	36	1431	399	764	327	435	238	565	1032	526
CSA (T=20)	340	12	660	328	12	3312	401	2008	328	413	259	587	2911	3164

Computational efficiency

The CSN has a larger number of states than the general spatial network. In order to check the computational efficiency of CSA, we compare the computational time (CPU time) of CSA to those of other STA algorithms using the grid networks in Figure 5.5. The network has n links on each side, i.e., it includes $2n(n + 1)$ links and $(n + 1)^2$ nodes. We assume 10 origins and 1 destination (10 OD pairs) for all settings of n . Table 5.5 shows the CPU time of Dial's algorithm, MTA and CSA with $T = 2n$, and each reported time is the average of 10 calculations of each assignment algorithm. Note that we use a sparse matrix coding in all assignments and the Dijkstra's method for calculating the shortest path in both Dial's algorithm and CSA. The CPU time of Dial's algorithm is the shortest in all cases of n . The CPU time of the MTA is smaller than that of CSA when n is small. As n is increasing, the difference between CPU times of MTA and CSA gets smaller, and when $n = 70, 80$, CSA is faster than MTA. The size of state space of CSA is larger than those of the other algorithms due to the incorporation of the choice-stage dimension T . However, reducing the number of states with the prism constraint allows the computation of the CSA in reasonable time. In the case of large networks, the MTA requires much time to solve

the system of linear equations with respect to the expected minimum costs. In contrast, as explained in Section 5.3, the computation of the expected minimum cost of the CSA requires only T iterations. That is, the computational effort increase at most linearly with respect to T , even though the CPU time of CSA depends on T .

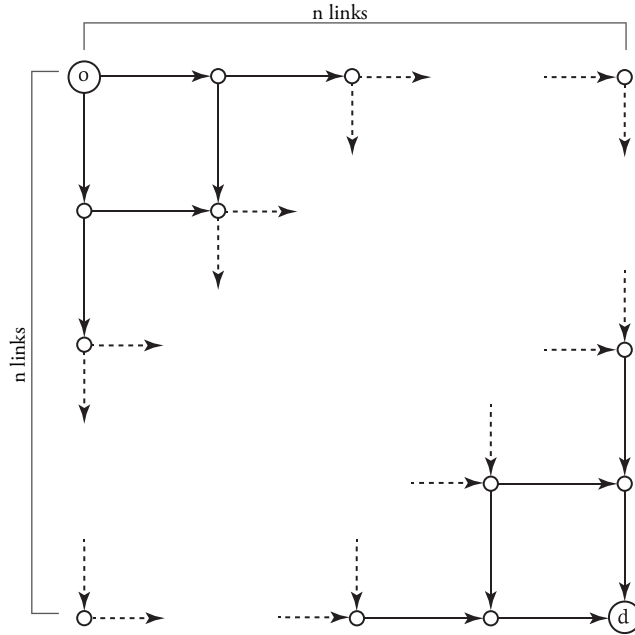


FIGURE 5.5: Grid network

TABLE 5.5: Loading time in seconds in grid networks

n	10	20	30	40	50	60	70	80
Dial	0.02	0.24	1.07	3.50	7.60	15.63	28.97	48.75
MTA	0.04	0.19	0.73	2.89	8.75	22.95	52.08	102.32
CSA	0.13	0.51	1.91	5.47	11.77	23.28	42.50	70.00

*The number is the average time of 10 calculations for each algorithm.

5.5.2 Cyclic flows

We herein consider the stochastic user equilibrium (SUE) problem to discuss the flow patterns that are performed by the three different assignment algorithms. We solve the problems with the partial linearization method (Patriksson, 1993). In the algorithm, the sub-problem where the first term of the objective function (Equation (5.40)) is partially linearized is equivalent to the CSA-STA.

To compare the assignment results given by the three algorithms, we implemented SUE assignments in the *Sioux Falls* network with 24 nodes, 76 links, 576 OD pairs and 36650 total demands. In this calculation, we set the perception parameter $\theta = 1$. We denote the assignment results given by the three algorithms as Dial-SUE, MTA-SUE and CSA-SUE, respectively. Figure 5.6 shows the difference of link flows between MTA-SUE and Dial-SUE (a) and between CSA-SUE and Dial-SUE (b). Colors exhibit the degree of difference: gray and black links indicate that the difference from Dial-SUE is small, on the other hand, orange and red links indicate the large increase. The assignment result given by MTA-SUE (a) shows that

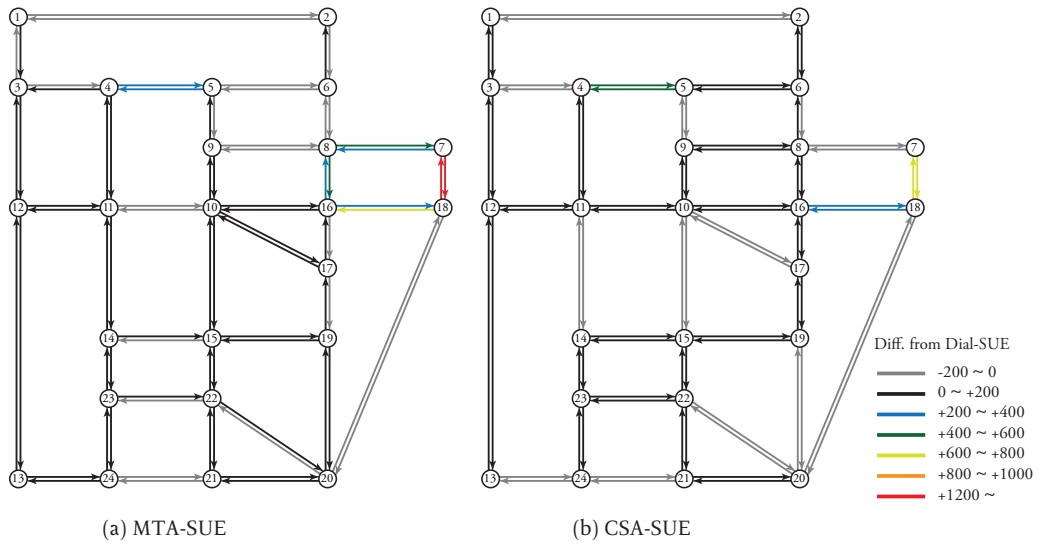


FIGURE 5.6: Stochastic user equilibrium results

flows of the cycle consisting of node 7, 8, 16 and 18 increase by more than 200, and this indicates that the MTA algorithm generates unreasonable cyclic flows. The assignment result given by CSA-SUE (b) with $T = \max[2D^o(d)]$ indicates the increase of link 7-18 and 18-7, too; however, the overall increase of link flows are restrained. These results conclude that the CSA algorithm can reduce the unreasonable cyclic flow of the MTA algorithm by incorporating the time-constraint concept, which is based on a behavioral mechanism.

5.5.3 Overlapping paths in cyclic networks

Finally, we show the model properties in terms of overlapping descriptions by extending the model to a network-GEV based model.

Formulation of a network-GEV model in CSN

Following the literature (Papola and Marzano, 2013; Hara and Akamatsu, 2014), we extend the proposed model to a network-GEV (n-GEV) based route choice model. The application of the n-GEV requires the network to be acyclic (see Bierlaire, 2002; Daly and Bierlaire, 2006), and in the literature of n-GEV based route choice models, the network was edited to remove cyclic structures. In contrast, in this paper all paths in CSNs, network states are decomposed by choice-stage, and any paths do not pass the same node more than once. Therefore, we do not need to remove any links and the spatial connection condition is retained.

The state transition probabilities of the n-GEV based route choice model in CSNs (CSN-nGEV) are formulated as follows:

$$p_t(m|n) = \frac{\Delta_t(m|n) \cdot \alpha_{nm} e^{-\theta_n \{c_{nm} + \mu_{t+1}(m)\}}}{\sum_{m' \in \mathcal{N}} \Delta_t(m'|n) \cdot \alpha_{nm'} e^{-\theta_n \{c_{nm'} + \mu_{t+1}(m')\}}}, \quad (5.41)$$

where θ_n is the scale parameter peculiar to node n , and states $s = (t, n)$, $\forall t$ have the same scale parameter with each other. α_{nm} is the allocation parameter peculiar to the node pair (n, m) and edges $e = ((t, n), (t + 1, m))$, $\forall t$ have the common value. Note that the allocation parameter describes the relationship between neighboring node

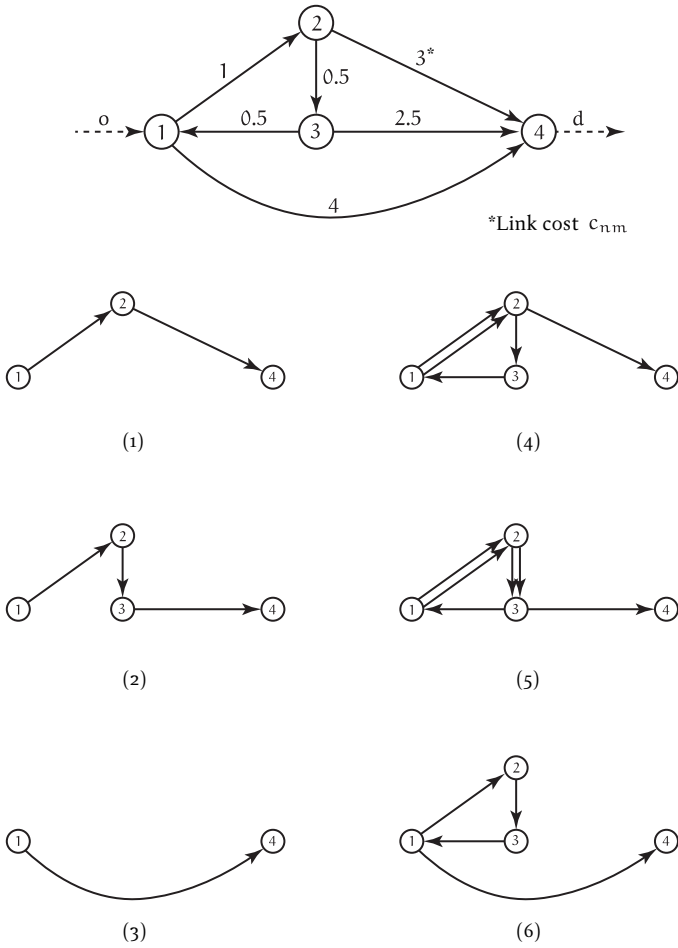


FIGURE 5.7: Network and alternatives

pairs and satisfies $\sum_m \alpha_{nm}, \alpha_{nm} > 0, \forall (n, m) \in \mathcal{A}$. By incorporating these parameters, the Bellman equation can be re-formulated as follows:

$$v_{tn} = \sum_{m \in \mathcal{N}} w_{tnm} (v_{t+1,m})^{\frac{\theta_n}{\theta_m}} \quad (5.42)$$

where,

$$v_{tn} = e^{-\theta_n \mu_t(n)} \quad (5.43)$$

$$w_{tnm} = \Delta_t(m|n) \cdot \alpha_{nm} e^{-\theta_n c_{nm}} \quad (5.44)$$

Equation (5.42) is non-linear, but we can solve the equation using the backward induction algorithm, similarly to as is shown in Section 5.3, because the value function v_{tn} is structured based on choice-stage.

TABLE 5.6: Path probabilities

Model	Path probability					
	P_1	P_2	P_3	P_4	P_5	P_6
logit	0.333	0.333	0.333	-	-	-
nGEV	0.250	0.250	0.500	-	-	-
CSN-logit	0.294	0.294	0.294	0.040	0.040	0.040
CSN-nGEV	0.281	0.140	0.562	0.005	0.002	0.010

Path probability

The probability of a path r in the CSN-nGEV model is formulated using the transition probabilities:

$$\mathbb{P}(r = [n_0, \dots, n_t, \dots, n_T]) = \prod_{t=0}^{T-1} p_t(n_{t+1}|n_t) \quad (5.45)$$

Using Equation (5.45), we calculate path probabilities in the network of Figure 5.7 and compare the results with previous models (logit, n-GEV). We set $T = 6$, then obtain the six paths shown in the bottom of Figure 5.7. The costs of the paths are 4, 4, 4, 6, 6 and 6, and we denote the path probabilities as P_1, P_2, P_3, P_4, P_5 and P_6 , respectively. The scale parameters and allocation parameters are formulated as

$$\theta_n = \frac{D^o(d)}{D^d(n)} \quad (5.46)$$

$$\alpha_{nm} = \frac{\delta(m|n)}{N(n)}, \quad (5.47)$$

where $N(n)$ is the degree of node n .

Table 5.6 shows the path probabilities given by logit (acyclic), n-GEV (acyclic), CSN-logit (cyclic) and CSN-nGEV (cyclic). The results of the logit-based route choice model that does not consider cycles are $P_1 = P_2 = P_3 = 0.333$. Although paths 1 and 2 share the link 1-2 and are assumed to be correlated with each other, all path probabilities are equal to each other because of the IIA property of the logit model. The n-GEV based route choice model is able to describe the correlation among paths, and the path probabilities are $P_1 = P_2 = 0.250$ and $P_3 = 0.500$. Application of the n-GEV model requires the removal of the link 3-1 to remove cyclic structures, and thus P_4, P_5 and P_6 can not be evaluated. The results of the logit-based route choice model including cyclic paths (CSN-logit) are $P_1 = P_2 = P_3 = 0.294$ and $P_4 = P_5 = P_6 = 0.040$. This model can not consider the overlapping paths as well as the first logit model. Compared to the three models, the CSN-nGEV model reports the result $P_3 > P_1 > P_2 > P_6 > P_4 > P_5$: all path probabilities are different from each other. P_1 becomes larger than P_2 because of the correlation among the path alternatives that includes the cyclic paths. P_4, P_5 and P_6 are evaluated to be smaller than the result of the CSN-logit model, since the CSN-nGEV model considers a mechanism that travelers take more cost when they pass the same node more than once, which is referred to as *cycle reluctance* in this paper. In disaster or pedestrian contexts, we cannot ignore the cyclic paths, and it is assumed inappropriate to remove the cyclic structure from the networks (Oyama and Hato, 2017). The proposed CSN-nGEV model is able to consider the mechanism of cycle reluctance, and thus it is able to avoid the assignment of unreasonable probabilities to cyclic paths.

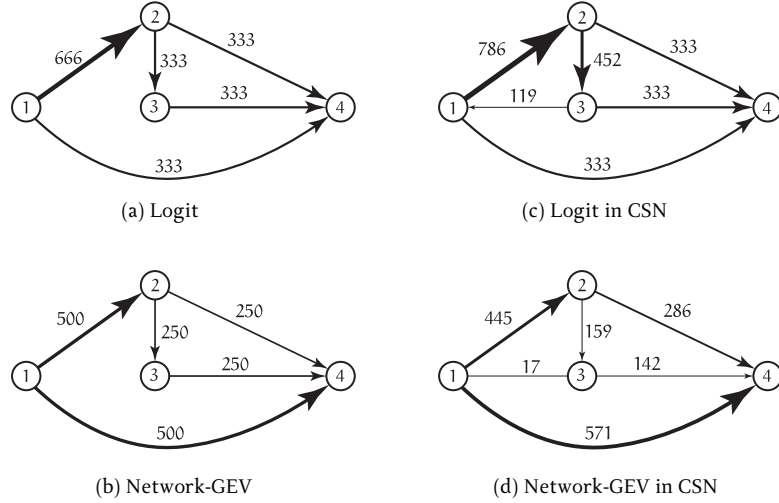


FIGURE 5.8: Logit-based and network-GEV-based assignment results with CSN

Assignment results

Figure 5.8 shows the assignment results given by the four models that are used in the previous section. Note that this example does not consider congestion. Figure 5.8 (a) and (b) are the results considering only the path 1, 2, and 3. In the case of Figure 5.8(a), link 1-2 has excessive flow, and on the other hand in the case of Figure 5.8(b), the flow was alleviated as the result of the consideration of the path overlapping. Figure 5.8(c) is the result given by the CSN-logit model, and it shows that more excessive flows were loaded on link 1-2 and 2-3 than the result of Figure 5.8(a). The flow of link 3-1 that constitutes cyclic paths is 119. In contrast, Figure 5.8(d) that is the result given by the CSN-nGEV model shows that the unreasonable flows generated in the case of Figure 5.8(a), (b) and (c) are alleviated. This is because the CSN-nGEV model is able to consider the correlation structure among the path set including cyclic paths. The result of considering cyclic link 3-1 is that more flow is loaded on path 3 (link 1-4) and less flow is loaded on link 1-2 than the results of the case of not considering cyclic paths. The difference of flow of link 3-4 is large among the results: 333 in cases (a) and (c), without considering cyclic paths; 250 in case (b); and 142 in case (d). Previous studies could not describe the change of flow due to the correlation structure of cyclic paths; however, our model is able to evaluate the effect of a variety of paths even if a network includes cyclic paths.

5.6 Conclusions and Discussion

This paper proposes an algorithm for stochastic traffic assignment that is referred to as a choice-stage-structured assignment (CSA). We decompose the network states by the choice-stage, and the new network description is able to remove the cyclic structure from the calculation. Moreover, we incorporate the concept of choice-stage-constraint into the route choice model and propose an algorithm for systematically restricting path sets. The set of all feasible paths after the restriction forms so-called the time-space prism, i.e., the method reflects behavioral limitation of travelers. Thus, we are able to remove unrealistic paths that are considered in the MTA

such as paths including infinite cycles. The restriction method also reduces the number of states that are considered in the model, and this allows the reduction of memory spaces and computational burden.

It is known that the MTA has a challenge with respect to computational instability: whether the Bellman equation can be solved is dependent on the structure and conditions of network. In contrast, in the CSN, the Bellman equation can be solved stably by the backward induction with only T iteration, because we assume that the states are different even if they are at the same spatial node. A numerical example shows that the CSA is always able to output the link flows, while the MTA is not able to do so when link costs or the perception parameter are small. The CSA is also able to examine the change of link flow by varying the parameter of choice-stage constraint T .

Also, the result of the SUE indicates the possibility that the application of the CSA algorithm could alleviate the unreasonable cyclic flow given by the MTA. Finally, we extend the proposed model to the network-GEV model in choice-stage-structured networks (CSN-nGEV) and show that the CSN-nGEV model is able to describe the effect of overlapping among the path set including cyclic paths.

These results conclude that the CSA algorithm is the one of the solution of the remaining challenges of the MTA: 1) computational instability dependent on network structure and conditions, 2) unreasonable cyclic flows, and 3) the amplification of the IIA property, with reasonable computational time.

We believe that our method is also useful for parameter estimation problems of Markovian route choice models, including so-called recursive logit models (Fosgerau, Frejinger, and Karlstrom, 2013). Also, the method can be applied to other transportation networks such as transit networks with uncertainties (Bell, 2009; Ma and Fukuda, 2015), pedestrian activity-scheduling networks (Oyama, and Hato, 2016).

As to the limitation of this algorithm, it is worth mentioning about the settings of the parameter T . Although we set arbitrary values for T in the paper, in the future work, we will examine the way of setting the parameter T and obtain an interpretation as a behavioral parameter using real data.

Chapter 6

Application to pedestrian activity-scheduling network

In this chapter, we use a Markovian route choice model to describe the path choice behavior in time-space networks, and present a framework that evaluate the use of time and space integrally. We apply it to a pedestrian network design problem. This is the collaboration work with Dr. Michel Bierlaire and Dr. Riccardo Scarinci at EPFL.

In the pedestrian route choice context, the continuity between behavior of walking in networks and of staying for conducting activities is very high. For this reason, the activity path choice approach, which is a route choice model in time-space networks, is applicable to describe integrally the combination of choices of routes, activity locations and durations. Activity paths are often complicated, and it is difficult to solve the activity path choice problem. Most of previous models deal with the problem as the deterministic one and optimize in the restricted path set in rough networks. However, pedestrian activities are often probabilistic and should be described in high resolution networks. In this study, we propose a Markovian activity assignment model for dealing with the computational challenges of the pedestrian activity path choices. Moreover, we present a method for systematically restricting the path set based on the concept of the time-space prism (Hägerstrand, 1970). We examine the properties of the model through several illustrative examples and a case study of the network in Matsuyama-city, Japan. In the end, we present a pedestrian network design problem based on the activity assignment model. The problem is a multi-level and multi-objective programming, and the Pareto front is investigated by a neighborhood search algorithm.

Keywords: Activity assignment, Route choice model, Time-space constraint, Pedestrian, Traffic assignment

6.1 Introduction

Pedestrian behavior is an important evaluation index for public space design and retail planning in city centers. Recent social needs such as the environmental conservation and the health awareness are paying much attention to pedestrians, and many municipal governments and retail planning authorities require the models that evaluate the pedestrian behavior in city centers. Borgers and Timmermans, 1986b; Borgers and Timmermans, 1986c developed a pedestrian simulation model and applied it to the questionnaire data of Maastricht, and recently, some studies have reported the analysis of pedestrian behavior using Global Positioning System (GPS) and detailed sensors (Hato, 2010) or WiFi data (Danalet, Farooq, and Bierlaire, 2014; Danalet et al., 2016). Likewise, the data collection of pedestrian behavior has been improved in these decades; however, there are still only a few operational models. In this paper, focusing of these trends, we aim at developing a novel framework for evaluating pedestrian route choice and time allocation behavior in city centers. Note that we focus on not microscopic and two-dimensional pedestrian behavior (e.g., Hoogendoorn and Bovy, 2004; Antonini, Bierlaire, and Weber, 2006; Robin et al., 2009; Hänseler et al., 2017) but the behavior at about 1km square scale based on the path choice behavior in activity-scheduling networks.

The pedestrian behavior in a city center is the scheduling behavior from the entry to the exit and can include multiple activities and multiple route choices within the district. In many cases, this behavior is restricted by the time-constraint. For this reason, we can assume the pedestrian behavior as an analogy of the home-based daily activity-scheduling behavior. Over the past decades, a large number of activity-scheduling models have been proposed (e.g., Bowman and Ben-Akiva, 2000; Miller and Roorda, 2003; Arentze and Timmermans, 2004b; Habib, 2011). Most of activity-scheduling models are based on the multiple choices, for instance, the destination and activity duration are firstly chosen and then the routes are chosen. On the other hand, in pedestrian route choice context in city centers, the choice of activity does not necessarily precede trips, and unplanned activities can be generated on the way of trips context-dependently. For this reason, this paper formulates an activity path choice model in pedestrian activity-scheduling networks.

The activity path choice model is applicable to describing continuous decisions in time-space networks. Recker, 1995 proposed an optimization model referred to as household activity pattern problem (HAPP) to assign households to activity agendas, and Arentze and Timmermans, 2004a proposed a state-expanded network to consider the sequence of changes of activity and vehicle states. Some studies extend the activity path choice to the dynamic user equilibrium model (e.g., Lam and Yin, 2001; Liu et al., 2015). Kang and Recker, 2013 and Liao, Arentze, and Timmermans, 2013 extended the activity path choice models by including location choices. Activity path choice models are often difficult to solve due to its combinatorial explosion, and previous studies restricted solution set by defining constraints. Chow and Recker, 2012 used an inverse optimization methodology to solve HAPP model. These activity path choice models focus on the household daily activity-scheduling patterns in the macro scale and low-resolution networks and based on *pre-trip* decision. The activity agendas are given as the necessary activities and the models are often formulated as the deterministic problem. However, pedestrian behavior are probabilistic and should be described in high-resolution networks. Pedestrians are not always based on *pre-trip* nor global optimal decision. These aspects make the problem more complicated, because probabilistic models require the choice set definition, and high-resolution networks increase the number of states. Danalet and

Bierlaire, 2015 formulated a probabilistic activity path choice model to describe the pedestrian activity sequences inner the campus of a university and use an importance sampling method proposed by Flötteröd and Bierlaire, 2013 for path set generation of the route choice model. Even though they do not consider the location choices, the path set can be huge, and the model is based on the *pre-trip* decision.

This paper is the first to describe probabilistic pedestrian activities with route choices and to analytically evaluate the network flow including time-use pattern. We focuses on the computational challenges of pedestrian activity scheduling networks and introduces an activity assignment model based on the Markov decision process. This approach is based on the Markov chain assignment (Bell, 1995; Akamatsu, 1996; Baillon and Cominetti, 2008), which is a well-known implicit network loading assignment as well as Dial's algorithm (Dial, 1971). It uses a sequential link choice model instead of the pre-trip path choice model and does not require the path enumeration. We apply this approach to the pedestrian activity-scheduling networks. The Markov model also enables us to describe the sequential and dynamic decision, while previous activity-scheduling models are based on the *pre-trip* decision. However, this type of network assignment model suffers from the computation of huge matrix and the computational instability because it can generate unrealistic cyclic paths. Focusing on the computational challenges, we present a network restriction method for the activity assignment model based on the Markov decision process, using the concept of the time-space prism. It is useful to reduce the number of states and the path set and calculate the transition probabilities more efficiently. Because the framework is based on a route choice model, we can consider the correlation structure among activity paths. In this paper, we focus on evaluating pedestrian space-time flows rather than the specification of the model, and we apply the proposed model to a pedestrian network design problem as a case study.

6.2 Time-space constraints

6.2.1 Network description

In order to model the activity path choice, which includes both moving and staying behavior, we use a graph incorporating the concept of scheduling. We first define a directed graph $\mathcal{G}^s = (\mathcal{N}, \mathcal{A})$ representative of the *spatial* network. \mathcal{N} is the set of nodes, and \mathcal{A} is the set of links. The set of nodes \mathcal{N} includes two kind of node sets, i.e., the set of nodes for only moving \mathcal{N}^m and for both moving and staying \mathcal{N}^s . Thus, $\mathcal{N} = \mathcal{N}^m \cup \mathcal{N}^s$. Likewise, the set of links \mathcal{A} contains both the set of moving links \mathcal{A}^m and the set of staying links \mathcal{A}^s , then $\mathcal{A} = \mathcal{A}^m \cup \mathcal{A}^s$. A moving link $a^m = (i, j) \in \mathcal{A}^m$ connects two different nodes $i, j \in \mathcal{N}$, i.e., $\mathcal{A}^m = \{a^m = (i, j) | i \neq j, i, j \in \mathcal{N}\}$. A staying link $a^s = (i, j) \in \mathcal{A}^s$ links the same nodes included in \mathcal{N}^s , i.e., $\mathcal{A}^s = \{a^s = (i, j) | i = j, i, j \in \mathcal{N}^s\}$.

We then define a time-structured *activity state* network $\mathcal{G}^a = (\mathcal{S}, \mathcal{E})$ by incorporating the time axis into the *spatial* network \mathcal{G}^s . \mathcal{S} is the set of states and \mathcal{E} is the set of edges, where a state s is defined as the pair of time and space (node) and an edge e connects two different states. Time t is discretized at each interval τ , and has the time-constraint T , i.e., $t \in \{0, 1, \dots, T\}$. Thus, the set of states \mathcal{S} and the set of edges \mathcal{E} are decomposed as $\mathcal{S} = [\mathcal{S}_1, \dots, \mathcal{S}_t, \dots, \mathcal{S}_T]$ and $\mathcal{E} = [\mathcal{E}_1, \dots, \mathcal{E}_t, \dots, \mathcal{E}_{T-1}]$. The set of states at time t \mathcal{S}_t is defined as $\mathcal{S}_t = \{s_t = (t, i) | t \in \{0, 1, \dots, T\}, i \in \mathcal{N}\}$ and the set of edges between time t and $t+1$ \mathcal{E}_t is defined as $\mathcal{E}_t = \{e_t = (s, s') | s \in \mathcal{S}_t, s' \in \mathcal{S}_{t+1}\}$, respectively. According to this notation, an activity path ψ is described as a sequence

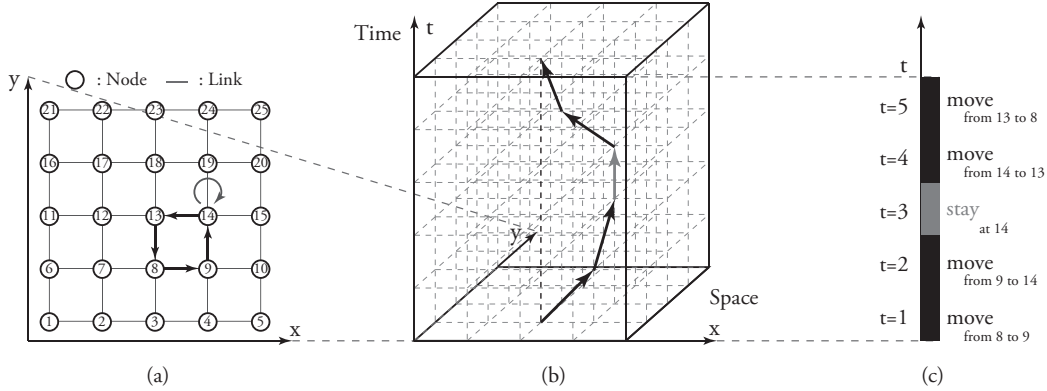


FIGURE 6.1: An activity path $\psi_{0:5} = [(8,9), (9,14), (14,14), (14,13), (13,8)]$ in time-structured network and its projections. (a) Spatial network graph, (b) time-structured network with time constraint $T = 5$ and (c) time use pattern.

of states from $t = 0$ to $t = T$, $\psi_{1:T} = [e_0, \dots, e_t, \dots, e_{T-1}]$. Figure 6.1(a) shows an illustration of a *spatial* network, and Figure 6.1(b) is the time-structured *activity state* network based on the spatial network (a). By projecting an activity path in the network (b) on x-y plain, we can evaluate spatial route choice. Figure 6.1(c) is the projection of the activity path on the time-axis and describes the pattern of time use. With the description of time-structured network, we are able to evaluate the use of time and space at the same time.

6.2.2 Network restriction

The activity path choice in the time-structured *activity state* network has a huge number of alternatives, which requires large memory space and makes computation expensive. Moreover, the existence of unreasonable paths causes the computational instability dependently on network conditions. In order to reduce the network and make computation stable, we propose a method for restricting state and edge sets based on Markovian approach.

We assume that an individual necessarily transitions from the current state s_t to the next state s_{t+1} at every discretized time t , and the initial state $s_0 = (0, o)$ and the final state $s_T = (T, d)$ are always given and fixed for each individual. Where the origin node o and the destination node d are contained in the set of node \mathcal{N} . These assumptions indicate that every state transition takes the same time τ , and an individual who departs from the origin node $o \in \mathcal{N}$ at time $t = 0$ must arrive at the destination node $d \in \mathcal{N}$ within the time-constraint T . Of course, an individual can arrive at the destination earlier than time $t = T$.

With the state constraints $s_0 = (0, o)$ and $s_T = (T, d)$, we restrict the set of states \mathcal{S} and the set of edges \mathcal{E} . We at first define the variables for topological ordering; the minimum number of steps from the origin node o to an node i $D^o(i)$, and the minimum number of steps from an node i to the destination node d $D^d(i)$. These equal to the shortest path travel time between two nodes when the travel time of all links are one. Using these variables, the set of states at time t is restricted as $\mathcal{S}_t = \{s_t = (t, i) | i \in \mathcal{N}, I_t(i) = 1\}$ where the state existence indicator $I_t(i)$ is formulated

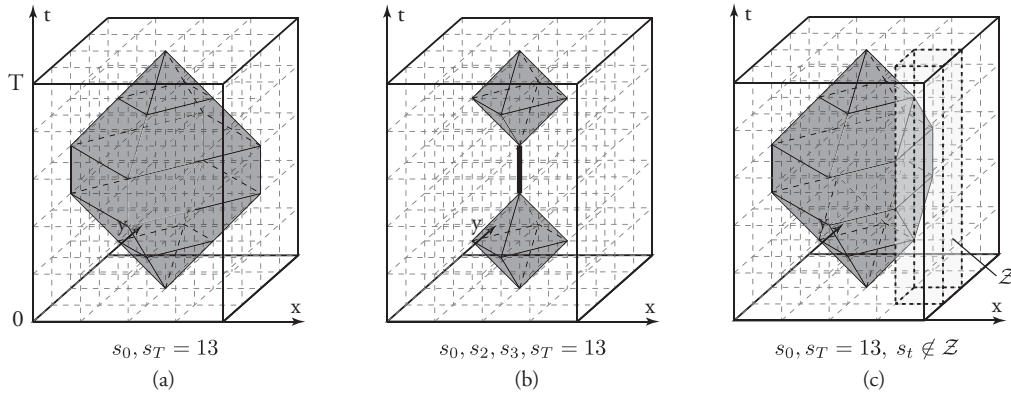


FIGURE 6.2: Time-space constraints and path restriction. (a) *Prism* constraint when the constraints are $s_0 = 13$ and $s_T = 13$ ($T = 5$), (b) *Bundle* constraint when the constraints are $s_0 = s_2 = s_3 = s_5 = 13$ and (c) *Domain* constraint.

as follows,

$$I_t(i) = \begin{cases} 1, & \text{if } D^o(i) \leq t, D^d(i) \leq T - t \\ 0, & \text{otherwise.} \end{cases} \quad (6.1)$$

Moreover, the constrained set of edges is described as $\mathcal{E}_t = \{e_t = (s_t, s_{t+1}) | s_t = (t, i) \in \mathcal{S}_t, s_{t+1} = (t+1, j) \in \mathcal{S}_{t+1}, \Delta_t(j|i) = 1\}$ where the time-space state connection indicator $\Delta_t(j|i)$ is formulated as follows,

$$\Delta_t(j|i) = I_t(i)\delta(j|i)I_{t+1}(i) \quad \forall t \in \{0, 1, \dots, T\}, \forall i, j \in \mathcal{N} \quad (6.2)$$

where $\delta(j|i)$ is the spatial connection indicator that equals one if the link (i,j) is contained in the link set \mathcal{A} , and zero otherwise. The time-space state connection indicator $\Delta_t(j|i)$ denotes the existence of the edge to transition from node i at time t to node j at time $t+1$. We can also denote it based on link description $\Delta_t(j|i) = \Delta_t(a)$, $a = (i,j) \in \mathcal{A}$. The connection between two edges $e_t = a$, $e_{t+1} = a'$ is conditioned as follows,

$$\iota_t(a'|a) = \Delta_t(a)\Delta_{t+1}(a') \quad \forall t \in \{0, 1, \dots, T-1\}, \forall a, a' \in \mathcal{A} \quad (6.3)$$

This time-space link connection variable $\iota_t(a'|a)$ is used in Markovian state transition model for describing activity path choice behavior in a later section.

6.2.3 Time-space prism

As an example, consider the network of Figure 6.1. We set the time-constraint $T = 5$, and the initial and final state are assumed as $s_0 = (0, 13)$ and $s_5 = (5, 13)$. The set of states after restricted is ¹: $\mathcal{S}_0 = \{13\}$, $\mathcal{S}_1 = \{8, 12, 13, 14, 18\}$, $\mathcal{S}_2 = \{3, 7, 8, 9, 11, 12, 13, 14, 15, 17, 18, 19, 23\}$, $\mathcal{S}_3 = \{3, 7, 8, 9, 11, 12, 13, 14, 15, 17, 18, 19, 23\}$, $\mathcal{S}_4 = \{8, 12, 13, 14, 18\}$ and $\mathcal{S}_5 = \{13\}$. Likewise, the set of restricted edges can be defined as the edges which connect restricted states. By piling up the restricted set of states and edges, we get the illustration shown in Figure 6.2(a). The activity paths

¹For the sake of simplicity, we omit the notation of time from states. It is expected to not disturb the understanding of readers because all states included in the set of states S_t are always at time t .

never pass outside of the polyhedron colored in gray. This constraint corresponds to the concept of *time-space prism* proposed by Hägerstrand, 1970.

Hägerstrand, 1970 also proposed *bundle* and *domain* as the time-space constraints of activity paths, and our method can describe these constraints in the same way. The *bundle* constraint indicates the existence of activity that binds an individual on a certain space during specific time period. For example, the bundle means activities such as appointment with someone or ones with high-priority. In our notation, the bundle constraint is described as $s_{t_b^-:t_b^+} = i$ ($t_b^- < t_b^+, t_b^-, t_b^+ \in \{0, 1, \dots, T\}$, $i \in \mathcal{N}$). We show an illustration of the activity path set in Figure 6.2(b) when the bundle constraint $s_{2:3} = a$ is added. The *domain* constraint indicates a certain time-space sphere where an individual cannot enter such as a shop with limitation of opening hours and private buildings. In our model, the domain constraint is described as $s \notin \mathcal{Z}$ where the domain \mathcal{Z} is defined as the set of states.

6.3 Activity assignment model

Base on the network described in Section 6.2, we propose an activity assignment model for evaluating the use of time and space of travelers especially in pedestrian context. We at first formulate an activity path choice model based on Markovian approach, and then propose an assignment method in time-space networks.

6.3.1 Activity path choice model

We formulate an activity path choice model using the sequential edge transition model based on Markovian approach. It is assumed that an individual on edge $e_t = a$ chooses the next edge $e_{t+1} = a'$ which maximizes the sum of direct utility of transition $u_{aa'}^t$ and the expected maximum utility of subsequent paths from state $e_{t+1} = a'$ to the final state $s_T = (T, d)$, $\varphi_{t+1}^{s_T}(a')$. We define v^t as the constant or monotonic decreasing function of time. $\varphi_t^{s_T}(a)$ is the function that evaluates the expected utility of prism with $s_t = (t, i)$ and $s_T = (T, d)$ as the vertexes, and is formulated as the Bellman equation (Bellman, 1957) as below (for the sake of simplicity, we omit the notation of the final state s_T),

$$\begin{aligned}\varphi_t(a) &= \max_{e_{t+1}} \mathbb{E} \left[\sum_{\tau=t}^{T-1} \beta^{\tau-t} \tilde{u}(e_{\tau+1}|e_\tau) \right] \\ &= \mathbb{E} \left[\max_{a' \in \mathcal{E}_{ta}^+} \{ u_{aa'}^t + \beta \varphi_{t+1}(a') + \varepsilon_{t+1}(a') \} \right],\end{aligned}\quad (6.4)$$

where ε is the random term of transition utility and *i.i.d.* extreme value type I and its scale parameter μ is strictly positive. \mathcal{E}_{ta}^+ is the set of successive edges connected with $e_t = a$; $\mathcal{E}_{ta}^+ = \{e_{t+1} = a' \in \mathcal{E}_{t+1} | \iota_t(a'|a) = 1\}$. β is the time-space discount rate of expected utility and satisfies $0 \leq \beta \leq 1$. Based on the assumption of distribution of ε , the transition probability from $e_t = a$ to $e_{t+1} = a'$ is given by the multinomial logit model as follows (see Rust, 1987 for the derivation of the equation),

$$p_t(a'|a) = \frac{e^{\mu \{ u_{aa'}^t + \beta \varphi_{t+1}(a') \}}}{\sum_{a' \in \mathcal{E}_{ta}^+} e^{\mu \{ u_{aa'}^t + \beta \varphi_{t+1}(a') \}}}.\quad (6.5)$$

The choice probability of activity path $\psi_{1:T} = [e_1, \dots, e_t, \dots, e_T] = [a_1, \dots, a_t, \dots, a_T]$ is formulated as the product of transition probabilities²,

$$\mathbb{P}(\psi_{1:T} = [a_1, \dots, a_t, \dots, a_T]) = \prod_{t=1}^{T-1} p_t(a_{t+1}|a_t). \quad (6.6)$$

By the property of maximum value distribution, Equation (6.4) can be re-formulated as the logsum,

$$\varphi_t(a) = \begin{cases} \frac{1}{\mu} \log \sum_{a' \in \mathcal{A}} \iota_t(a'|a) e^{\mu \{ u_{aa'}^t + \beta \varphi_{t+1}(a') \}}, & t \neq T \wedge a \neq d, \\ 0, & t = T \vee a = d. \end{cases} \quad (6.7)$$

The activity path choice model proposed in this paper describes the path choice behavior in time-space networks without path enumeration, and the prim constraint Δ_t reduces unreasonable paths and computational burden. Moreover, the time-space discount rate β is important to describe decision making dynamics as we will mention later.

6.3.2 Path correlation

It is well-known that Logit type route choice models have the IIA (*Independence from Irrelevant Alternatives*) property. In case of activity path choices, the similarity of paths is a more considerable problem. Three activity paths shown in Figure 6.3 are different from each other in terms of only time when an activity is implemented, while all of them share moving route and staying location with each other. That is, there are points of similarity among the three paths, however they are assumed to be independent from each other in Logit model because of the IIA property. The ignorance of the similarity among activity paths can cause the wrong evaluation of the use of time and space.

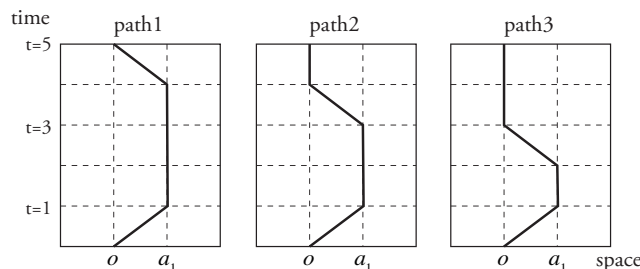


FIGURE 6.3: Example of activity paths which have similarity with each other

Recently some literatures have presented route choice models considering the correlation structure among alternatives without path enumeration (Papola and Marzano, 2013; Hara and Akamatsu, 2014; Mai, Fosgerau, and Freijinger, 2015; Mai, 2016). These models are based on the network-GEV (n-GEV) model proposed by Bierlaire, 2002 and Daly and Bierlaire, 2006. However, the application of the n-GEV model requires the network to be acyclic. For this reason, in literature of n-GEV based route

² a_t does not include the information of time while it has the suffix of time t conveniently. For this reason, we add the suffix of time t to the transition probability, $p_t(a_{t+1}|a_t)$ for distinguishing it from the spatial transition probability.

choice models the network was edited to remove cyclic structures. On the other hand, time-space networks naturally have no cycle and satisfy the condition for applying the n-GEV model. In this paper, for describing the activity path correlation, we formulate a n-GEV based activity path choice model with time-space discount rate and prism constraint.

We here assume that time-space discount rate β and the scale parameter μ are the variables specific on each state, β_{s_t} and φ_{s_t} . Using these parameters and taking exponential, we re-formulate Equation 6.4 as follows,

$$e^{\mu_{ta}\varphi_t(a)} = \sum_{a' \in \mathcal{A}} \iota_t(a'|a) e^{\mu_{ta}\{v_{aa'}^t + \beta_{ta}\varphi_{t+1}(a')\}} \quad (6.8)$$

We then divide the deterministic term of state transition utility $u_{aa'}^t$ into the utility dependent on only state $e_{t+1} = a'$, $\hat{u}_{e_{t+1}}$ and the other,

$$u_{aa'}^t = \hat{u}_{t+1,a'} + \frac{1}{\mu_{ta}} \log \alpha_{aa'}^t \quad (6.9)$$

Moreover, we define $y_t(a) = e^{\varphi_t(a)}$ and $G^{t,a}(y) = y_t(a)^{\mu_{ta}}$, and re-formulate Equation 6.8 as follows,

$$G^{t,a}(y) = \sum_{a' \in \mathcal{A}} e^{\mu_{t,a}\hat{u}_{t+1,a'}} \alpha_{aa'}^t \left\{ G^{t+1,a'}(y)^{\frac{\mu_{ta}}{\mu_{t+1,a'}}} \right\}^{\beta_{ta}} \quad (6.10)$$

Equation 6.10 describes the relationship between upstream node $e_t = a$ and downstream node $e_{t+1} = a'$ in GEV-network, and α is the allocation parameter. The state transition probability of an arbitrary node pair is given by the following equation,

$$p(e_{t+k}|e_t) = \sum_{e_{t+k-1}} p(e_{t+k}|e_{t+k-1}) p(e_{t+k-1}|e_t) \quad (6.11)$$

where,

$$p(e_{t+1}|e_t) = \frac{\eta_{aa'}^t \left\{ G^{t+1,a'}(y)^{\frac{\mu_{ta}}{\mu_{t+1,a'}}} \right\}^{\beta_{ta}}}{\sum_{a' \in \mathcal{A}} \eta_{aa'}^t \left\{ G^{t+1,a'}(y)^{\frac{\mu_{ta}}{\mu_{t+1,a'}}} \right\}^{\beta_{ta}}} \quad (6.12)$$

$$\eta_{aa'}^t = e^{\mu_{ta}\hat{u}_{t+1,a'}} \alpha_{aa'}^t \quad (6.13)$$

β_{ta} means that the weight of future expected utility can change at each edge. In pedestrian activity context, it is assumed that whether an individual consider the future utility or not is dependent on his/her situation at that time. We examine these parameters through sensitivity analyses in Section 6.4.

6.3.3 Solving the Bellman equation

Note that we have to solve the Bellman equation (6.8) in order to evaluate the maximum expected utility and the state transition probability. Since previous implicit route choice models solve the maximum expected utility at the steady state, they need to apply inverse matrix or iterative calculation which may cause computational instability dependently on network conditions. On the other hand, in this

paper $\varphi_t(a)$ has different value at each state (space and time), therefore we can solve the Bellman equation using following backward induction algorithm:

Step 1: Preliminaries. Set the initial edge $e_0 = o$, the final edge $e_T = d$ and $\varphi_t^{ST}(d) = 0, \forall t$. Calculate I, Δ, ι .

Step 2: Initialization. Set $t = T$, and $\varphi_t^{ST}(a) = 0, \forall a \in \mathcal{A}$.

Step 3: Backward calculation. Set $t = t - 1$, and calculate $\varphi_t^{ST}(a)$ based on Equation (6.8).

Step 4: Finalization. Finish the calculation if $t = 0$, return *Step 3* otherwise.

6.3.4 Assignment algorithm

We define g_a^t and $f_{aa'}^t$ as the state flow at (t, a) , $\forall t \in \{0, 1, \dots, T\}, \forall a \in \mathcal{A}$ and edge flow from states (t, a) to $(t + 1, a')$, $\forall t \in \{0, 1, \dots, T - 1\}, \forall a, a' \in \mathcal{A}$, respectively. The relationship between state and edge flows is formulated as follow,

$$g_a^t = \begin{cases} \sum_{k \in \mathcal{A}} f_{ka}^{t-1}, & t \neq 0 \\ q_{od}, & t = 0 \wedge a = o \\ 0, & t = 0 \wedge i \neq l \end{cases} \quad (6.14)$$

and

$$f_{aa'}^t = g_a^t p_t(a'|a), \quad \forall t \in \{0, \dots, T - 1\}, \quad (6.15)$$

where q_{od} is a generating flow from the origin $o \in \mathcal{O} \subseteq \mathcal{A}$ to the destination $d \in \mathcal{D} \subseteq \mathcal{A}$. The assignment algorithm is following. We first set the generating flow $g_o^0 = q_{od}$, and calculate the edge flows at time $t = 1$ using Equation (6.15). Then, the state flows at time $t = 2$ can be calculated by Equation (6.14). All of other state and edge flows can be calculated alternately until time $t = T$. Moreover, we obtain spatial link flow of $a \in \mathcal{A}$, g_a by summation g_a^t as follow,

$$g_a = \sum_{t=0}^T g_a^t, \quad (6.16)$$

where f_a in Equation (6.16) corresponds to link flow in previous loading models. Note that the activity network assignment is computationally expensive if the number of links and/or times are large. The propose method of time-space constraint description helps for reducing network size and the path alternatives.

6.4 Illustrative example

We evaluated activity patterns using a simple network of Figure 6.4(a). Figure 6.4(b) indicates the possible path set under the time-space constraints; $T = 5$, $s_0 = (0, 0)$ and $s_T = (5, 14)$. For simplicity, the transition utility $u_{aa'}^t$ depends on only the utility of link a' $u_{aa'}^t = \hat{u}_{a'}$, and the value of $\hat{u}_{a'}$ is given in the parenthesis on each link. The utility of staying link $a \in \mathcal{A}^s$ is defined as $\hat{u}_a = b_a + c_a t$ where $b_a > 0$ and $c_a < 0$ are dependent on each activity location and shown on the network.

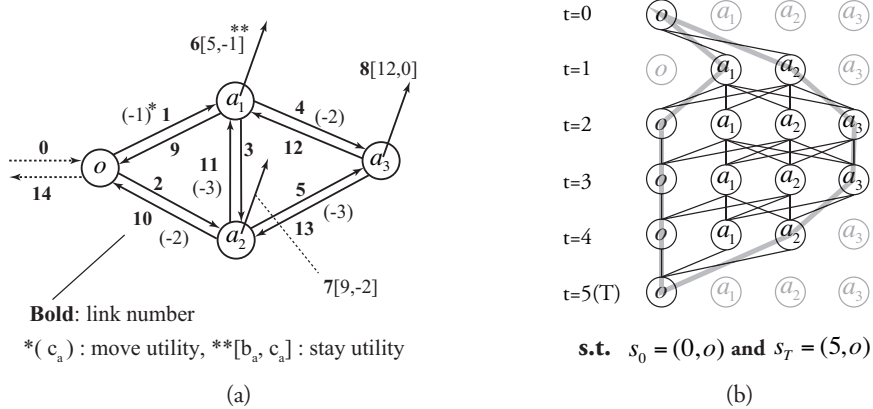


FIGURE 6.4: A simple network with three nodes for staying. (a) Network and parameter setting and (b) Time-structured network and prism constraint.

6.4.1 Activity assignment

Figure 6.5 shows the results of activity assignment where the total demand is 1000 and all of them have the state constraint $s_0 = (0, 0)$ and $s_T = (5, 14)$, $T = 5$. Each column shows the top three frequent activity patterns, link flows and the number of activities. Activity patterns are generated based on random walk algorithm using transition probabilities. Link flows are calculated by the time-structured assignment algorithm proposed by Section 6.3.4. We can also calculate the duration time at each node by multiplying the flows of staying link by the interval of time discretization, that is, our activity assignment model in time-space network can evaluate the use of time and space simultaneously.

Each row corresponds to the result with different value of the time-space discount rate. The time-space discount rate does is common value for all states in this example. When $\beta = 1$, an individual evaluate the instantaneous utility $u_{aa'}^t$ and future expected utility $\varphi_{t+1}(a')$ at equal weights, i.e., they consider the total utility of activity paths. As the result, the activity pattern which includes the stay at a_3 where the access cost is high but the utility is large enough was the most frequent. In contrast, when $\beta = 0$, activities are based on myopic decision without consideration of future utility. As the result, the pattern including activity at a_1 where the access cost is low was the most frequent, and the flow of staying at a_3 was only 6. The result in the case of $\beta = 0.5$ showed the eclectic patterns. These results concluded that the time-space discount rate β is a parameter describing the difference of decision making and had a large impact on the evaluation of activity patterns.

6.4.2 Time-space discount rate

In order to examine of the effect of time-space discount rate, we changed the value of each link and calculated probabilities of eight paths in Table 6.1. We show the path probabilities in Table 2, where "Original" column presents the probabilities when $\beta_a = 1, \forall a \in \mathcal{A}$ and the right four columns indicate the probabilities when the value of the time-space discount rate of some links change. The probabilities of paths including activity at a_2 (C, D) and a_3 (E, F, G, H) increased when the discount rate of links corresponding to each activity became small, because the (dis)utilities for

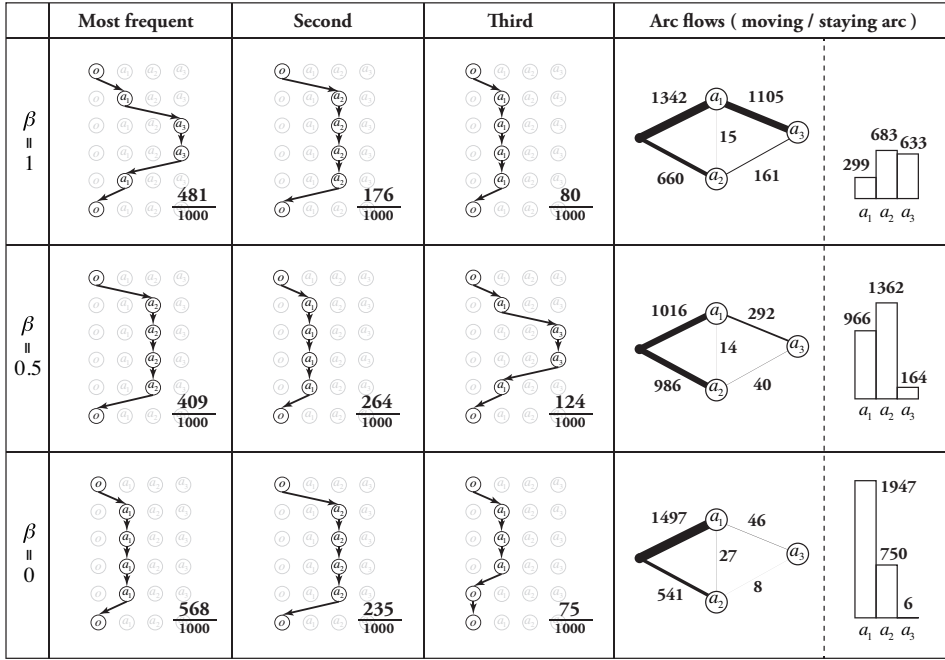


FIGURE 6.5: Evaluation of activity path and its change with various β

return (u_{back}) were evaluated as the discounted value. In the real contexts, it is assumed that the weight of future expected utility is large on link which is likely to be passed, while the weight of myopic utility is large on link with many shops or heterogeneous characteristics. The results indicated the possibility to describe the decision making dynamics by changing the value of β on each link. When $\beta_8 = 0$, there was a large difference between the probabilities of path F and H that have the same u_{total} , and this result indicates the tendency that people want to arrive early at the main destination because the access cost ($-u_{\text{go}}$) of path F is smaller than that of path H. In the case of $\beta_6 = \beta_7 = \beta_8 = 0$, the probabilities of path C, F and G increased. We confirmed that the effect of the time-space discount rate depends on the relationship among activity utility, future expected utility, access and egress costs.

6.4.3 Activity path correlation

In order to examine the activity path correlation, we changed the value of scale parameter φ_a and calculated the path probabilities. For the sake of simplicity, in this case study we set time-space discount rate $\beta_a = 1, \forall a \in \mathcal{A}$. We show in Figure 6.6 the change of eight path probabilities when the scale parameter of stay links μ_6, μ_7, μ_8 change. When $\mu_6 = \mu_7 = \mu_8 = 1$, the probabilities of path A, D, F and H are the same value, because they are based on the same path-based utility u_{total} . According to the change of μ , the activity path probabilities changed, and when $\mu_6 = \mu_7 = \mu_8 = 0$ the probabilities of only 4 paths are non-zero. This result shows the transition between paths with the same activity place (A and B; C and D; E and F; G and H), and we can describe the path correlation among similar paths by changing the scale parameter μ .

Here, we examine the effects of removal of specific states when $\mu_6 = \mu_7 = \mu_8 = 0.5$. In this study, we can describe not only spatial state removals (ex. road closing)

TABLE 6.1: Eight dominant activity paths and their utilities

path: [links]	stay	u_{total}	u_{stay}	u_{go}	u_{back}
A: [0,1,6,6,6,9,14]	a_1	4	6	-1	-1
B: [0,1,6,6,9,14,14]	a_1	3	5	-1	-1
C: [0,2,7,7,7,10,14]	a_2	5	9	-2	-2
D: [0,2,7,7,10,14,14]	a_2	4	8	-2	-2
E: [0,1,4,8,12,9,14]	a_3	6	12	-3	-3
F: [0,1,4,8,13,10,14]	a_3	4	12	-3	-5
G: [0,2,5,8,13,10,14]	a_3	2	12	-5	-5
H: [0,2,5,8,12,9,14]	a_3	4	12	-5	-3

TABLE 6.2: Time-space discount rate and path probabilities

path	original*	probability with β varied			
		$\beta_6 = 0$	$\beta_7 = 0$	$\beta_8 = 0$	$\beta_{6,7,8} = 0.5$
A	0.067	0.060	0.054	0.027	0.044
B	0.025	0.008	0.020	0.010	0.010
C	0.182	0.187	0.375	0.074	0.258
D	0.067	0.069	0.019	0.027	0.035
E	0.496	0.508	0.400	0.549	0.460
F	0.067	0.069	0.054	0.202	0.103
G	0.009	0.009	0.007	0.027	0.014
H	0.067	0.069	0.054	0.074	0.062
AB*	0.092	0.068	0.074	0.037	0.054
CD*	0.249	0.256	0.394	0.101	0.293
EFGH*	0.639	0.655	0.515	0.852	0.639

*Original: $\beta_a = 1, \forall a \in A$

*AB, CD, EFGH: Total value of path probabilities

but also the temporal state removals (ex. operation time saving of shop; *Domain constraint* in Figure 6.2C), because the activity path choice model includes the concept of scheduling. Table 6.3 shows the change of path probabilities with additional state constraints. When state $s_4 = 6$ is excluded from the network, path A cannot be chosen and the choice probability of path B largely increased, and when state $s_4 = 7$ is removed, travelers cannot choose path C and the choice probability of path D largely increased, respectively. Regarding the state removal of move links, when states $s_t = 4, \forall t$ are removed, the choice probability of path E and F, which include link 4 in the path, became zero. In that case, choice probability not only of paths which share the activity location a_3 with E and F but also of path C which has the largest utility u_{total} except for path E increased. On the other hand, when states $s_t = 13, \forall t$ are excluded, the choice probability of paths that has high similarity with removed paths increased. These results show the tendency of keeping activity locations even with additional state constraints, and the relaxation of IIA property of logit model.

6.5 Case study

We finally show a case study using a simple network of the city center of Matsuyama-city, Japan. For applying the activity assignment model to the network where the travel time of links is different, we first introduce a method of network standardization. Then we define the utility of links and implement the activity assignment in Matsuyama-network. Moreover, we apply the framework to a pedestrian network design problem and investigate the Pareto front solutions in Section 6.5.4.

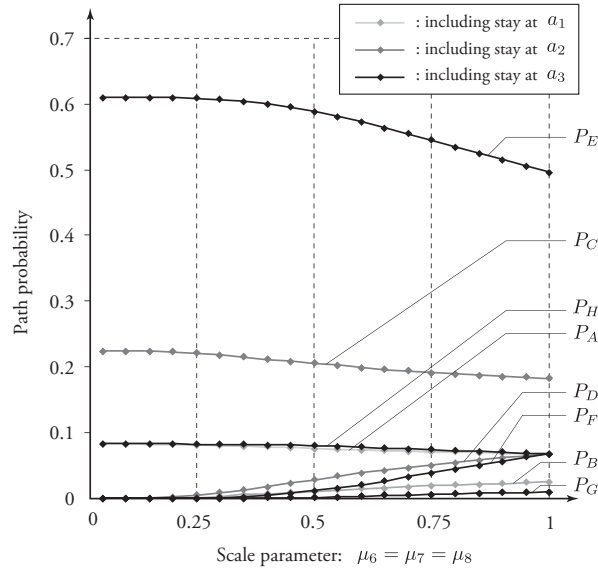


FIGURE 6.6: Scale parameter and path probabilities

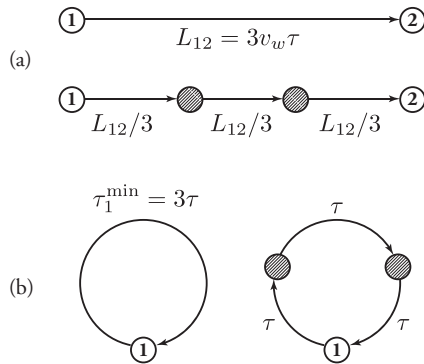


FIGURE 6.7: Network standardization

6.5.1 Network standardization

In the time-structured activity network, travelers are assumed to necessarily transition to the next state at each discretized time, and the interval of time discretization τ is a constant value. This constraint can cause a problem when the length of link is varied, i.e., discretized time τ can be largely different from the time for passing links. For this reason, we standardize a network before applying the activity assignment. Figure 6.7(a) shows an example of standardizing link length. In this case, the length of link $(1, 2)$ is $l_{12} = 3v_w\tau$ where v_w is walking speed. In order to solve this problem, we add two pseudo nodes and divide the link into three links, where the length of each divided link is $l_{12}/3$ then passing time is $l_{12}/3v_w = \tau$. In the same way, we can consider the minimum duration time at each node $i \in \mathcal{N}^s$, τ_i^{\min} . In the case of Figure 6.7(b), the minimum duration time at node 1 is $\tau_1^{\min} = 3\tau$. Then we add two pseudo nodes and divide the link into three links as well as moving links.

TABLE 6.3: Addition of state constraint and path probabilities

path	original	probability with state removed			
		$s_4 = 6$	$s_4 = 7$	$s_4 = 8$	
A	0.075	0	-	0.089	+0.014(+18.67%)
B	0.010	0.031	+0.021(+210%)	0.012	+0.002(+20.00%)
C	0.205	0.217	+0.012(+5.85%)	0	-
D	0.028	0.029	+0.001(+3.57%)	0.094	+0.066(+235.7%)
E	0.589	0.623	+0.034(+5.77%)	0.694	+0.105(+17.83%)
F	0.011	0.011	$\pm 0.000(\pm 0.00\%)$	0.013	+0.002(+18.18%)
G	0.001	0.002	+0.001(+100%)	0.002	+0.001(+100.0%)
H	0.080	0.084	+0.004(+5.00%)	0.094	+0.014(+17.50%)

path	original	probability with state removed			
		$s_t = 4, \forall t$	$s_t = 13, \forall t$	$s_t = 14, \forall t$	
A	0.075	0.188	+0.113(+150.67%)	0.076	+0.001(+1.33%)
B	0.010	0.025	+0.015(+150.00%)	0.01	$\pm 0.000(\pm 0.00\%)$
C	0.205	0.511	+0.306(+149.27%)	0.206	+0.001(+0.49%)
D	0.028	0.069	+0.041(+146.43%)	0.028	$\pm 0.000(\pm 0.00\%)$
E	0.589	0	-	0.598	+0.009(+1.53%)
F	0.011	0	-	0	-
G	0.001	0.004	+0.003(+300.00%)	0	-
H	0.080	0.199	+0.119(+148.75%)	0.081	+0.001(+1.25%)

* $\beta_a = 1, \forall a \in \mathcal{A}, \mu_6 = \mu_7 = \mu_8 = 0.5, \mu_a = 1, \forall a \notin \{6, 7, 8\}$

6.5.2 Modeling utility

Travelers can move on moving links $a^m \in \mathcal{A}^m$, which are directed and have the attributes: link length l_a , sidewalk width x_a^w and shopping street dummy variable x_a^s . There are also links for staying $a^s \in \mathcal{A}^s$ with the deviated function of staying utility: $\hat{u}_a^s(\omega) = x_{ij}^c + x_{ij}^d\omega$, where ω is continuos time from departure at the origin. The utility function of link is defined as:

$$\hat{u}_a^t = \underbrace{\theta_{tt} tt_a}_{\text{travel time}} + \underbrace{(\theta_w x_a^w + \theta_s x_a^s) \left(\frac{l_a}{L} \right)}_{\text{utility of moving sidewalk and shopping street}} + \underbrace{\theta_u \int_{t\tau}^{(t+1)\tau} (x_{ij}^c + x_{ij}^d\omega) d\omega}_{\text{utility of staying}} \quad (6.17)$$

where θ is a vector of coefficients and tt_a is the travel time of link a . L is a standardization constant of link length. Then,

$$\hat{u}_a^t = \begin{cases} \theta_{tt} tt_{ij} + (\theta_w x_a^w + \theta_s x_a^s) \left(\frac{l_{ij}}{L} \right), & a \in \mathcal{A}^m \quad (\text{moving an link}) \\ \theta_u \int_{t\tau}^{(t+1)\tau} (x_{ij}^c + x_{ij}^d s) ds, & a \in \mathcal{A}^s \quad (\text{staying a node}) \end{cases} \quad (6.18)$$

In the time-structured activity network, tt_{ij} has to be always same value, i.e., $tt_{ij} = \tau, \forall (i, j) \in \mathcal{A}, i \neq j$. As mentioned above, we standardize the network in order to make all of link length same $l_{ij} = L$, therefore the travel time of all links is $\tau = L/v_w$.

6.5.3 Assignment result in Matsuyama network

Based on the proposed model, we calculated the pedestrian assignment in a grid network of the city center in Matsuyama-city, Japan (Figure 6.8). We set the standardization constant of link length $L = 100$ [m], which is the length of the shortest link. The length of the longest links is 300 [m]. Moreover, the walking speed v_w is assumed to be 4.0 [km/h], thus $\tau = 1.5$ [min].

We show the assignment results in Figure 6.9 where the upper is the link flow and the lower is the average of activity duration per person at each staying node $i \in \mathcal{N}^s$. When the time-constraint was one hour (Figure 6.9A), most of activities occurred at node 4 or 18 and link flows were locally distributed. When the time-constraint is two hours (Figure 6.9B), activity locations and link flows are distributed around node 4 and 18. In real measurement (not appeared in this paper) we could also see the deviation of activity locations in the city center of Matsuyama-city, therefore the results in this paper described the expanse of pedestrian activity sphere corresponding to time-constraint. Moreover, when the time-constraint is three hours (Figure 5C), the distribution of activity duration barely changed from the case B while the link flows were widely distributed. It is assumed that the result came from the utility decreasing as time went by.

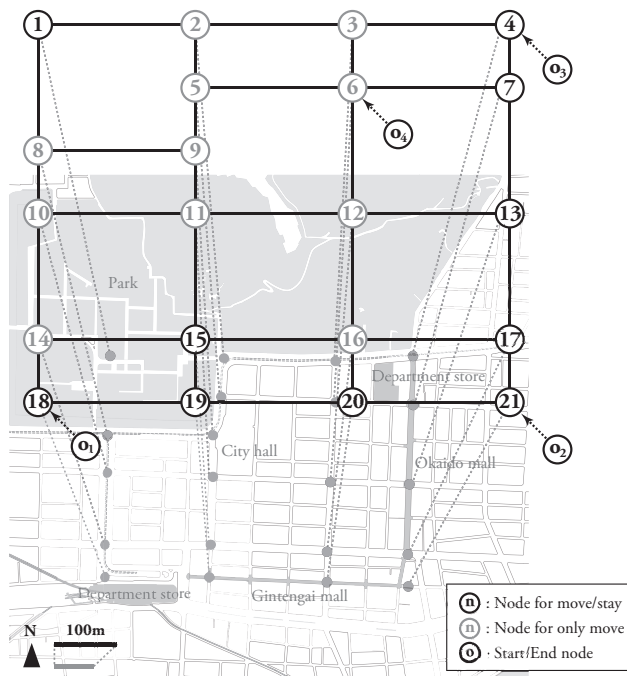


FIGURE 6.8: Network of the city center in Matsuyama-city, Japan

6.5.4 Application to network design

We finally apply the activity assignment model above to a network design problem. Recently in Japanese cities including Matsuyama-city, street space conversion attracts more attention as a urban design method for increasing pedestrian activities. Focusing this kind of design, in this study we assume the widening the sidewalk width. Given a network of interconnected streets, we are looking for the configuration of a network that satisfies the travel demand with the maximum activity time for different increasing sidewalk area [m^2]. We assume that the capital cost of widening sidewalk width is proportional to the area. Our problem decides on which links and how wide we increase the sidewalk width in meters, i.e., the decision variable is the sidewalk width $n_{ij} = x_{ij}^w$ on each moving link $a^m = (i, j) \in \mathcal{A}^m$. We assume that each moving link has the possible maximum sidewalk width n_{ij}^{\max} and the minimum sidewalk width n_{ij}^{\min} because of geometrical limitation. The minimum

TABLE 6.4: Attributes of links

source	sink	l_a	n_a^{\min}	n_a^{\max}	x_a^s	x_a^c	x_a^d	link
1	2	200	8	8	1	0	0	move
2	3	300	4	8	0	0	0	move
3	4	200	4	8	0	0	0	move
5	6	300	2	8	0	0	0	move
6	7	200	2	8	0	0	0	move
8	9	200	4	8	0	0	0	move
10	11	200	2	8	0	0	0	move
11	12	300	2	8	0	0	0	move
12	13	200	2	8	0	0	0	move
14	15	200	2	8	0	0	0	move
15	16	300	2	8	0	0	0	move
16	17	200	2	8	0	0	0	move
18	19	200	8	8	1	0	0	move
19	20	300	8	8	1	0	0	move
20	21	200	8	8	1	0	0	move
1	8	200	4	8	0	0	0	move
2	5	100	4	8	0	0	0	move
3	6	100	0	8	0	0	0	move
4	7	100	8	8	1	0	0	move
5	9	100	4	8	0	0	0	move
8	10	100	4	8	0	0	0	move
9	11	100	2	8	0	0	0	move
6	12	200	0	8	0	0	0	move
7	13	200	8	8	1	0	0	move
10	14	200	4	8	0	0	0	move
11	15	200	2	8	0	0	0	move
12	16	200	0	8	0	0	0	move
13	17	200	8	8	1	0	0	move
14	18	100	4	8	0	0	0	move
15	19	100	0	8	0	0	0	move
16	20	100	0	8	0	0	0	move
17	21	100	8	8	1	0	0	move
1	1	0	0	0	0	0.5	-0.005	stay
4	4	0	0	0	0	0.8	-0.015	stay
7	7	0	0	0	0	0.4	-0.003	stay
13	13	0	0	0	0	0.3	-0.001	stay
15	15	0	0	0	0	0.5	-0.006	stay
17	17	0	0	0	0	0.3	-0.001	stay
18	18	0	0	0	0	0.8	-0.015	stay
19	19	0	0	0	0	0.3	-0.001	stay
20	20	0	0	0	0	0.3	-0.001	stay
21	21	0	0	0	0	0.4	-0.002	stay

*All links are bidirectional and paired link have same attributes with each other

TABLE 6.5: OD patterns

Pattern	s_0	s_T	Flow	Pattern	s_0	s_T	Flow
1	$(0, o_1)$	(T, o_1)	400	3	$(0, o_3)$	(T, o_3)	300
2	$(0, o_2)$	(T, o_2)	100	4	$(0, o_4)$	(T, o_4)	200

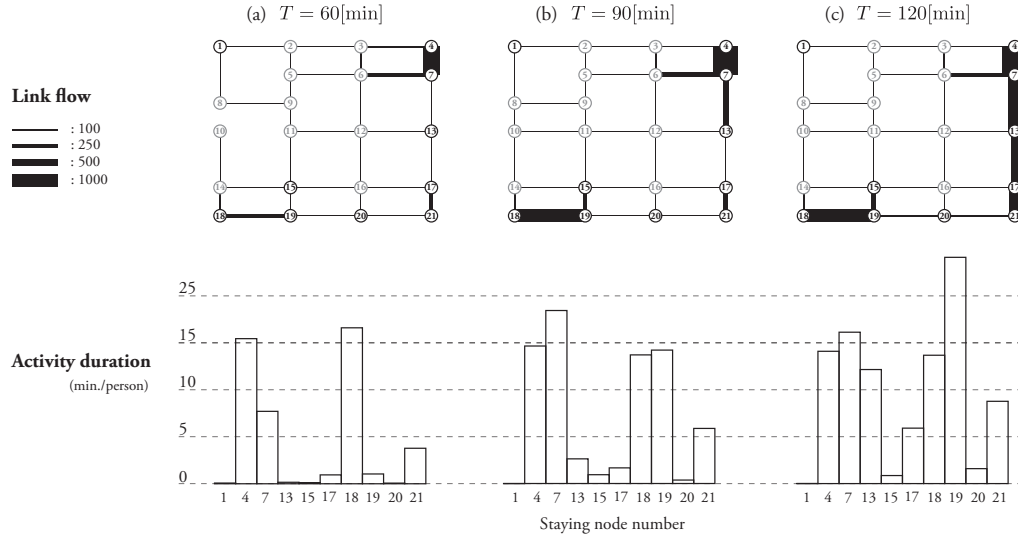


FIGURE 6.9: Time constraint and pedestrian activity assignment results

sidewalk width n_{ij}^{\min} is assumed to equal to the current sidewalk width on link (i, j) because we consider only the widening in this study. Then, the sidewalk width n_{ij} must satisfy the following constraint,

$$n_{ij}^{\min} \leq n_{ij} \leq n_{ij}^{\max} \quad \forall (i, j) \in \mathcal{A}^m \quad (6.19)$$

We investigate the trade-off curve between the total activity time and the total increasing sidewalk area. This Pareto front indicates the possible activity time increase for different levels of investment in building a pedestrian network. Therefore, our problem has two conflicting objectives, maximizing the total activity time in the district and minimizing the capital cost (increasing sidewalk area). The objective function for the activity time is,

$$\max z_1 = \sum_{(i,j) \in \mathcal{A}} \sum_t f_{ij}^t \tau, \quad (6.20)$$

where f_{ij}^t is the flow on link (i, j) at time t and τ is the interval of time discretization. The objective function for the capital cost is,

$$\min z_2 = \sum_{(i,j) \in \mathcal{A}^{\ddagger}} (n_{ij} - n_{ij}^{\min}) l_{ij} \hat{c}, \quad (6.21)$$

where \hat{c} is the unit capital cost for widening sidewalk width [yen/m²] and multiplied by the area which is the product of the increased width $n_{ij} - n_{ij}^{\min}$ [m] and the link length l_{ij} [m]. Our problem is a bi-objective optimization problem as mentioned above, and it is also bi-level programming because travelers react the network configuration and change their activity locations, durations and routes, and vice versa.

We adopt the network update algorithm as the solution methodology (Scarinci et al., 2016) of the optimization problem. This algorithm has two main steps: activity assignment and network update. The activity assignment proposed in former sections is used to evaluate the flows f_{ij}^t on an activity network. The flows are used to calculate the total activity time associated to the first objective in Equation (6.20). The

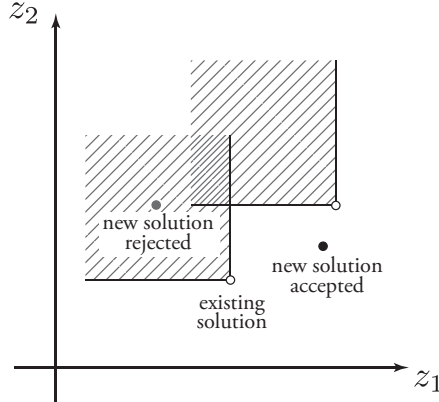


FIGURE 6.10: Acceptance criterion of new solutions

network update modifies the current network, and the new solution is evaluated as a Pareto front solution if it satisfies the following condition,

$$\neg\{\exists f \in \mathcal{F}, z_1 \geq z_1^{(f)} \wedge z_2 \geq z_2^{(f)}\}, \quad (6.22)$$

where, \mathcal{F} is the set of the Pareto front solutions. We also show the acceptance criterion of new solutions in Figure 6.10.

The network update algorithm consists of four neighborhood structures based on Scarinci et al., 2016: 1) Remove-random-width 2) Add-random-width 3) Remove-worst-width 4) Add-best-width , subject to the constraint of Equation (6.19). In order to identify the *worst* and *best* link, we introduce two link-performance-value: *loss* φ^{loss} and *gain* φ^{gain} formulated as follows,

$$\begin{aligned} \varphi_{ij}^{\text{loss}} &= \{\hat{u}_{ij}(n_{ij}^{(h)} - \tilde{n}) - \hat{u}_{ij}(n_{ij}^{(h)})\} \cdot f_{ij} \quad \forall(i, j) \in \mathcal{A}^m \\ \varphi_{ij}^{\text{gain}} &= \{\hat{u}_{ij}(n_{ij}^{(h)} + \tilde{n}) - \hat{u}_{ij}(n_{ij}^{(h)})\} \cdot f_{ij} \quad \forall(i, j) \in \mathcal{A}^m, \end{aligned} \quad (6.23)$$

where $n_{ij}^{(h)}$ is the sidewalk width on link (i, j) at the h -th iteration. The unit removal/additional width \tilde{n} is set as 1 [m] in this case study. These performance values give an upper bound on the possible loss/gain of pedestrian utility associated with the removal/addition. We start with the network equipped with the maximum possible sidewalk, i.e., $n_{ij}^{(1)} = n_{ij}^{\max} \forall(i, j) \in \mathcal{A}^m$, and iterate this activity assignment and network update process for 1000 times.

The main characteristics of explored solutions are shown in Figure 6.11. Figure 6.11(a) shows all investigated solutions and they indicate the trade-off curve between total activity time and total area of widened sidewalk. The black circles are the set of Pareto front solutions which are not dominated by any other solution. Figure 6.11(b) shows the variation of total sojourn time in iteration process, and indicates the decrease of activity time according to iteration. As seen in Figure 6.11(c), that is because the total area of widened sidewalk is decreasing as the iteration proceeds. As the result, we can see the clear Pareto front in Figure 6.11(a).

In Figure 6.12, we also show an example solution A in Figure 6.11(a). Figure 6.12(a) shows the network configuration of solution A, where on eleven links the sidewalk width increase. These links are located near the origins/destinations or shopping streets. Figure 6.11(b) shows the activity assignment result in case of the

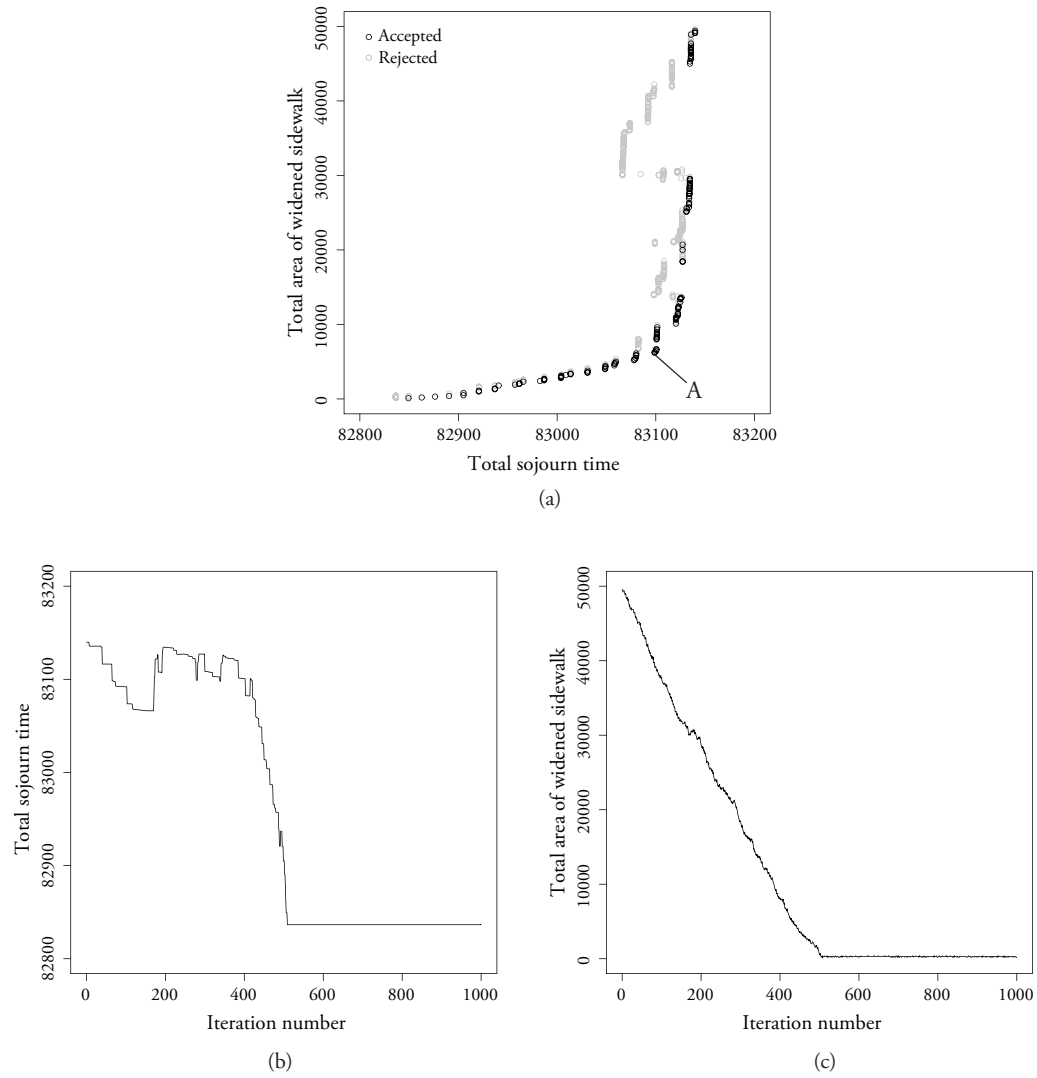


FIGURE 6.11: Network design results. (a) Trade-off curve between total sojourn time and total area of widened sidewalk, the variation of (b) Total sojourn time and (c) Total area of widened sidewalk in iteration process.

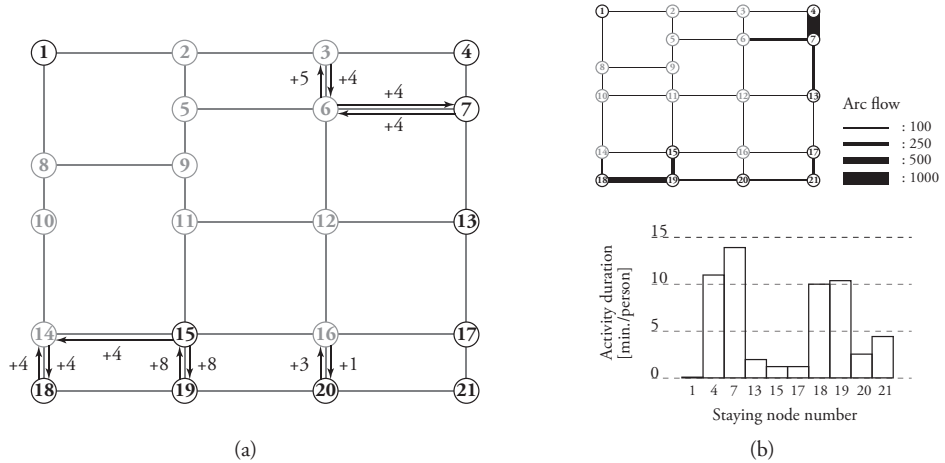


FIGURE 6.12: Network design results. (a) Example of pedestrian network corresponding to *example solution A* in Figure 6.11(a) and (b) The activity assignment result in case of the network.

network configuration.

6.6 Conclusions and discussion

This paper propose an activity assignment model based on Markovian approach, focusing on the high continuity between walking and staying behavior in pedestrian contexts. We formulate an activity path choice model based on implicit path enumeration as one type of network-GEV based model. In order to solve the computational challenges of Markovian assignment model, we introduced the three following methods: 1) time-structured network as a description of activity network, 2) network restriction based on time-space constraints which can be interpreted as the time-space prisms and 3) the dynamic sequential discrete choice model with time-space discount rate . The model allows us to compute the activity assignment with cyclic, multi-trip and time attributes. The assignment results show that time-space discount rate of expected utility and the prism constraint are important parameters that have an influence on pedestrian decision-making. Moreover, we applied the model to a network design problem in pedestrian context. We investigated the Pareto front based on network update algorithm and solved a multi-objective and bi-level programming.

Chapter 7

Conclusions and future works

This thesis proposes a number of methods for solving issues of Markovian route choice analysis. Proposed methods are regarding *Data and Estimation*, *Model*, *Assignment algorithm*, and *Application*, respectively. Therefore, this thesis is based on a collection of papers, which are rather independent from each other. The contributions of this thesis and their relationship are shown in Figure 1.4. In this chapter, we present an overview of this thesis again and some future research plans.

7.1 Conclusion of the thesis

In Chapter 3, we focus on estimating parameters of route choice models using GPS data with measurement uncertainties. Recently, the development of technologies is facilitating one to observe micro-scale trajectories, such as walking trips and moves in buildings, using GPS or WiFi technologies. However, in these cases, the measurement errors are still large and the path observations are difficult, because networks are often dense and spatial attributes affect the size of measurement errors. Since previous works have focused on networks of vehicles, they have often assumed that the variance of GPS measurement errors is constant over a network. Some studies use bayesian approaches and incorporate the prior with given preferences of route choices to correct the measurement probabilities. We focus on that these parameter settings cause the biases in the process of estimating route choice models, and propose two methods to reduce the biases: the *sequential link measurement model* and the *structural estimation method*. The sequential link measurement model is based on the time-decomposition of states and the Markovian route choice model. It enables us to estimate the link-specific variance of GPS measurement errors, while in previous studies the variance is given as a constant value over a network and causes the biases. The structural estimation method solves the fixed point of the parameters of route choice and measurement models, and it can remove the biases included in the prior information. Through twins experiments, we examine the effectiveness of the proposed methods from the viewpoint of measurement accuracy and the difference between estimated parameters and the true values. The structural estimation results show that the proposed method allows to achieve estimates close to the true value regardless of the initial parameter settings and refine the accuracy of link measurements. Moreover we validate the method in the case of using real data. We use Probe Person data collected in Matsuyama-city, Japan, and obtain the parameter estimation results of the pedestrian route choice model. The results show that the iteration process makes estimates get better by refining path estimations. The estimated preferences of route choices using the structural estimation method are less biased and show the different trend from those using the biased route choice observations. Moreover, the variance of GPS measurement errors, which has been assumed to be independent of spatial attributes in networks in previous studies, is estimated for

each link in the proposed model, and the estimated values are realistic.

In Chapter 4, we propose the β -scaled recursive logit (β -SRL) model that incorporates a parameter of the sequential discount rate, which is the discount factor of the dynamic discrete choice model (e.g., Rust, 1987), for capturing the diversity of decisions under congestions. Through some illustrative examples using simple networks, we present the properties of the β -SRL model in terms of the path probability and the link flow prediction, and we also show the differences from several existing route choice models. The sequential discount rate reflects the drivers' decision-making dynamics and has a large impact on the order of path probabilities of routes. It also affects network assignment results, and we conclude that the evaluation of appropriate sequential discount rates is important for precise demand forecasting. Moreover, we mention the selectivity of cyclic paths, which have not been discussed in detail in previous works and may cause the divergence of expected utilities, and show the effect of the balance between the parameter of link cost and the sequential discount rate. We then estimate the model using both simulation data and real data, including GPS traces in the time of the Great East Japan Earthquake. The estimated parameters using real data show that the difference of route choice mechanisms between the normal day and the disaster day, and among the time periods. On the disaster day, all parameters systematically change as time goes by after the earthquake occurrence, and the estimation results of the sequential discount rate indicate myopic route choice behavior in gridlock networks. We conclude that the β -SRL model enable us to examine the decision-making dynamics in route choices and also to forecast demand more precisely by estimating appropriate sequential discount rates. The case study is of the gridlock network, however, it is assumed that the bias of link utility perception can be seen also in pedestrian and general vehicle networks.

In Chapter 5, we focus on the computational challenges in Markovian route choice models. We propose an algorithm referred to as the time-structured assignment (TSA), which is a method for stochastic network loading. Time-structuring of networks decomposes the state by the timing of decision-making, and it can remove the cyclic structure from the network for calculations. Moreover, we incorporate the concept of time-constraint into the route choice model and propose an algorithm for systematically restricting path sets. Thanks to these ideas, we can solve the Bellman equation easily and stably with backward induction, which is a simple solution method, and we can calculate the expected minimum cost regardless of network conditions. A numerical example of network loading shows that the TSA can always output the link flows, while the Markov chain assignment (MCA) cannot do so when link costs are small. The TSA can also examine the change of link flow by varying the parameter of time-constraint. The result of the stochastic user equilibrium indicates the possibility that the application of the TSA algorithm can alleviate the unreasonable cyclic flow given by the MCA. Moreover, we extend the model to the network-GEV model in time-structured networks (n-GEV-t) and show that the n-GEV-t model can describe the effect of overlapping among the path set including cyclic paths. The TSA algorithm is the one of solution of the challenges that the MCA algorithm remains; 1) computational instability dependent on network conditions, 2) unreasonable cyclic flows and 3) the amplification of the IIA property, with reasonable computational time. These challenges occur in the econometric models (see Fosgerau, Frejinger, and Karlstrom, 2013); therefore, our method can be applied to the discrete choice analysis to solve the computational problems.

In Chapter 6, we propose an activity assignment model based on a Markovian route choice model, focusing on the high continuity between walking and staying behavior in pedestrian contexts. We formulate an activity path choice model based on the proposed framework of the Markovian route choice analysis and describe a pedestrian activity-scheduling problem. By assuming that individuals always change their state at a certain time interval, the model can describe the choices of routes, activity locations and durations simultaneously. Moreover, in the context of assignment, we can evaluate both the spatial link flow and the aggregate duration time at each node. In the same way in previous sections, we restrict the path set based on the time-space prism and incorporate the time discount rate to model dynamic decisions of travelers. Illustrative examples show that these parameters of the time-constraint and the discount rate show the critical impact on the time-use patterns of pedestrians. A case study in the network of the city center of Matsuyama-city, Japan also presents the expanse of pedestrian activity sphere corresponding to the time-constraint. Finally we apply the activity assignment model to a pedestrian activity-based network design problem. We formulate the problem of widening sidewalk width in the pedestrian network of Matsuyama as a multi-objective and bi-level programming. We investigate the Pareto front solutions of the problem using the network update algorithm, which is a heuristic method to search neighborhood solutions. An example solution indicates that the streets whose sidewalks are widened connect directly to the shopping streets.

By using the models proposed in Chapter 3-6, we identify the preference of route choice behavior and evaluate network flow even in pedestrian networks in the same framework. Therefore as the main conclusion, we solve the computational challenges of previous Markovian route choice models and develop a integrated framework of Markovian route choice analysis regarding *Data and Estimation, Model, Assignment algorithm, and Application*.

7.2 Future research

This study is halfway to the completion, and we are proceeding the continuing research. In the following we present the future work related to the content of this thesis.

In Chapter 3, we point out that previous frameworks of estimating route choice models include biases in the process of route observations, and propose a new measurement model and a novel estimation method: *sequential link measurement model* and *structural estimation method*.

As the next work, we are planning to develop a more generalized framework, which is the joint estimation of the measurement model and route choice model. Our proposed measurement model identifies links sequentially, and it achieves the reduction of the number of iteration and enables to analyze the model property by investigating the convergence process of parameters. The framework retains the problem regarding the analytical characteristics, such as the existence of the fixed point and the solution stability of the convergence. As a more generalized framework, in the future work, we are planning to maximize the joint probability of the

two model. Based on the proposed measurement and route choice models, we formulate a problem maximizing the probability of reproducing the vector of measurements by the two models. As we mentioned in Chapter 2, the definition of the set of path candidates is required for evaluating the probabilities. In the framework of our model, it is difficult to memorize path candidates naively because the number of paths increases sequentially and becomes huge soon. For this reason, the development of algorithms of generating and resampling paths sequentially in the process of path observations will be required. Moreover, for maximizing the joint probability, the application of the EM algorithm or the variational Bayesian method and perhaps the development of a new estimation method will be discussed in the future work.

We will also examine the relationship between the definition of the time discretization interval and the sequential route choice model. For applying the sequential link measurement model, we have to assume that travelers make decisions at a certain time interval. When the lengths of links in a network differ from each other, the interval of time discretization is often defined by the travel time of the shortest link. In this case, we will assume that travelers choose the same link iteratively when they move on long links. The distribution of the true location on link and the definition of the utility function of staying at the same link will be examined in the future work.

Since the model includes the aspect of time, we will develop the framework to the activities in time-space networks. Based on the activity path choice model, which is presented in Chapter 6, we will identify the path in time-space networks and estimate the mechanisms of the activity path choice behavior, using GPS data. We have collected GPS data of pedestrians in city centers through multiple surveys, and will use it to investigate the paths in time-space networks.

The structural estimation method proposed in Chapter 3 is applicable to not only route choice models but also other transportation behavior models with uncertain measurements. We expect the development based on various data and models.

In Chapter 4, we propose a Markovian route choice model with the sequential discount rate and present its application to the gridlock network analysis. By considering the sequential discount rate, we can describe the mechanisms of myopic decisions in route choice behavior, which is dependent on the environment close to the decision makers.

In the future work, we will investigate the interpersonal heterogeneity of the sequential discount rate, because the parameter indicates the decision making dynamics and it is assumed to largely depends on personal characteristics of travelers. In the analysis in Chapter 4, it is assumed that all travelers have the same value of the sequential discount rate. We will examine its dispersion among travelers by extending the model to e.g., the mixed logit model or the latent class model. We will also investigate the relationship between the value of the sequential discount rate and the temporal and spatial situations of networks, using the large amount of data source.

The framework of estimating Markovian route choice models using real-time trajectories will be developed in the future work. Markovian route choice models, such as the RL model and β -SRL model, which is proposed in Chapter 4, do not require the information of entire trips but only the destination and link transitions for estimating parameters. The destination is required for evaluating the value functions, which are the expected maximum utilities of dynamic discrete choice models. However, the identification of the destinations is a big issue in the case of using real-time

trajectories. We are developing algorithms for identifying destinations, and their validation will be presented in the future work.

The estimation of the β -SRL model takes time to calculate, because the system of non-linear equations has to be solved to evaluate the route choice probabilities. As is discussed in Mai, Frejinger, and Bastin, 2015, methods for reducing the computational time are required for applying the model to real large-scale networks.

In Chapter 5, we focus on that the cyclic structures in networks cause the divergence of the Bellman equation and unreasonable flows, and introduce a method for restricting path set by incorporating the parameter of the time-constraint. The method does not remove all cyclic paths, and do solve the computational challenges of Markovian route choice models in reasonable time.

We define the value of the time-constraint arbitrarily in the analyses of Chapter 5, but in the future work, we will discuss the way of the definition and the validation of the time-constraint. We will examine the set of paths that are used in real networks, using real trajectories, and present a method for defining the time-constraint.

We also will apply the method to estimating route choice models, which is discussed in Chapter 3 and 4. Because the same problem of the divergence of the Bellman equation can be seen in the model estimation, it is meaningful to examine the possibility of application of the path restriction to estimators.

We show that the divergence of the expected maximum utilities is restrained using a simple network analysis, and we also discuss the condition of the convergence as the inequality of the spectral radius of the incidence matrix defining link costs. The theoretical discussion of the convergence condition in the case of incorporating the time-constraint will be presented in the future work.

In Chapter 6, we apply the Markovian route choice model with the sequential discount rate and the time-constraint to an activity network, and present a pedestrian activity-based network design problem as the framework of bi-level and bi-objective programming.

We define the utility function of the time use in an activity network as a quadratic function of the elapsed time from departing the initial node. More realistically, the utility function should be defined as a function of the duration time at each location to describe the law of diminishing marginal utility. However, in Markovian route choice models, the utilities of paths are always calculated in the *link additive* way, which is a problem for expressing realistic path utilities, such as considering effects of the elapsed time or the distance from the middle of the paths. The way of defining utility functions of Markovian route choice models will be discussed in the future work. The balance between the size of staying utilities and moving costs will also be examined.

For solving the network design problem, we investigate the Pareto front using a simple solution method of metaheuristics. This algorithm may result in the local optimal solution; therefore, the test and the development of solution methods to obtain more precise solutions will be presented in the future work. More efficient algorithms of solving both the network design problem and the activity assignment are required for applying to large-size networks.

Appendix A

Appendix to Chapter 3

A.1 Link switching

The link-based route measurement model often involves difficulties with respect to link connectivity due to its myopic optimization. Figure A.1 illustrates an example in which a path $r = [2, 4, 6]$ (expressed as the bold solid line) is estimated given measurements $(\hat{\mathbf{m}}^1, \hat{\mathbf{m}}^2, \hat{\mathbf{m}}^3)$ although the actual path is $r = [2, 7, 10]$ (expressed as the dashed line), as follows. Link $a_1 = 2$ is initially identified as the true state at $t = 1$ by the link-based route measurement model, and then the set of candidate states for a_2 is $\mathcal{A}(a_1 = 2) = \{2, 4, 5, 7\}$. Based on the calculation of link likelihoods $p(a_2 | \hat{\mathbf{m}}^2, 2)$, a_2 is determined as link 4. In this case, the set of possible states for a_3 is $\mathcal{A}(a_2 = 4) = \{1, 3, 4, 6\}$; however, given the locations of $\hat{\mathbf{m}}^3 = (\hat{m}_1^3, \hat{m}_2^3, \hat{m}_3^3)$, it seems that the measurements are not likely to correspond to any links in $\mathcal{A}(a_2)$. Nevertheless, since $a_2 = 4$ is identified as the true state at $t = 2$, the model has to determine the true state at $t = 3$ from $\mathcal{A}(a_2)$, and thus a_3 is identified as link 6. The example depicts a failure case in which a measurement error at a certain time period causes the subsequent errors, and this is a problem of the link-based route measurement model.

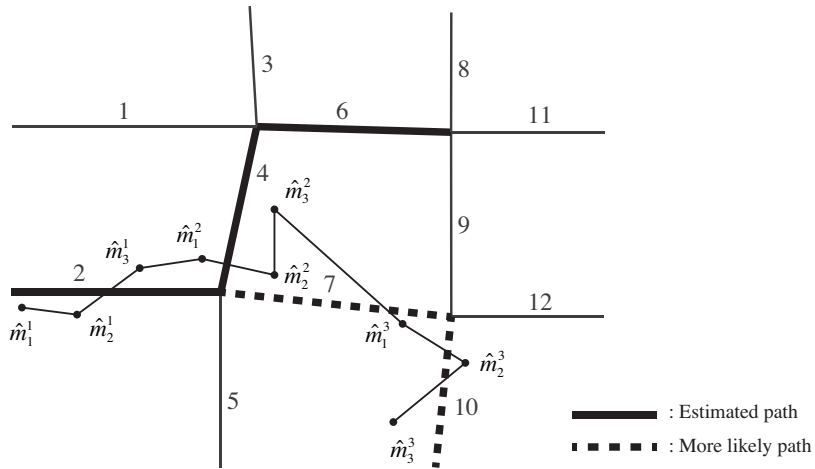


FIGURE A.1: Example of errors in path estimation

In order to solve this problem, we introduce the link switching algorithm (Figure A.2) to the link based measurement model. The algorithm is described as follows:

Step 1: Calculate the link likelihoods $p(a_t | \hat{\mathbf{m}}^t, a_{t-1})$ of all candidates for $a_t \in \mathcal{A}(a_{t-1})$ using Equation (3.5).

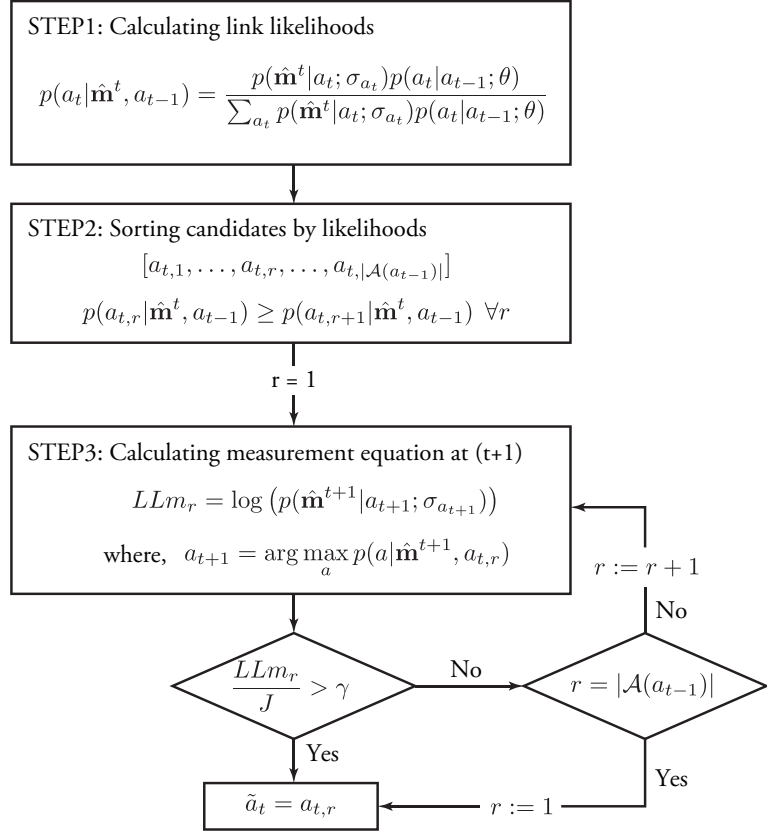


FIGURE A.2: Flow of link switching algorithm

Step 2: Sort and label the candidate links by the likelihoods $p(a_t|\hat{\mathbf{m}}^t, a_{t-1})$ as $[a_{t,1}, \dots, a_{t,k}, \dots, a_{t,|\mathcal{A}(a_{t-1})|}]$ which satisfy:

$$p(a_{t,1}|\hat{\mathbf{m}}^t, a_{t-1}) \geq \dots \geq p(a_{t,k}|\hat{\mathbf{m}}^t, a_{t-1}) \geq \dots \geq p(a_{t,|\mathcal{A}(a_{t-1})|}|\hat{\mathbf{m}}^t, a_{t-1}), \quad (\text{A.1})$$

where $1 \leq k \leq |\mathcal{A}(a_{t-1})|$ is the suffix of rank.

Step 3: Set $k = 1$, and calculate the measurement log-likelihood LLm_k of a_{t+1} given the measurements $\hat{\mathbf{m}}^{t+1}$ and the state $a_{t,k}$:

$$LLm_k = \log \left(p(\hat{\mathbf{m}}^{t+1}|a_{t+1}; \sigma_{a_{t+1}}) \right), \quad (\text{A.2})$$

where

$$a_{t+1} = \arg \max_a p(a|\hat{\mathbf{m}}^{t+1}, a_{t,k}). \quad (\text{A.3})$$

Step 4: Finish the algorithm if the following inequality with the convergence tolerance γ is satisfied:

$$\frac{LLm_r}{J} > \gamma, \quad (\text{A.4})$$

then identify $a_t = a_{t,k}$. Otherwise, go to *Step 3*.

Step 5: If $k = |\mathcal{A}(a_{t-1})|$, finish the algorithm and identify $a_t = a_{t,1}$, and otherwise, set $k = k + 1$ and go back to *Step 3*.

A.2 Fluctuation of estimated values of parameters

Figure A.3 shows the fluctuation of estimated parameter values in the structural estimation process, which is the result of the case study in Section 3.6.2.

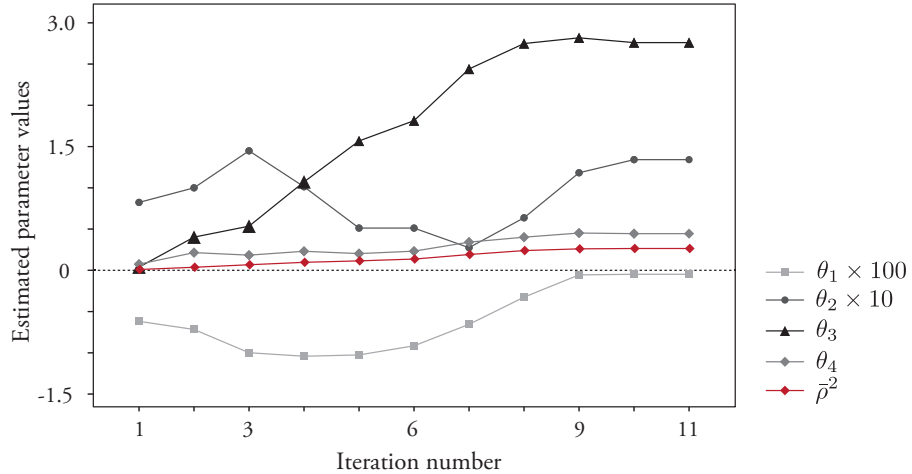


FIGURE A.3: Fluctuation of estimated values of parameters

Appendix B

Appendix to Chapter 5

B.1 Condition to solve Bellman equation

For the MTA, the inequality (5.17) regarding the spectral radius of the incidence matrix \mathbf{W} is a necessary and sufficient condition to solve the Bellman equation. We here discuss the relationship between the network condition and the spectral radius through a numerical example with a simple network.

Using a cyclic network, illustrated in Figure B.1, we calculate the spectral radii of the matrices \mathbf{W} with various values of θ shown in Table B.1. The results show that Equation (5.17) is not satisfied and the expected minimum cost diverges when the network includes cycles and θ is small. In this case, we cannot solve the Bellman equation when θ is less than or equal to 0.4. From above discussions it is concluded that the expected minimum cost cannot be solved with a small perception parameter. In other words, existing approaches retain the instability in the calculation of convergence.

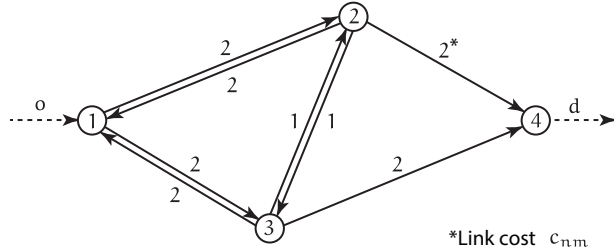


FIGURE B.1: A simple cyclic network

TABLE B.1: Spectral radius of the matrix \mathbf{W}

θ	1	0.9	0.8	0.7	0.6	0.5	0.4	0.3	0.2	0.1
$\rho(\mathbf{W})$	0.45	0.51	0.59	0.68	0.78	0.91	1.05	1.23	1.44	1.70

Appendix C

Appendix to Chapter 6

C.1 Equivalent optimization model

The activity network loading problem is:

$$\begin{aligned} \min z(f) = & - \sum_{ij} \sum_t v_{ij}^t f_{ij}^t + \sum_{o \in \mathcal{O}} \sum_{ij} \sum_t \frac{1}{\mu} f_{ij}^{o,t} \log f_{ij}^{o,t} \\ & - \sum_{o \in \mathcal{O}} \sum_{i \in \mathcal{N}} \sum_t \frac{1}{\mu} \left(\sum_{j \in \mathcal{N}} f_{ij}^{o,t} \right) \log \left(\sum_{j \in \mathcal{N}} f_{ij}^{o,t} \right), \end{aligned} \quad (\text{C.1})$$

subject to,

$$\sum_h f_{hi}^{o,t-1} - \sum_j f_{ij}^{o,t} - \eta_{oi}^t q_{od} + \eta_{id}^t q_{od} = 0, \quad \forall i \in \mathcal{N}, \forall t \in \{0, 1, \dots, T\} \quad (\text{C.2})$$

$$f_{ij}^t = \sum_l f_{ij}^{l,t}, \quad \forall (i, j) \in \mathcal{A}, \forall t \in \{0, 1, \dots, T\} \quad (\text{C.3})$$

$$f_{ij}^{l,t} \geq 0, \quad \forall (i, j) \in \mathcal{A}, \forall t \in \{0, 1, \dots, T\}, \forall o \in \mathcal{O} \quad (\text{C.4})$$

where η_{li}^t equals one if $t = T$ and $i = l$ and zero otherwise, and η_{il}^t equals one if $t = 0$ and $i = l$ and zero otherwise. The edge flow f_{ij}^t is not defined and equals zero if it is smaller than zero or larger than T . It is described that Equations (C.1)-(C.4) are equivalent to the path choice model in the activity network as follows.

Proof. We first define the Lagrangian as follows:

$$\begin{aligned} \mathcal{L}(f, \mu, \lambda) = & z(f) + \sum_t \sum_l \sum_i \varphi_{t,i}^l \left(\sum_h f_{hi}^{l,t-1} - \sum_j f_{ij}^{l,t} - \eta_{li}^t q_l + \eta_{il}^t q_l \right) \\ & + \sum_{ij} \sum_t \lambda_{ij}^t \left(f_{ij}^t - \sum_l f_{ij}^{l,t} \right), \end{aligned} \quad (\text{C.5})$$

then KKT-conditions is formulated as below:

$$\frac{\partial \mathcal{L}}{\partial f_{ij}^{l,t}} = \frac{1}{\mu} \log \frac{f_{ij}^{l,t}}{\sum_j f_{ij}^{l,t}} - v_{ij}^t + \varphi_{t+1,j}^l - \varphi_{t,i}^l = 0, \text{ if } f_{ij}^{l,t} > 0, \quad (\text{C.6})$$

$$\frac{\partial \mathcal{L}}{\partial f_{ij}^{l,t}} = \frac{1}{\mu} \log \frac{f_{ij}^{l,t}}{\sum_j f_{ij}^{l,t}} - v_{ij}^t + \varphi_{t+1,j}^l - \varphi_{t,i}^l > 0, \text{ if } f_{ij}^{l,t} = 0, \quad (\text{C.7})$$

$$\frac{\partial \mathcal{L}}{\partial \varphi_{t,i}^l} = \sum_h f_{hi}^{l,t-1} - \sum_j f_{ij}^{l,t} - \eta_{li}^t q_l + \eta_{il}^t q_l, \quad (\text{C.8})$$

$$\frac{\partial \mathcal{L}}{\partial \lambda_{ij}^t} = f_{ij}^t - \sum_l f_{ij}^{l,t}. \quad (\text{C.9})$$

Assuming $f_{ij}^{l,t} > 0$, Equation (C.6) is re-formulated as:

$$\begin{aligned} & \frac{1}{\mu} \log \frac{f_{ij}^{l,t}}{\sum_j f_{ij}^{l,t}} - v_{ij}^t + \varphi_{t+1,j}^l - \varphi_{t,i}^l = 0 \\ \Leftrightarrow & \frac{f_{ij}^{l,t}}{\sum_j f_{ij}^{l,t}} = \exp[\mu(v_{ij}^t + \varphi_{t+1,j}^l - \varphi_{t,i}^l)] \\ \Leftrightarrow & p_t^l(j|i) = \exp[\mu(v_{ij}^t + \varphi_{t+1,j}^l - \varphi_{t,i}^l)], \end{aligned} \quad (\text{C.10})$$

where the transition probability between states (t, i) and $(t+1, j)$, $p_t^l(j|i)$ is equivalent to the branching fraction of flow $f_{ij}^{l,t} / \sum_j f_{ij}^{l,t}$. Because the sum of the probability equals one, we get the following equation:

$$\varphi_{t,i}^l = \frac{1}{\mu} \sum_j \exp[\mu(v_{ij}^t + \varphi_{t+1,j}^l)]. \quad (\text{C.11})$$

This formulation is equivalent to the expected minimum cost from states (t, i) to (T, l) , and finally we get the formulation of the transition probability by substituting Equation (C.11) to Equation (C.10):

$$p_t^{(T,l)}(j|i) = \frac{\exp[\mu(v_{ij}^t + \varphi_{t+1,j}^{(T,l)})]}{\sum_{j'} \exp[\mu(v_{ij'}^t + \varphi_{t+1,j'}^{(T,l)})]}. \quad (\text{C.12})$$

This is equivalent to the probability of the path choice model in time-structured network. ■

C.2 Activity patterns with different β

The time-space discount rate β in the activity path choice model describes the decision-making dynamics of traveler. We change the parameter β and generate 1000 activity paths, which depart at node 18 in the Matsuyama network in Chapter 6 with the time-constraint of 90 minutes. Figure C.1 shows the most frequent activity patterns in the case that β is 1 (a) and 0.8 (b), respectively. When $\beta = 1$, travelers optimize their activities within the time-constraint and spend 81 minutes in the network. On the other hand, when $\beta = 0.8$, travelers stay at only node 18 and the total duration

time is only 45 minutes. It is because travelers behave myopically and optimize their decisions at each timing.

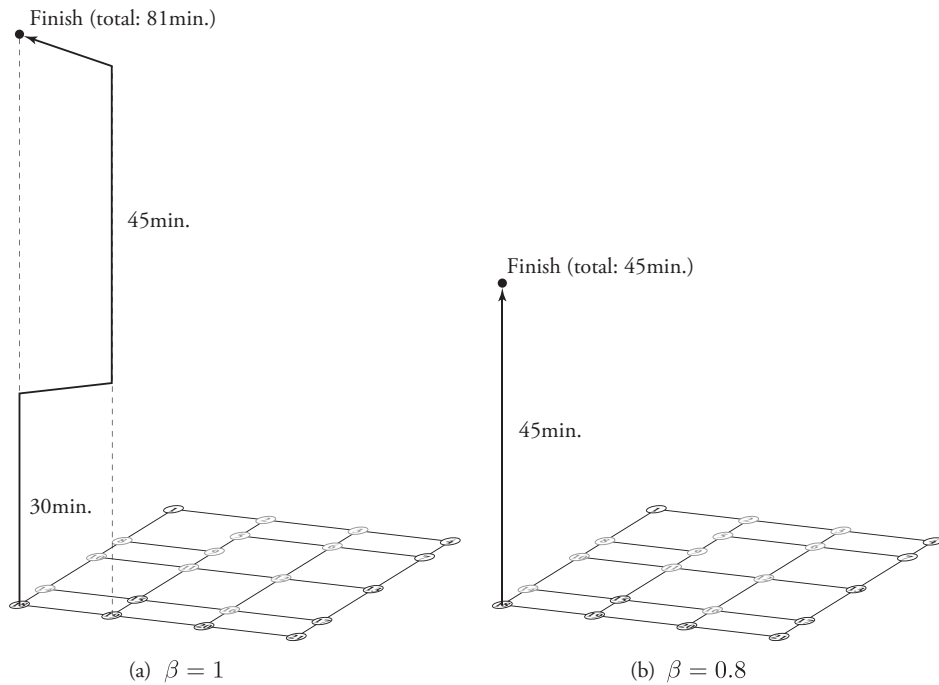


FIGURE C.1: The most frequent activity patterns with different β s

C.3 Flow of the solution algorithm

Figure C.2 shows the flow of the solution algorithm, which is used for the case study in Section 6.5 in Chapter 6.

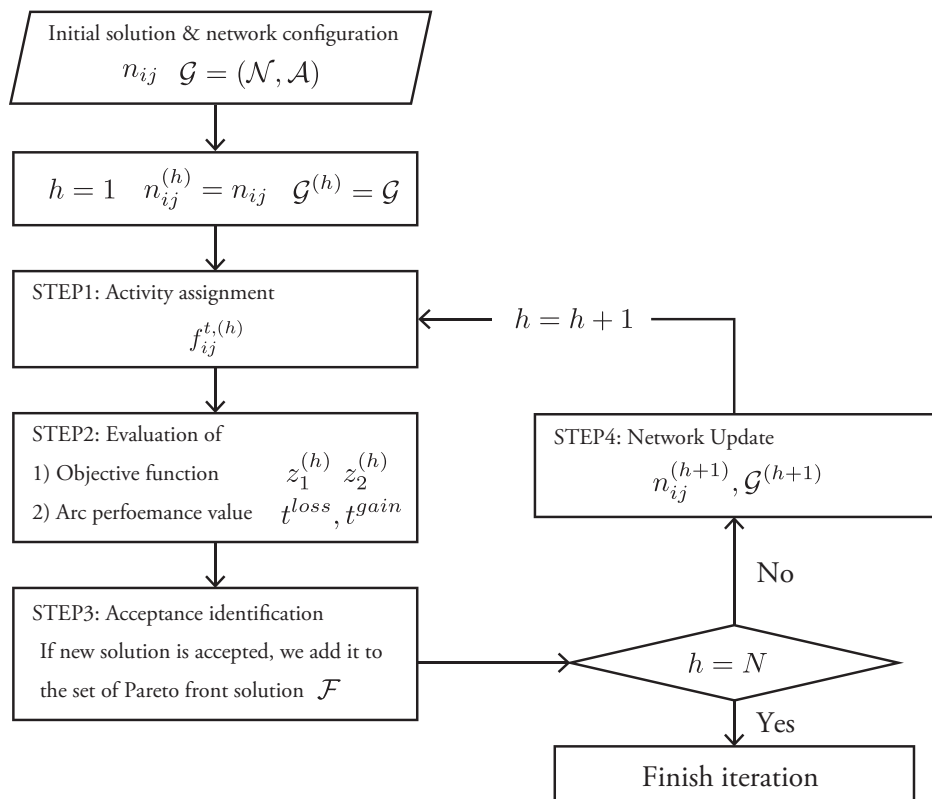


FIGURE C.2: Flow of Network Update algorithm

Appendix D

Related publications

This chapter has been updated on January 4, 2018.

- Chapter 3 has been presented by Yuki Oyama at the conference of *hEART 2016* in Delft as *A link-based map matching algorithm with structural estimation method* and published as:

Oyama, Y. and Hato, E., 2017. Structural estimation for route choice models considering link specificity of measurement error variances, Journal of JSCE Series D3: Infrastructure Planning and Management, 73(5), 597-608, and also submitted to as:

Oyama, Y., Hato, E. Link-based measurement model to estimate route choice parameters in urban pedestrian networks, for publication on Transportation Research Part C: Emerging Technologies..

- The content of Chapter 4 has been presented by Yuki Oyama at the conference of *11th ERTICO* in Glasgow as *Trajectory-oriented traffic management using sequential discount rate: a case study of the Great East Japan Earthquake*, and has been published as:

Oyama, Y. and Hato, E., 2017. A discounted recursive logit model for dynamic gridlock network analysis, Transportation Research Part C: Emerging Technologies 85, pp.509-527 and

Oyama, Y. and Hato, E., 2017. Route choice analysis in disaster network using generalized recursive logit model, Journal of Traffic Engineering 3(5), 1-10.

- The content of Chapter 5 has been published as:

Oyama, Y. and Hato, E., 2017. Stochastic traffic assignment in time-structured networks, Journal of JSCE Series D3: Infrastructure Planning and Management 73(4), 186-200 (in Japanese), and also submitted as:

Oyama, Y., Hato, E. Prism-based path set restriction for solving Markovian traffic assignment problem, for publication on Transportation Research Part B: Methodological.

- The contents of Chapter 6 have been presented by Yuki Oyama in the conferences of *21st International Conference of Hong Kong for Transportation Studies (HK-STS)* as *Pedestrian activity model based on implicit path enumeration* and *6th symposium arranged by European Association for Research in Transportation (hEART)* as *Markov assignment for a pedestrian activity-based network design problem*. They have also been published as:

Oyama, Y. and Hato, E., 2016. Pedestrian activity assignment problem with time-space constraint and path correlation, Journal of City Planning 51(3), 680-687 and

Oyama, Y. and Hato, E., 2017. Pedestrian activity-based network design based on multi-objective programming, Journal of City Planning 52(3), 810-817.

Bibliography

- Abdel-Aty, Mohamed A and M Fathy Abdalla (2006). "Examination of multiple mode/route-choice paradigms under ATIS". In: *IEEE Transactions on Intelligent Transportation Systems* 7.3, pp. 332–348.
- Abdel-Aty, Mohamed A, Ryuichi Kitamura, and Paul P Jovanis (1997). "Using stated preference data for studying the effect of advanced traffic information on drivers' route choice". In: *Transportation Research Part C: Emerging Technologies* 5.1, pp. 39–50.
- Aguirregabiria, Victor and Pedro Mira (2002). "Swapping the Nested Fixed Point Algorithm: A Class of Estimators for Discrete Markov Decision Models". In: *Econometrica* 70.4, pp. 1519–1543. ISSN: 0012-9682. DOI: [10.1111/1468-0262.00340](https://doi.org/10.1111/1468-0262.00340). arXiv: [arXiv:1011.1669v3](https://arxiv.org/abs/1011.1669v3).
- (2010). "Dynamic discrete choice structural models: A survey". In: *Journal of Econometrics* 156.1, pp. 38–67. ISSN: 03044076. DOI: [10.1016/j.jeconom.2009.09.007](https://doi.org/10.1016/j.jeconom.2009.09.007). URL: <http://dx.doi.org/10.1016/j.jeconom.2009.09.007>.
- Akamatsu, Takashi (1996). "Cyclic flows, Markov process and stochastic traffic assignment". In: *Transportation Research Part B: Methodological* 30.5, pp. 369–386. ISSN: 01912615. DOI: [10.1016/0191-2615\(96\)00003-3](https://doi.org/10.1016/0191-2615(96)00003-3).
- (1997). "Decomposition of Path Choice Entropy in General Transport Networks". In: *Transportation Science* 31.4, pp. 349–362. ISSN: 0041-1655. DOI: [10.1287/trsc.31.4.349](https://doi.org/10.1287/trsc.31.4.349).
- Antonini, Gianluca, Michel Bierlaire, and Mats Weber (2006). "Discrete choice models of pedestrian walking behavior". In: *Transportation Research Part B: Methodological* 40.8, pp. 667–687. ISSN: 01912615. DOI: [10.1016/j.trb.2005.09.006](https://doi.org/10.1016/j.trb.2005.09.006).
- Arentze, T. and H. Timmermans (2004a). "Multistate supernetwork approach to modelling multi-activity, multimodal trip chains". In: *International Journal of Geographical Information Science* 18.7, pp. 631–651. ISSN: 1365-8816. DOI: [10.1080/13658810410001701978](https://doi.org/10.1080/13658810410001701978).
- Arentze, Theo A. and H. J P Timmermans (2004b). "A learning-based transportation oriented simulation system". In: *Transportation Research Part B: Methodological* 38.7, pp. 613–633. ISSN: 01912615. DOI: [10.1016/j.trb.2002.10.001](https://doi.org/10.1016/j.trb.2002.10.001).
- Asakura, Yasuo, Eiji Hato, and Takuya Maruyama (2014). "Behavioural data collection using mobile phones". In: *Mobile Technologies for Activity-Travel Data Collection and Analysis*, pp. 17–35.
- Azevedo, JoseAugusto et al. (1993). "An algorithm for the ranking of shortest paths". In: *European Journal of Operational Research* 69.1, pp. 97–106.
- Baillon, J. B. and R. Cominetti (2008). "Markovian traffic equilibrium". In: *Mathematical Programming* 111.1-2, pp. 33–56. ISSN: 00255610. DOI: [10.1007/s10107-006-0076-2](https://doi.org/10.1007/s10107-006-0076-2).
- Barra, Tomas de la, B Perez, and J Anez (1993). "Multidimensional path search and assignment". In: *PTRC Summer Annual Meeting, 21st, 1993, University of Manchester, United Kingdom*.
- Beckmann, Martin, CB McGuire, and Christopher B Winsten (1956). *Studies in the Economics of Transportation*. Yale University Press.

- Bekhor, S and J Prashker (2001). "Stochastic user equilibrium formulation for generalized nested logit model". In: *Transportation Research Record: Journal of the Transportation Research Board* 1752, pp. 84–90.
- Bekhor, Shlomo, Moshe Ben-Akiva, and M Scott Ramming (2002). "Adaptation of logit kernel to route choice situation". In: *Transportation Research Record: Journal of the Transportation Research Board* 1805, pp. 78–85.
- Bekhor, Shlomo, Moshe E. Ben-Akiva, and M. Scott Ramming (2006). "Evaluation of choice set generation algorithms for route choice models". In: *Annals of Operations Research* 144.1, pp. 235–247. ISSN: 02545330. DOI: [10.1007/s10479-006-0009-8](https://doi.org/10.1007/s10479-006-0009-8).
- Bell, Michael G H (1995). "Alternatives to Dial's logit assignment algorithm". In: *Transportation Research Part B* 29.4, pp. 287–295. ISSN: 01912615. DOI: [10.1016/0191-2615\(95\)00005-X](https://doi.org/10.1016/0191-2615(95)00005-X).
- Bell, Michael GH (2009). "Hyperstar: A multi-path Astar algorithm for risk averse vehicle navigation". In: *Transportation Research Part B: Methodological* 43.1, pp. 97–107.
- Bellman, Richard E (1957). *Dynamic programming*. Princeton University Press.
- Ben-Akiva, Moshe and Michel Bierlaire (1999). "Discrete choice methods and their applications to short term travel decisions". In: *Handbook of transportation science*. Springer, pp. 5–33.
- Ben-Akiva, Moshe, Michèle Cyna, and André de Palma (1984). "Dynamic model of peak period congestion". In: *Transportation Research Part B* 18.4-5, pp. 339–355. ISSN: 01912615. DOI: [10.1016/0191-2615\(84\)90016-X](https://doi.org/10.1016/0191-2615(84)90016-X).
- Ben-Akiva, Moshe, Andre De Palma, and Kaysi Isam (1991). "Dynamic network models and driver information systems". In: *Transportation Research Part A: General* 25.5, pp. 251–266.
- Ben-Akiva, Moshe et al. (1997). "Development of a route guidance generation system for real-time application". In: *Proceedings of the IFAC Transportation Systems 97 Conference, Chania*. Citeseer.
- Ben-Akiva, Moshe et al. (2002). "Hybrid Choice Models : Progress and Challenges Massachusetts Institute of Technology". In: *Marketing Letters* 13.3, pp. 163–175. ISSN: 0923-0645. DOI: [10.1023/A:1020254301302](https://doi.org/10.1023/A:1020254301302).
- Ben-Akiva, Moshe E and Steven R Lerman (1985). *Discrete choice analysis: theory and application to travel demand*. Vol. 9. MIT press.
- Bierlaire, Michel (2002). "The Network GEV". In: *Swiss Transport Research Conference*.
- Bierlaire, Michel, Jingmin Chen, and Jeffrey Newman (2013). "A probabilistic map matching method for smartphone GPS data". In: *Transportation Research Part C: Emerging Technologies* 26, pp. 78–98. ISSN: 0968090X. DOI: [10.1016/j.trc.2012.08.001](https://doi.org/10.1016/j.trc.2012.08.001). URL: <http://dx.doi.org/10.1016/j.trc.2012.08.001>.
- Bierlaire, Michel and Emma Frejinger (2008). "Route choice modeling with network-free data". In: *Transportation Research Part C: Emerging Technologies* 16.2, pp. 187–198. ISSN: 0968090X. DOI: [10.1016/j.trc.2007.07.007](https://doi.org/10.1016/j.trc.2007.07.007).
- Bolduc, Denis and Moshe Ben-Akiva (1991). "A multinomial probit formulation for large choice sets". In: *Proceedings of the 6th International Conference on Travel Behaviour* 2, pp. 243–258.
- Borgers, A. and H. J P Timmermans (1986a). "City centre entry points, store location patterns and pedestrian route choice behaviour: A microlevel simulation model". In: *Socio-Economic Planning Sciences* 20.1, pp. 25–31. ISSN: 00380121. DOI: [10.1016/0038-0121\(86\)90023-6](https://doi.org/10.1016/0038-0121(86)90023-6).

- Borgers, Aloys and Harry Timmermans (1986b). "A Model of Pedestrian Route Choice and Demand for Retail Facilities within Inner-City Shopping Areas". In: *Geographical Analysis* 18.2, pp. 115–128. ISSN: 00167363. DOI: [10.1111/j.1538-4632.1986.tb00086.x](https://doi.org/10.1111/j.1538-4632.1986.tb00086.x). URL: <http://dx.doi.org/10.1111/j.1538-4632.1986.tb00086.x>.
- Borgers, Aloys and HJP Timmermans (1986c). "City centre entry points, store location patterns and pedestrian route choice behaviour: A microlevel simulation model". In: *Socio-economic planning sciences* 20.1, pp. 25–31.
- Borst, Hieronymus C. et al. (2008). "Relationships between street characteristics and perceived attractiveness for walking reported by elderly people". In: *Journal of Environmental Psychology* 28.4, pp. 353–361. ISSN: 02724944. DOI: [10.1016/j.jenvp.2008.02.010](https://doi.org/10.1016/j.jenvp.2008.02.010).
- Bovy, Piet HL (2009). "On modelling route choice sets in transportation networks: a synthesis". In: *Transport reviews* 29.1, pp. 43–68.
- Bovy, Piet HL and Eliahu Stern (1990). *Route choice: Wayfinding in transportation networks*.
- Bowman, J. L. and M. E. Ben-Akiva (2000). "Activity-based disaggregate travel demand model system with activity schedules". In: *Transportation Research Part A: Policy and Practice* 35.1, pp. 1–28. ISSN: 09658564. DOI: [10.1016/S0965-8564\(99\)00043-9](https://doi.org/10.1016/S0965-8564(99)00043-9).
- Cascetta, Ennio et al. (1996). "A modified logit route choice model overcoming path overlapping problems: specification and some calibration results for interurban networks". In: *Proceedings of the 13th International Symposium on Transportation and Traffic Theory*. Pergamon Lyon, France, pp. 697–711.
- Chen, Jingmin and Michel Bierlaire (2015). "Probabilistic multimodal map matching with rich smartphone data". In: *Journal of Intelligent Transportation Systems* 19.2, pp. 134–148.
- Chow, Joseph YJ and Will W Recker (2012). "Inverse optimization with endogenous arrival time constraints to calibrate the household activity pattern problem". In: *Transportation Research Part B: Methodological* 46.3, pp. 463–479.
- Cirillo, Cinzia and Renting Xu (2011). "Dynamic Discrete Choice Models for Transportation." In: *Transport Reviews* 31.4, pp. 473–494. ISSN: 01441647. DOI: [10.1080/01441647.2010.533393](https://doi.org/10.1080/01441647.2010.533393). URL: [10.1080/01441647.2010.533393\\$\\backslash\\$http://ezproxy.lib.utexas.edu/login?url=http://search.ebscohost.com/login.aspx?direct=true&db=a9h&AN=62667369&site=ehost-live](http://ezproxy.lib.utexas.edu/login?url=http://search.ebscohost.com/login.aspx?direct=true&db=a9h&AN=62667369&site=ehost-live).
- Daganzo, Carlos F. (2007). "Urban gridlock: Macroscopic modeling and mitigation approaches". In: *Transportation Research Part B: Methodological* 41.1, pp. 49–62. ISSN: 01912615. DOI: [10.1016/j.trb.2006.03.001](https://doi.org/10.1016/j.trb.2006.03.001).
- Daganzo, Carlos F and Yosef Sheffi (1977). "On stochastic models of traffic assignment". In: *Transportation science* 11.3, pp. 253–274.
- Dailey, Daniel J and Frederick W Cathey (2002). *AVL-equipped vehicles as traffic probe sensors*. Tech. rep. Washington State Department of Transportation.
- Daly, Andrew and Michel Bierlaire (2006). "A general and operational representation of Generalised Extreme Value models". In: *Transportation Research Part B: Methodological* 40.4, pp. 285–305. ISSN: 01912615. DOI: [10.1016/j.trb.2005.03.003](https://doi.org/10.1016/j.trb.2005.03.003).
- Danalet, Antonin and Michel Bierlaire (2015). "Importance sampling for activity path choice". In: *Proceedings of the 15th Swiss Transport Research Conference*. EPFL-CONF-207458.
- Danalet, Antonin, Bilal Farooq, and Michel Bierlaire (2014). "A Bayesian approach to detect pedestrian destination-sequences from WiFi signatures". In: *Transportation*

- Research Part C: Emerging Technologies* 44, pp. 146–170. ISSN: 0968090X. DOI: [10.1016/j.trc.2014.03.015](https://doi.org/10.1016/j.trc.2014.03.015). URL: <http://dx.doi.org/10.1016/j.trc.2014.03.015>.
- Danalet, Antonin et al. (2016). "Location choice with longitudinal WiFi data". In: *Journal of choice modelling* 18, pp. 1–17.
- Dia, Hussein (2002). "An agent-based approach to modelling driver route choice behaviour under the influence of real-time information". In: *Transportation Research Part C: Emerging Technologies* 10.5, pp. 331–349.
- Dial, R B (1971). "A probabilistic multipath traffic assignment algorithm which obviates pathenumeration". In: *Transportation Research* 5.2, pp. 83–111.
- Diggelen, Frank van (2007). "SYSTEM DESIGN & TEST-GNSS Accuracy-Lies, Damn Lies, and Statistics-This update to a seminal article first published here in 1998 explains how statistical methods can create many different". In: *GPS World* 18.1, pp. 26–33.
- Dijkstra, Edsger W (1959). "A note on two problems in connexion with graphs". In: *Numerische mathematik* 1.1, pp. 269–271.
- Eppstein, David (1998). "Finding the k shortest paths". In: *SIAM Journal on computing* 28.2, pp. 652–673.
- Fisk, Caroline (1980). "Some developments in equilibrium traffic assignment". In: *Transportation Research Part B: Methodological* 14.3, pp. 243–255. ISSN: 01912615. DOI: [10.1016/0191-2615\(80\)90004-1](https://doi.org/10.1016/0191-2615(80)90004-1).
- Flötteröd, Gunnar and Michel Bierlaire (2013). "Metropolis-Hastings sampling of paths". In: *Transportation Research Part B: Methodological* 48, pp. 53–66. ISSN: 01912615. DOI: [10.1016/j.trb.2012.11.002](https://doi.org/10.1016/j.trb.2012.11.002).
- Fosgerau, Mogens, Emma Freijinger, and Anders Karlstrom (2013). "A link based network route choice model with unrestricted choice set". In: *Transportation Research Part B: Methodological* 56, pp. 70–80. ISSN: 01912615. DOI: [10.1016/j.trb.2013.07.012](https://doi.org/10.1016/j.trb.2013.07.012). URL: <http://dx.doi.org/10.1016/j.trb.2013.07.012>.
- Freijinger, E. and M. Bierlaire (2007). "Capturing correlation with subnetworks in route choice models". In: *Transportation Research Part B: Methodological* 41.3, pp. 363–378. ISSN: 01912615. DOI: [10.1016/j.trb.2006.06.003](https://doi.org/10.1016/j.trb.2006.06.003).
- Freijinger, E., M. Bierlaire, and M. Ben-Akiva (2009). "Sampling of alternatives for route choice modeling". In: *Transportation Research Part B: Methodological* 43.10, pp. 984–994. ISSN: 01912615. DOI: [10.1016/j.trb.2009.03.001](https://doi.org/10.1016/j.trb.2009.03.001). URL: <http://dx.doi.org/10.1016/j.trb.2009.03.001>.
- Freijinger, Emma (2008). "Route Choice Analysis : Data, Models, Algorithms and Applications". PhD thesis. École polytechnique fédérale de Lausanne.
- Friedrich, Markus, Ingmar Hofsäß, and Steffen Wekeck (2001). "Timetable-based transit assignment using branch and bound techniques". In: *Transportation Research Record: Journal of the Transportation Research Board* 1752, pp. 100–107.
- Fuse, Takashi and Wataru Nakanishi (2012). "A study on multiple human tracking by integrating pedestrian behavior model". In: *Journal of Japan Society of Civil Engineers, Ser. D3 (Infrastructure Planning and Management)* 68, pp. 92–104.
- Gale, Nathan et al. (1990). "The acquisition and integration of route knowledge in an unfamiliar neighborhood". In: *Journal of Environmental Psychology* 10.1, pp. 3–25.
- Gao, Song, Emma Freijinger, and Moshe Ben-Akiva (2010). "Adaptive route choices in risky traffic networks: A prospect theory approach". In: *Transportation Research Part C: Emerging Technologies* 18.5, pp. 727–740. ISSN: 0968090X. DOI: [10.1016/j.trc.2009.08.001](https://doi.org/10.1016/j.trc.2009.08.001). URL: <http://dx.doi.org/10.1016/j.trc.2009.08.001>.

- Gentile, G. and Andrea Papola (2006). "An alternative approach to route choice simulation: the sequential models". In: *European Transport Conference 2006*. DOI: [10.1.1.157.3774](https://doi.org/10.1.1.157.3774).
- Geroliminis, Nikolas and Carlos F Daganzo (2008). "Existence of urban-scale macroscopic fundamental diagrams: Some experimental findings". In: *Transportation Research Part B: Methodological* 42.9, pp. 759–770.
- Greenfeld, Joshua S (2002). "Matching GPS observations to locations on a digital map". In: *Transportation Research Board 81st Annual Meeting*.
- Habib, Khandker M Nurul (2011). "A random utility maximization (RUM) based dynamic activity scheduling model: Application in weekend activity scheduling". In: *Transportation* 38.1, pp. 123–151.
- Hägerstrand, Torsten (1970). "What about people in regional science?" In: *Regional Science Association* 24.
- Hänseler, Flurin S et al. (2017). "A dynamic network loading model for anisotropic and congested pedestrian flows". In: *Transportation Research Part B: Methodological* 95, pp. 149–168.
- Hara, Yusuke and Takashi Akamatsu (2014). "Stochastic User Equilibrium Traffic Assignment with a Network GEV Based Route Choice Model". In: *Journal of Japan Society of Civil Engineers, Ser. D3 (Infrastructure Planning and Management)* 70, p. 611.
- Hato, Eiji (2006). "Development of MoALs (Mobile Activity Loggers supported by gps-phones) for travel behavior analysis". In: *Transportation Research Board 85th Annual Meeting*. 06-2862.
- (2010). "Development of behavioral context addressable loggers in the shell for travel-activity analysis". In: *Transportation Research Part C: Emerging Technologies* 18.1, pp. 55–67.
- Hoogendoorn, Serge P and Piet HL Bovy (2004). "Pedestrian route-choice and activity scheduling theory and models". In: *Transportation Research Part B: Methodological* 38.2, pp. 169–190.
- Hunter, Timothy, Pieter Abbeel, and Alexandre Bayen (2014). "The path inference filter: model-based low-latency map matching of probe vehicle data". In: *IEEE Transactions on Intelligent Transportation Systems* 15.2, pp. 507–529.
- Kang, Jee Eun and Will Recker (2013). "The location selection problem for the household activity pattern problem". In: *Transportation Research Part B: Methodological* 55, pp. 75–97. ISSN: 01912615. DOI: [10.1016/j.trb.2013.05.003](https://doi.org/10.1016/j.trb.2013.05.003). URL: <http://dx.doi.org/10.1016/j.trb.2013.05.003>.
- Kasemsuppakorn, Piyawan and Hassan A Karimi (2013). "A pedestrian network construction algorithm based on multiple GPS traces". In: *Transportation research part C: emerging technologies* 26, pp. 285–300.
- Kurose, Shigeyuki, Aloys WJ Borgers, and Harry JP Timmermans (2001). "Classifying pedestrian shopping behaviour according to implied heuristic choice rules". In: *Environment and Planning B: Planning and Design* 28.3, pp. 405–418.
- Lam, William H K and Yafeng Yin (2001). "An activity-based time-dependent traffic assignment model". In: *Transportation Research Part B: Methodological* 35, pp. 549–574.
- Leurent, Fabien M (1997). "Curbing the computational difficulty of the logit equilibrium assignment model". In: *Transportation Research Part B: Methodological* 31.4, pp. 315–326.
- Li, Dawei, Tomio Miwa, and Takayuki Morikawa (2014). "Considering en-route choices in utility-based route choice modelling". In: *Networks and Spatial Economics* 14.3-4, pp. 581–604.

- Liao, Feixiong, Theo Arentze, and Harry Timmermans (2013). "Incorporating space – time constraints and activity-travel time profiles in a multi-state supernetwork approach to individual activity-travel scheduling". In: *Transportation Research Part B: Methodological* 55, pp. 41–58. ISSN: 0191-2615. DOI: [10.1016/j.trb.2013.05.002](https://doi.org/10.1016/j.trb.2013.05.002). URL: <http://dx.doi.org/10.1016/j.trb.2013.05.002>.
- Liu, Peng et al. (2015). "Dynamic activity-travel assignment in multi-state supernetworks". In: *Transportation Research Part B: Methodological* 81, pp. 656–671. ISSN: 01912615. DOI: [10.1016/j.trb.2015.08.006](https://doi.org/10.1016/j.trb.2015.08.006). URL: <http://dx.doi.org/10.1016/j.trb.2015.08.006>.
- Ma, Jiangshan and Daisuke Fukuda (2015). "A hyperpath-based network generalized extreme-value model for route choice under uncertainties". In: *Transportation Research Part C: Emerging Technologies* 59, pp. 19–31. ISSN: 0968090X. DOI: [10.1016/j.trc.2015.05.015](https://doi.org/10.1016/j.trc.2015.05.015). URL: <http://dx.doi.org/10.1016/j.trc.2015.05.015>.
- Mahmassani, Hani S and Yu-Hsin Liu (1999). "Dynamics of commuting decision behaviour under advanced traveller information systems". In: *Transportation Research Part C: Emerging Technologies* 7.2, pp. 91–107.
- Mahmassani, Hani S., Meead Saberi, and Ali Zockaei (2013). "Urban network gridlock: Theory, characteristics, and dynamics". In: *Transportation Research Part C: Emerging Technologies* 36, pp. 480–497. ISSN: 0968090X. DOI: [10.1016/j.trc.2013.07.002](https://doi.org/10.1016/j.trc.2013.07.002). URL: <http://dx.doi.org/10.1016/j.trc.2013.07.002>.
- Mahmassani, HaniS. (2001). "Dynamic Network Traffic Assignment and Simulation Methodology for Advanced System Management Applications". In: *Networks and Spatial Economics* 1.3-4, pp. 267–292. ISSN: 1566-113X. DOI: [10.1023/A:1012831808926](https://doi.org/10.1023/A:1012831808926). URL: <http://dx.doi.org/10.1023/A:1012831808926>.
- Mai, Tien (2015). "Dynamic programming approaches for estimating and applying large-scale discrete choice models". PhD thesis. Université de Montréal.
- (2016). "A method of integrating correlation structures for a generalized recursive route choice model". In: *Transportation Research Part B: Methodological* 93, pp. 146–161.
- Mai, Tien, Mogens Fosgerau, and Emma Frejinger (2015). "A nested recursive logit model for route choice analysis". In: *Transportation Research Part B: Methodological* 75, pp. 100–112. ISSN: 01912615. DOI: [10.1016/j.trb.2015.03.015](https://doi.org/10.1016/j.trb.2015.03.015).
- Mai, Tien, Emma Frejinger, and Fabien Bastin (2015). "A dynamic programming approach for quickly estimating large scale MEV models". In:
- McFadden, Daniel (1973). "Conditional logit analysis of qualitative choice behavior". In:
- (1978). *Modelling the choice of residential location*. URL: <http://cowles.econ.yale.edu/P/cd/d04b/d0477.pdf>.
- Miller, Eric J and Matthew J Roorda (2003). "Eric J. Miller and Matthew J. Roorda 1". In: 416, pp. 1–20.
- Morikawa, Taka and Tomio Miwa (2006). "Preliminary analysis on dynamic route choice behavior: Using probe-vehicle data". In: *Journal of advanced transportation* 40.2, pp. 140–163.
- Ochieng, Washington Y, Mohammed A Quddus, and Robert B Noland (2003). "Map-matching in complex urban road networks". In:
- Oyama, Yuki, and Eiji Hato (2016). "Pedestrian activity model based on implicit path enumeration". In: *Proceedings of the 21st International Conference of Hong Kong for Transportation Studies (HKSTS)*, pp. 331–338.
- (2017). "A discounted recursive logit model for dynamic gridlock network analysis". In: *Transportation Research Part C: Emerging Technologies* 85, pp. 509–527.

- ISSN: 0968-090X. DOI: [10.1016/j.trc.2017.10.001](https://doi.org/10.1016/j.trc.2017.10.001). URL: <http://dx.doi.org/10.1016/j.trc.2017.10.001>.
- Oyama, Yuki et al. (2016). "Trajectory-oriented traffic management using sequential discount rate: a case study of the Great East Japan Earthquake". In: *Proceeding of 11th ITS European Congress (ERTICO), Glasgow*.
- Palma, Andre de and Nathalie Picard (2005). "Route choice decision under travel time uncertainty". In: *Transportation Research Part A: Policy and Practice* 39.4, pp. 295–324.
- Papola, Andrea and Vittorio Marzano (2013). "A network generalized extreme value model for route choice allowing implicit route enumeration". In: *Computer-Aided Civil and Infrastructure Engineering* 28.8, pp. 560–580. ISSN: 10939687. DOI: [10.1111/mice.12007](https://doi.org/10.1111/mice.12007).
- Patriksson, Michael (1993). "Partial linearization methods in nonlinear programming". In: *Journal of Optimization Theory and Applications* 78.2, pp. 227–246.
- Peeta, Srinivas and Jeong Whon Yu (2005). "A hybrid model for driver route choice incorporating en-route attributes and real-time information effects". In: *Networks and Spatial Economics* 5.1, pp. 21–40.
- Pel, Adam, Michiel Bliemer, and Serge Hoogendoorn (2009). "Hybrid route choice modeling in dynamic traffic assignment". In: *Transportation Research Record: Journal of the Transportation Research Board* 2091, pp. 100–107.
- Pel, Adam J, Michiel CJ Bliemer, and Serge P Hoogendoorn (2012). "A review on travel behaviour modelling in dynamic traffic simulation models for evacuations". In: *Transportation* 39.1, pp. 97–123.
- Prashker, J and Shlomo Bekhor (1998). "Investigation of stochastic network loading procedures". In: *Transportation Research Record: Journal of the Transportation Research Board* 1645, pp. 94–102.
- Prashker, Joseph N and Shlomo Bekhor (2004). "Route choice models used in the stochastic user equilibrium problem: a review". In: *Transport reviews* 24.4, pp. 437–463.
- Prato, Carlo and Shlomo Bekhor (2006). "Applying branch-and-bound technique to route choice set generation". In: *Transportation Research Record: Journal of the Transportation Research Board* 1985, pp. 19–28.
- Pyo, Jong-Sun, Dong-Ho Shin, and Tae-Kyung Sung (2001). "Development of a map matching method using the multiple hypothesis technique". In: *IEEE Intelligent Transportation Systems Conference Proceedings*, pp. 23–27. DOI: [10.1109/ITSC.2001.948623](https://doi.org/10.1109/ITSC.2001.948623).
- Quddus, Mohammed A, Robert B Noland, and Washington Y Ochieng (2005). "Validation of Map Matching Algorithms using High Precision Positioning with GPS". In: *Journal of Navigation* 58.2, pp. 257–271. ISSN: 0373-4633. DOI: [10.1017/S0373463305003231](https://doi.org/10.1017/S0373463305003231).
- Quddus, Mohammed A., Washington Y. Ochieng, and Robert B. Noland (2006). "Integrity of map-matching algorithms". In: *Transportation Research Part C: Emerging Technologies* 14.4, pp. 283–302. ISSN: 0968090X. DOI: [10.1016/j.trc.2006.08.004](https://doi.org/10.1016/j.trc.2006.08.004).
- (2007). "Current map-matching algorithms for transport applications: State-of-the art and future research directions". In: *Transportation Research Part C: Emerging Technologies* 15.5, pp. 312–328. ISSN: 0968090X. DOI: [10.1016/j.trc.2007.05.002](https://doi.org/10.1016/j.trc.2007.05.002).
- Quddus, Mohammed a. et al. (2003). "A general map matching algorithm for transport telematics applications". In: *GPS Solutions* 7.3, pp. 157–167. ISSN: 1080-5370. DOI: [10.1007/s10291-003-0069-z](https://doi.org/10.1007/s10291-003-0069-z). URL: <http://link.springer.com/10.1007/s10291-003-0069-z>.

- Ramming, Michael Scott (2001). "Network knowledge and route choice". PhD thesis. Massachusetts Institute of Technology.
- Recker, W W (1995). "The Household Activity Pattern Problem - General Formulation and Solution". In: *Transportation Research Part B-Methodological* 29.1988, pp. 61–77. URL: {\textless}GotoISI{\textgreater}://A1995QK23900004.
- Robin, Th. et al. (2009). "Specification, estimation and validation of a pedestrian walking behavior model". In: *Transportation Research Part B: Methodological* 43.1, pp. 36–56. ISSN: 01912615. DOI: 10.1016/j.trb.2008.06.010. URL: <http://linkinghub.elsevier.com/retrieve/pii/S0191261508000763>.
- Rust, John (1987). "Optimal replacement of GMC bus engines: An empirical model of Harold Zurcher". In: *Econometrica: Journal of the Econometric Society*, pp. 999–1033.
- Samuelson, Paul A (1937). "A note on measurement of utility". In: *The Review of Economic Studies* 4.2, pp. 155–161.
- Sasaki, Tsuna (1965). "Theory of traffic assignment through absorbing Markov process". In: *Transactions of the Japan Society of Civil Engineers* 1965.121, pp. 28–32.
- Scarinci, Riccardo, Iliya Markov, and Michel Bierlaire (2017). "Network design of a transport system based on accelerating moving walkways". In: *Transportation Research Part C: Emerging Technologies* 80, pp. 310–328. DOI: 10.1016/j.trc.2017.04.016.
- Scarinci, Riccardo et al. (2016). "An exploration of moving walkways as a transport system in urban centers". In: *TRANSP-OR Report*.
- Shafique, Muhammad Awais, Eiji Hato, and Hideki Yaginuma (2014). "Using Probe Person Data for Travel Mode Detection". In: *Int. J. Comput. Inf. Syst. Control Eng. World Acad. Sci. Eng. Technol* 94, pp. 1501–1505.
- Sheffi, Yosef (1985). "Urban transportation network". In: *Pretince Hall*.
- Su, Che-Lin and Kenneth L Judd (2012). "Constrained Optimization Approaches to Estimation of Structural Models". In: *Econometrica* 80.5, pp. 2213–2230. ISSN: 1468-0262. DOI: 10.3982/ECTA7925. URL: <http://dx.doi.org/10.3982/ECTA7925>.
- Timmermans, Harry, Xavier van der Hagen, and Aloys Borgers (1992). "Transportation systems, retail environments and pedestrian trip chaining behaviour: Modelling issues and applications". In: *Transportation Research Part B: Methodological* 26.1, pp. 45–59.
- Tversky, Amos (1972). "Elimination by aspects: A theory of choice." In: *Psychological review* 79.4, p. 281.
- Tversky, Amos and Daniel Kahneman (1992). "Advances in prospect theory: Cumulative representation of uncertainty". In: *Journal of Risk and uncertainty* 5.4, pp. 297–323.
- Van Vliet, Dirck (1981). "Selected node-pair analysis in Dial's assignment algorithm". In: *Transportation Research Part B: Methodological* 15.1, pp. 65–68.
- Velaga, Nagendra R., Mohammed A. Quddus, and Abigail L. Bristow (2009). "Developing an enhanced weight-based topological map-matching algorithm for intelligent transport systems". In: *Transportation Research Part C: Emerging Technologies* 17.6, pp. 672–683. ISSN: 0968090X. DOI: 10.1016/j.trc.2009.05.008. URL: <http://dx.doi.org/10.1016/j.trc.2009.05.008>.
- Vovsha, Peter and Shlomo Bekhor (1998). "Link-nested logit model of route choice: overcoming route overlapping problem". In: *Transportation Research Record: Journal of the Transportation Research Board* 1645, pp. 133–142.
- Wardrop, John Glen (1952). "Some theoretical aspects of road traffic research". In: *Proceedings of the institution of civil engineers Part II* 1.3, pp. 325–362.

- White, Christopher E., David Bernstein, and Alain L. Kornhauser (2000). "Some map matching algorithms for personal navigation assistants". In: *Transportation Research Part C: Emerging Technologies* 8.1-6, pp. 91–108. ISSN: 0968090X. DOI: [10.1016/S0968-090X\(00\)00026-7](https://doi.org/10.1016/S0968-090X(00)00026-7). arXiv: [arXiv:1011.1669v3](https://arxiv.org/abs/1011.1669v3).
- Yai, Tetsuo, Seiji Iwakura, and Shigeru Morichi (1997). "Multinomial probit with structured covariance for route choice behavior". In: *Transportation Research Part B: Methodological* 31.3, pp. 195–207.
- Zadeh, Lotfi (1965). "Fuzzy logic and its applications". In: *New York, NY, USA*.